

Value-added products from bio-based platform chemicals

Kumulative Dissertation

zur Erlangung des akademischen Grades

Doctor rerum naturalium (Dr. rer. nat.)

der Mathematisch-Naturwissenschaftlichen Fakultät

der Universität Rostock

Vorgelegt von

Andrea Dell'Acqua, M.Sc.

Geboren am 18.02.1994 in Varese (Italien)

Rostock, den 22.08.2022

Die vorliegende Arbeit entstand in der Zeit von Oktober 2019 bis August 2022 am Leibniz-Institut für Katalyse e.V. an der Universität Rostock unter der Betreuung von Prof. Dr. Johannes G. de Vries.

Gutachter 1: Prof. Dr. Johannes G. de Vries

Leibniz-Institut für Katalyse e.V. an der Universität Rostock

Albert-Einstein-Straße 29a

18059 Rostock

Gutachter 2: Prof. Dr. Gert-Jan Gruter

Faculty of Science, Van 't Hoff Institute for Molecular Sciences, University of Amsterdam

Postbus 94157, 1090 GD Amsterdam, Niederlande

Datum der Einreichung: 22.08.2022

Datum der Verteidigung: 15.11.2022

Erklärung

Hiermit versichere ich an Eides statt, dass ich die vorliegende Arbeit selbständig angefertigt und ohne fremde Hilfe verfasst habe. Dazu habe ich keine außer den von mir angegebenen Hilfsmitteln und Quellen verwendet. Die aus den benutzten Werken inhaltlich und wörtlich entnommenen Stellen sind als solche kenntlich gemacht.

Andrea Dell'Acqua

Rostock, den 22.08.2022

Acknowledgments

This work would have never seen the light without the help, guidance and support of many people.

First of all, many thanks to my supervisor, **Prof. Johannes de Vries**. Thanks for the trust you put in me from the very beginning of my experience in LIKAT, for the amazing discussions and exchanges of ideas in the last 4 years, for your constant enthusiasm and knowledge in catalysis and applied chemistry. And for the great and convivial atmosphere that you always bring with you, inside and outside working hours.

Thanks to my group leader, **Dr. Sergey Tin**, for all the constant support and help. Thanks for always finding time to discuss my projects and for valuing all my suggestions.

My time in LIKAT was part of a very fruitful collaboration with Henkel KGa & Co, that is acknowledged for funding my PhD. Thanks to **Dr. Horst Beck**, **Dr. Adrian Brandt**, **Dr. Kenji Ito**, **Dr. Andreas Taden**, and **Dr. Felix Geitner** for the very collaborative atmosphere and the nice exchange of different point of views that a collaboration with industry offers.

Dr. Bernhard Stadler deserves a huge thank for initiating some of the projects that will be discussed in this thesis, for the amazing working atmosphere and all the interesting discussions.

Claas Schünemann is acknowledged for all the practical help in the lab, particularly when it comes to clean the glassware from my attempted polymerizations. Thanks also for the great atmosphere you brought with you into our group.

Lukas Wille is acknowledged for the great help with the ozonolysis project.

Thanks to the new department leader **Dr. habil. Eszter Barath** for the help with the last projects, the nice atmosphere and the energy you brought into the group.

Thanks to the analytical department of LIKAT for the helpful support with characterizations.

Thanks to all the members of the group *Catalysis with renewables and platform chemicals* for the amazing time, inside and outside LIKAT. In the last 4 years I had the pleasure to work with amazing people, who made my stay in Rostock way easier. Thanks for giving me a good reason to come to work every morning!

In particular I want to mention Bartosz, Bernhard, Pim, Thibault, Roberto, Brian, Fabian, Soumyadeep, Shasha, Zahra, Sergey and Claas for the great time at work and after work.

My 4 years in Rostock would have been incredibly boring without amazing people as David, Thibault, Thomas, Dario, Veronica, Fabrizio, Peter, Johannes, Eva, Niklas, Clara, Svenja, Max and many others. It was an amazing time that I'll always bring with me.

Grazie alla mia famiglia, soprattutto a mamma, papà ed Alice, per tutto il supporto, anche a distanza. Nonostante i chilometri che ci separano non mi sono mai sentito davvero solo. Credete in me e mi supportate (sopportate) da 28 anni, e non passa giorno in cui non sia fiero di voi.

Last but not least, Valerie. Your love, support and help go way beyond any possible written word. Simply thanks for all of it.

Kurzzusammenfassung

Aufgrund der sich zusehends abzeichnenden Ressourcenverknappung und des zunehmenden sozialen Bewusstseins für die durch die extensive Nutzung fossiler Rohstoffe entstehenden Umweltprobleme ist besonders die chemische Industrie zum Paradigmenwechsel gezwungen, nämlich zur Nutzung erneuerbarer Ressourcen als Ausgangsmaterialien. Ein potenzieller Ansatz besteht in der Verwendung sogenannter *Plattformchemikalien*, d. h. Verbindungen, die durch chemische oder enzymatische Reaktionen direkt aus Zuckern gewonnen werden können und deren weitere Umwandlung zu Bulk- und Feinchemikalien führt. Diese Arbeit zielt darauf ab, mögliche neue Anwendungen von drei Plattformchemikalien aufzuzeigen: Angelikalakton, Glykolaldehyd und Methylvinylglykolat.

α -Angelikalakton wird durch reaktive Destillation der Plattformchemikalie Lävulinsäure unter sauren Bedingungen hergestellt. Seine C-C-Doppelbindung wurde für die weitere Funktionalisierung anvisiert. Zunächst wurde eine neue atomökonomische, basenkatalysierte Isomerisierung zum β -Angelikalakton, mit anschließender katalytischer Diels-Alder-Reaktion und Ringöffnungsmetathesepolymerisation entwickelt, um funktionalisierte Polynorborene herzustellen, die als hochtransparente Materialien verwendet werden können. Ein weiterer Ansatz zur Wertschöpfung von α -Angelikalakton ist dessen oxidative Spaltung durch Ozonolyse zu Malonsäure und ihren Estern, wichtigen Zwischenprodukten, die derzeit in großen Mengen aus Petrochemikalien hergestellt werden, oder 3-Hydroxypropionaten, die für die Synthese von bioabbaubaren Polyestern in Betracht gezogen werden.

Glykolaldehyd ist der kleinste reduzierende Zucker und kann in hoher Ausbeute aus lignozellulosehaltiger Biomasse gewonnen werden, beispielsweise aus Pyrolyseöl. Seine Verwendung als C2-Baustein ist bekannt; in dieser Arbeit wurde Glykolaldehyd als C1 Baustein für die selektive *N*-Formylierung sekundärer Amine mit Luft als Oxidationsmittel verwendet. Die Reaktion ist vollständig atomökonomisch und verläuft nachweislich über einen radikalischen Mechanismus.

Methylvinylglykolat (MVG) kann als Nebenprodukt der säurekatalysierten Synthese von Methylaktat aus Zuckern, einschließlich Glykolaldehyd, erhalten werden. Seine C-C-Doppelbindung wurde zur Herstellung neuer Produkte genutzt. Die Hydroformylierung mittels bewährter Rhodium-Katalyse ergab ein Gemisch aus linearen und verzweigten Aldehyden, die weiter zu Diolen und Triolen reduziert werden können. Diese können verschiedenen Anwendungen zugeführt werden, zum Beispiel als reaktive Vernetzer in Spezialpolyestern. Die Methoxycarbonylierung des funktionalisierten MVG ergab lineare Diester, die erfolgreich zu amorphen Polyestern mit niedriger Glasübergangstemperatur polymerisiert wurden und die als biobasierte thermoplastische Elastomere Anwendung finden könnten.

Abstract

Due to the upcoming shortage of fossil resources, together with an increasing social awareness of the environmental problems due to their extensive exploitation, the chemical industry must switch to a new paradigm based on the use of renewable resources. One approach that has been proposed consists in the use of the so-called *platform chemicals*, compounds that can be directly obtained from sugars by chemical or enzymatic reactions and whose further transformations yield bulk and fine chemicals. This work aims to show possible novel applications of three platform-derived chemicals: angelica lactone, glycolaldehyde and methyl vinyl glycolate.

α -Angelica lactone is prepared by reactive distillation of the platform chemical levulinic acid under acidic conditions. Its carbon-carbon double bond was targeted for further functionalization. First, a new atom economic base-catalysed isomerization to its β -isomer followed by catalytic Diels-Alder reaction and ring-opening metathesis polymerization was designed to prepare functionalized *poly-norbornenes* that can be employed as highly transparent materials. Another approach to valorise α -angelica lactone is its oxidative cleavage using ozonolysis to malonic acid and its esters, important intermediates currently produced in bulk from petrochemicals, or 3-hydroxy propionates, that are considered for the synthesis of bio-degradable polyesters.

Glycolaldehyde is the smallest reducing sugar and can be obtained from lignocellulosic biomass in high yields, for example from pyrolysis oil. Its use as C2 building block is known. In this work, glycolaldehyde was employed for the selective *N*-formylation of secondary amines using air as oxidant. The reaction is fully atom economic and was shown to proceed *via* radical mechanism.

Methyl vinyl glycolate (MVG) can be obtained as side stream of the acid-catalysed production of methyl lactate from sugars. It is also possible to synthesise it from glycolaldehyde. Its carbon-carbon double bond was targeted in order to synthesise new compounds. Hydroformylation using well-established rhodium catalysis gave a mixture of linear and branched aldehyde that could be further reduced to diols and triols. The latter compounds might have several applications, for example as reactive cross-linkers in specialty polyesters. Methoxycarbonylation of functionalised MVGs afforded linear diesters that were successfully polymerised to amorphous polyesters with low glass transition temperatures, that might have applications as bio-derived thermoplastic elastomers.

List of Abbreviations

2-MeTHF		2-Methyltetrahydrofuran
ACN		Acetonitrile
AL		Angelica lactone
Cat.		Catalyst
Conv.	[%]	Conversion
Cp		Cyclopentadiene
\bar{D}	$[M_w M_n^{-1}]$	Dispersity
DCM		Dichloromethane
DMF		<i>N,N</i> -dimethylformamide
DSC		Differential Scanning Calorimetry
EA		Ethyl acetate
EPR		Electron paramagnetic resonance
Eq.		Equivalent
ESI		Electro spray ionization
FCC		Flash column chromatography
GA		Glycolaldehyde
GPC		Gel permeation chromatography
LA		Levulinic acid
IR		Infrared
MA		Malonic acid
<i>m</i> CPBA		3-Chloroperbenzoic acid
MIBK		Methylisobutylketone
ML		Methyl levulinate
M_n	$[\text{g mol}^{-1}]$	Number average molecular weight
mol		Moles
MS		Mass spectroscopy
MTBE		Methyl tert-butyl ether
MVG		Methyl vinyl glycolate
M_w	$[\text{g mol}^{-1}]$	Average molecular weight by weight
NMR		Nuclear magnetic resonance

p	[bar]	Relative pressure
Ref.		Reference
Sel.	[%]	Selectivity
Sub.		Substrate
t	[h]	Time
T	[°C]	Temperature
T_g	[°C]	Glass transition temperature
THF		Tetrahydrofuran
UV-vis.		Ultraviolet-visible light
θ	[°]	Contact angle

Table of Contents

1. Introduction	1
1.1 The need for bio-based chemicals	1
1.2 The biorefinery approach	3
2. Platform chemicals	5
2.1 Levulinic acid (LA)	7
2.1.1 Synthesis of LA	7
2.1.2 Synthetic applications of LA	8
2.1.3 Angelica lactones	8
2.2 Glycolaldehyde	11
2.2.1 Synthesis of glycolaldehyde	11
2.2.2 Reactivity of glycolaldehyde	12
2.3 Methyl vinyl glycolate	13
2.3.1 Synthesis of methyl vinyl glycolate	13
2.3.2 Synthetic applications of methyl vinyl glycolate	15
3. Aim and results of the dissertation	17
3.1 New polymers from a scalable β-Angelica lactone derived monomer	17
3.2 Production of malonates and 3-oxopropanoates via ozonolysis of α-angelica lactone	22
3.3 N-Formylation of amines using glycolaldehyde as C1 building block	25
3.4 Methyl vinyl glycolate as renewable difunctional monomer for novel polymers	31
4. Conclusions	37
5. References	38
6. Selected publications	44
6.1 Scalable synthesis and polymerisation of a β-angelica lactone derived monomer	44
6.2 Ozonolysis of α-angelica lactone: a renewable route to malonates	52
6.3 Glycolaldehyde as a Bio-based C1 Building Block for Selective N-Formylation of Secondary Amines	57
6.4 New Bifunctional Monomers from Methyl Vinyl Glycolate.	64
7. Appendix	71
7.1 Contributions to the Individual Publications	71
7.2 Supporting Information	72
7.3 Curriculum Vitae	159

1. Introduction

1.1 The need for bio-based chemicals

Fossil fuels, such as petroleum and coal, are naturally occurring mixtures of a huge number of chemical compounds, among them hydrocarbons, that originated from organic sediments from the Cenozoic and Mesozoic eras (10 to 200 mln. years ago) that have formed under specific pressure and temperature conditions. Although its use has been exploited by humans since the early days of history, it is only from the 19th century that the “petroleum age” started.¹ This span of 200 years is also characterized by the fastest and most significant growth of humankind, both in terms of World population and wealth. The chemical industry as we know it was also boosted in the same time frame due to the availability of so many compounds that can be easily, and most important cheaply, obtained from petroleum and other fossil sources. However, this age is approaching its end. Although new technologies, such as hydraulic fracturing, make the exploitation of a larger number of less accessible oilfields possible, and it is therefore not clear when exactly all the reserves will come to an end, this moment is bound to happen. On top of that, the usage of fossil fuels has led to massive issues with air pollution and emissions of carbon dioxide, that contributed to generate tangible consequences such as global warming, ice melting and climate changes, together with a huge increase of waste (above all, plastics) spread into the environment, particularly into seas and oceans.² Nonetheless, fossil resources still account for the largest contribution to global energy production, approaching 80% in 2019 (Figure 1), while renewable resources are far behind, at the 4th position.³

World total energy supply by source, 1971-2019

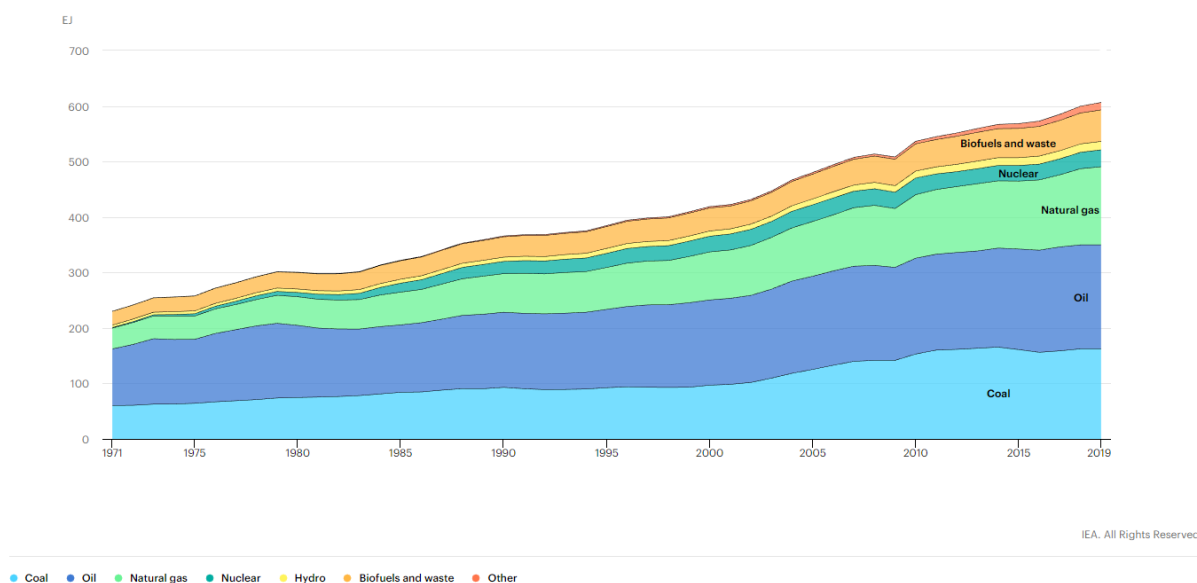


Figure 1. World total energy supply by source in the period 1971-2019. Credits: IEA.

Chemical industry is the biggest consumer of fossil fuels (oil and gas), both as energy source and as raw material, and the third CO₂ emitter after cement and steel industries. The demand of chemicals is foreseen to increase even stronger in the upcoming years.⁴ In 2015 the Paris Agreement set the goal of achieving carbon neutrality by year 2050. Thus, there is an urgent need for a paradigm change from fossil-based to renewable-based chemical economy.

Fossil fuels can be seen as very old biomass, that favourable conditions had gradually turned into chemical compounds that are easily exploitable for our needs. Nature generates around 170 billion

metric tons of renewable biomass per year from wood, aquatic plants, waste (industrial, agricultural and municipal), and energy crops (used in the production of biofuels such as biodiesel). Biomass is a complex mixture of many chemicals bearing several different functionalities. Its main components are sugars, lignin, proteins and fats (mainly as triglycerides).⁵⁻⁹ Concerning its chemical composition, the main difference with fossil resources concerns the oxygen content, which accounts for up to 40% of biomass' weight, whereas in the latter it rarely exceeds 10%. The carbon content ranges between around 40 and 60% (in oil and coal can be up to 94%); sulfur is higher in oil (up to 6%), but in other fossil resources its content is comparable to biomass. Nitrogen levels are in both cases between 0.1 and 2%.¹⁰

Lignocellulosic biomass is the most abundant on the planet, coming for example from agricultural wastes such as sugarcane bagasse and corn stover, paper and wood industry. It comprises three polymers: cellulose, hemicellulose, and lignin (Figure 2), that together constitute the cell walls of plants. Cellulose is made by glucose units whose positions 1 and 4 are linked by β -glycosidic bonds. Hemicellulose contains mainly xylose units, together with smaller amounts of other sugars such as mannose, galactose and others. These two are held together by covalent and non-covalent bonds, and encapsulated by lignin. The latter contains aromatic moieties (lignols) connected by C-C and C-O bonds, forming a complex amorphous polymer. The amount of each component largely varies with the source of biomass: cellulose is generally the main component (30 – 50% weight), followed by hemicellulose (20 – 40%) and lignin (10 – 20%).¹¹

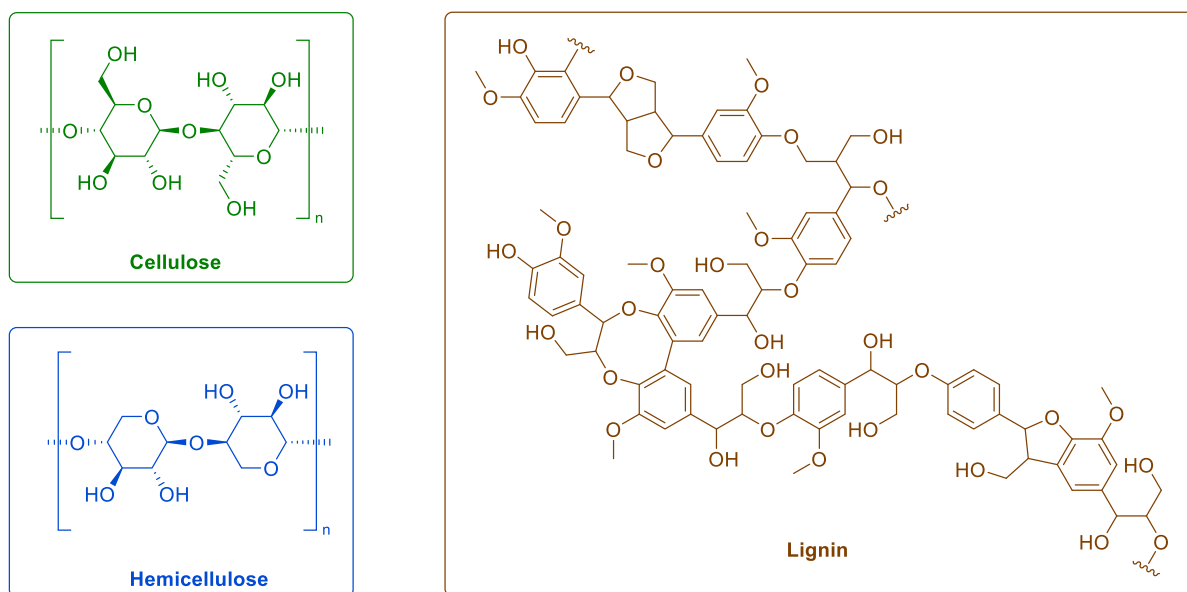


Figure 2. Components of lignocellulosic biomass.

Despite its abundance, its variety of chemical compounds and its renewable nature, nowadays only a very small amount of biomass, below 5%, is actually employed as source of food, fuels and chemicals.⁹

1.2 The biorefinery approach

Analogously to what an oil refinery makes with crude oil, a biorefinery converts biomass into added-value products through a series of chemical and separation processes.^{9, 12} Different kind of biomass can lead to very different products (Table 1). The largest application of biomass rich in starch and sugar is the production of ethanol by fermentation. Bioethanol itself accounts for more than 90% of the world's production of bio-fuels.¹³ However, fuels are low-value products, thus making the investment in a biorefinery not necessarily economic, in particular when it concerns lignocellulose-based bio-ethanol. It is more convenient to aim to higher-value chemicals, making this approach more profitable and therefore attractive for companies.¹⁴ Bioethanol can be further converted into several products such as ethylene, diethyl ether, higher hydrocarbons, aromatics, etc. Longer alcohol like butanols, that are mainly used as fuels and solvents, can be made by using different (engineered) yeasts.^{15, 16} Fine chemicals such as lactic, itaconic, succinic acids are obtained by numerous (catalytic and biocatalytic) transformations of sugars, such as retro-aldol condensations and dehydration.¹¹



Figure 3. Dupont's biorefinery for producing cellulosic ethanol, Nevada. Source: www.refiningandpetrochemicalsme.com

Lignocellulosic biomass can be valorised by several methods. Its direct combustion generates heat and energy. This represents the oldest and at the moment largest application of lignocellulose.¹⁷ Gasification at high temperature in the presence of air to syngas, that can be further converted by Fisher-Tropsch chemistry and Water-gas shift reaction to green hydrogen is another way to valorise it. However, the syngas originated from this process contains rather high levels of methane and char.¹⁸ Pyrolysis or liquefaction of biomass affords bio-oils, mixtures of many small molecules that can be then converted by dehydration, deoxygenation, decarboxylation etc. of the (hemi)cellulose component to obtain carbohydrates, and other compounds.^{10, 19} This approach suffers from the harsh conditions necessary (acids, high temperature and pressure) for the reactions, thus requiring corrosion-resistant equipment which increases the costs of the processes.^{20, 21} Hydrolysis of the lignocellulose into lignin and cellulose is usually required to fully exploit both components. The lignin fraction is rich in phenolic compounds and can in principle be used to obtain valuable aromatic products, although its depolymerisation to monomeric products still remains challenging.²² Several important small molecules can be obtained by catalytic dehydration of the sugars present in lignocellulose, for example furfural, levulinic acid and HMF.^{23, 24} This part will be discussed in detail in the following paragraphs.

Fatty acids in the form of triglycerides are converted to biodiesel *via* catalytic transesterification at mild temperatures with methanol. A by-product of the process (10% of the total biodiesel weight) is glycerol, that has several applications in pharma, cosmetics, material science and fine chemistry.^{25, 26} It can also be converted to highly valuable chemicals such as acrolein,²⁷ propanediols,²⁸ epichlorohydrin and others.^{29, 30}

Table 1. Examples of different biorefineries products from different biomass feedstocks.

Biomass type	Technique	Example of products
Cellulose/starch	Fermentation	Ethanol, ABE (acetone, butanol, ethanol), higher alcohols, lactic acid, succinic acid, itaconic acid
	Microbial digestion	Fuels
	Dehydrocyclization	HMF
	Reforming	Hydrogen
Lignocellulose	Combustion	Heat and electricity
	Gasification	Syngas
	Pyrolysis	Bio-oils
	Catalytic pyrolysis	Aromatics, alkenese, CO ₂ , CO
	Liquefaction	Bio-oils
	Steam explosion	Lignin, sugars Levulinic acid, furfural
Triglycerides	Dehydration	Fatty acids, glycerol
	Transesterification	Fatty acids, glycerol
	Hydrolysis	Fuels
	Pyrolysis or cracking	Syngas
	Reforming	

Many challenges have still to be addressed in order to pave the way for biorefineries to replace their fossil counterparts. Biomass is inherently inconsistent in nature, with a composition that highly depends not only on its type, but also on the location and even on the moment of the year when the biomass is collected. High volumes of biomass are extracted and have to be transported to the refinery. Thus, the logistics may become a limiting factor. This is particularly true for lignocellulose, where the amount of material needed for refining requires expensive transport often over long distances. Moreover, the existing infrastructure that was designed for petrochemicals should in an ideal scenario be maintained as much as possible, in order to save the time and costs that would be required to completely design a new one. The overall biorefinery approach should be, from an economic point of view, at least comparable with the existing fossil-based market, both for chemicals and fuels. Last but not least, we should all learn the lesson we got from the extensive exploitation of fossil resources: the new chemical landscape must be as sustainable as possible. Food resources should neither be used for fuels production, nor land should be taken away from this purpose. Their use as raw materials for the production of chemicals should always be carefully considered within the frame of circular and sustainable economy, for example by valorising food wastes. Any new process has to be designed in accordance with the “12 principle of green chemistry” and the “17 sustainable developments goals”,^{31, 32} since any deviation from these pillars would nullify the overall approach.

2. Platform chemicals

One valuable way that has been proposed to convert biomass to useful compounds consists into the use of the so-called platform chemicals. They are a number of molecules that can be directly obtained from carbohydrates by either chemical or fermentative processes, and that can be further transformed on a commercial scale into useful compounds such as fuels, monomers or fine chemicals. Platform chemicals are all known and well-studied compounds, either already produced on large scale, or new compounds that could replace existing fossil-based ones, as in the case of furandicarboxylic acid.^{14, 33} Several molecules have been proposed in the last 20 years as potential platform chemicals according to this definition (Fig. 4).

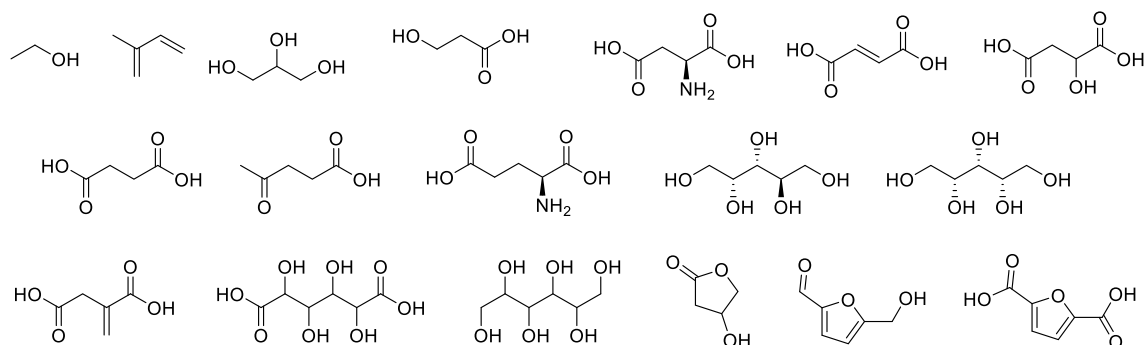


Figure 4. Proposed platform chemicals from references 13 and 33.

Table 2 shows an overview of the so-far proposed platform chemicals and their main production methods and applications. The use of ethanol as biofuel and its conversion to other products, as well as the uses of glycerol, have been already mentioned in the previous section. Furans (furfural and HMF) are obtained by dehydration of C5 and C6 sugars, respectively.³⁴ Furfural is also a side stream from the production of paper, it being abundant in the sulfite liquor that originates from the separation of the lignin and cellulose fractions.³⁵ 90% of the produced furfural is further hydrogenated to furfuryl alcohol, whose largest application is as monomer for resins used in moulding.³⁶ Furan-2,5-dicarboxylic acid (FDCA) is gaining attention as a potential replacement for terephthalic acid for polyesters production, especially for packaging applications, due to its lower carbon footprint and superior gas barrier properties when compared to the existing petrochemical PET.³⁷ FDCA can be produced directly from fructose by dehydration-oxidation in a 2-steps catalytic process.^{38, 39} The first commercial-scale plant utilizing this approach will be operative from 2024, with a yearly production capacity of 5 kt of FDCA.⁴⁰

Isoprene has a billion-dollar market share for its use as monomer in the production of elastomers. It has been originally proposed as platform chemical because it could be obtained by fermentation of sugars using different bacteria.^{41, 42} However, in the best of my knowledge, none of these renewable routes have been ever implemented on an industrial scale. Higher hydrocarbons may also be produced by microalgae fermentation using both sugars or fatty acids as feedstock.⁴³

Several organic acids are included in the list of platform chemicals. Lactic acid is commercially available from the fermentation of glucose. In the process its calcium salt is produced, thus requiring stoichiometric sulfuric acid for its neutralization. This affords a 1:1 mass of calcium sulfate, generating a huge waste problem and increases its cost.⁴⁴ Another possibility is to produce lactic acid esters by acid-catalysed degradation of sugars. Other than improving the overall atom efficiency of the process, this approach also generates other valuable molecules as side stream, as will be shown in this work.^{38, 45} Lactic acid is used for the production of biodegradable polyesters, acrylic acid, propylene glycol, and

lactate esters as green solvents and in the production of acrylates.⁴⁶ Another high value product is succinic acid, that can be also produced by fermentation of sugars.⁴⁷ Its esters can be hydrogenated to 1,4-butanediol, THF, γ -butyrolactone and others.⁴⁸ Succinic acid is mostly employed in the synthesis of polyesters and polyamides (nylon). 3-Hydroxypropionic acid comes as product of glucose as well as glycerol fermentation.⁴⁹ Its hydrogenation yields 1,3-propanediol, added-value monomer for polyesters. Acrolein and acrylic acid can be also produced by its dehydration.⁵⁰ Biodegradable polyesters can be obtained from (co)polymerization of hydroxypropionic acid. Levulinic acid will be discussed in more details in the next paragraphs.

Sugar alcohols are readily obtainable by hydrogenation of sugars and have their biggest commercial application as low-calory food additives. Xylitol can be either produced from xylol or by biochemical reduction of cellulosic biomass.⁵¹ Analogously, sorbitol is produced from glucose. Sugar alcohols applications include their deoxydehydration to the corresponding hydrocarbons, and reforming to CO, H₂, and methane.¹⁹ The Chinese company Dacheng Polyol Investment produces different diols and polyols from sorbitol on commercial scale.⁵²

Table 2. Overview of some production methods and applications of platform chemicals.

Platform chemical	Production method from biomass	Main products and applications
Ethanol	Fermentation	Fuel, ethylene, acetic acid, diethyl ether, olefins
Furfural	Dehydration of xylose	THF, pyrroles
HMF	Dehydration of hexoses	Levulinic acid, FDCA
FDCA	Dehydration-oxidation of fructose	Polyesters
Glycerol	Transesterification of fatty acids	Glycols, hydrocarbons, acrolein, hydroxyacetone, 1,3-propanediol, carbonates, epichlorohydrin
Isoprene ^[a]	Bacterial fermentation of sugars	Elastomers
Higher hydrocarbons	Microalgae fermentation of sugars and fatty acids	Monomers, solvents, fuels
Lactic acid and lactates	Fermentation of glucose, acid-catalysed degradation of sugars	Polyesters, acrylic acid, acrolein, solvents
Succinic acid	Fermentation of sugars	Polyesters, polyamides
3-Hydroxypropionic acid	Fermentation of sugars	Acrolein, acrylic acid
Levulinic acid	Acid-catalysed degradation of hexoses	GVL, caprolactam, acrylates, MVK, angelica lactones, adipic acid, 2-methyl-THF
Xylitol	(Bio)catalytic reduction of xylose	Hydrocarbons
Sorbitol	(Bio)catalytic reduction of glucose	Hydrocarbons

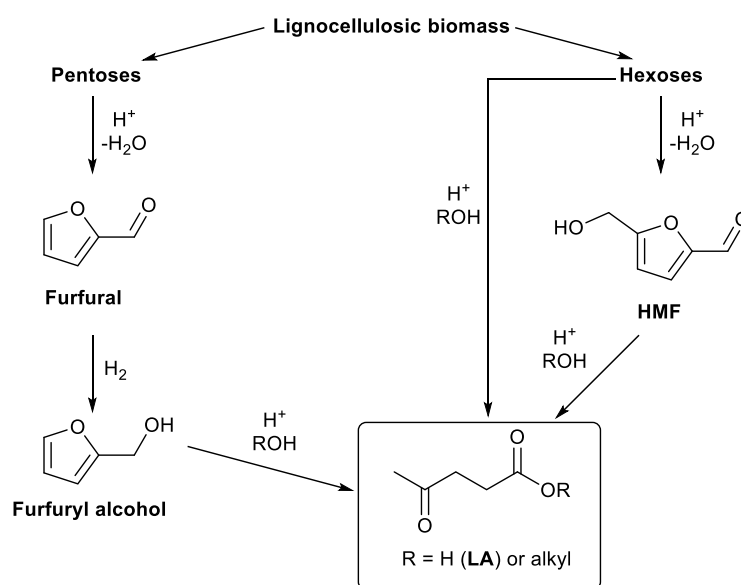
^[a]No commercial production from renewables up to date.

In this work, the use of platform-derived angelica lactones was investigated. Moreover, glycolaldehyde and methyl vinylglycolate, that can be both conveniently obtained from sugars, were envisaged as promising novel platform chemicals for their use as C1 building block and monomer for polymers, respectively.

2.1 Levulinic acid (LA)

2.1.1 Synthesis of LA

Levulinic acid was isolated for the first time by Mulder in the mid-19th century by heating fructose (levulose, hence LA's name) in the presence of aqueous acids.⁵³ It can be also obtained directly from cellulose or lignocellulosic biomass. Already in 1956 it was recognised as potential raw material for the chemical industry, due to the large availability of lignocellulose and its low price.⁵⁴ Different mechanisms of LA formation have been described, depending on the starting feedstock and particularly on the sugars involved (Scheme 1).^{55, 56}



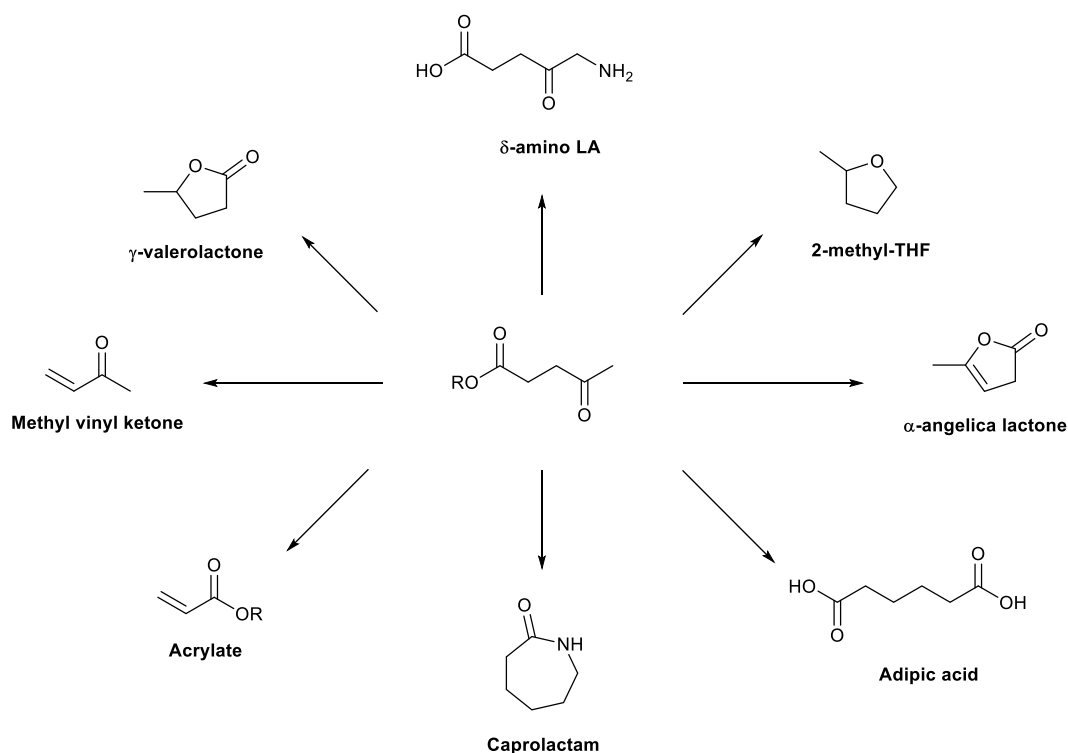
Scheme 1. Overview of synthetic pathways from biomass to LA.

Starting from pentose sugars such as xylose, their acid-catalysed dehydration affords furfural, which is then hydrogenated to furfuryl alcohol typically over heterogeneous catalysts.⁵⁷ Solvolysis of the latter in the presence of acids leads to LA or LA esters. Starting from hexoses on the other hand involves their dehydration to hydroxymethyl furfural (HMF), that can be then re-hydrated or undergo solvolysis to LA or alkyl levulinates. Even more interestingly in view of a biorefinery approach, lignocellulosic biomass can be directly converted into LA in a multistep synthesis that involves a pre-treatment of the biomass in diluted acids followed by the hydrolysis step that affords LA in around 50% final yield. The reaction gives formic acid as co-product, that itself has a market of almost 900 kt/year.⁵⁸ This process has been run on pilot scale, but never got to production.⁵⁹ Alternatively, levulinates can be obtained as side products of the production of furandicarboxylic acid (FDCA) from fructose (as discussed earlier in this section) *via* 5-methoxymethyl furfural, namely during the acid-catalysed dehydration of the sugar.⁶⁰

The (potential) demand for LA has been forecasted to be increasing in the upcoming years (3437 t/y between 2022 and 2026).⁶¹ Several estimations of LA's price have been made in the last years, showing that the use of lignocellulosic feedstock might reduce its price down to 0.09 €/kg in the very best case, although this is still far from being the reality, at the moment.⁶² In spite of the apparently favourable ground for LA's production on bulk scale, there is only one producer of alkyl levulinates on the market, and the scale of the process is, in the best of my knowledge, not known.⁶³

2.1.2 Synthetic applications of LA

As mentioned in the introduction, one of the key features of platform chemicals is their applicability in the synthesis of new or existing substances that have potential large-scale application, and LA fully meets this requirement (Scheme 2). Levulinate esters are mainly employed as fragrances, and have been additionally proposed as oxygenated fuels, even though their price would be far too high.^{64, 65} Moreover, it was shown that methyl levulinate can be converted with very high yields into methyl acrylate and acetic acid *via* the intermediate methyl 3-acetoxypropionate by gas-phase pyrolysis.⁶⁰ 5-Aminolevulinic acid has applications as herbicide and growth-promoting factor for plants.⁶⁶ Its hydrogenation, depending on the specific reaction conditions, gives three very useful compounds: the renewable solvent and monomer 2-methyl-THF,⁶⁷ γ -valerolactone (GVL),⁶⁸ and 1,4-pentanediol.⁶⁹ GVL has also been further converted to nylon intermediates such as caprolactam and adipic acid.⁷⁰⁻⁷⁵ Methyl vinyl ketone is used as building block in the synthesis of various fine chemicals, among them vitamin A, and as monomer; it can be obtained from methyl levulinate either by oxidation or decarboxylation.⁷⁶⁻⁷⁸ This second possible path involves the intermediate α -angelica lactone, that will be discussed more in details in the following paragraphs.

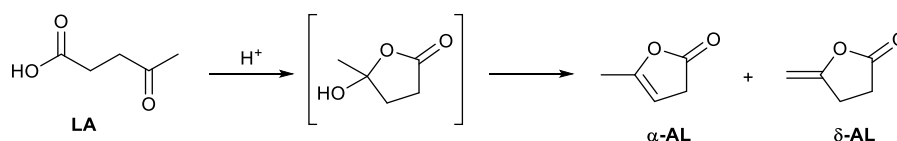


Scheme 2. Overview of some possible products obtainable from LA and its esters.

2.1.3 Angelica lactones

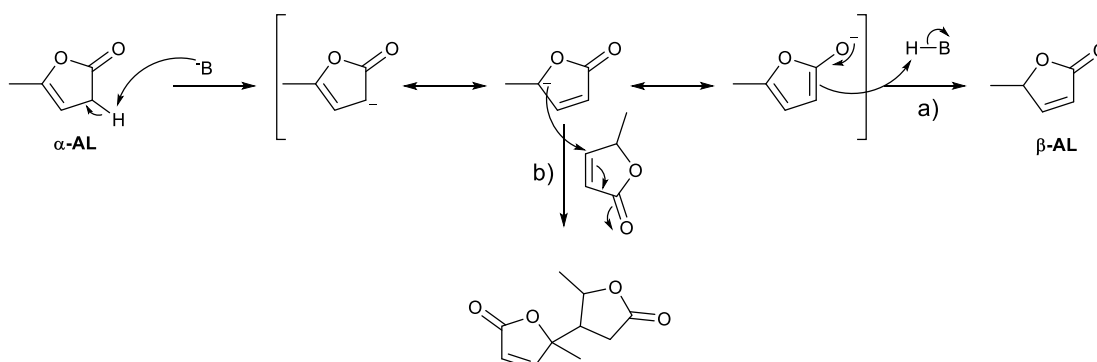
Distilling levulinic acid, Ludwig Wolf obtained and reported for the first time in 1883 the isolation of α -angelica lactone (α AL).⁷⁹ The mechanism of α AL formation (Scheme 3) involves a first, acid-catalysed cyclization of LA, with subsequent elimination of water from the unstable hydroxy lactone (pseudolevulinic acid). Typical reaction conditions for the reactive distillation are 160 °C, under reduced pressure (in the order of 10^{-2} bar) and in the presence of 1% weight of phosphoric acid.⁸⁰ AL

can exist in principle as mixture of three isomers (α , β and δ). The described reaction affords mainly the α isomer, with some minor amounts of the less stable δ isomer, that further isomerises to α AL.



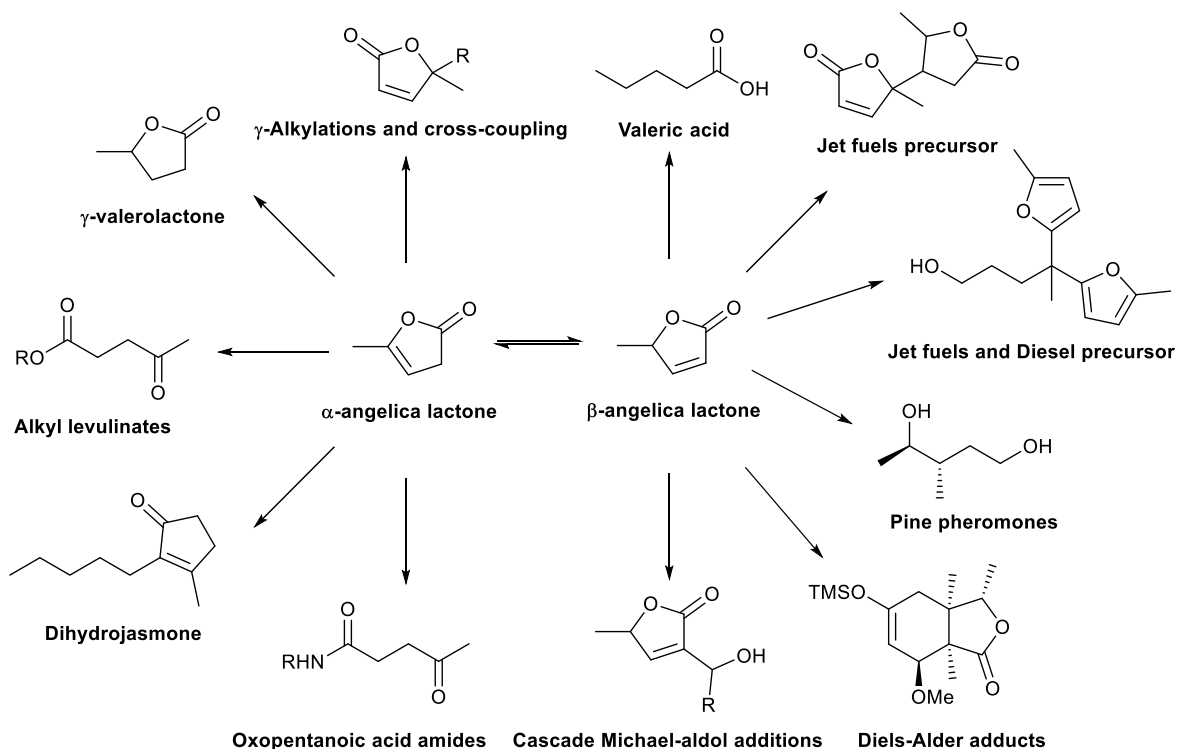
Scheme 3. Synthesis of angelica lactones from LA.

In the presence of catalytic amounts of a base, isomerization of this mixture to the β isomer occurs (Scheme 4a). The reaction proceeds *via* an aromatic intermediate furanolate, that gets re-protonated in the more thermodynamically stable α -position. However, the reaction being an equilibrium, the reported yields do not exceed 60%.^{54, 81-83} This problem will be tackled in section 3.1. Other than the thermodynamic limitations for the synthesis of pure β -AL, there is another base-promoted reaction that might limit the outcome of the isomerization, *i.e.* dimerization (Scheme 4b). The dimer has been applied in the synthesis of bio-based jet fuels by the group of Mascal, by converting α -AL to the dimer in quantitative yield using potassium carbonate followed by hydrogenation over a supported Iridium catalyst to branched olefins.⁸⁴



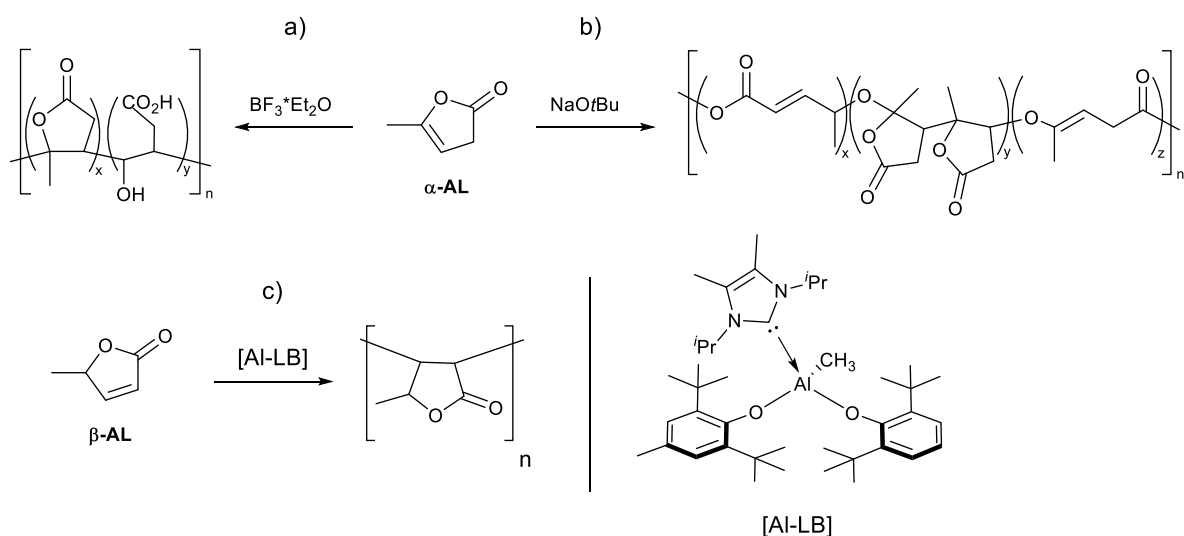
Scheme 4. Base-promoted: a) α - to β AL isomerization; b) dimerization.

Angelica lactones have been already applied in several fields. Zhang and co-workers also investigated the use of angelica lactone derivatives as precursors for jet fuels and diesel-type branched alkanes, in this case by reacting AL (both α and β) with 2-methylfuran and hydrogenating or hydrodeoxygenating the products.⁸⁵ Moreover, α -AL has been used as fragrance and food additive due to its intense fruity (coconut-like) flavour. It can be converted to dihydrojasnone, another important aroma.⁸⁶ Starting from both the α and β isomers, various pharmaceutically relevant building blocks have been prepared by Michael addition, Morita-Baylis-Hillman reaction, Mannich-type addition, and many more. Scheme 5 gives an overview of some of the synthetic approaches that have been applied on angelica lactones so far. A more detailed discussion of all the applications of AL in the synthesis of fine chemicals goes beyond the scope of this work.⁸⁷



Scheme 5. Overview of the synthetic applications of angelica lactones.

Polymers based on AL have been already reported in the past. Cationic polymerization of α -AL using BF_3 as initiator only leads to oligomers (800 g/mol), where some of the pending lactone groups are opened, probably due to the aqueous conditions employed for the workup (Scheme 6a).⁸⁸ Anionic polymerization and copolymerization of α -AL is also known, and affords as in the previous case only oligomeric species after two weeks reaction time. Sodium tert-butoxide has been used as initiator, and a large number of the lactones were also opened during the reaction (Scheme 6b).⁸⁹⁻⁹¹ In both of the cases the irregular structures and the low molecular weights limit the possible real-life application of these polymers. On the other hand, β -AL was efficiently polymerised to an acrylate-like polymer by means of a Lewis-pair catalyst. Very high molecular weights (up to 26 kg/mol) could be achieved



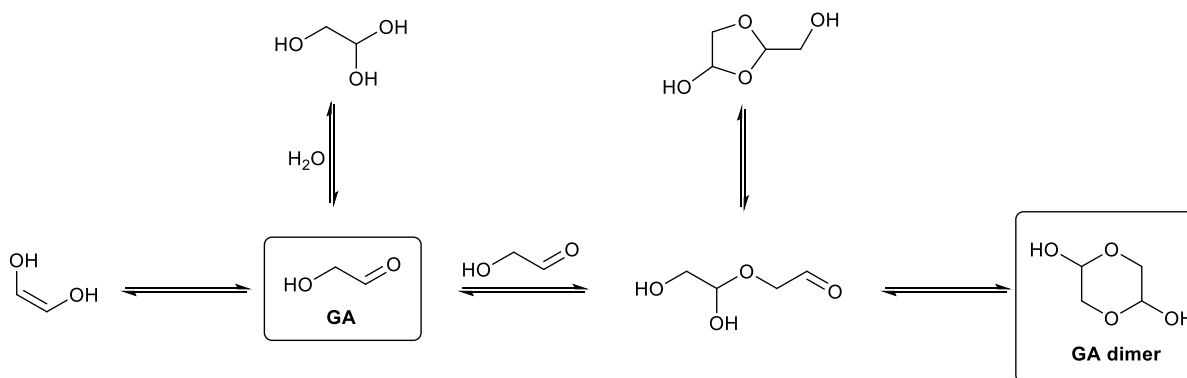
Scheme 6. Reported polymerizations of angelica lactones: a) cationic and b) anionic polymerizations of α AL; c) Lewis-pair catalysed polymerization of β AL.

(Scheme 6c). Moreover, a frustrated-Lewis-pair catalyst is used in the same work to synthesise β AL dimers in high yields. Interestingly, when radical initiators such as AIBN were tried, no polymerization occurred.⁹² Within the scope of this thesis, angelica lactones were investigated as building blocks for polymers using two different approaches: α - to β -AL isomerization followed by Diels-Alder and ring-opening metathesis polymerization (3.1) and oxidative cleavage of the double bond of α -AL using ozone (3.2).

2.2 Glycolaldehyde

2.2.1 Synthesis of glycolaldehyde

Glycolaldehyde (GA) is a reducing sugar, the smallest in the homologue series, that exists at room temperature as a crystalline dimer (GA dimer, Scheme 7) that gradually becomes a mixture of open dimer and monomer upon heating, turning purely monomeric in the gas phase.⁹³ In solution, different species in equilibrium have been shown to be present in amounts that largely vary according to the solvent. In protic solvent such as methanol or water, the monomeric species are favored due to stabilization by hydrogen bonding.⁹⁴ For example, in water only 4% of GA exists as monomeric hydroxyaldehyde and 9% as cyclic dimer, the hydrated GA being the major species at 70%.⁹³ On the other hand, in DMSO and acetone the monomerization of the dimer is comparably slower. Other than these equilibria, due to its two reactive groups GA is prone to undergo aldol condensation, which might limit the commercial applicability of GA as such, making it preferable to react it further to ethylene glycol by hydrogenation, or to amino alcohols by reductive amination.⁹⁵



Scheme 7. Equilibria between different monomeric and dimeric forms of GA.

Notwithstanding the limitations due to its instability, GA has been gaining attention in the last years as a potentially safer and environmentally friendlier replacement for ethylene oxide as C2 building block.⁹⁵ GA can be obtained from sugar-containing biomass in several ways. Biomass pyrolysis oil contains up to 13% of GA, even though its isolation in a pure form can be challenging.⁹⁶ A potentially scalable method involves its reactive extraction using amines, that has been shown to be economically feasible for a yearly production of 13 Kt of GA on a price that would compete with petrochemical ethylene oxide.^{97, 98} Similar to this route, gasification of biomass to syngas could be employed. Syngas is used in the current synthesis of GA *via* hydroformylation of formaldehyde with homogeneous rhodium catalysts.⁹⁹ Formaldehyde can also be converted to GA using the Butlerov (or formose) reaction,¹⁰⁰ that affords aldose sugars by a sequence of aldol condensations and aldose-ketose rearrangements. The reaction is catalysed by bases, but its selectivity to the C2 product is rather low.

Table 3. Overview of methods for the synthesis of GA from biomass.

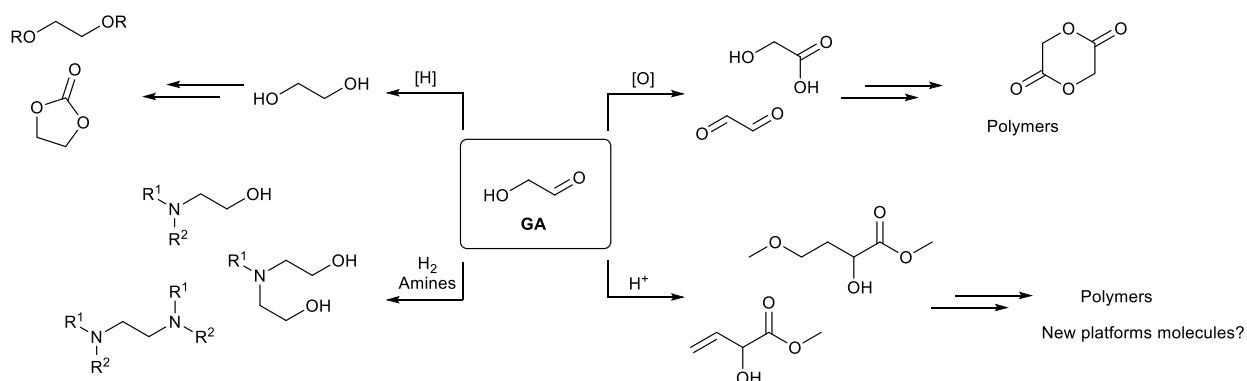
Entry	Method	Representative conditions	GA yield [%]	Ref.
1	Biomass pyrolysis	500 °C, then reactive extraction	13	96-98
2	Hydroformylation of formaldehyde	100 °C, 138 bar syngas, Rh-phosphine catalyst	80	99
3	Butlerov reaction of formaldehyde	NaOH (substoichiometric), zeolites, 94 °C	32	101-103
4	Cellulose hydrolysis with supercritical water	373 °C, 220 bar	64	104
5	Retro-aldol of sugars	240 °C, Tungsten catalyst, O ₂ , methanol, then H ₂ , Cu/SiO ₂ catalyst	74 ^[a]	105-107
6	Hydrous thermolysis of sugars	500-600 °C, fluidized sand bed reactor	70	108

^[a]Ethylene glycol as product.

Progress has been made by employing zeolites,¹⁰¹ N-heterocyclic carbenes,¹⁰² or thiazolium salts.¹⁰³ Cellulose can be decomposed by supercritical water, with up to 64% selectivity for GA.¹⁰⁴ Retro-aldol condensation of glucose also yields GA. However, as previously mentioned, it is more convenient to convert it directly by hydrogenation to the corresponding diol without isolating the intermediate GA.¹⁰⁵⁻¹⁰⁷ Recently, Haldor Topsøe and Braskem have launched a demonstration plant that produces ethylene glycol by hydrous thermolysis of sugars, that achieves up to 74% GA that is then reduced to the diol. The process is planned to get to commercial scale in the upcoming years.¹⁰⁹ The stream of GA can also be used for the synthesis of lactates and other derivatives,¹⁰⁸ and will be further discussed in Section 2.3. A recent process by Avantium, that is currently on pilot scale, directly converts glucose to ethylene glycol by a single-step retro-aldol followed by hydrogenation over a tungsten-ruthenium catalyst.¹¹⁰

2.2.2 Reactivity of glycolaldehyde

Due to the relative small-scale availability of GA, its current applications are limited to flavour and food additive.¹¹¹ However, assuming a larger production coming from a future bio-refinery approach, a wide spectrum of compounds can be envisaged (Scheme 8). As already mentioned, ethylene glycol can be readily obtained by GA hydrogenation using different homogeneous or heterogeneous catalysts. Ethylene glycol is produced in a million metric ton scale and widely employed as a refrigerant liquid, monomer, anti-freezing agents and production of fine chemicals.¹¹² GA oxidation yields glycolic acid or glyoxal, respectively. The former is used in the production of bio-degradable polyesters, usually by ring-opening polymerization of the cyclic dimeric lactone. These materials have several applications in medicinal products.¹¹³ The latter is used in pharmaceuticals and as wood and leather tanning agent.^{114, 115} Reductive amination of GA finds application in the synthesis of monoethanolamine, used as monomer and in the preparation of detergents, emulsifiers, and other fine chemicals. Other alkanol- and diamines have been made from GA, such as dimethylethanolamine and tetramethylethylenediamine.¹¹⁶ During GA synthesis from sugars, different retro-aldol condensations take place. Some interesting side products have also been isolated, and they were shown to be obtainable in good yield also starting directly from GA. For example, methyl-4-methoxy-2-hydroxybutanoate (MMHB) and methyl vinyl glycolate (MVG) can be further converted into specialty *poly*-(α -hydroxyacids), that are promising bio-degradable replacements for engineering plastics.^{45, 117-119} The use of MVG as new platform chemical will be further discussed in the next session.



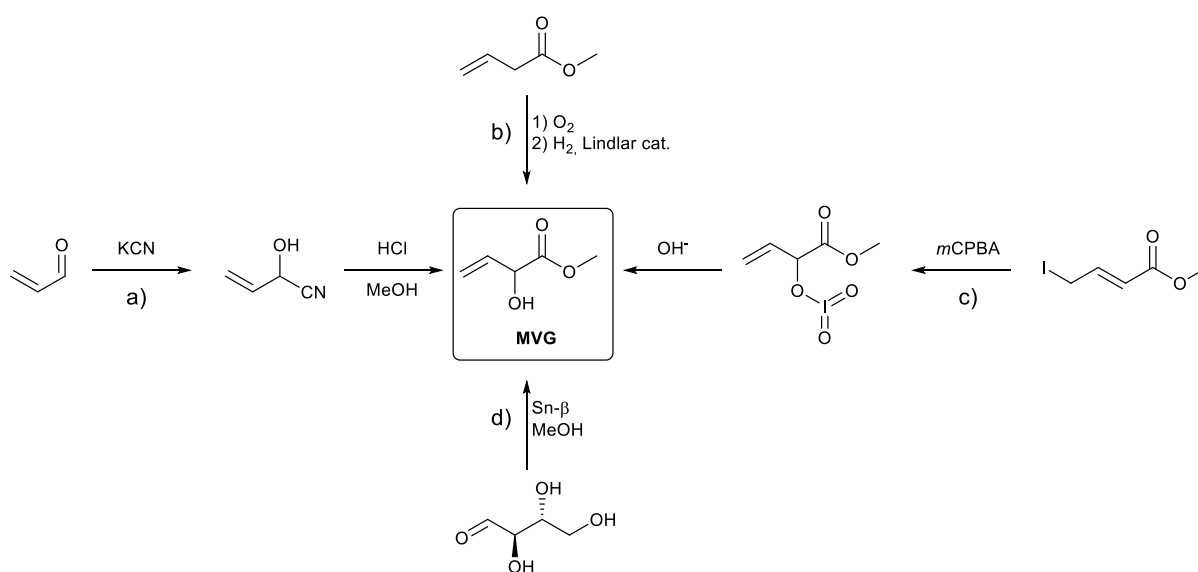
Scheme 8. Example of products that can be obtained from GA.

This work presents the use of glycolaldehyde as C1 building block for the selective synthesis of secondary formamides. The results will be discussed in Paragraph 3.3.

2.3 Methyl vinyl glycolate

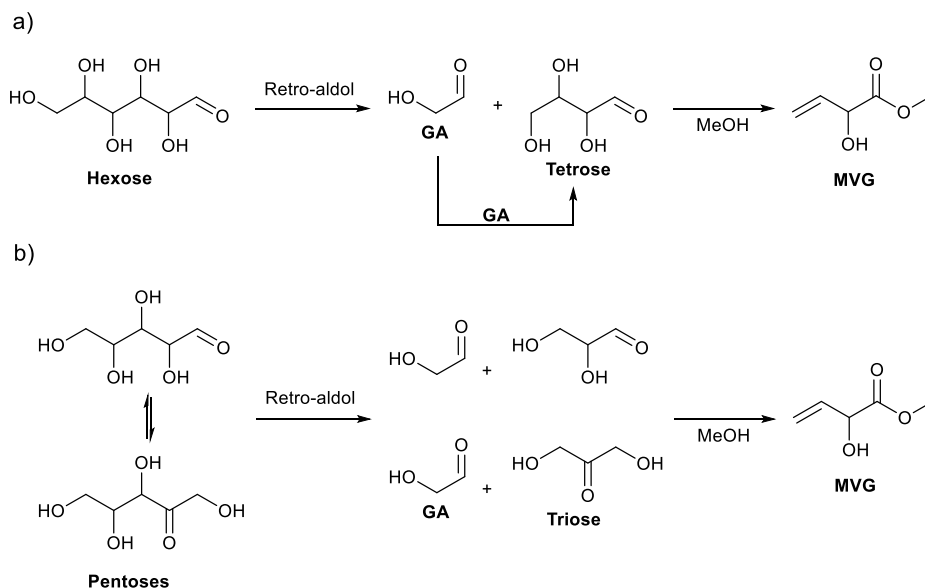
2.3.1 Synthesis of methyl vinyl glycolate

Methyl vinyl glycolate (2-hydroxybut-3-enoate, MVG), was synthesised for the first time by Rambaud in the 1930s by nucleophilic substitution of cyanide on acrolein, followed by acid methanolysis of the obtained cyanohydrine (Scheme 9a).¹²⁰ Rieche and co-workers prepared MVG by shaking vinylacetic acid in the presence of oxygen at 65 °C, hydrogenating then the intermediate α -peroxide on Lindlar catalyst (Scheme 9b).¹²¹ Yamamoto reported the oxidation of allyl iodides and following rearrangement and hydrolysis, achieving MVG in 67% yield (Scheme 9c).¹²² What brought MVG to be a potential platform chemical was initiated by the group of Taarning in 2010, namely the conversion of sugars over a tin- β zeolite to methyl lactate (ML). The selectivity can be directed towards MVG by using erythrose as substrate in methanol at 160 °C, that gave 56% yield (Scheme 9d).⁴⁵



Scheme 9. Reported synthesis of MVG.

After this first report, several other studies focused on understanding the mechanism of the sugar conversion to lactate and MVG using different sugars as feed. The same group showed that many C5 and C6 sugars can be efficiently converted to methyl lactate under the same experimental conditions, affording MVG as by-product up to 11%.¹²³ Interestingly, when glycolaldehyde was used as substrate MVG's yield increased to 30%. This behaviour can be explained by looking into the possible mechanisms involved (Scheme 10).



Scheme 10. Mechanism of the conversion of hexoses (a) and pentoses (b) to MVG.

Retro-aldol condensation of (aldo)hexoses affords one equivalent of glycolaldehyde and one of tetrose sugar (Scheme 10a), whereas starting from pentoses one equivalent of glycolaldehyde and one of triose sugar are obtained (Scheme 10b). Two molecules of GA can also undergo aldol condensation to form another equivalent of tetrose. This latter, in the presence of methanol and under acidic conditions, can dehydrate to form MVG. The proposed mechanism is consistent with the higher yields of MVG from C4 sugars and from GA that were reported. The group of Sels has shown that homogeneous Tin(II and IV) chlorides can also catalyse the reaction, although the highest yield of MVG observed was only 7%.¹²⁴ The same group also investigated dealuminated tin- β , that can convert erythrulose to up to 50% MVG in methanol at 90 °C for 20 hours.¹²⁵ Glucose was also attempted as feed, affording 18% of MVG in the presence of potassium carbonate.¹²⁶ The tin- β catalyst can be further optimized to convert glucose to MVG in more than 20% yield.¹²⁷ A few years later, they showed that even cellulose can be used as feed: using metal triflates and ball-milled cellulose, MVG was obtained together with other α -hydroxyesters, but the high temperature required (200 °C) decreased the selectivity by promoting other reaction pathways.¹²⁸ Table 4 contains a summary of all the mentioned methods to convert sugars to MVG. At the moment, there are no commercial producers of MVG from renewables. However, the Danish company Haldor Topsoe recently launched, in collaboration with Braskem, a new process for producing ethylene glycol from biomass by a 2-step catalytic cracking of sugars, having MVG and glycolic acid as side products.^{129, 130} The process is currently in the demonstration phase, aiming at a commercial plant by the year 2025. This may lead to a larger availability of MVG in the upcoming years, thus its use as platform chemical was one of the aims of this thesis.

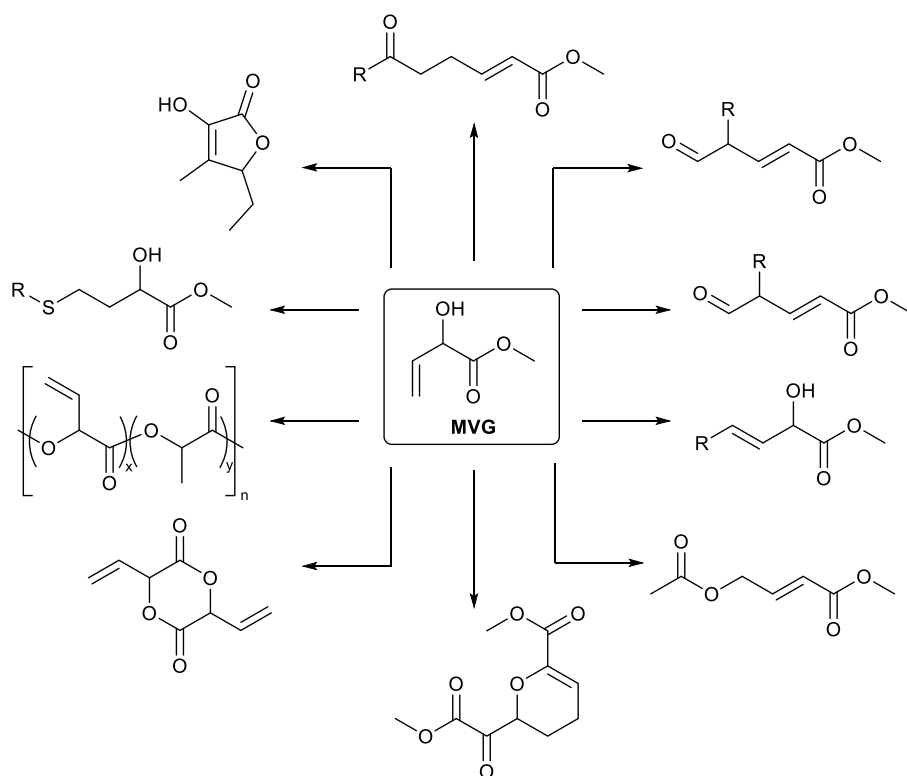
Table 4. Overview of methods for the conversion of sugars to MVG using methanol as solvent.

Entry	Feed	Catalyst	Representative conditions	MVG yield [%]	Ref.
1	Glycolaldehyde	Sn- β	140 °C, 16 h	30	123
2	Xylose	Sn- β	140 °C, 16 h	9	123
3	Glucose	Sn- β	160 °C, 16 h	10	123
4	Glucose-xylose (1:1)	Sn- β	140 °C, 16 h	9	123
5	Xylose-GA (1:1)	Sn- β	140 °C, 16 h	20	123
6	Pseudo-hemicellulose ^[a]	Sn- β	160 °C, 16 h	5	123
7	Erythrose	Sn- β	160 °C, 16 h	56	45
8	Glycolaldehyde	SnCl ₄ *5H ₂ O	90 °C, 20 h	7	124
9	Erythrulose	Dealuminated Sn- β	120 °C, 5 h	24	125
10	Glucose	Post-synthetic Sn- β	160 °C, 6 h, K ₂ CO ₃ (0.3 M)	18-20	126, 127
11	Cellulose	Sn(OTf) ₂	200 °C, 2 h	6	128

^[a]Equimolar mixture of monosaccharides.

2.3.2 Synthetic applications of methyl vinyl glycolate

MVG contains three reactive groups (carbon-carbon double bond, hydroxy group and ester) that can be envisaged for further functionalizations. Nevertheless, its uses in synthetic chemistry are so far rather limited (Scheme 11). Maple furanone, an important food additive, can be prepared by MVG isomerization followed by enolization and cyclization.¹³¹ Thiol-ene reaction of the double bond of MVG, *i.d.* the addition of a thiol catalysed by radical initiators such as Azobisisobutyronitrile (AIBN) has been reported.¹³² The hydroxy group of MVG can be reacted with aldehydes to form hemiacetals; this latter dehydrates to vinyl ethers, that undergo Claisen rearrangement ([3,3]-sigmatropic) to 6-oxohex-2-enoates.¹³³ Analogously to the cyclic dimer of other α -hydroxy acids such as lactic and glycolic acid, also hydrolysed MVG can cyclize in the presence of acidic catalysts, although in lower yields when compared to similar compounds.¹¹⁸ This cyclic dilactone could have a big potential as co-monomer to novel polyesters that bear pending C=C groups, useful for post-polymerization reactions such as the above-mentioned thiol-ene reaction. MVG-containing polyesters have been prepared by copolymerization with lactic acid.¹²⁴ Olefin homo- and cross-metathesis using Grubbs catalyst was used to prepare either diesters or long-chain α -hydroxyesters, that can have similar uses as fatty acid methyl esters.¹¹⁹ Functionalized MVG bearing an acetyl group undergoes Pd-catalysed allylic transposition, forming the linear α,β -unsaturated isomer.¹³⁴ MVG can be oxidised to the corresponding α -ketoester. However, the product is unstable and hetero-Diels Alder immediately occurs affording a cyclic dimer.¹³⁵



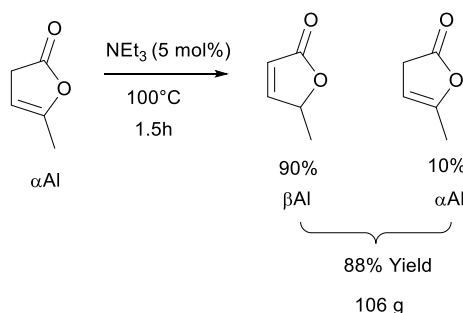
Scheme 11. Example of reactions involving MVG.

MVG's reactivity for the synthesis of new monomers and polymers *via* reaction with carbon monoxide will be treated in paragraph 3.4.

3. Aim and results of the dissertation

3.1 New polymers from a scalable β -Angelica lactone derived monomer

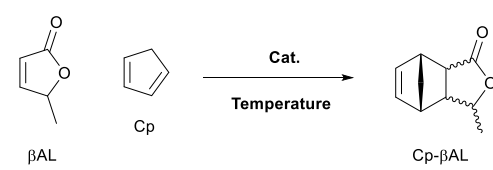
As mentioned in paragraph 2.1.3, α -AL dimerization goes through its α,β -unsaturated isomer.^{84, 136} We aimed to investigate the reactivity of the α,β -unsaturated bond in β -AL in order to introduce new (polymerizable) functional groups *via* Diels-Alder reaction. The reaction itself has recently gained attention in the field of green chemistry due to its discernible advantage in terms of atom economy as well as the typical experimental conditions, that employ cheap catalysts and neat conditions.¹³⁷⁻¹⁴⁰ While investigating the α to β isomerization step, which is reported using catalytic base in apolar solvents such as dichloromethane or toluene,⁷² we found out that the reaction can proceed under solvent free conditions without significant loss in yield (Scheme 12). A 90:10 β : α mixture was obtained in 1.5 h upon distillation under reduced pressure. We selected 90:10 as best compromise between purity and yield: higher purity (up to 99% β) could be obtained by carefully conducting the distillation step, but the yield would consequently be lowered. More extended reaction times lead to a drop in the yield, due to competing dimerization and oligomerization of AL. The reaction was successfully scaled up to 100 g scale.



Scheme 12. Isomerization of α AL to a 90% β -enriched mixture.

The reactivity of the mixture in the solvent-free Diels-Alder reaction was then investigated. Cyclopentadiene was chosen as diene for screening the reaction conditions (Table 5). Use of aluminum triflate as catalyst afforded a black char, with no product detected. Both catalyst-free conditions and use of anhydrous zinc chloride gave only moderate yields, so it was reasoned that the problem may be the competing di- and trimerization of the cyclopentadiene. Indeed, when a larger excess of diene was employed in the presence of the catalyst, the isolated yield was improved to 90%. Aiming at a sustainable process collides with the use of large excess of one reagent, so a semi-batch process was designed: 2 equivalents of diene were slowly added over 10 h to the solution of dienophile and catalyst. At this stage the separation and purification of the product was studied in detail. Distillation must be avoided, since retro-Diels-Alder could take place (from DSC the back-reaction starts at 136°C). Addition of acetone to the crude precipitated the catalyst, while washing with methanol could efficiently crash out the oligomeric species of the diene. The remaining 10% of α AL can be effectively removed by drying the material under vacuum. Eventually, 82% pure Diels-Alder adduct was obtained on a 50 g scale, with an *endo/exo* ratio of 10/90.

Table 5. Screening of the reaction conditions for the Diels-Alder reaction between β AL and cyclopentadiene.

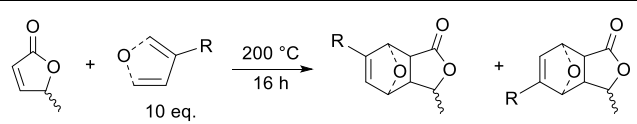


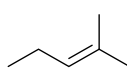
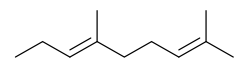
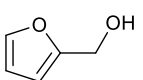
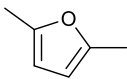
Entry	Catalyst	Eq. CPD	T [°C]	t [h]	Yield ^[a] [%]	Endo/Exo ^[a]
1	Al(Otf) ₃	3	RT	16	-	-
2	Al(Otf) ₃	3	100	2	-	-
3	-	3	80	0.5	19	91/9
4	-	3	100	0.5	40 ^b	70/30
5	-	3	60	0.5	25	95/5
6	ZnCl ₂	3	80	0.5	40	84/16
7	ZnCl ₂	3	RT	16	63	89/11
8	ZnCl ₂	10	RT	16	90 (86) ^[b]	90/10

General conditions: Reactions were carried out in closed reaction tubes and heated with microwave irradiation. ^[a]Determined by ¹H-NMR spectroscopy; ^[b]Isolated by column chromatography.

Other dienes from renewable resources were investigated under different reaction conditions (Table 6). The reaction was successful, although the yields were generally lower than in the previously discussed case, where terpenes were used at high temperature and catalyst-free conditions.

Table 6. Diels-Alder reaction between β AL and renewable dienes.



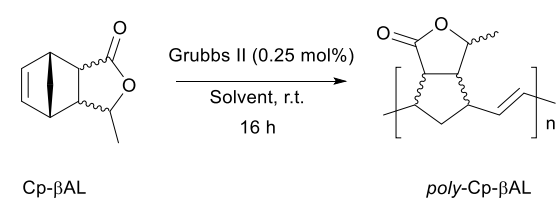
Entry	Diene	Yield ^[a] [%]
1	Isoprene (R = Me)	60
2	Myrcene (R = )	54
3	β -Farnesene (R = )	18
4	Furane 	0
5	Furfuryl alcohol 	0
6	2,5-dimethylfuran 	0

^[a]Isolated yields.

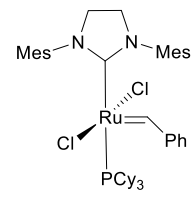
On the other hand, furans turned out more problematic. Several catalysts and conditions have been attempted, but the formation of humins (polymeric material formed by acid-catalysed reaction of furans) always prevailed.

The Cp- β -AL monomer was polymerised *via* ring-opening metathesis polymerization (ROMP) employing Grubbs' 2nd generation catalyst in dichloromethane.¹⁴¹⁻¹⁴³ The other Diels-Alder adducts shown in table 6 did not react under the same conditions, due to lack of the ring strain that thermodynamically drives ROMP towards the product. Cp- β -AL turned out to be extremely reactive in ROMP, indicated by the almost instantaneous gel formation after the addition of the monomer to the solution with the catalyst. DCM is on the "blacklist" of toxic and non-green solvents.¹⁴⁴ Consequently, we investigated the use of greener alternatives (Table 7). 2-Me-THF has similar polarity as DCM, but low toxicity and it is renewable.¹⁴⁵ Ethyl acetate and MIBK are among the safest solvents concerning both toxicity and flammability.^{146, 147} MTBE, in spite of growing environmental concern, has a lower tendency to build up peroxides compared to the related diethyl ether and it is still widely employed on industrial scale. In each solvent but DCM a precipitate immediately formed upon monomer addition, suggesting poorer solubility of the growing chain, which leads to its precipitation once a certain molecular weight is reached. Nevertheless, polymerization always occurred. The living character of the polymerization can be assessed by comparing the experimental molecular weights with the predicted one. DCM and to 2-Me-THF afforded higher values than calculated (by dividing the molecular weight of the monomer per the catalyst loading; table 7, entry 1), likely due to the higher solubility of high-MW chains in these solvents. Ethyl acetate performed the best, which together with considerations about its greenness and safeness makes it the best choice.

Table 7. Influence of different solvents in the ROMP of Cp- β -AL.



Cp- β -AL $\xrightarrow[\text{Solvent, r.t.}]{\text{Grubbs II (0.25 mol\%)}, 16 \text{ h}}$ poly-Cp- β -AL



Grubbs II

Entry	Solvent	Yield ^[a] [%]	M_n ^[b] [kg/mol]	M_w ^[b] [kg/mol]	\mathcal{D} ^[b]
-	Calc.	-	65.9	-	-
1	DCM	78	122	264	2.17
2	2-MeTHF	69	80.6	154	1.91
3	EtOAc	61	64.1	118	1.85
4	MIBK	52	70.9	1.46	2.06
5	MTBE	70	67.8	138	2.04

^[a]Isolated yield; ^[b]Determined by GPC (DMF/LiBr).

The linearity between the substrate-to-catalyst ratio and molecular weight was shown by performing the reaction at different loading of [Ru] (Figure 5). Substantial linearity was found in the range between 100:1 and 600:1 (mol_{subst}/mol_{cat}), thus indicating the possibility to tune the outcome of the reaction.

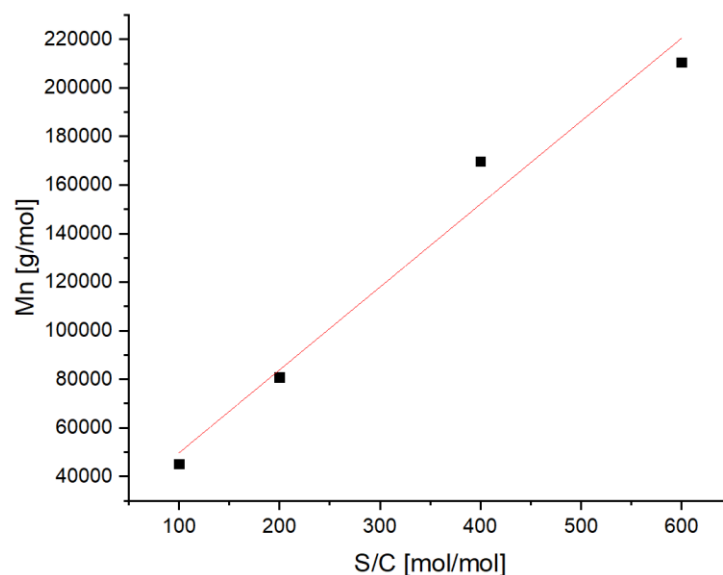


Figure 5. Obtained M_n values via ROMP of Cp- β AL performed at different substrate to catalyst ratios (S/C).

The DSC trace of the polymer is shown in Figure 6. The amorphous nature of the polymer is shown by the absence of melting points. The material has a rather high decomposition onset (378 °C). Remarkably, no T_g could be detected: the transition has to occur at or above the decomposition temperature. This latter property drastically deviates from known poly-norbornenes, showing a T_g at 35 °C.¹⁴⁸ A possible explanation from this behavior is the high stereoregular nature of the material: all the double bonds of the polymer are in *trans* configuration, which might favour a better packing of the chains thus increasing significantly the T_g .

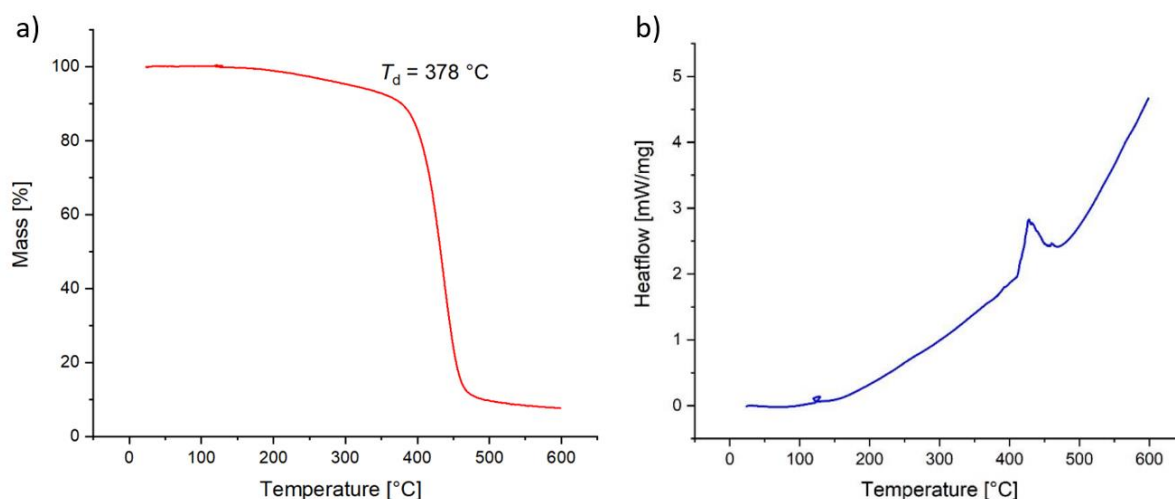


Figure 6. TGA (a) and DSC (b) of *poly*-Cp- β AL.

The polymer can be easily cast into films, whose physical and optical properties were investigated and compared to analogous *poly*-norbornene prepared by the same method (Grubbs' 2nd gen. catalyst in DCM). Contact angle measurements (Figure 7) showed that *poly*-Cp- β AL has increased hydrophilicity in comparison to *poly*-norbornene, due to the presence of the lactone moiety. The transparency of the films does not differ, as can be seen by the UV-Visible absorbance spectrum.

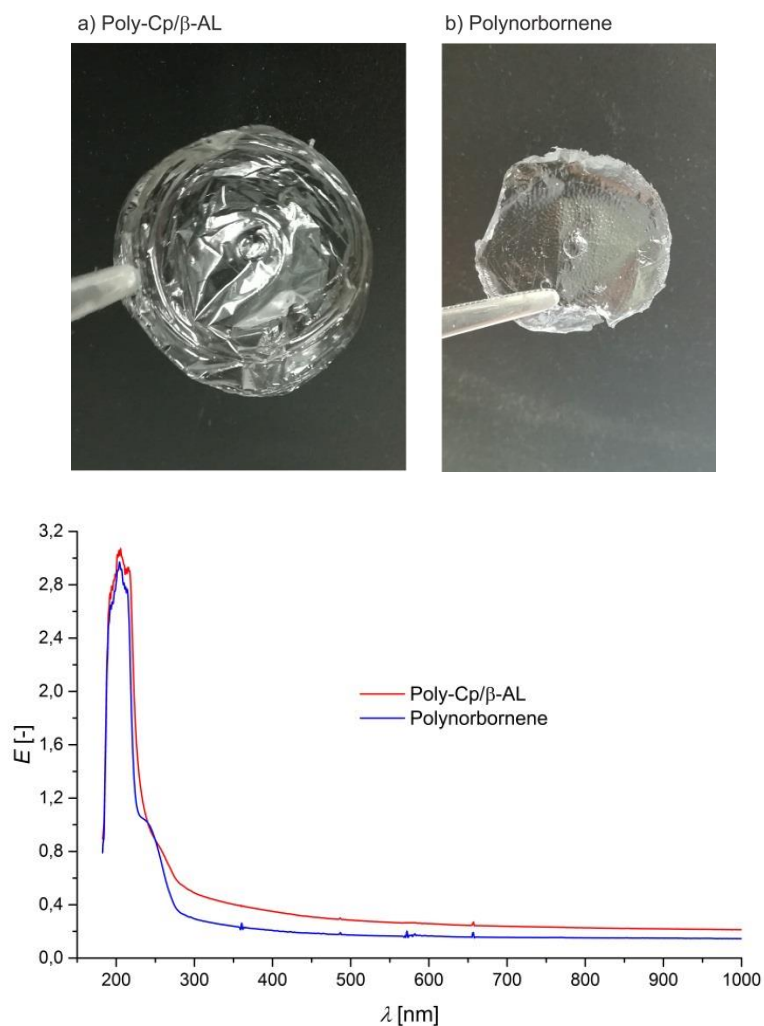


Figure 7. Films obtained from a) poly-Cp/ β AL and b) polynorbornene obtained by solution castings. Below: absorbance spectra of these films in the range from 150-1000 nm. E=Extinction.

In light of these properties, the new material could be potentially employed where high transparency is desired,¹⁴⁹ such as optical fibers,¹⁵⁰ and transparent coatings.¹⁵¹

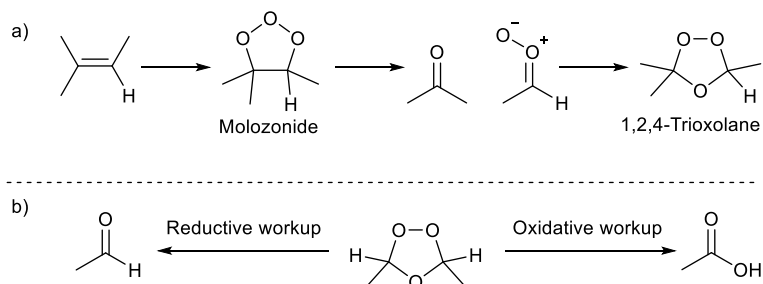
In summary, an atom economic and efficient α to β AL isomerization protocol was developed. The Diels-Alder reaction with several dienes and β AL was then used to prepare new monomers for ROMP. A bio-based, functionalized *poly*-norbornene was prepared and fully characterized, showing interesting properties such as high transparency.

The publication concerning this work can be found in section 6.1.

3.2 Production of malonates and 3-oxopropanoates via ozonolysis of α -angelica lactone

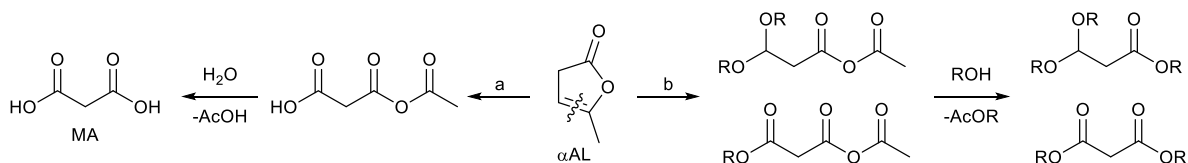
Malonic acid (MA) and its esters are important building blocks for the synthesis of fine chemicals such as fragrances, fertilizers and drugs, with an estimated annual market of 20.000 t.¹⁵² Industrially, MA is mainly produced from the petrochemical chloroacetic acid via cyanation followed by hydrolysis. This route employs toxic reagents, and an overstoichiometric amount of salt is produced as side product (2 equivalents: the cyanide is also hydrolysed, leading to an extra equivalent of ammonium salt). An alternative synthesis based on alkoxycarbonylation of chloroacetic acid has been proposed but has never gotten to industrial implementation. A fermentative route is also known, but it requires high dilution and two equivalents of salt are also produced.^{153, 154} Finally, catalytic oxidation of fermentative 3-oxopropionic acid has been reported but never scaled.¹⁵⁵

We envisioned that MA and other analogous derivatives could be produced upon oxidative cleavage of the carbon-carbon double bond of α AL. Ozonolysis is a cheap, easy to scale and 100% atom economic reaction, that typically proceeds under mild conditions and affords high yields. It has been used from small to industrial scale for the production of a number of aldehydes, ketones and carboxylic acids.¹⁵⁶⁻¹⁵⁸ Unsaturated fatty acids have been cleaved by ozonolysis, e.g. for the production of pelargonic acid and azelaic acid from oleic acid.^{159, 160} Lignin can be effectively depolymerised by ozone, as shown by Heeres and co-workers.¹⁶¹ The mechanism of the reaction has been thoroughly studied for decades (Scheme 13).^{157, 158} According to the experimental conditions, different products can be obtained. If the workup of the unstable 1,2,4-trioxolane intermediate is done under reductive conditions (e.g. with dimethylsulfide, triphenylphosphine, Zn), an aldehyde or its acetal is obtained in case of non-tetrasubstituted double bonds. If, on the other hand, oxidants as hydrogen peroxide or organic peroxides are employed, the product is a carboxylic acid.



Scheme 13. a) Mechanism of ozonolysis; b) products obtained by reductive or oxidative workups.

Therefore, the ozonolysis of α -AL would either produce oxidized products such as MA and its esters, or reduced products such as 3-oxopropanoates (Scheme 14). The latter are valuable intermediates for the synthesis of 3-hydroxypropionic acid, starting material for the synthesis of bio-based acrylonitrile and acrylic acid.^{60, 162, 163}



Scheme 14. Synthesis of malonates and oxo-propanoates by ozonolysis of α AL. a) Ozonolysis in aprotic media; b) ozonolysis in protic media (R=H, alkyl).

Initial attempts were performed at -78 °C and focused on non-participating solvents (Table 8). The use of DCM and aqueous hydrogen peroxide for the workup – although leading to full conversion of α AL – led to problems in extracting MA from the water phase due to the high polarity of the latter. Switching to ethyl acetate afforded up to 90% pure MA after evaporation of the solvent and removal under high vacuum of the stoichiometric co-product acetic acid. Kula showed that the safest temperature range of ozonolysis in batch conditions spans between -20 and +10 °C.¹⁶⁴ The reaction was attempted at 0 °C, showing no significant change in the yield. Efforts on obtaining the corresponding aldehyde, 3-oxopropanoic acid, were less successful. Quenching with dimethyl sulfide, even at low temperature, always led to decomposition. This may be due to the poor stability of the aldehyde under acidic conditions. Sodium borohydride was then tried, aiming at reducing the aldehyde to 3-hydroxypropanoic acid *in situ*. However, no product could be detected.

Table 8. Ozonolysis of α AL in non-participating solvents.

CC1=CC(=O)OC1 $\xrightarrow[2) \text{ Quenching agent, r.t., 20 h}]{1) \text{ O}_3, \text{ solvent, temperature}}$ OC(=O)CC(=O)O
 α AL MA

Entry ^[a]	Solvent	Temperature (°C)	Work-up	Product	MA (%)
1	DCM	-78	H ₂ O ₂ / H ₂ O	MA	89
2	EA	-78	H ₂ O ₂ / H ₂ O	MA	90
3	EA	0	H ₂ O ₂ / H ₂ O	MA	90
4	DCM	-78	Me ₂ S	-	-
5	EA	-78	Me ₂ S	-	-
6	EA	0	Me ₂ S	-	-
7	EA	0	NaBH ₄	-	-
8 ^[b]	EA	0	H ₂ O ₂ / H ₂ O	MA	86

^[a]Reaction conditions: α -AL 25.5 mmol, 2 mL*min⁻¹ O₃ bubbled through the solution; reaction times 30 – 60 min (titration with KI); quenched with 10 eq of quenching agent. ^[b]Reaction performed on 25 g scale.

The problem of poor stability of the aldehyde was addressed by switching to a nucleophilic solvent, i.e. methanol (Table 9). Reductive quenching with dimethylsulfide at -78 °C afforded 43% of the corresponding acetal, with some traces of aldehyde detected by ¹H-NMR: stability of the aldehyde itself seems to improve in participating solvents. Higher temperature afforded the acetal only in 46% isolated yield. Ethanol can also be used, although with lower yield. The co-produced methyl or ethyl acetate, that can be easily separated by distillation, are also valuable chemicals, typically employed as solvents and bulk chemicals. Oxidative workup was attempted as well, aiming at esters of MA. The monoester of MA was obtained at 0 °C using hydrogen peroxide as quenching agent.

In light of the better stability of the aldehyde in nucleophilic solvents, water was investigated. To our surprise, reductive quenching afforded solely the oxidized product, MA. After optimizing the conditions, 5% water in acetonitrile was found to give the best result, comparable to what was obtained in non-participating solvents. Higher water content led to partial hydrolysis of the lactone prior to cleavage of the double bond (levulinic acid was detected by GC-MS of the crude mixture).

Table 9. Ozonolysis of α -AL in participating solvents.

Entry ^[a]	Solvent	Temperature (°C)	Work-up	Product		Yield (%)
				Structure	Yield (%)	
				<chem>RO-C(=O)-CH2-CH2-C(=O)-OR</chem> R = H: MA R = Me: MM	<chem>HO-C(=O)-CH2-CH2-C(=O)-OR</chem> mMM	<chem>RO-C(OR)(R)-CH2-CH2-C(=O)-OR</chem> R = Me: MOP-Acetal R = Et: EOP-Acetal
1	MeOH	-78	Me ₂ S	MOP-acetal	43	
2	MeOH	0	Me ₂ S	MOP-acetal	46	
3	MeOH	0	H ₂ O ₂ / H ₂ O	mMM	52	
4	EtOH	0	Me ₂ S	EOP-acetal	21	
5	H ₂ O	0	NaHSO ₃	MA	67	
6	H ₂ O	0	Me ₂ S	MA	77	
7	EA + 10% H ₂ O	0	NaHSO ₃	MA	63	
8	ACN + 5% H ₂ O	0	NaHSO ₃	MA	91	

^[a] Reaction conditions: α -AL 25.5 mmol, 2 mL*min⁻¹ O₃ bubbled through the solution; reaction times 30 – 60 min (titration with KI); quenched with 10 eq. of quenching agent.

To gain a better insight in this unexpected behaviour, the reaction was performed in deuterated water and a ¹³C-NMR recorded on the reaction crude before quenching (Figure 8a).

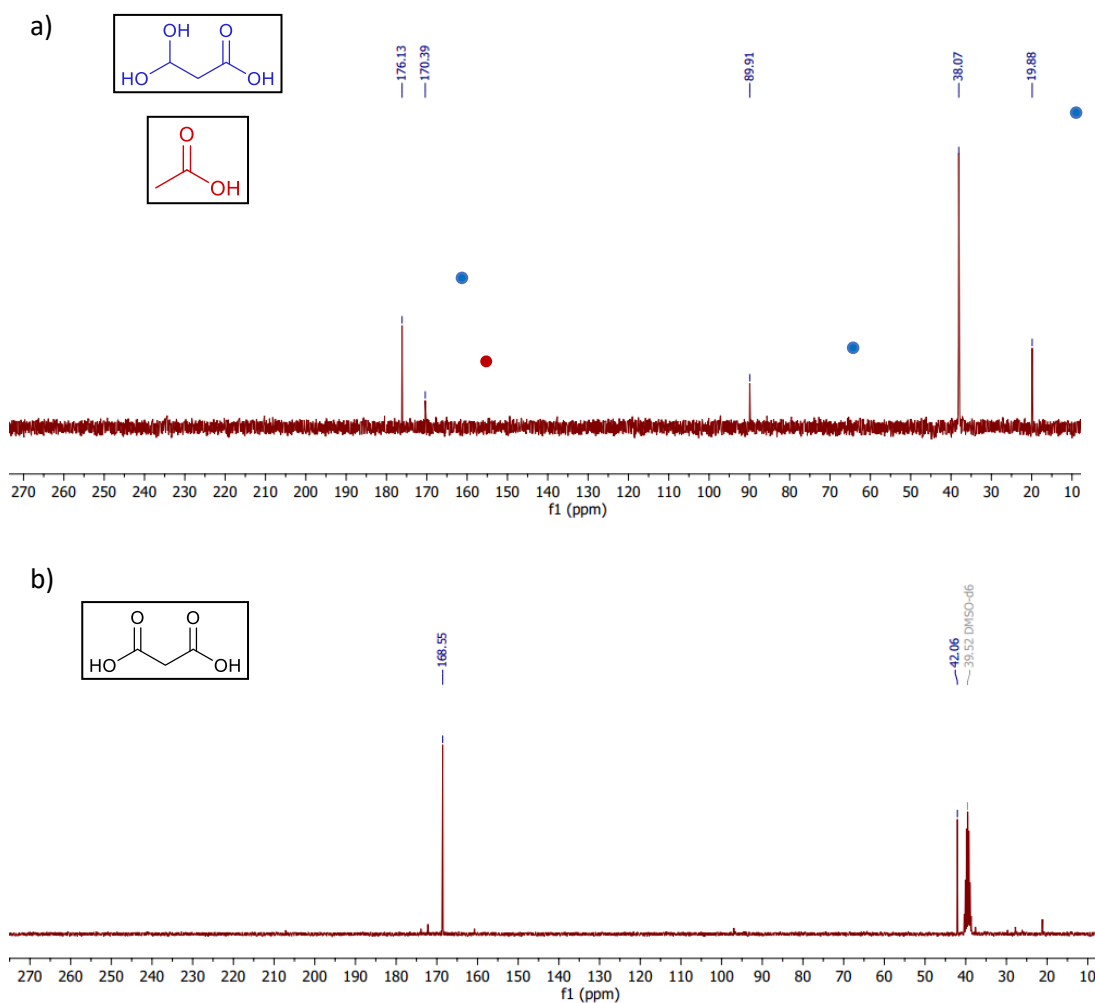
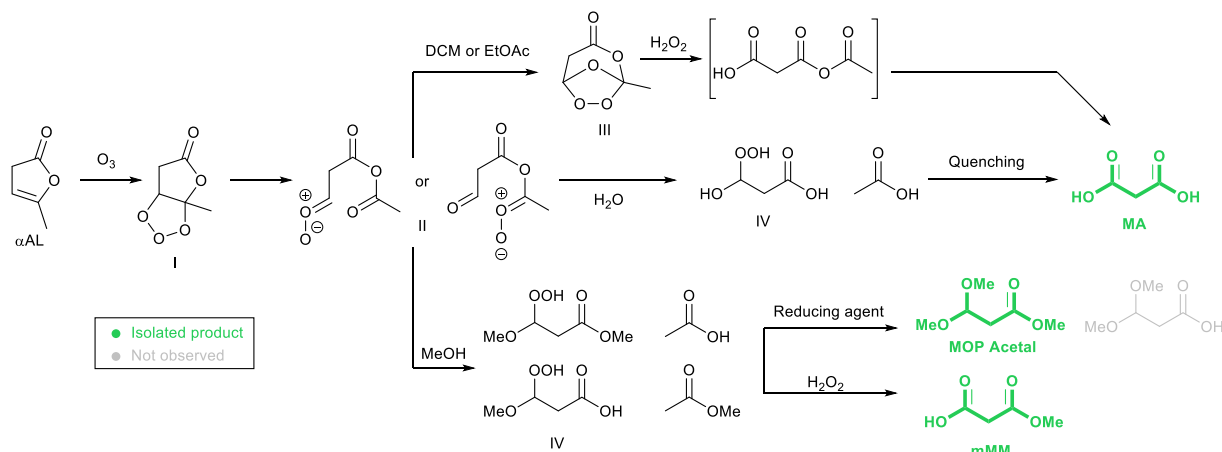


Figure 8. ¹³C-NMR of the ozonolysis of α AL in water: a) before quenching; b) after quenching with Me₂S and solvent removal.

The spectrum shows signals compatible to the co-presence of the hydrated aldehyde (e.g. 89.9 ppm) and acetic acid: this suggests that the oxidation likely occurs during the workup phase, the aldehyde being too unstable towards oxidation to be isolated. A mechanism which is in accord to what is observed experimentally and to the known literature was proposed (Scheme 15). The first step involves the [3+2] cycloaddition of ozone to the double bond, forming the molozonide (I). The latter breaks down in one of the possible carbonyl oxides (II). In the absence of nucleophiles, a highly energetic trioxolane (III) is formed, whose cleavage affords the monoacetic anhydride of MA, eventually formed upon hydrolysis. Different is the case in the presence of a nucleophilic solvent: the carbonyl oxide reacts forming hydroperoxides (IV), that are quenched by a reducing agent to afford the corresponding acetal or oxidized to a dicarboxylic species.



Scheme 15. Proposed mechanism for the ozonolysis of α AL.

To sum up, ozonolysis of the platform chemical-derived α -angelica lactone was established as an efficient alternative method to produce malonic acid and other potentially useful C3 derivatives. Different products can be obtained by simply tuning the reaction conditions such as solvents or quenching agent.

The publication concerning this work can be found in section 6.2.

3.3 N-Formylation of amines using glycolaldehyde as C1 building block

N-Formamides are widely employed chemicals, with applications ranging from solvents (above all, DMF) to fragrances, from drugs to softening agents for polymers.^{165, 166} Common ways to access N-formamides involve the reaction of amines with the mixed anhydride of acetic acid and formic acid (which is made *in situ* from a mixture of formic acid and acetic anhydride), trichloroacetaldehyde (chloral) or carbon monoxide.¹⁶⁷ Carbon dioxide in combination with hydrogen has also been reported.¹⁶⁸⁻¹⁷¹ The last two synthetic methods, particularly the use of carbon monoxide, are well in agreement with the principles of green chemistry (good atom economy, only water as co-product, etc.).³¹ Nonetheless, the use of alternative, non-gaseous C1 building blocks, ideally directly derived from renewable resources, could be more practical on a laboratory scale. Glycerol, as well as some of its derivatives (dihydroxyacetone, glyceraldehyde and glycolic acid) have been shown to effectively perform the reaction in the presence of a copper catalyst and an oxidant.^{25, 172, 173} While attempting to prepare novel cleavable conjugated polymers, it was found by our group that glycolaldehyde (GA) reacts with secondary amines affording the N-formylated product. This serendipitous finding prompted us to investigate the use of GA as potential C1 building block. It can be readily obtained from

renewable resources, for example from biomass pyrolysis oil or by cracking glucose (as described in the introduction); moreover, its toxicity is low.¹⁷⁴ The reaction of GA with amines under reductive conditions has already been reported, for example by the groups of Zheng and Sels, as a method to prepare alkanolamines and diamines (Figure 9).^{95, 175, 176}

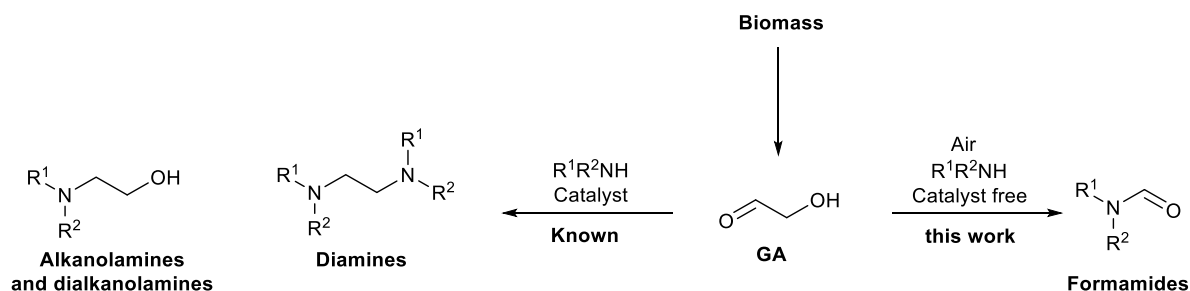


Figure 9. Reaction of GA with primary and secondary amines. Left: GA as C2 building block. Right: GA as C1 building block.

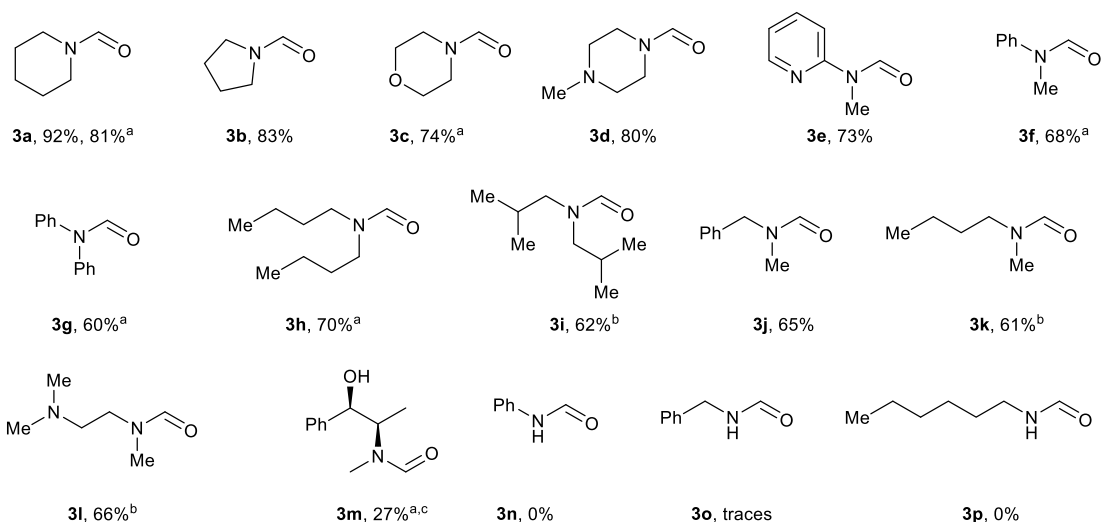
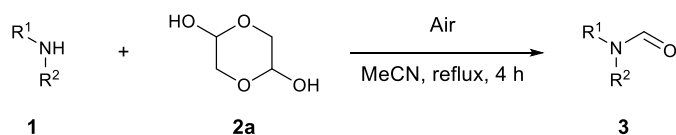
Table 10. Optimization of the reaction conditions.

The reaction scheme shows piperidine (1a) reacting with the dimer of glycolaldehyde (2a) in the presence of an additive (1 mol%) and a solvent, under reflux for 4 hours, to produce formamide (3a) and a secondary amide (4a).

Entry	Solvent	Additive	Conv./ %	3a/ %	4a/ %
1	THF	–	>99	64	31
2	CH ₂ Cl ₂	–	75	71	3
3	CHCl ₃	–	84	81	2
4	toluene	–	81	73	6
5	MeCN	–	99	92	5
6	acetone	–	81	75	5
7	MeCN	CuCl	72	55	7
8	MeCN	Pd(OAc) ₂	88	78	10
9 ^[a]	MeCN	–	97	92	3
10 ^[b]	MeCN	–	90	–	–
11 ^[c]	MeCN	–	99	91	4

Reaction conditions: **1a** (2.0 mmol), **2a** (0.5 mmol), solvent (5 mL), reflux, 4 h. Yields were determined by GC using mesitylene as the internal standard. ^[a]Using O₂ balloon with Schlenk flask. ^[b]Under argon. ^[c]Reaction was run in the dark.

Piperidine **1a** was used in the preliminary screenings, as shown in Table 10. GA is typically sold as its dimer **2a**, which in solution is in equilibrium with the free monomer. The reaction was run under air in refluxing solvent. Acetonitrile was found to perform best among different solvents. Interestingly, the use of known oxidation metal catalysts decreased the yield of formamide **3a**. The presence of oxygen is crucial: inert atmosphere did not afford the formamide. On the other hand, the use of pure oxygen did not improve the yield further. The absence of light did not seem to have any effect. With the optimized conditions in hands, different secondary amines were investigated (Scheme 16).



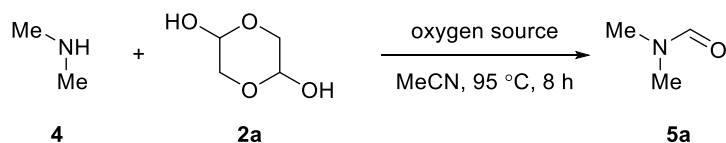
Reaction conditions: **1** (2.0 mmol), **2a** (0.5 mmol), MeCN (5.0 mL), reflux, 4 h. Yields were determined by GC using mesitylene as the internal standard. ^[a]Isolated yields are given. ^[b]**1** (1.0 mmol), **2a** (0.5 mmol), 12 h. ^[c]16 h, O₂ (1 atm).

Scheme 16. Scope of *N*-formylation of secondary amines with GA.

The reaction afforded good to high yields with cyclic and acyclic aliphatic amines, as well as aromatic ones. The good reactivity observed with acyclic amines is particularly remarkable, since acyclic secondary amines are generally less reactive under standard formylation conditions, for example due to competing metal-catalysed transalkylation to primary and tertiary amines.^{177, 178} On the other hand, primary amines did not work at all, which makes the method selective to secondary amine groups only.

N-Dimethylformamide (DMF, **5a**) is probably the most used *N*-formamide, due to its outstanding properties as polar aprotic solvent.^{179, 180} Formylation of dimethylamine **4** was thus investigated as an alternative synthesis of DMF. Several commercial solutions of **4** were tested, yielding up to 24% when

Table 11. Formylation of dimethylamine to DMF.

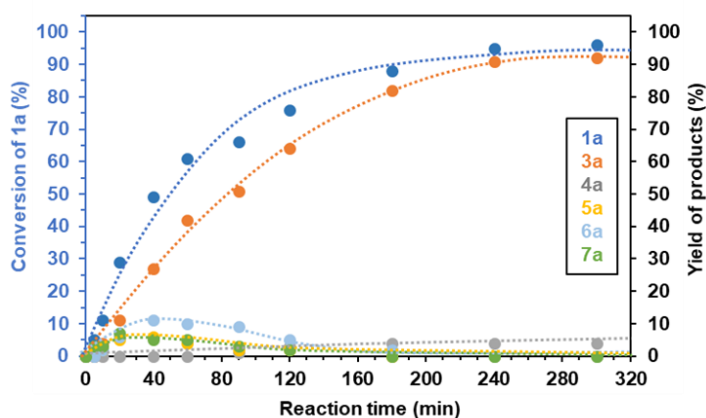
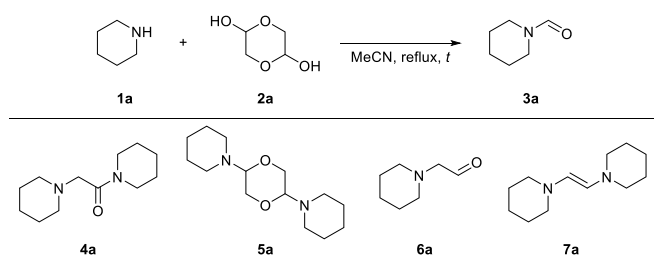


Entry	Dimethylamine solution 4	Oxygen source	5a / %
1	2.0 M in THF	O ₂ balloon	24
2	40 wt. % in H ₂ O	O ₂ balloon	0
3	2.0 M in methanol	O ₂ balloon	0
4	5.6 M in ethanol	O ₂ balloon	0
5	(CH ₃) ₂ NH · (CH ₃) ₂ NCOOH	O ₂ balloon	21
6	2.0 M in THF	air (10 bar) ^[a]	57
7	(CH ₃) ₂ NH · (CH ₃) ₂ NCOOH	air (10 bar) ^[a]	45

Reaction conditions: **1a** (1.0 mmol), **2a** (0.5 mmol), MeCN (5 mL), 95 °C, 8 h. Yields were determined by GC using mesitylene as the internal standard. ^a Autoclave instead of Schlenk flask.

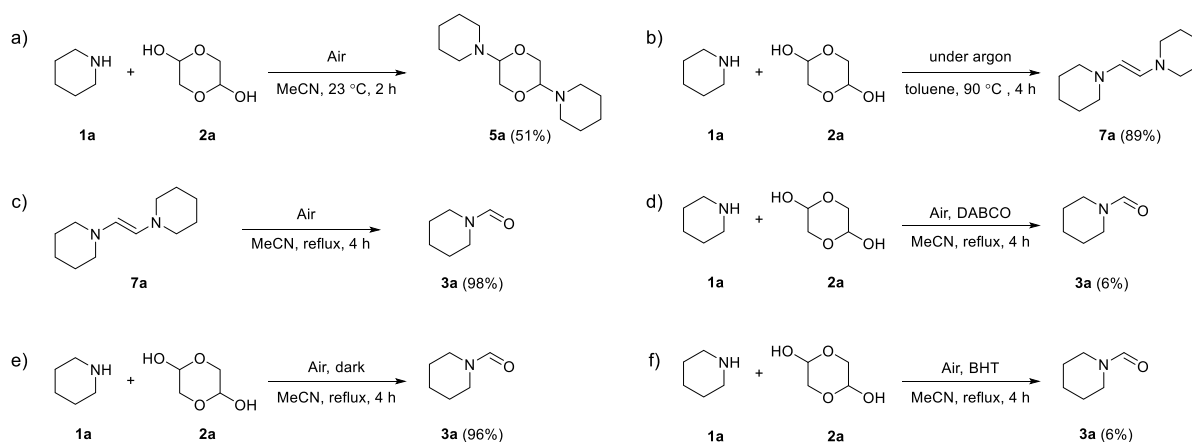
oxygen was used as oxidant at ambient pressure and THF as solvent. Dimethylammonium dimethyl carbamate, typically employed as starting material in DMF synthesis,¹⁷⁰ did not improve the results. Eventually, compress air at higher pressure turned out to be the best performing system, and DMF was obtained in up to 57% yield.

The reaction between **1a** and **2a**, including the formation of intermediate species, was monitored over time (Scheme 17). The desired product started forming almost immediately. Amide **4a**, on the other hand, only appeared after 90 minutes, thus suggesting that this may be a byproduct rather than an intermediate.



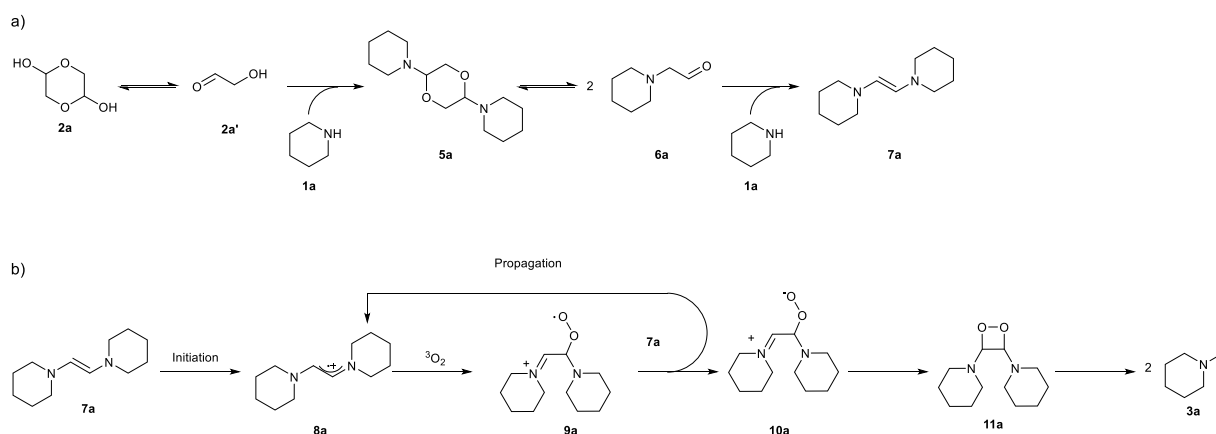
Scheme 17. Time - conversion profile of the reaction between **1a** and **2a**.

Three other species were detected at the initial stage, but were gradually being consumed over time: amination **5a**, C2-addition product **6a** and dienamine **7a**. The role of these alleged intermediates was further investigated, and several control experiments were performed (Scheme 18).



Scheme 18. Mechanistic investigations and control experiments.

Intermediate **5a** was obtained as a crystalline solid and fully characterized by stirring **1a** and **2a** at room temperature. When left in solution (CDCl_3 , or even faster in C_6D_6), **5a** readily monomerizes to **6a**. Absence of air only afforded dienamine **7a**. When the latter was subjected to the standard reaction conditions, product **3a** was obtained in quantitative yield. This suggests that the oxygen atom of the product actually comes from air and not from the water that is produced upon condensation between the amine and GA. The oxidation step could potentially be performed by singlet oxygen ($^1\text{O}_2$), which might in theory be formed by light-driven excitation of triplet oxygen with the dienamine (or any reaction impurity) acting as photosensitizer. To verify this alternative, the reaction was performed in the presence of 1,4-diazabicyclo[2.2.2]octane (DABCO), a quencher for $^1\text{O}_2$.¹⁸¹ The reaction only produced traces of the product. To further exclude the role of light, the formylation was run in the dark. The yield of **3a** was almost quantitative. This points towards a radical oxidation by $^3\text{O}_2$. Indeed, the common radical inhibitor butylated hydroxytoluene (BHT) suppressed the reaction, and only traces of the product were obtained. With these control experiments in hand, a mechanism was proposed (Scheme 19a). Initially, GA (which exists in solution as equilibrium between dimer and monomer), forms aminal **5a** that monomerizes to **6a**. The latter reacts with a further equivalent of amine, yielding dienamine **7a**. At this stage, radical oxidation takes place (Scheme 19b). An iminium radical cation (**8a**) is formed by reaction of molecular oxygen with **7a**. Oxygen adds on the double bond, forming the peroxy-radical **9a**, that extracts a radical from **7a** generating a new iminium radical cation on one hand and the zwitterionic **10a** on the other. Such compounds have been shown to be unstable,¹⁸²⁻¹⁸⁴ converting immediately to the dioxetane ring **11a**. Oxetanes are known to easily decompose to formamides.¹⁵⁷ Thermal cleavage of **11a** eventually generates the product.



Scheme 19. Proposed mechanism for the *N*-formylation of **1a** with GA (a) and detailed radical oxidation path (b).

EPR was envisaged to bring further insight regarding the proposed radical mechanism. Indeed, a triplet of sextets ($g = 2.006$) was detected when **7a** and 5,5-dimethyl-1-pyrroline N-oxide (DMPO) as spin trap were measured under oxygen atmosphere. This indicates the formation of a nitrogen-centered radical, that is trapped by DMPO as DMPO- $\cdot\text{N}$ adduct (Figure 10).¹⁸⁵ A weaker, three-line signal (1:1:1, $g = 2.006$) was also detected, and it could be assigned to the aminoxyl radical deriving from a partial degradation of the spin trap. The same set of measurements under inert atmosphere gave no EPR signals at all, thus confirming the active role of oxygen in the reaction.

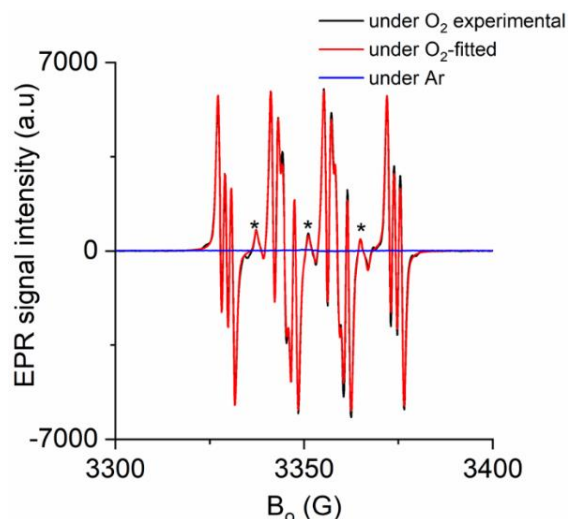


Figure 10. EPR spectra (at 20 °C) of **7a** in the presence of DMPO after keeping it 4h at 80 °C under a) Ar (blue-line); b) O₂ (black-line); c) Fitted spectrum of (b) using Bruker SpinFit package program (red line). *EPR signal of DMPOX due to the oxidation of DMPO.

Finally, ¹H NMR was used in order to detect some of the reaction intermediates. The focus was put on oxetane **11a**, that in spite of its known instability could possibly give a distinguishable transient signal for the protons in the 4-membered ring. Indeed, dissolving **7a** in CD₃CN and flushing the tube with oxygen, time-resolved ¹H NMR showed a small peak at 4.92 ppm that gradually disappeared while the formiate peak (7.92 ppm) increased (Figure 11). With this information in hand, the radical mechanism depicted in Scheme 19b was further supported.

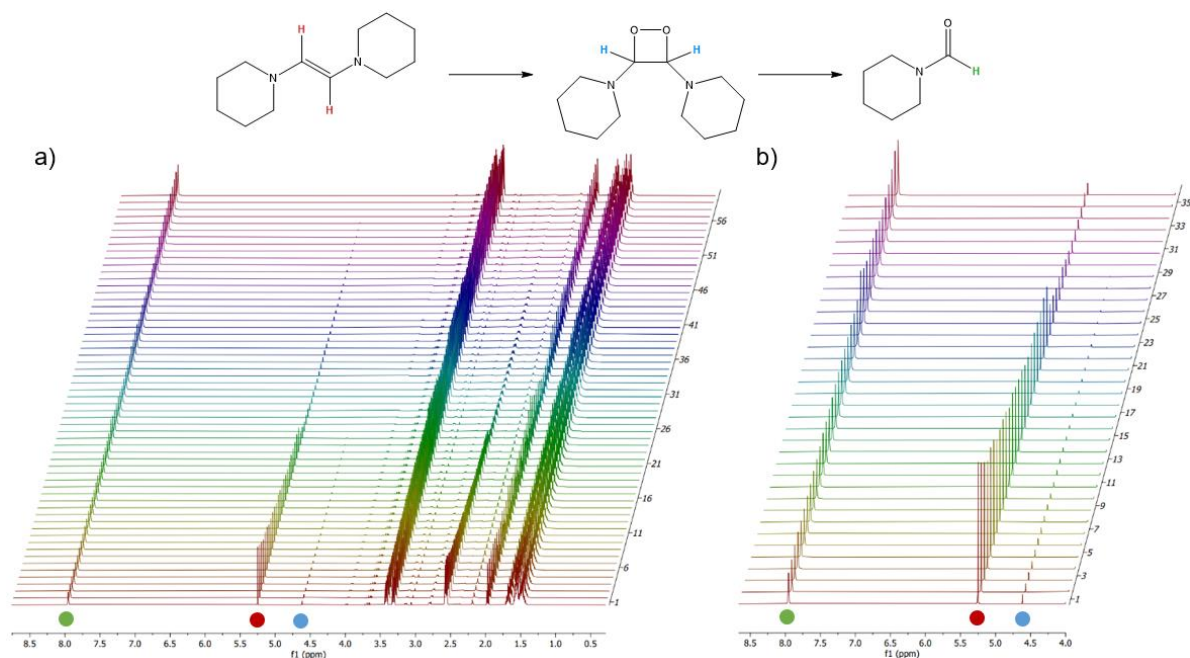


Figure 11. Reaction profile using ¹H NMR in CD₃CN (16 h, room temperature, 1 atm O₂): a) full spectrum; b) zoom between 4.0 and 8.5 ppm.

In conclusion, glycolaldehyde was applied for the first time as C1 building block for the synthesis of N-formamides. The reaction proceeds effectively under ambient air and is selective for secondary amines. Mechanistic studies suggested a radical oxidation path in which triplet oxygen acts as oxidant.

The publication concerning this work can be found in section 6.3.

3.4 Methyl vinyl glycolate as renewable difunctional monomer for novel polymers

Methyl vinyl glycolate (MVG) bears three different reactive groups that can be envisaged as handles for further functionalization to a variety of new molecules, as discussed in Section 2.3. Specifically, we aimed to functionalize the carbon-carbon double bond, in order to produce new valuable bifunctional monomers and from them novel polyesters. One of the biggest industrial processes that works under homogeneous catalysis is hydroformylation of olefins using syngas.^{186, 187} It involves the formal addition of carbon monoxide and hydrogen to double bonds, affording the C1-homologated aldehyde, typically using cobalt or rhodium catalysts. Syngas is produced in several ways, including steam reforming of hydrocarbon feedstocks, dry reforming of carbon dioxide, and from biomass, for example by (partial) oxidation.^{20, 188, 189} Hydroformylation of MVG using dicarbonyl(acetylacetonato)rhodium(I) was attempted in the presence of an excess (10:1 to the metal) of different phosphorus containing ligands, from simple triphenylphosphine (**L1**) to the more hindered Xantphos (**L2**) and Xantphenoxaphos (**L3**) to the bisphosphite **L4** (Figure 12).

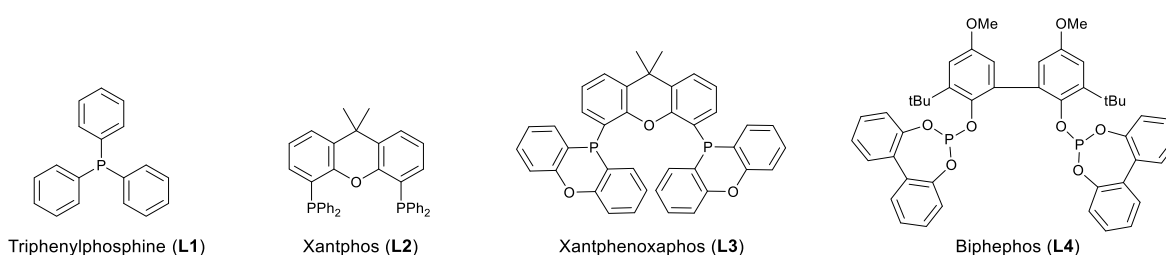


Figure 12. Ligands used for the hydroformylation of MVG

Use of 10 bar of syngas at 80 °C turned out to be effective to achieve full conversion of the starting material in most of the cases (Table 12). The CO can add to both sides of the carbon-carbon bond, affording in theory a linear (**12**) and a branched (**13**) isomer. On top of that, due to the presence of the hydroxyl group of MVG, cyclization to a stable 5-membered hydroxyacetal can occur. Within the shown screening, only the 5-membered acetal **14** originated from the linear isomer was detected. Figure 13 shows the ¹H-NMR of the crude reaction mixture from entry 1 and the assignment of the characteristic signals.

Table 12 Hydroformylation of MVG.

Entry	Ligand	Solvent	MVG Conversion [%] ^[a]	12 [%] ^[a]	13 [%] ^[a]	14 [%] ^[a]	L/B ^[b]
1	L1	Toluene	>99	6	39	55	61:39
2	L1	THF	>99	6	33	61	67:33
3	L2	Toluene	>99	10	3	87	97:3
4	L2	THF	>99	9	2	89	98:2
5	L3	Toluene	71	17	6	48	91:9
6	L4	Toluene	>99	11	5	84	95:5

^[a]NMR conversion; ^[b]Linear to branched ratio = [(conc.(1) + conc.(3)) / conc.(2)] * 100%.

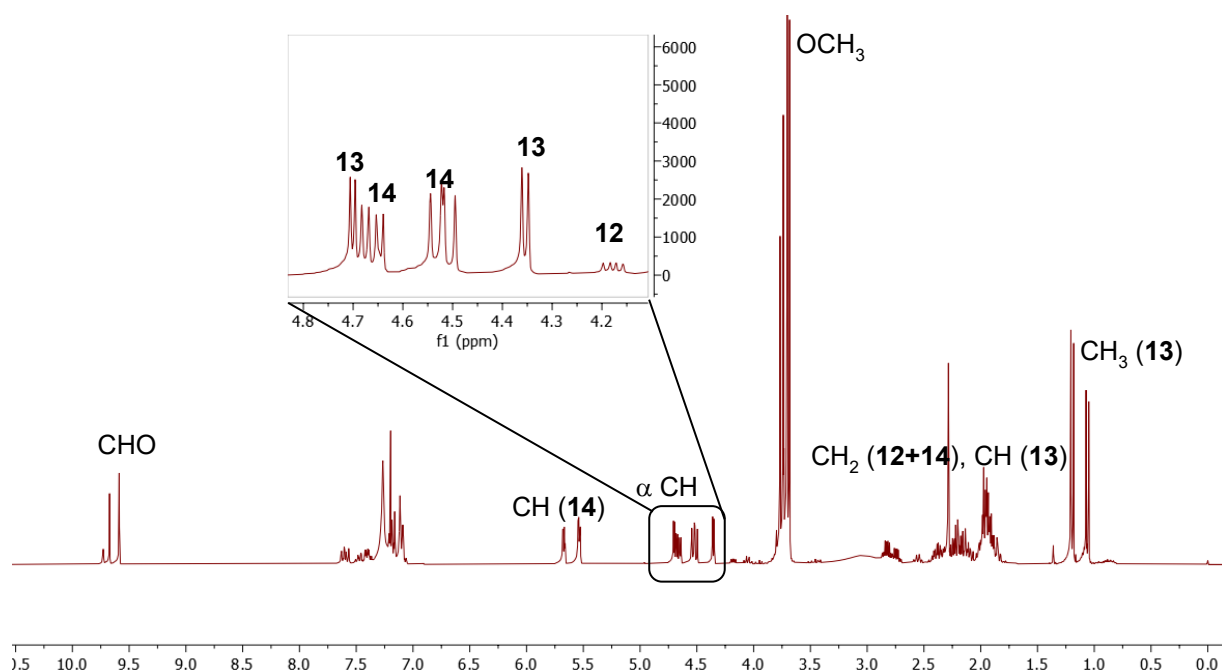
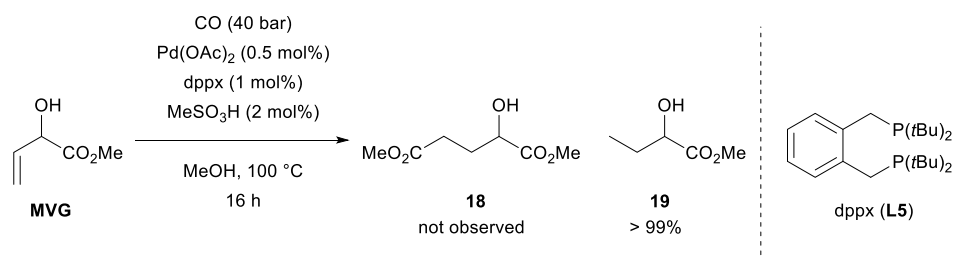


Figure 13. $^1\text{H-NMR}$ of the crude mixture from Table 12 entry 1 with assignment of the characteristic signals.

Although it led to full conversion of the starting material, **L1** was not selective neither for the linear nor for the branched isomer. When switching to bisphosphine **L2**, high linear to branched ratios could be achieved in both THF and toluene, again with full conversion of MVG. Interestingly, most of the linear product exists as 5-membered cyclic acetal, which presumably is more thermodynamically stable. Moving to **L3** led to a slower reaction, at the same time slightly lowering the linear to branched ratio. Bisphosphite **L4** gave full conversion and very high linear selectivity. Both the branched isomer **13** and the lactone **14** exists as roughly 50:50 mixture of *cis* and *trans* diastereoisomers. Aldehydes resulting from hydroformylation processes are rarely used as such by industry, and typically their subsequent hydrogenation to alcohols or oxidation to carboxylic acids is performed. MVG-derived aldehydes may be envisaged as precursors to di- and triols, as well as diesters or diacids, that might find applications as monomers or cross-linkers for bio-based polymers.¹⁹⁰

As the previously discussed hydroformylation, alkoxy carbonylation (*i.e.* the reaction of a carbon-carbon multiple bond with carbon monoxide in the presence of an alcohol to produce the corresponding ester) is also widely employed by industry to produce a large number of bulk and fine chemicals, above all methyl propionate from ethylene (intermediate to methyl methacrylate), the so-called Lucite Alpha Process.^{191, 192} The latter example employs a Palladium(II) salt in the presence of a bulky diphosphine ligand (dppx, Scheme 20) and a protic source. Starting from these conditions, methoxycarbonylation of MVG was investigated (Scheme 20). However, the reaction did not afford any of the desired diester **18**, but only the product of MVG hydrogenation (**19**). This is probably due to a Pd-catalysed transfer hydrogenation of the allylic double bond, where the methanol acts as hydrogen donor. The reaction is probably too fast compared to the hydroformylation path, thus consuming all the starting MVG before any product can be formed.



Scheme 20. Attempted methoxycarbonylation of MVG using ligand L5.

To circumvent the problem, the OH moiety could be protected: more steric hindrance around the C=C might help in slowing down the unwanted reduction of the bond. Moreover, electron withdrawing groups such as an acetyl are also reducing its reactivity. Finally, isomerization to the internal position might also occur, thus making the double bond less reactive in hydrogenation.

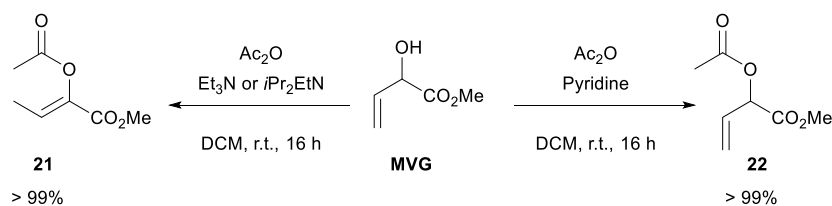
The OH protection turned out less obvious than expected on paper. When attempting to methylate MVG, after trying several reaction conditions (Table 14) the only effective method involved the use of silver(I) oxide and a slight excess of methyl iodide.¹⁹³ The reaction was rather slow, with full conversion obtained only after 60 hours (Entry 9).

Table 13. Screening of reaction conditions for the methylation of MVG.

Reaction scheme showing the methylation of MVG (methyl vinyl glycidate) to 20 (methyl 2-methoxyprop-1-enoate) using MeI (2 eq).

Entry	Conditions	Outcome
1	NaH, THF, 0 °C – r.t., 16 h	C=C isomerization
2	K ₂ CO ₃ , THF, 80 °C, 1 h	-
3	K ₂ CO ₃ , MeOH, 80 °C, 1 h	MeOMVG dimerization
4	K ₂ CO ₃ , neat, 80 °C, 1 h	-
5	K ₂ CO ₃ , acetone, 80 °C, 1 h	-
6	NaOMe, MeOH, 80 °C, 1 h	C=C isomerization
7	DIPEA, Et ₂ O, r.t., 48 h	C=C isomerization
8	Ag ₂ O, Et ₂ O, r.t., 24 h	20 (49 % after FCC)
9	Ag ₂ O, Et ₂ O, r.t., 60 h	20 (> 99%, no FCC needed)

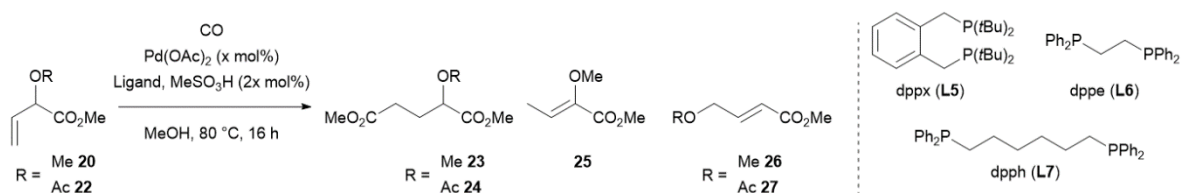
When attempting to acetylate MVG using acetic anhydride in the presence of a tertiary base (triethylamine, Scheme 21), the double bond always isomerized from the terminal to the internal position. The weaker pyridine was found to be effective in promoting the reaction while leaving the double bond in the terminal position. Quantitative yield of the desired acetylated MVG **22** could be eventually obtained.¹¹⁹



Scheme 21. Protection of the OH group of MVG.

Having the protected MVGs in hand, their methoxycarbonylation was explored (Table 15). Diphosphines with different bite angles were tried (Table 15, **L5-7**), using palladium(II) acetate as metal source. Methylated MVG (**20**) was converted at best by dppx (entry 1), while the other ligands only afforded traces of the desired diester. Increasing the catalyst loading up to 2 mol% the conversion only slightly increased (entries 4 and 5). In all the cases the main by-product was the methylated MVG with the C=C bond in the internal position. This can be easily explained by the formation of an allylic-Pd species that can then afford both isomeric olefins. Since this reaction is likely reversible, whereas the formation of the diester is not, an increase of the CO pressure and / or of the reaction temperature should increase the selectivity. Gratefully, this turned out to be the case, and the formation of **24** could be completely prevented. Up to 77% isolated yield of **23** was achieved in a multi-gram reaction (entry 9).

Table 14. Methoxycarbonylation of functionalised MVG **20** and **22**.

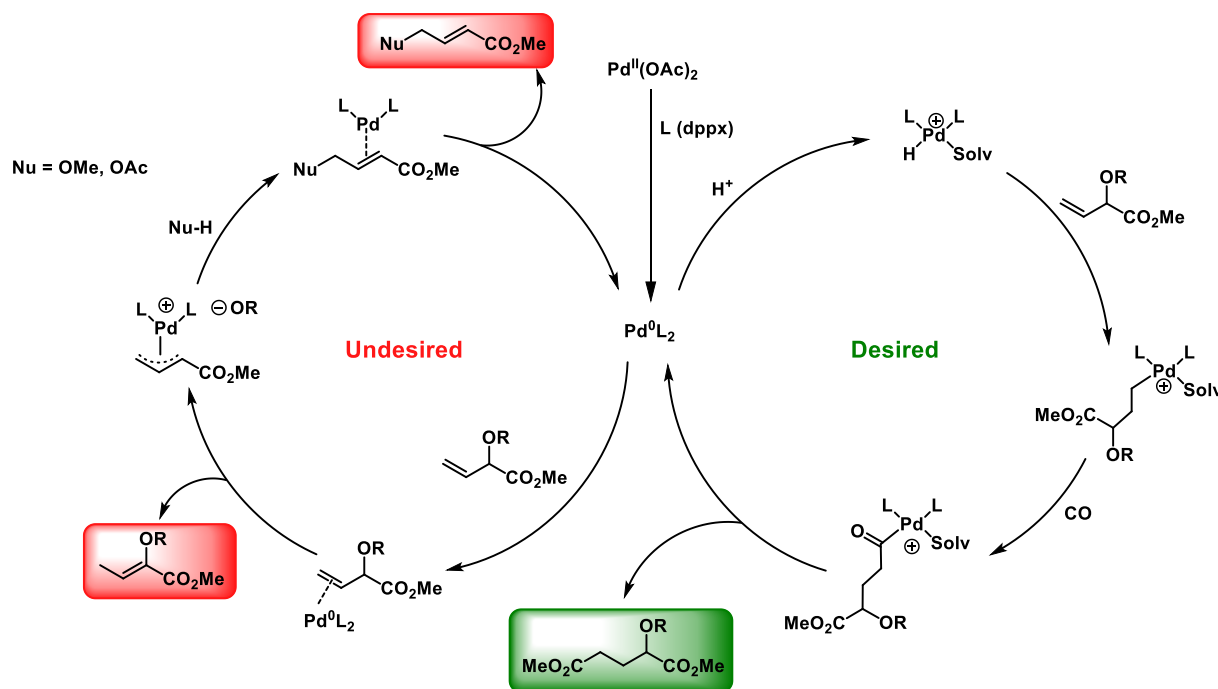


Entry	Substr.	[Pd] [mol%]	Ligand	ρ [bar]	Conv. [%] ^[a]	Product (23 or 24) [%] ^[a]	Isomerization (25) [%] ^[a]	Allylic rearrangement 26 [%] ^[a]	27 [%] ^[a]
1	6	0.5	L5	20	67	30	32	0	0
2	6	0.5	L6	20	<2	Traces	Traces	0	0
3	6	0.5	L7	20	<2	Traces	Traces	0	0
4	6	1.0	L5	20	86	31	28	0	0
5	6	2.0	L5	20	>99	33	24	0	0
6	6	1.0	L5	40	>99	71	27	0	0
7 ^[b]	6	1.0	L5	40	>99	47	31	0	0
8 ^[c]	6	1.0	L5	40	>99	63	32	0	0
9 ^[d]	6	1.0	L5	40	>99	>99 (77 ^[e])	0	0	0
10	7	0.5	L5	20	56	Traces	0	36	Traces
11	7	0.5	L6	20	44	0	0	Traces	Traces
12	7	0.5	L7	20	83	Traces	0	20	55
13	7	1.0	L5	20	54	9	0	21	0
14	7	2.0	L5	20	>99	18	0	17	Traces
15	7	1.0	L5	40	47	6	0	14	0
16 ^[b]	7	1.0	L5	40	82	21	0	0	0
17 ^[c]	7	1.0	L5	40	>99	Traces	0	27	Traces

^[a]GC yields; *n*-dodecane as internal standard. ^[b]20 mol% of MeSO₃H. ^[c]100 °C. ^[d]120 °C. ^[e]isolated yield.

Acetylated MVG **22** was explored in a similar manner as described for **20**. In this case the reaction was less clean than the previous case due to a wider spectrum of by-products that was obtained. Other than the already mentioned isomerization of the olefin, that in this case was never observed, one can expect allylic rearrangement to the linear isomer, that can afford either the acetyl or the methoxy

product (Table 15, **26** or **27**).¹³⁴ The same considerations made for **20** also applies here, so higher temperature and pressure should favour the desired product (Scheme 22). However, though the by-products were reduced in the same fashion, the product yield did not significantly increase (Table 15, entries 15-17). This can be explained with the inferior stability of the acetyl group compared with the methoxy moiety. Solvolysis of the ester in methanol gives back MVG, that can isomerize to the ketone or oligomerize under the acidic reaction conditions, thus lowering the output of **24**. For this reason, methoxy derivative **23** was selected as the more promising monomer for the preparation of polyesters *via* polycondensation.



Scheme 22. Catalytic cycles involved in the reaction of MVG derivatives under the conditions reported in Table 15.

A widely employed and commercially available catalyst for polycondensation reactions is titanium(IV) isopropoxide. The reaction between **23** and several diols was performed at 150 °C, first under argon atmosphere and after 6 hours under vacuum to completely remove the produced methanol thus pushing the reaction to full conversion. A 1:1 molar ratio between diols and diester was used (Table 16).

Table 16. Polycondensation of **23** with different aliphatic diols.

Entry	Diol	Yield [%]	M_n^{GPC} [kg/mol]	M_w^{GPC} [kg/mol]	\bar{D}	T_g [°C] ^[a]
1	1,4- butanediol	91	20.6	45.4	2.2	-37
2	1,6-hexanediol	82	11.3	18.1	1.6	-43
3	1,12-dodecanediol	93	22.1	41.8	1.9	-20
4	1,4-pentanediol	87	28.5	61.7	2.1	-22

^[a]Measured by DSC.

Linear diols with different carbon chains were successfully polymerised with **23**, affording products with molecular weights around 10-20 kg/mol. 1,4-Pentanediol, that can be obtained from renewable levulinic acid, was also successfully incorporated into polyesters with similar yield and molecular weight (entry 4). DSC of all the obtained materials showed amorphous polymers, with glass-transition temperatures always below 0 °C (Figure 14).

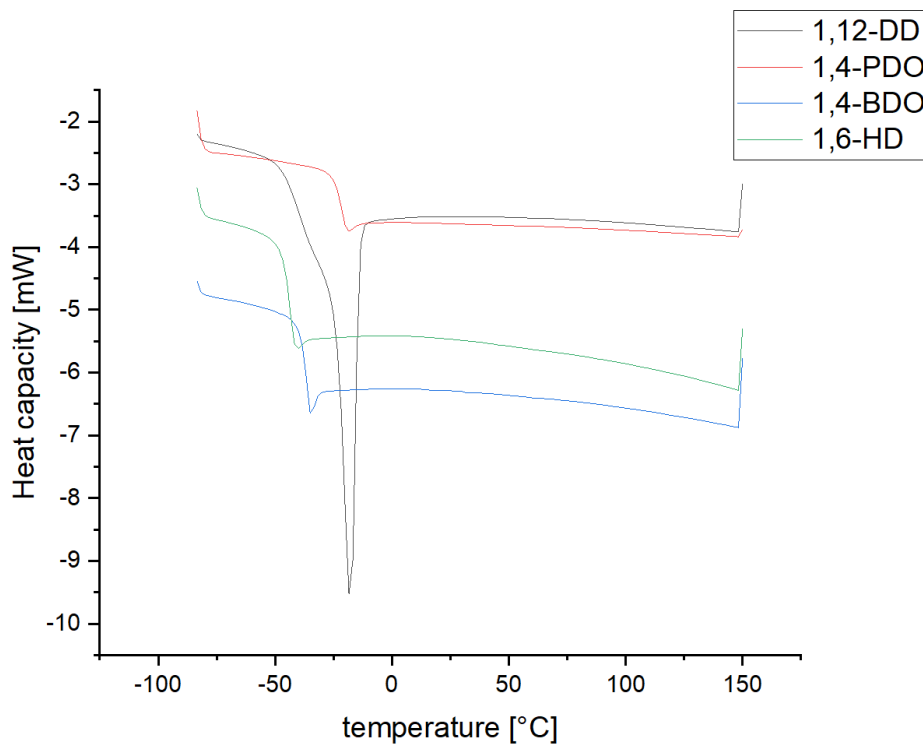


Figure 14. DSC traces of MVG-derived polyesters **28-31**.

In summary, hydroformylation and methoxy carbonylation reactions were explored to prepare novel bifunctional monomers from MVG. New MVG-derived polyesters were prepared and fully characterized, showing another possible practical application of this sugar-derived platform chemical.

The publication concerning this work can be found in section 6.4.

4. Conclusions

There are many ways to imagine a chemical economy based on renewable resources. The use of platform chemicals is currently being investigated in order to produce bulk and fine chemicals, as well as fuels, efficiently from sugars. Strong connections between industry and academia are crucial to enlarge the portfolio of biobased alternatives to petrol-derived products and design novel (catalytic) methods for high-yielding conversion of biomass to useful chemicals.

Levulinic acid, although not yet available in large amounts from renewables, might have a huge potential due to the manifold chemicals that can be prepared from it. Angelica lactones, readily obtained by reactive distillation of LA, were targeted in this work as potential novel building blocks for fine chemicals and polymers. An atom economic, efficient and easily scalable route was designed to convert α - to β AL and functionalize it with different dienes through a catalytic Diels-Alder reaction. This monomer can be then polymerised using Grubbs catalyst in green solvents to afford novel and biobased polynorbornene that retains the properties of their petrol-based analogue (such as high transparency), but at the same time bears the lactone ring that can be further utilized for post-polymerisation reactions.

α -AL was furthermore converted to malonic acid and malonates in very high yield *via* ozonolysis of its double bond. Malonic acid and its esters represent a very important chemical that are yearly produced in a multi-ton scale and function as building blocks for the synthesis of fine chemical and specialty polymers. Moreover, by changing the solvent and the work-up conditions, 3-oxopropionic acid and esters were obtained. These are intermediates to 3-hydroxypropionic acid, that is used for preparing biodegradable polyesters.

Glycolaldehyde is directly obtained from retro-aldol condensation of hexoses and pentoses. It is a major component of pyrolysis oil and is getting the attention of industry as intermediate in the production of ethylene glycol from sugars. In this work, GA was used for the first time as C1 building block, namely for the *N*-formylation of secondary amines. The reaction is highly selective and can be used to convert a range of aliphatic and aromatic amines. Mechanistic studies showed that the reaction proceeds via a radical pathway, using atmospheric oxygen as oxidant.

Methyl vinyl glycolate is a side stream product in the synthesis of methyl lactate from sugars under acidic conditions. Its hydroformylation with rhodium-phosphine catalysts was investigated. High selectivity for the linear product was achieved. This can be used for the synthesis of new diols and triols, potentially useful as monomers in polymers. Methoxycarbonylation of MVG is another valuable approach to prepare linear diesters, that were successfully polymerised to new and bio-based polyesters. This approach can widen the scope of MVG in polymer chemistry, for example in the field of elastomers.

This work focused on both already established (*e.g.*, malonic acid) and novel (*e.g.* MVG-derived) products. Biomass valorisation is a valuable method to obtain both drop-in chemicals, that already have a market, and new compounds that might have different properties and wider applications, opening an enormous number of new possibilities for chemists.

5. References

1. J. Connan, *Philos. Trans. R. Soc. London, Ser. B*, 1999, **354**, 33-50.
2. M. Höök and X. Tang, *Energy policy*, 2013, **52**, 797-809.
3. IEA, *Key World Energy Statistics 2021*, <https://www.iea.org/reports/key-world-energy-statistics-2021>, 2021.
4. C. Ladder, C&EN's World Chemical Outlook, *Chem. Eng. News*, 2022.
5. A. Corma, S. Iborra and A. Velty, *Chem. Rev.*, 2007, **107**, 2411-2502.
6. H. Kopetz, *Nature*, 2013, **494**, 29-31.
7. L. T. Mika, E. Csefalvay and A. Nemeth, *Chem. Rev.*, 2018, **118**, 505-613.
8. M.-A. Perea-Moreno, E. Samerón-Manzano and A.-J. Perea-Moreno, *Sustainability*, 2019, **11**, 863.
9. S. K. Maity, *Renew. Sust. Energ. Rev.*, 2015, **43**, 1427-1445.
10. A. Corma, S. Iborra and A. Velty, *Chem. Rev.*, 2007, **107**, 2411-2502.
11. C.-H. Zhou, X. Xia, C.-X. Lin, D.-S. Tong and J. Beltramini, *Chem. Soc. Rev.*, 2011, **40**, 5588-5617.
12. B. Kamm and M. Kamm, *Chem. Biochem. Eng. Q.*, 2004, **18**, 1-7.
13. A. Demirbas, *Appl. Energy*, 2011, **88**, 17-28.
14. J. J. Bozell and G. R. Petersen, *Green Chem.*, 2010, **12**, 539-554.
15. E. Taarning, C. M. Osmundsen, X. Yang, B. Voss, S. I. Andersen and C. H. Christensen, *Energy & Environ. Sci.*, 2011, **4**, 793-804.
16. C. A. Rabinovitch-Deere, J. W. Oliver, G. M. Rodriguez and S. Atsumi, *Chem. Rev.*, 2013, **113**, 4611-4632.
17. M. M. Maghanki, B. Ghobadian, G. Najafi and R. J. Galogah, *Renew. Sust. Energ. Rev.*, 2013, **28**, 510-524.
18. R. Luque, A. R. de la Osa, J. M. Campelo, A. A. Romero, J. L. Valverde and P. Sanchez, *Energy & Environ. Sci.*, 2012, **5**, 5186-5202.
19. G. W. Huber and J. A. Dumesic, *Catal. Today*, 2006, **111**, 119-132.
20. M. B. Figueirêdo, I. Hita, P. J. Deuss, R. H. Venderbosch and H. J. Heeres, *Green Chem.*, 2022, **24**, 4680-4702.
21. S. Xiu and A. Shahbazi, *Renew. Sust. Energ. Rev.*, 2012, **16**, 4406-4414.
22. X. Wu, M. V. Galkin, T. Stern, Z. Sun and K. Barta, *Nat. Commun.*, 2022, **13**, 1-12.
23. J. G. de Vries, *Chem. Rec.*, 2016, **16**, 2787-2800.
24. I. Delidovich, P. J. C. Hausoul, L. Deng, R. Pfützenreuter, M. Rose and R. Palkovits, *Chem. Rev.*, 2016, **116**, 1540-1599.
25. X. Dai, J. Rabeah, H. Yuan, A. Brückner, X. Cui and F. Shi, *ChemSusChem*, 2016, **9**, 3133-3138.
26. C.-H. C. Zhou, J. N. Beltramini, Y.-X. Fan and G. M. Lu, *Chem. Soc. Rev.*, 2008, **37**, 527-549.
27. B. Katryniok, S. Paul and F. Dumeignil, *ACS Catal.*, 2013, **3**, 1819-1834.
28. Y. Wang, J. Zhou and X. Guo, *RSC Adv.*, 2015, **5**, 74611-74628.
29. P. Krafft, US8344185B2, 2006.
30. G. M. Lari, G. Pastore, C. Mondelli and J. Pérez-Ramírez, *Green Chem.*, 2018, **20**, 148-159.
31. P. Anastas and N. Eghbali, *Chem. Soc. Rev.*, 2010, **39**, 301-312.
32. J. D. Sachs, G. Schmidt-Traub, M. Mazzucato, D. Messner, N. Nakicenovic and J. Rockström, *Nat. Sustain.*, 2019, **2**, 805-814.
33. T. Werpy and G. Petersen, *Top Value Added Chemicals from Biomass: Volume I -- Results of Screening for Potential Candidates from Sugars and Synthesis Gas*, National Renewable Energy Lab., Golden, CO (US), 2004.
34. A. Gandini, T. M. Lacerda, A. J. F. Carvalho and E. Trovatti, *Chem. Rev.*, 2016, **116**, 1637-1669.
35. C. Rueda, M. Marinova, J. Paris, G. Ruiz and A. Coz, *J. Chem. Technol. Biotechnol.*, 2016, **91**, 2646-2653.
36. K. Dalvand, J. Rubin, S. Gunukula, M. Clayton Wheeler and G. Hunt, *Biomass Bioenergy*, 2018, **115**, 56-63.

37. B. M. Stadler, C. Wulf, T. Werner, S. Tin and J. G. de Vries, *ACS Catal.*, 2019, **9**, 8012-8067.
38. J. Iglesias, I. Martínez-Salazar, P. Maireles-Torres, D. Martín Alonso, R. Mariscal and M. López Granados, *Chem. Soc. Rev.*, 2020, **49**, 5704-5771.
39. O. R. Schade, P.-K. Dannecker, K. F. Kalz, D. Steinbach, M. A. R. Meier and J.-D. Grunwaldt, *ACS Omega*, 2019, **4**, 16972-16979.
40. <https://www.avantium.com/press-releases/avantium-reaches-financial-close-for-its-fdca-flagship-plant/>, (accessed 09/08/2022).
41. L. Ye, X. Lv and H. Yu, *Metab. Eng.*, 2016, **38**, 125-138.
42. T. Kuzuyama and H. Seto, *Nat. Prod. Rep.*, 2003, **20**, 171-183.
43. J. Fortman, S. Chhabra, A. Mukhopadhyay, H. Chou, T. S. Lee, E. Steen and J. D. Keasling, *Trends Biotechnol.*, 2008, **26**, 375-381.
44. F. A. C. Martinez, E. M. Balciunas, J. M. Salgado, J. M. D. González, A. Converti and R. P. de Souza Oliveira, *Trends Food Sci. Technol.*, 2013, **30**, 70-83.
45. M. S. Holm, S. Saravanamurugan and E. Taarning, *Science*, 2010, **328**, 602-605.
46. S. Aparicio and R. Alcalde, *Green Chem.*, 2009, **11**, 65-78.
47. I. Bechthold, K. Bretz, S. Kabasci, R. Kopitzky and A. Springer, *Chemical Engineering & Technology: Industrial Chemistry-Plant Equipment-Process Engineering-Biotechnology*, 2008, **31**, 647-654.
48. C. Delhomme, D. Weuster-Botz and F. E. Kühn, *Green Chem.*, 2009, **11**, 13-26.
49. L. Matsakas, K. Hrůzová, U. Rova and P. Christakopoulos, *Fermentation*, 2018, **4**, 13.
50. S. S. Bhagwat, Y. Li, Y. R. Cortés-Peña, E. C. Brace, T. A. Martin, H. Zhao and J. S. Guest, *ACS Sustain. Chem. Eng.*, 2021, **9**, 16659-16669.
51. A. Yamaguchi, O. Sato, N. Mimura and M. Shirai, *Catal. Today*, 2016, **265**, 199-202.
52. 徐周文, CN1683293A, 2005.
53. G. Mulder, *J. prakt. Chem.*, 1840, **21**, 321-370.
54. R. H. Leonard, *Ind. Eng. Chem. Res.*, 1956, **48**, 1330-1341.
55. M. Signoretto, S. Taghavi, E. Ghedini and F. Menegazzo, *Molecules*, 2019, **24**, 2760.
56. D. Di Menno Di Bucchianico, Y. Wang, J.-C. Buvat, Y. Pan, V. Casson Moreno and S. Leveneur, *Green Chem.*, 2022, **24**, 614-646.
57. K. Yan, C. Jarvis, J. Gu and Y. Yan, *Renew. Sustain. Energy Rev.*, 2015, **51**, 986-997.
58. Formic acid market - growth, trends, COVID-19 impact, and forecasts (2022 - 2027), <https://www.mordorintelligence.com/industry-reports/formic-acid-market#:~:text=The%20Global%20Formic%20Acid%20Market,during%20the%20period%202022%2D2027.>, (accessed 14/07/2022).
59. D. J. Hayes, S. Fitzpatrick, M. H. Hayes and J. R. Ross, *Biorefineries—Industrial Processes and Product*, 2006, **1**, 139-164.
60. F. El Ouahabi, M. Polyakov, G. P. M. van Klink, S. Wohlrab, S. Tin and J. G. de Vries, *ACS Sustain. Chem. Eng.*, 2020, **8**, 1705-1708.
61. Global Levulinic Acid Market 2022-2026, https://www.reportlinker.com/p06293140/Global-Levulinic-Acid-Market.html?utm_source=GNW, (accessed 08/08/2022).
62. M. Sajid, U. Farooq, G. Bary, M. M. Azim and X. Zhao, *Green Chem.*, 2021, **23**, 9198-9238.
63. Bringing levulinic acid derivatives to the market through technology innovation, <http://www.gfbiochemicals.com/technology/#atlas-technology>, (accessed 22/08/2022).
64. E. Koivisto, N. Ladommatos and M. Gold, *Energy & Fuels*, 2015, **29**, 5875-5884.
65. A. M. Api, D. Belsito, D. Botelho, M. Bruze, G. A. Burton, J. Buschmann, M. L. Dagli, M. Date, W. Dekant, C. Deodhar, M. Francis, A. D. Fryer, L. Jones, K. Joshi, S. La Cava, A. Lapczynski, D. C. Liebler, D. O'Brien, A. Patel, T. M. Penning, G. Ritacco, J. Romine, N. Sadekar, D. Salvito, T. W. Schultz, I. G. Sipes, G. Sullivan, Y. Thakkar, Y. Tokura and S. Tsang, *Food Chem. Toxicol.*, 2019, **127**, S48-S54.
66. S. Liu, G. Zhang, X. Li and J. Zhang, *Appl. Microbiol. Biotechnol.*, 2014, **98**, 7349-7357.
67. B. M. Stadler, S. Tin, A. Kux, R. Grauke, C. Koy, T. D. Tiemersma-Wegman, S. Hinze, H. Beck, M. O. Glocker, A. Brandt and J. G. de Vries, *ACS Sustain. Chem. Eng.*, 2020, **8**, 13467-13480.

68. D. M. Alonso, S. G. Wettstein and J. A. Dumesic, *Green Chem.*, 2013, **15**, 584-595.
69. B. M. Stadler, A. Brandt, A. Kux, H. Beck and J. G. de Vries, *ChemSusChem*, 2020, **13**, 556-563.
70. J.-P. Lange, J. Z. Vestering and R. J. Haan, *Chem. Commun.*, 2007, DOI: 10.1039/b705782b, 3488-3490.
71. J. G. de Vries, N. Sereinig, E. W. M. van de Vondervoort and M. C. C. Janssen, *NLD Pat.*, WO2012131028 A1, 2012.
72. B. Lu, J. Li, G. Lv, Y. Qi, Y. Wang, T. Deng, X. Hou and Y. Yang, *RSC Adv.*, 2016, **6**, 93956-93962.
73. Y. Yang, X. R. Wei, F. X. Zeng and L. Deng, *Green Chem.*, 2016, **18**, 691-694.
74. A. Marckwordt, F. El Ouahabi, H. Amani, S. Tin, N. V. Kalevaru, P. C. J. Kamer, S. Wohlrab and J. G. de Vries, *Angew. Chem., Int. Ed.*, 2019, **58**, 3486-3490.
75. J. Lin, H. Song, X. Shen, B. Wang, S. Xie, W. Deng, D. Wu, Q. Zhang and Y. Wang, *Chem. Commun.*, 2019, **55**, 11017-11020.
76. J. A. Dumesic and R. M. West, *US Pat.*, WO002011087962 A1, 2011.
77. F. El Ouahabi, W. Smit, C. Angelici, M. Polyakov, U. Rodemerck, C. Fischer, V. N. Kalevaru, S. Wohlrab, S. Tin, G. P. M. van Klink, J. C. van der Waal, F. Orange and J. G. de Vries, *ACS Sustain. Chem. Eng.*, 2022, **10**, 766-775.
78. Y. Gong, L. Lin and B. Zhang, *Chin. J. Chem.*, 2012, **30**, 327-332.
79. L. Wolff, *Justus Liebigs Ann Chem.*, 1885, **229**, 249-285.
80. J. H. Helberger, S. Ulubay and H. C. Civelekoglu, *Justus Liebigs Ann Chem.*, 1949, **561**, 215-220.
81. R. Zhu, A. Chatzidimitriou, B. Liu, D. J. Kerwood and J. Q. Bond, *ACS Catal.*, 2020, **10**, 1555-1565.
82. Y. Wu, R. P. Singh and L. Deng, *J. Am. Chem. Soc.*, 2011, **133**, 12458-12461.
83. L. Zhou, L. Lin, J. Ji, M. Xie, X. Liu and X. Feng, *Org. Lett.*, 2011, **13**, 3056-3059.
84. M. Mascals, S. Dutta and I. Gandarias, *Angew. Chem.*, 2014, **126**, 1885-1888.
85. W. Wang, N. Li, S. Li, G. Li, F. Chen, X. Sheng, A. Wang, X. Wang, Y. Cong and T. Zhang, *Green Chem.*, 2016, **18**, 1218-1223.
86. J. Ficini, J. d'Angelo, J.-P. Genêt and J. Noiré, *Tetrahedron Lett.*, 1971, **12**, 1569-1571.
87. C. G. S. Lima, J. L. Monteiro, T. de Melo Lima, M. Weber Paixao and A. G. Correa, *ChemSusChem*, 2018, **11**, 25-47.
88. C. S. Marvel and C. L. Levesque, *J. Am. Chem. Soc.*, 1939, **61**, 1682-1684.
89. V. E. Tarabanko and K. L. Kaygorodov, *Chem. Sus. Dev*, 2010, 321-328.
90. V. E. Tarabanko and K. L. Kaygorodov, *Macromol Symp.*, 2015, **354**, 367-373.
91. K. L. Kaygorodov, V. E. Tarabanko and N. Tarabanko, *Cogent Chem.*, 2018, **4**.
92. X.-J. Wang and M. Hong, *Angew. Chem. Int. Ed.*, 2020, **59**, 2664-2668.
93. Y. Kobayashi, H. Takahara, H. Takahashi and K. Higasi, *J. Mol. Struct.*, 1976, **32**, 235-246.
94. C. I. Stassinopoulou and C. Zioudrou, *Tetrahedron*, 1972, **28**, 1257-1263.
95. W. H. Faveere, S. Van Praet, B. Vermeeren, K. N. Dumoleijn, K. Moonen, E. Taarning and B. F. Sels, *Angew. Chem. Int. Ed.*, 2021, **133**, 12312-12331.
96. C. R. Vitasari, G. W. Meindersma and A. B. de Haan, *Sep. Purif. Technol.*, 2012, **95**, 103-108.
97. J. A. Stradal and G. L. Underwood, US5252188A, 1992.
98. V. K. Venkatakrisnan, J. C. Degenstein, A. D. Smeltz, W. N. Delgass, R. Agrawal and F. H. Ribeiro, *Green Chem.*, 2014, **16**, 792-802.
99. K. Q. A. Leñero, E. Drent, R. V. Ginkel and R. I. Pugh, US7449607B2, 2004.
100. A. Butlerow, *CR Acad. Sci*, 1861, **53**, 145-147.
101. A. H. Weiss, US4238418A, 1979.
102. A. J. Vetter, M. E. Janka and J. R. Zoeller, US7498469 B1, 2007.
103. W. H. E. Gehrer, K. Ebel, J.-P. Melder, J. H. Teles, US5298668 A, 1992.
104. M. Sasaki, K. Goto, K. Tajima, T. Adschiri and K. Arai, *Green Chem.*, 2002, **4**, 285-287.
105. G. Xu, A. Wang, J. Pang, X. Zhao, J. Xu, N. Lei, J. Wang, M. Zheng, J. Yin and T. Zhang, *ChemSusChem*, 2017, **10**, 1390-1394.

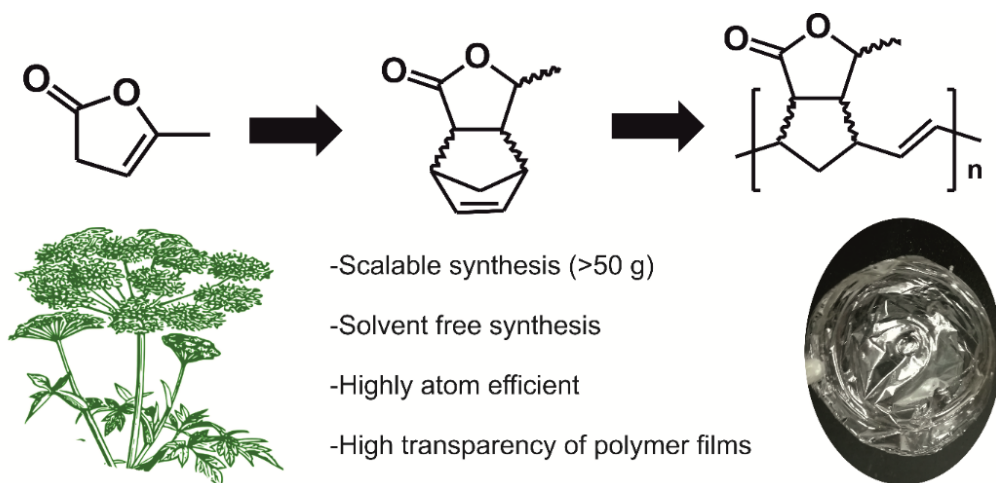
106. C. Yang, Z. Miao, F. Zhang, L. Li, Y. Liu, A. Wang and T. Zhang, *Green Chem.*, 2018, **20**, 2142-2150.
107. M. Yang, H. Qi, F. Liu, Y. Ren, X. Pan, L. Zhang, X. Liu, H. Wang, J. Pang, M. Zheng, A. Wang and T. Zhang, *Joule*, 2019, **3**, 1937-1948.
108. M. S. Holm, I. S. Zubiri, S. Tolborg, C. M. Osmundsen and E. Taarning, US9573123 B2, 2015.
109. A. Tullo, *Chem. Eng. News*, 2017, **95**, 10.
110. J. Singh, P. Dekker, J. C. V. D. Waal and B. Mckay, WO2019175365A1, 2019.
111. T. Hofmann, W. Bors and K. Stettmaier, *J. Agric. Food. Chem.*, 1999, **47**, 379-390.
112. H. Yue, Y. Zhao, X. Ma and J. Gong, *Chem. Soc. Rev.*, 2012, **41**, 4218-4244.
113. P. K. Samantaray, A. Little, D. M. Haddleton, T. McNally, B. Tan, Z. Sun, W. Huang, Y. Ji and C. Wan, *Green Chem.*, 2020, **22**, 4055-4081.
114. A. Ballerini, A. Despres and A. Pizzi, *Holz als Roh- und Werkstoff*, 2005, **63**, 477-478.
115. M. A. Salaev, A. A. Krejker, O. V. Magaev, V. S. Malkov, A. S. Knyazev, E. S. Borisova, V. M. Khanaev, O. V. Vodyankina and L. N. Kurina, *Chem. Eng. J.*, 2011, **172**, 399-409.
116. M. Pelckmans, W. Vermandel, F. Van Waes, K. Moonen and B. F. Sels, *Angew. Chem. Int. Ed.*, 2017, **56**, 14540-14544.
117. M. Dusselier, P. Van Wouwe, F. de Clippel, J. Dijkmans, D. W. Gammon and B. F. Sels, *ChemCatChem*, 2013, **5**, 569-575.
118. M. Dusselier, P. V. Wouwe, A. Dewaele, P. A. Jacobs and B. F. Sels, *Science*, 2015, **349**, 78-80.
119. A. Sølvhøj, E. Taarning and R. Madsen, *Green Chem.*, 2016, **18**, 5448-5455.
120. R. Rambaud, *Bull. Soc. Chim. Fr.*, 1934, **1**, 1317-1341.
121. A. Rieche, M. Schulz, H. Seyfarth and G. Gottschalk, *Fette, Seifen, Anstrichmittel*, 1962, **64**, 198-205.
122. S. Yamamoto, H. Itani, T. Tsuji and W. Nagata, *J. Am. Chem. Soc.*, 1983, **105**, 2908-2909.
123. M. S. Holm, Y. J. Pagán-Torres, S. Saravanamurugan, A. Riisager, J. A. Dumesic and E. Taarning, *Green Chem.*, 2012, **14**, 702-706.
124. M. Dusselier, P. Van Wouwe, S. De Smet, R. De Clercq, L. Verbelen, P. Van Puyvelde, F. E. Du Prez and B. F. Sels, *ACS Catal.*, 2013, **3**, 1786-1800.
125. R. De Clercq, M. Dusselier, C. Christiaens, J. Dijkmans, R. I. Iacobescu, Y. Pontikes and B. F. Sels, *ACS Catal.*, 2015, **5**, 5803-5811.
126. S. Tolborg, S. Meier, I. Sádaba, S. G. Elliot, S. K. Kristensen, S. Saravanamurugan, A. Riisager, P. Fristrup, T. Skrydstrup and E. Taarning, *Green Chem.*, 2016, **18**, 3360-3369.
127. L. Botti, R. Navar, S. Tolborg, J. S. Martínez-Espín and C. Hammond, *ACS Sust. Chem. Eng.*, 2022, **10**, 4391-4403.
128. M. Dusselier, R. De Clercq, R. Cornelis and B. F. Sels, *Catal. Today*, 2017, **279**, 339-344.
129. A. Wójcik, <https://blog.topsoe.com/braskem-and-haldor-topsoe-achieve-first-production-of-bio-based-meg-from-sugar>, (accessed 09/08/2022).
130. S. Ravn, <https://blog.topsoe.com/braskem-and-haldor-topsoe-start-up-demo-unit-for-developing-renewable-meg>, (accessed 09/08/2022).
131. H. Stach, W. Huggenberg and M. Hesse, *Helv. Chim. Acta*, 1987, **70**, 369-374.
132. K. E. Koenig, 1998.
133. M. Freiría, A. J. Whitehead, D. A. Tocher and W. B. Motherwell, *Tetrahedron*, 2004, **60**, 2673-2692.
134. B. M. Jessen, J. M. Ondozabal, C. M. Pedersen, A. Sølvhøj, E. Taarning and R. Madsen, *ChemistrySelect*, 2020, **5**, 2559-2563.
135. B. M. Jessen, E. Taarning and R. Madsen, *Eur. J. Org. Chem.*, 2021, **2021**, 4049-4053.
136. J. Xu, N. Li, X. Yang, G. Li, A. Wang, Y. Cong, X. Wang and T. Zhang, *ACS Catal.*, 2017, **7**, 5880-5886.
137. A. D. Pehere, S. Xu, S. K. Thompson, M. A. Hillmyer and T. R. Hoye, *Org. Lett.*, 2016, **18**, 2584-2587.
138. Y. Bai, M. De bruyn, J. H. Clark, J. R. Dodson, T. J. Farmer, M. Honoré, I. D. V. Ingram, M. Naguib, A. C. Whitwood and M. North, *Green Chem.*, 2016, **18**, 3945-3948.

139. M. Iqbal, R. A. Knigge, H. J. Heeres, A. A. Broekhuis and F. Picchioni, *Polymers*, 2018, **10**, 1177.
140. A. Blanpain, J. H. Clark, T. J. Farmer, Y. Guo, I. D. V. Ingram, J. E. Kendrick, S. B. Lawrenson, M. North, G. Rodgers and A. C. Whitwood, *ChemSusChem*, 2019, **12**, 2393-2401.
141. I. Choinopoulos, *Polymers*, 2019, **11**, 298.
142. A. K. Pearce, J. C. Foster and R. K. O'Reilly, *J. Polym. Sci., Part A: Polym. Chem.*, 2019, **57**, 1621-1634.
143. J.-A. Song, B. Park, S. Kim, C. Kang, D. Lee, M.-H. Baik, R. H. Grubbs and T.-L. Choi, *J. Am. Chem. Soc.*, 2019, **141**, 10039-10047.
144. D. Prat, J. Hayler and A. Wells, *Green Chem.*, 2014, **16**, 4546-4551.
145. V. Antonucci, J. Coleman, J. B. Ferry, N. Johnson, M. Mathe, J. P. Scott and J. Xu, *Org. Process Res. Dev.*, 2011, **15**, 939-941.
146. F. P. Byrne, S. Jin, G. Paggiola, T. H. M. Petchey, J. H. Clark, T. J. Farmer, A. J. Hunt, C. Robert McElroy and J. Sherwood, *Sustain. Chem. Process.*, 2016, **4**, 7.
147. C. M. Alder, J. D. Hayler, R. K. Henderson, A. M. Redman, L. Shukla, L. E. Shuster and H. F. Sneddon, *Green Chem.*, 2016, **18**, 3879-3890.
148. K. Sakurai and T. Takahashi, *J. Appl. Polym. Sci.*, 1989, **38**, 1191-1194.
149. M.-C. Choi, J.-C. Hwang, C. Kim, S. Ando and C.-S. Ha, *J. Polym. Sci., Part A: Polym. Chem.*, 2010, **48**, 1806-1814.
150. M. Singh and K. Weidner, in *Optical Interconnects for Data Centers*, eds. T. Tekin, R. Pitwon, A. Håkansson and N. Pleros, Woodhead Publishing, 2017, DOI: 10.1016/B978-0-08-100512-5.00006-1, pp. 157-170.
151. G. Sung, M.-C. Choi, S. Nagappan, W.-K. Lee, M. Han and C.-S. Ha, *Polym. Bull.*, 2012, **70**, 619-630.
152. S. H. Harald Strittmatter, Peter Pollak, in *Ullmann's Encyclopedia of Industrial Chemistry*, Wiley-VCH Verlag GmbH & Co, 2007.
153. J. L. F. Jeffrey A. Dietrich, Eric J. Steen, WO 2013/134424 A1, 2013.
154. U. Horn, A. Siering, K. Martin, G. Krauter, P.-J. Mueller, B. Bardl, J.-H. Ozegowski and K. Herold, DE102005052338A1, 2007.
155. T. Haas, M. Meier, C. Brossmer, D. Arntz and A. Freund, US5817870A, 1998.
156. in *Ullmann's Encyclopedia of Industrial Chemistry*, DOI: 10.1002/14356007.a18_349.
157. R. Criegee, *Angew. Chem., Int. Ed. Engl.*, 1975, **14**, 745-752.
158. R. L. Kuczkowski, *Chem. Soc. Rev.*, 1992, **21**, 79-83.
159. in *Ullmann's Encyclopedia of Industrial Chemistry*, DOI: 10.1002/14356007.a08_523.pub3, pp. 1-18.
160. G. C. Brown AC, Oehlschlaeger HF, Rolfes RP, 1957.
161. M. B. Figueirêdo, F. W. Keij, A. Hommes, P. J. Deuss, R. H. Venderbosch, J. Yue and H. J. Heeres, *ACS Sust. Chem. Eng.*, 2019, **7**, 18384-18394.
162. E. M. Karp, T. R. Eaton, V. S. i. Nogué, V. Vorotnikov, M. J. Bidy, E. C. D. Tan, D. G. Brandner, R. M. Cywar, R. Liu, L. P. Manker, W. E. Michener, M. Gilhespy, Z. Skoufa, M. J. Watson, O. S. Fruchey, D. R. Vardon, R. T. Gill, A. D. Bratis and G. T. Beckham, *Science*, 2017, **358**, 1307-1310.
163. L. T. Mika, E. Cséfalvay and Á. Németh, *Chem. Rev.*, 2018, **118**, 505-613.
164. J. Kula, *Chemical Health and Safety*, 1999, **6**.
165. H. Bipp and H. Kieczka, in *Ullmann's Encyclopedia of Industrial Chemistry*, DOI: https://doi.org/10.1002/14356007.a12_001.pub2.
166. J. R. Dunetz, J. Magano and G. A. Weisenburger, *Org. Process Res. Dev.*, 2016, **20**, 140-177.
167. G. A. Olah, L. Ohannesian and M. Arvanaghi, *Chem. Rev.*, 1987, **87**, 671-686.
168. N. Ortega, C. Richter and F. Glorius, *Org. Lett.*, 2013, **15**, 1776-1779.
169. L. Zhang, Z. Han, X. Zhao, Z. Wang and K. Ding, *Angew. Chem. Int. Ed.*, 2015, **127**, 6284-6287.
170. M. Hulla, G. Laurency and P. J. Dyson, *ACS Catal*, 2018, **8**, 10619-10630.
171. M. Nasrollahzadeh, N. Motahharifar, M. Sajjadi, A. M. Aghbolagh, M. Shokouhimehr and R. S. Varma, *Green Chem.*, 2019, **21**, 5144-5167.

172. X. Dai, S. Adomeit, J. Rabeah, C. Kreyenschulte, A. Brückner, H. Wang and F. Shi, *Angew. Chem. Int. Ed.*, 2019, **58**, 5251-5255.
173. X. Dai, X. Wang, J. Rabeah, C. Kreyenschulte, A. Brückner and F. Shi, *Chem. Eur. J.* 2021 **27**, 16889-16895.
174. C. B. Schandel, M. Høj, C. M. Osmundsen, A. D. Jensen and E. Taarning, *ChemSusChem*, 2020, **13**, 688-692.
175. G. Liang, A. Wang, L. Li, G. Xu, N. Yan and T. Zhang, *Angew. Chem. Int. Ed.*, 2017, **129**, 3096-3100.
176. W. Faveere, T. Mihaylov, M. Pelckmans, K. Moonen, F. Gillis-D'Hamers, R. Bosschaerts, K. Pierloot and B. F. Sels, *ACS Catal.*, 2019, **10**, 391-404.
177. S. Murahashi, N. Yoshimura, T. Tsumiyama and T. Kojima, *J. Am. Chem. Soc.*, 1983, **105**, 5002-5011.
178. G. Bitsi and G. Jenner, *J. Organomet. Chem.*, 1987, **330**, 429-435.
179. J. Muzart, *Tetrahedron*, 2009, **65**, 8313-8323.
180. S. Ding and N. Jiao, *Angew. Chem. Int. Ed.*, 2012, **51**, 9226-9237.
181. C. Ouannes and T. Wilson, *J. Am. Chem. Soc.*, 1968, **90**, 6527-6528.
182. C. S. Foote and J. W.-P. Lin, *Tetrahedron Lett.*, 1968, 3267-3270.
183. J. E. Huber, *Tetrahedron Lett.*, 1968, 3271-3272.
184. H. H. Wasserman and S. Terao, *Tetrahedron Lett.*, 1975, 1735-1738.
185. F. Li, L. Xiao and L. Liu, *Sci. Rep.*, 2016, **6**, 22876.
186. R. Franke, D. Selent and A. Börner, *Chem. Rev.*, 2012, **112**, 5675-5732.
187. C. Schneider, T. Leischner, P. Ryabchuk, R. Jackstell, K. Junge and M. Beller, *CCS Chemistry*, 2021, **3**, 512-530.
188. V. S. Sikarwar, M. Zhao, P. Clough, J. Yao, X. Zhong, M. Z. Memon, N. Shah, E. J. Anthony and P. S. Fennell, *Energy Environ. Sci.*, 2016, **9**, 2939-2977.
189. S. Püschel, S. Störtte, J. Topphoff, A. J. Vorholt and W. Leitner, *ChemSusChem*, 2021, **14**, 5226-5234.
190. M. B. Buendia, A. E. Daugaard and A. Riisager, *Catal. Lett.*, 2021, **151**, 8-16.
191. K. Dong, X. Fang, S. Gülak, R. Franke, A. Spannenberg, H. Neumann, R. Jackstell and M. Beller, *Nat. Commun.*, 2017, **8**, 14117.
192. Y. Liu and S. Mecking, *Angew. Chem. Int. Ed.*, 2019, **58**, 3346-3350.
193. J. Savard and P. Brassard, *Tetrahedron*, 1984, **40**, 3455-3464.

6. Selected publications

6.1 Scalable synthesis and polymerisation of a β -angelica lactone derived monomer



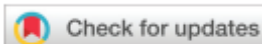
A. Dell'Acqua, † B. M. Stadler, † S. Kirchhecker, S. Tin, J. G. de Vries († equal contributions)

Green Chem. **2020**, *22*, 5267–5273.

DOI: 10.1039/D0GC00338G

Electronic supporting information for this article is available under:

<https://pubs.rsc.org/en/content/articlelanding/2020/gc/d0gc00338g>



Cite this: *Green Chem.*, 2020, **22**, 5267

Received 27th January 2020,

Accepted 19th April 2020

DOI: 10.1039/d0gc00338g

rsc.li/greenchem

Scalable synthesis and polymerisation of a β -angelica lactone derived monomer†

Andrea Dell'Acqua,[‡] Bernhard M. Stadler,[‡] Sarah Kirchhecker,[‡] Sergey Tin[‡] and Johannes G. de Vries^{‡*}

Bio-based levulinic acid is easily ring-closed to α -angelica lactone (α -AL). α -AL can be isomerized to the conjugated β -AL under the influence of base, but since this is an equilibrium mixture it is very hard to devise a scalable process that would give pure β -AL. This problem was circumvented by distilling the equilibrium mixture to obtain a 90 : 10 mixture of β - and α -AL in 88% yield. This mixture was used for Diels–Alder reactions on 3 terpenes and on cyclopentadiene in up to 100 g scale. The latter DA adduct was subjected to a ROMP reaction catalysed by the Grubbs II catalyst. The resulting polymer has some similarities to poly-norbornene but is more polar. The polymer can be processed into films with very good transparency.

Introduction

The debate about when fossil fuels will run out has been ongoing for many years. Technological advancements have made the exploitation of an increasing number of reservoirs profitable. However, there is a consensus that all the natural reservoirs may eventually become depleted, and thus a gradual switch to renewable feedstocks will be necessary. And although it will be impossible to fulfil the total global demand for fuel and energy with biomass-based analogues, there is more than enough biomass available on a yearly basis to serve as the raw material for all of the chemicals we need.¹

Platform chemicals are small molecules that can be produced in good yields from bio-based raw materials such as lignocellulose or sugars by fermentation or by using thermocatalytic reactions.^{2,3} Further (preferably catalytic) conversions of these chemicals allows the synthesis of fine chemicals,^{4–8} monomers,^{8–13} and fuels.^{14,15} Especially renewable polymers^{16–18} and adhesives¹⁹ based on them, often have novel properties which are considered an advantage beyond renewability. One very prominent example of a bio-based platform chemical is levulinic acid (LA) which can be efficiently obtained by the acid-catalysed decomposition of the C-6 sugars in lignocellulose.^{2,20–23} LA itself can be converted into a wide range of useful compounds.²⁴ The most studied and used ones are aminolevulinic acid (herbicide), 2-methyl tetrahydrofuran (solvent and fuel),^{25,26} γ -valerolactone²⁷ (solvent), ester

derivatives (plasticisers, fragrances and fuels),^{28–30} and the nylon intermediates adipic acid and caprolactam.^{31–37} LA can be converted into methyl vinyl ketone (monomer, vitamin A precursor) under oxidative conditions,³⁸ or *via* decarbonylation of the intermediate angelica lactone.^{39,40}

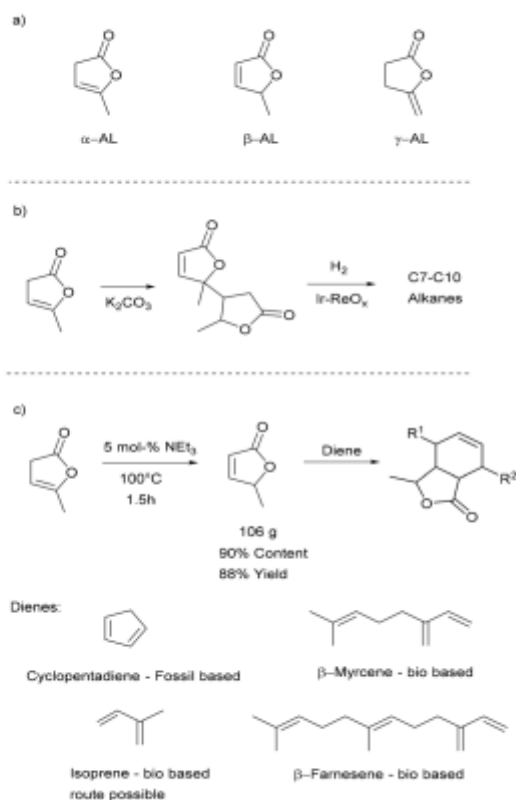
There are three isomers of angelica lactone (α -AL, β -AL, and γ -AL) which are shown in Scheme 1a. α -AL is conveniently obtained by reactive distillation of LA in high yields with water being the sole side product.^{41–43} This makes α -AL an interesting bio-based building block, which has been used as a monomer in UV-light induced, cationic and ring-opening polymerisations.⁴⁴ The UV-light induced and cationic polymerisations tend to afford only sticky colourful oligomers.^{45,46} The product obtained by anionic ring-opening polymerisation has a higher molecular weight but consists of a mixture of C–C and ester connected monomer units.⁴⁷ Such an irregular structure would make it rather challenging to use these polymers in applications where an exact control of the polymer structure is necessary. For instance, the oligomers that are typically used in the production of thermoplastic polyurethanes require well-defined end groups.⁴⁸ Higher molecular weight polyesters on the other hand are typically used in extrusion and spinning processes⁴⁹ for which high crystallinity and melting points are desirable traits, something poly α -AL may not provide due to the high stereo- and regio-irregularity. Other studies which were initiated by Mascial and co-workers focused on the utilisation of α -AL as a precursor for jet-fuels. Here α -AL is converted in the presence of K_2CO_3 to its di- and trimers, which can then be hydrodeoxygenated to the branched alkanes typically used in gasoline (Scheme 1b).^{50,51} The dimerisation step caught our attention as this reaction is known to occur *via* the β -isomer which we deem to be an interesting building block. β -AL itself has been dimerised to jet-fuels precursor and, for

Leibniz Institut für Katalyse, e. V. Albert-Einstein-Strasse 29a, 18059 Rostock, Germany. E-mail: johannes.devries@catalysis.de

† Electronic supplementary information (ESI) available. See DOI: 10.1039/d0gc00338g

‡ These authors contributed equally.





Scheme 1 a) Different isomers of angelica lactone. (b) The pioneering work of Mascal and co-workers regarding the conversion of AL to fuels. (c) Our approach to upgrade α -AL to functional monomers for ROMP.

the first time, polymerized to acrylic-type polymers by the group of Hong.⁵²

We have explored the synthesis of bio-based monomers *via* Diels-Alder reactions (Scheme 1c) to obtain lactone functionalised derivatives. Diels-Alder reactions for the preparation of bio-based monomers recently received much attention^{53–56} as they are very atom-efficient and usually can be conducted in the absence of a solvent. Such functionalised norbornenes can then be used for example as monomer for adhesives,⁵⁷ shape memory materials⁵⁸ and polymer based electrolytes in batteries.⁵⁹ Adducts containing the angelica lactone moiety have been prepared using this approach, but thus far the β -AL that was used in these reactions was not made from α -AL, likely due to the necessity to have pure β -AL.^{60–62}

We wanted to use these Diels-Alder adducts in ring-opening metathesis reactions (ROMP) to obtain bio-based norbornene polymers. They can be easily functionalised as it is known that the γ -valerolactone moiety readily undergoes reactions with primary amines.⁶³

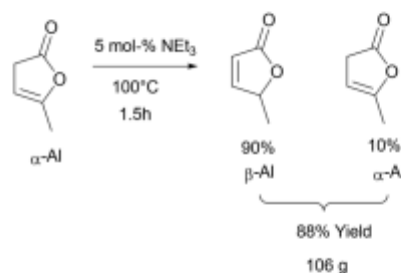
Results and discussion

α -AL and β -AL are in equilibrium with each other in the presence of base but also undergo dimerisation under the reaction conditions necessary for isomerisation, a fact that makes the

highly selective synthesis of pure β -AL from α -AL at high conversion a very challenging reaction that has not been achieved up to this date. Usually yields between 40–60% of β -AL can be achieved.^{64–66} This and the fact that in the existing protocols product separation needs to be carried out by column chromatography negatively affects the sustainability and scalability. Additionally, the formation of various azeotropes (see ESI†) of the isomers under vacuum distillation conditions results in a further yield penalty.

However, as shown in Scheme 2, we found that it is possible to obtain a high content of β -AL in the product fraction (90 mol%), if the reaction time is kept rather short and no solvent is used. The usage of triethylamine allows its easy separation during vacuum distillation preventing further dimerisation. The mixture of the two angelica lactones was thus obtained in 88% yield after distillation on a 100 g scale. A small forerun was obtained, containing mostly α -AL, which can be reused. The only side products that remain are the di- and trimers which might be interesting raw materials for fuels.^{50,67}

Next the solvent free Diels-Alder reaction of the AL-mixture containing 90% β -AL with cyclopentadiene (CPD) was investigated in the presence and absence of a catalyst (Table 1).



Scheme 2 Synthesis of a mixture enriched with β -AL.

Table 1 Screening of the reaction conditions for the DA-reaction between β -AL and CPD

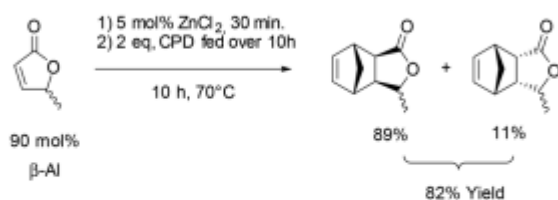
Entry	Catalyst	Eq. (CPD)	T [°C]	t [h]	Yield ^a [%]	Endo/exo ^a
1	5 mol% Al(OTf) ₃	3	RT	16	—	—
2	5 mol% Al(OTf) ₃	3	100	2	—	—
3	—	3	80	0.5	19	91/9
4	—	3	100	0.5	40 ^b	70/30
5	—	3	60	0.5	25	95/5
6	5 mol% ZnCl ₂	3	80	0.5	40	84/16
7	5 mol% ZnCl ₂	3	RT	16	63	89/11
8	5 mol% ZnCl ₂	10	RT	16	90 (86) ^b	90/10

General conditions: Reactions were carried out in closed reaction tubes and heated with microwave irradiation. ^a Determined by ¹HNMR spectroscopy. ^b Isolated by column chromatography.



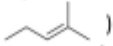
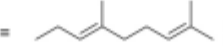
When aluminium triflate was used as the catalyst (entries 1 + 2) the contents were converted to a black charred residue and no desired product formation was observed. When no catalyst was used it was possible to obtain the product in 19 to 25% at 80 °C to 90 °C respectively (Table 1, entries 3 and 5). At a higher temperature (100 °C) it was possible to isolate 40% of the DA-adduct. A similar yield was obtained at 80 °C in 30 minutes when anhydrous zinc chloride was used as catalyst. Increasing the reaction time from 30 minutes to 16 hours only led to a yield of 63%. As it was apparent that the low yields are caused by the competing di- and trimerisation of the CPD with itself, the equivalents of CPD with respect to β -AL were increased up to 10. This resulted in 90% yield of the desired product. Since a process that uses 10 eq. of CPD is not very efficient and sustainable, we decided to perform the reaction under semi-batch conditions on a 50 g scale (see Scheme 3). After dissolving zinc chloride in the β -AL enriched mixture 2 equivalents of CPD were slowly added over 10 hours. The ZnCl_2 could be easily separated by adding acetone and any formed di- or trimers of CPD could be precipitated by simple dissolution of the product mixture in methanol. No column chromatography was necessary to obtain the product as a mixture of isomers in 82% yield. This is very fortunate as purification by distillation of the adduct is not an option since the retro-Diels-Alder reaction to β -AL commences at 136 °C (see ESI† for a DSC/TGA). Aiming for a higher renewable atom content, dienes other than cyclopentadiene have also been investigated. Use of furans was not successful under both catalysed and thermal conditions, due to rapid formation of humines (see ESI†). On the other hand, use of isoprene and terpenes (β -myrcene and farnesene) were more promising (Table 2). Upon reaction with β -AL at high temperature, full conversion was achieved. The diene oligomers formed as by-product were removed by a simple filtration through a short silica path, affording the Diels-Alder products in yields of up to 60%.

The ring-opening metathesis polymerisation (ROMP) of the DA adducts was next investigated.^{68–70} Grubbs' 2nd generation catalyst was chosen for this (Fig. 1). Dichloromethane (DCM) is the solvent of choice for this reaction, since the polymeric products normally dissolve in it, thus allowing the formation of higher molecular weight polymers. The fully bio-based adducts shown in Table 2 were not polymerizable under these conditions, probably due to the absence of the ring strain that is present in the norbornene-type structure. On the other hand, the polymerization of the Cp/ β -AL adduct was success-



Scheme 3 Synthesis of the DA-adduct with CPD on 50 g scale.

Table 2 Screening of dienes in the Diels-Alder reaction with β -AL

Entry	Diene	Yield ^a [%]
1	Isoprene (R = Me)	60
2	Myrcene (R = )	54
3	β -Farnesene (R = )	18

General conditions: reactions were carried out in 4 ml vials equipped with a septum and magnetic stirring bar placed into a stainless steel 300 ml autoclave pressurised with 20 bar of nitrogen. ^a Isolated yield.

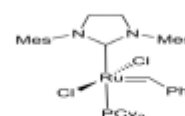
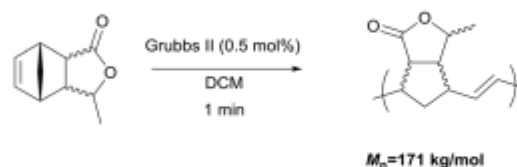


Fig. 1 Grubbs II metathesis catalyst.

ful. Interestingly, at the initial monomer concentration of 1 mol l⁻¹ after the addition of the initiator (0.5 mol% w.r.t. Cp/ β -AL) the reaction mixture formed a gel within one minute indicating a great reactivity of this monomer in ROMP reactions (see Scheme 4). To further fine tune the polymerisation conditions different solvents, commonly considered as "greener" or safer choices, beside DCM were investigated at a lower catalyst loading. These solvents and their influence on the ROMP of the CP adduct are shown in Table 3. 2-Methyltetrahydrofuran was chosen due to its similar polarity to DCM but lower toxicity⁷¹ and potential renewability. Ethyl acetate (EtOAc) was included as it is one of the safest solvents regarding flammability and toxicity,^{72,73} which is also applicable for methyl isobutyl ketone (MIBK). Although not a "green" compound in general we also included *tert*-butyl methyl ether (MTBE) since it remains still a common solvent in industry and does not form peroxides.

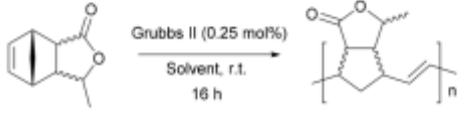
Notably, in all solvents except DCM a white precipitate appeared after a few minutes of reaction time. In all the attempts the DA adduct did polymerise, yielding white gummy materials after precipitation with cold methanol.

As expected, the polymer obtained in DCM had a substantially higher molecular weight than the one predicted assum-



Scheme 4 Initial ROMP experiment with Cp/ β -AL.



Table 3 Influence of different solvents in the ROMP of Cp/ β -AL


Entry	Solvent	Yield ^a [%]	M_n^b [kg mol ⁻¹]	M_w^b [kg mol ⁻¹]	D^b
—	Calc.	—	65.6	—	—
1	DCM	78	122	264	2.17
2	2-MeTHF	69	80.6	154	1.91
3	EtOAc	61	64.1	118	1.85
4	MIBK	52	70.9	1.46	2.06
5	MTBE	70	67.8	138	2.04

^a Isolated yield. ^b Determined by GPC (DMF/LiBr).

ing a living polymerization (Table 3, entry 1). When using 2-MeTHF the obtained molecular weight was reduced to 80.6 kg mol⁻¹. Ethyl acetate (EtOAc) and MTBE on the other hand afforded molecular weights of 64.1 kg mol⁻¹ and 67.8 kg mol⁻¹ respectively which are relatively close to the theoretical molecular weight of 65.6 kg mol⁻¹. These findings indicate that the very safe and potentially renewable solvent EtOAc does not lead to catalyst deactivation/inhibition compared to DCM.

Aiming to assess the relation between substrate to catalyst ratio and molecular weight of the polymer, different catalyst loadings were investigated. A substantial linearity in the range between 100 : 1 and 600 : 1 (mol of substrate per mol of catalyst) was achieved, showing that the final molecular weight can be controlled by varying the amount of catalyst (Fig. 2).

The obtained polymers tend to decompose at about 378 °C in a nitrogen atmosphere. No melting points were detected in the DSC analysis (as expected) confirming the amorphous nature of the polymer. In addition, a glass transition could also not be observed, which is an indication that the T_g occurs at or above the decomposition temperature (Fig. S8 and S9†). In contrast, poly-norbornene has a T_g at 35 °C. It is not easy to account for the huge difference in T_g between the two polymers. The high T_g of our polymer can possibly be explained by the stereoregular nature. For steric reasons, the polymer has to be *all trans*.

Contact angle measurement revealed that the presence of the lactone moiety in poly-Cp/ β -AL is increasing the hydrophilicity compared to poly-norbornene ($\theta(\text{Cp}/\beta\text{-AL}) = 75.7 \pm 1.9^\circ$; $\theta(\text{Cp}/\text{poly-norbornene}) = 83.9 \pm 2.3^\circ$).

As shown in Fig. 2 the polymer obtained *via* the ROMP of Cp/ β -AL can be cast into clear transparent films. Comparison with poly-norbornene (prepared with the same catalyst in DCM) shows there is no negative effect of the lactone group on transparency (Fig. 3). Therefore it might be possible to find similar applications in optical wave guides,⁷⁴ transparent coatings⁷⁵ or other applications where high transparency in a large range of wavelengths is necessary.⁷⁶

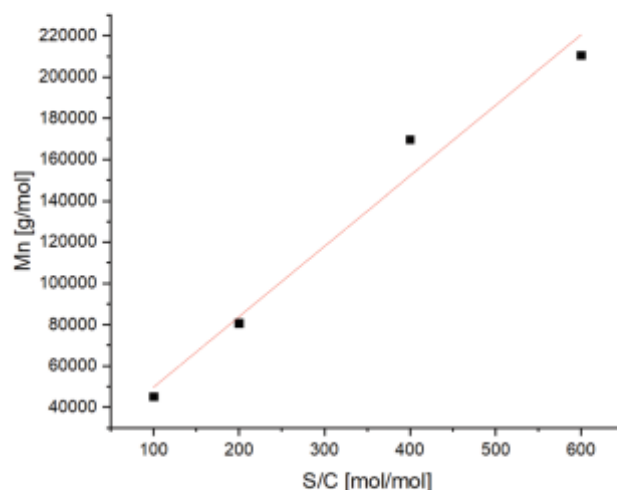


Fig. 2 Obtained M_n values via ROMP of Cp/ β -AL performed at different substrate to catalyst ratios (S/C).

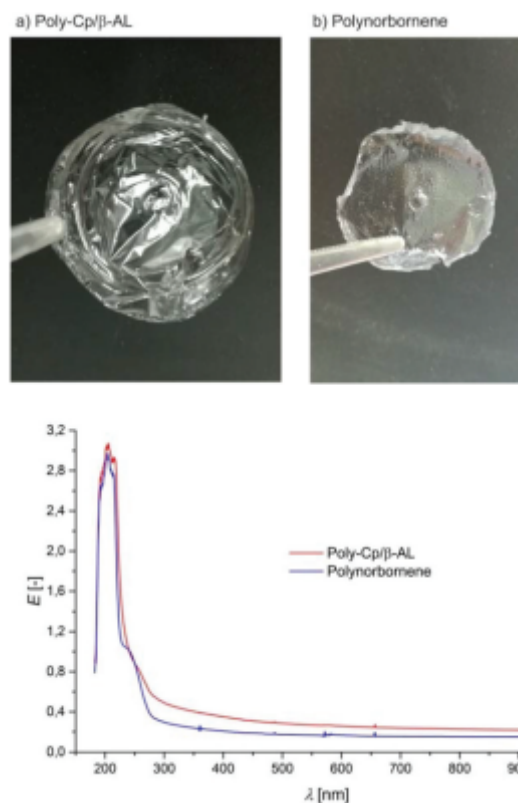


Fig. 3 Films obtained from (a) poly-Cp/ β -AL and (b) polynorbornene obtained by solution castings. Below: absorbance spectra of these films in the range from 150–1000 nm. E = extinction.

Conclusions

It is still challenging to obtain pure β -AL from renewable α -AL in a scalable and sustainable procedure. In this work we show that a 90 : 10 mixture of the two can be prepared in a scalable



procedure. This mixture is rich enough in β -AL to be used efficiently as dienophile in Diels–Alder reactions with cyclopentadiene, isoprene, myrcene and β -farnesene. The adduct obtained with cyclopentadiene can be efficiently polymerized in a ROMP reaction catalysed by the Grubbs II catalyst, either in DCM or alternatively using the renewable solvents 2-MeTHF or ethyl acetate. A linear relationship between M_n and the amount of catalyst is observed between a monomer to catalyst ratio of 100 to 600, thus allowing control of the molecular weight. The resulting polymers can be processed into films that have high transparency over a wide range of wavelengths. Compared with poly-norbornene the lactone moiety increases (surface) hydrophilicity, which could give rise to various benefits; for instance, higher miscibility with polar additives or better interaction with certain (wet) surfaces in coating applications. The lactone moiety does not only increase the bio-based carbon content of the materials, but it also enables further derivatization which gives easy access to a plethora of different polymers.

Experimental section

Preparation of a mixture of angelica lactones with 90 mol% content of the β -isomer

α -Angelica lactone (98%, 120 g, 1.2 mol) was added to a 250 ml two neck flask equipped with a condenser and a magnetic stirrer followed by the addition of triethyl amine (5 mol%, 8.5 ml). The mixture was heated to 100 °C under an argon atmosphere and monitored by $^1\text{H-NMR}$. After 1.5 hours a ratio of β/α -angelica lactone of 90–95/10–5 was reached and the condenser exchanged with a distillation head. Subsequent vacuum distillation at 6×10^{-2} mbar yielded two fractions: 38–42 °C containing mainly the α -isomer (this fraction can be reused for the next isomerisation run) and a fraction at 45–50 °C containing a mixture of angelica lactones with 90 mol% content of the β -isomer (106 g, 88% of theory).

$^1\text{H NMR}$ (400 MHz, CD_2Cl_2 , signals of β -isomer are reported) δ 7.46 (dd, $J = 5.7, 1.5$ Hz, 1H), 6.04 (dd, $J = 5.7, 2.0$ Hz, 1H), 5.11 (qt, $J = 6.9, 2.0, 1.5$ Hz, 1H), 1.41 (d, $J = 6.9$ Hz, 3H). $^{13}\text{C NMR}$ (101 MHz, CD_2Cl_2) δ 173.3, 158.0, 121.3, 80.0, 19.0.

Diels–Alder reaction between β -angelica lactone and cyclopentadiene

In a dry and argon purged 10 ml reaction tube the angelica lactone mixture (β -AL = 90%, 10 mmol, 900 μl) and the desired catalyst were mixed. Freshly prepared CPD (3.0–10 eq. 2.5–8.3 ml) was added, the tube was sealed and heated with a microwave oven to the desired reaction temperature where it is kept for the indicated time. The 2 diastereomers of the product were separated by flash column chromatography (heptane/ethyl acetate 8:2), affording the *endo* and *exo* isomers (each of them is a racemic mixture of 2 stereoisomers) adduct as colourless oils (*endo*: 949 mg, 5.9 mmol, 30%; *exo*: 119 mg, 0.7 mmol, 7%; *endo/exo* 89/11).

Exo: $^1\text{H NMR}$ (300 MHz, CD_2Cl_2) δ 6.21–6.04 (m, 2H), 4.17 (qd, $J = 6.4, 3.2$ Hz, 1H), 3.24–3.03 (m, 1H), 2.82 (dtq, $J = 3.1, 1.5, 0.8$ Hz, 1H), 2.59 (dt, $J = 8.3, 1.3$ Hz, 1H), 2.08–1.97 (m, 1H), 1.50–1.35 (m, 7H), 1.30 (d, $J = 6.4$ Hz, 3H). $^{13}\text{C NMR}$ (75 MHz, CD_2Cl_2) δ 177.4, 136.4, 134.9, 78.9, 51.6, 48.5, 48.2, 46.0, 45.6, 22.8.

Endo: $^1\text{H NMR}$ (300 MHz, CD_2Cl_2) δ 6.22–6.09 (m, 2H), 3.95 (qd, $J = 6.5, 3.1$ Hz, 1H), 3.26–2.97 (m, 3H), 2.67–2.54 (m, 1H), 1.57–1.46 (m, 1H), 1.39–1.29 (m, 1H), 1.25 (d, $J = 6.5$ Hz, 3H). $^{13}\text{C NMR}$ (75 MHz, CDCl_3) δ 177.3, 137.6, 137.5, 80.7, 50.0, 48.9, 47.6, 46.3, 43.1, 23.2.

Semi continuous synthesis of the β -angelica lactone CPD adduct

A 500 mL 2-neck round bottom flask was filled with dicyclopentadiene (100 mL) and iron(0) powder and equipped with a distillation setup. Cyclopentadiene was obtained by thermal cracking of its corresponding dimer at 180 °C and then condensed into a dropping funnel. 2 equivalents (84 mL, 67 g, 1.0 mol) were dropped over 10 hours into a 1 liter 3-necks round bottom flask containing the angelica lactone mixture (β -AL = 90%; 50 g, 0.5 mol) and zinc(II) chloride (3.5 g, 0.03 mol, 0.05 eq.) while heating up to 70 °C. Once the addition was complete, the reaction was stirred for another 10 hours and monitored by GC. After cooling down to room temperature, acetone (80–150 ml) was added to precipitate the Lewis acid catalyst. The remaining cyclopentadiene and α -angelica lactone were removed by vacuum distillation (50 °C/0.06 mbar) and the remaining cyclopentadiene dimers were precipitated by addition of ice-cold methanol (100 ml) followed by filtration. Solvent removal afforded the product as an orange liquid (69 g, 0.4 mol, 82% yield, *endo* : *exo* 89/11).

Ring-opening metathesis polymerization of the Cp/ β AL adduct

To a stirred solution of Grubbs II catalyst (4.7 mg, 0.006 mmol, 0.25 mol%) in the desired solvent (Table 3) the Cp/ β AL adduct (0.2 mL, 2.2 mmol, 1 eq.) was added under argon atmosphere. The reaction was stirred overnight. In few minutes after the addition, all the solutions turned opalescent and a whiteish precipitate appeared, except for the reaction in DCM. The reaction mixtures were then concentrated *in vacuo* and washed several times with methanol (using DCM to re-dissolve the polymer). All the reaction afforded a whiteish, gummy solid. A small portion of each sample was dissolved in a DMF/LiBr solution and analyzed by GPC. $^1\text{H-NMR}$ spectra were recorded in CDCl_3 .

$^1\text{H NMR}$ (300 MHz, CDCl_3) δ 5.84–5.12 (m, 2H, $-\text{CH}=\text{CH}-$), 4.53–4.09 (m, 1H, $\text{O}-\text{CH}-\text{CH}_3$), 3.33–2.38 (m, 4H, ring junction- and allylic- CH), 1.89 (m, 2H, bridged- CH_2), 1.62–0.92 (m, 3H, CH_3).

Film formation procedure

Films were obtained by casting a saturated solution of the polymer in DCM into a Teflon mold (depth 1 mm), letting the solvent evaporate over 4 hours.



Conflicts of interest

The authors declare no conflict of interest.

Acknowledgements

The authors greatly appreciate the help of C. Wulf with the GPC and DSC measurements and to A. Wotzka for further DSC and TGA measurements. AD and SK are highly thankful to Henkel AG & Co for the financial support. The authors are grateful to Andreas Taden, Kenji Ito, Adrian Brandt and Horst Beck (Henkel AG & Co) for the useful discussions.

This research was funded by the Bio-Based Industries Joint Undertaking under the European Union's Horizon 2020 research and innovation program, grant agreement no. 720695 (GreenSolRes).

Notes and references

- 1 P. N. R. Vennestrøm, C. M. Osmundsen, C. H. Christensen and E. Taarning, *Angew. Chem., Int. Ed.*, 2011, **50**, 10502–10509.
- 2 *Top Value-Added Chemicals from Biomass Vol. I—Results of Screening for Potential Candidates from Sugars and Synthesis Gas*, ed. T. Werpy and G. Petersen, U. S. Department of Energy (DOE) by the National Renewable Energy Laboratory a DOE national Laboratory, 2004.
- 3 J. J. Bozell and G. R. Petersen, *Green Chem.*, 2010, **12**, 539–554.
- 4 W. G. Fan, C. Verrier, Y. Queneau and F. Popowycz, *Curr. Org. Synth.*, 2019, **16**, 583–614.
- 5 C.-H. Zhou, X. Xia, C.-X. Lin, D.-S. Tong and J. Beltramini, *Chem. Soc. Rev.*, 2011, **40**, 5588–5617.
- 6 B. Wozniak, S. Tin and J. G. de Vries, *Chem. Sci.*, 2019, **10**, 6024–6034.
- 7 P. Gallezot, *Catal. Today*, 2007, **121**, 76–91.
- 8 J. G. de Vries, *Chem. Rec.*, 2016, **16**, 2787–2800.
- 9 I. Delidovich, P. J. C. Hausoul, L. Deng, R. Pfützenreuter, M. Rose and R. Palkovits, *Chem. Rev.*, 2016, **116**, 1540–1599.
- 10 X. Zhang, M. Fevre, G. O. Jones and R. M. Waymouth, *Chem. Rev.*, 2018, **118**, 839–885.
- 11 B. M. Stadler, C. Wulf, T. Werner, S. Tin and J. G. de Vries, *ACS Catal.*, 2019, **9**, 8012–8067.
- 12 O. R. Schade, P.-K. Dannecker, K. F. Kalz, D. Steinbach, M. A. R. Meier and J.-D. Grunwaldt, *ACS Omega*, 2019, **4**, 16972–16979.
- 13 T. Asano, H. Takagi, Y. Nakagawa, M. Tamura and K. Tomishige, *Green Chem.*, 2019, **21**, 6133–6145.
- 14 W. Leitner, J. Klankermayer, S. Pischinger, H. Pitsch and K. Kohse-Höinghaus, *Angew. Chem., Int. Ed.*, 2017, **56**, 5412–5452.
- 15 K. I. Galkin and V. P. Ananikov, *ChemSusChem*, 2019, **12**, 185–189.
- 16 Y. Zhu, C. Romain and C. K. Williams, *Nature*, 2016, **540**, 354.
- 17 J. A. Galbis, M. d. G. García-Martín, M. V. de Paz and E. Galbis, *Chem. Rev.*, 2016, **116**, 1600–1636.
- 18 A. Gandini, T. M. Lacerda, A. J. F. Carvalho and E. Trovatti, *Chem. Rev.*, 2016, **116**, 1637–1669.
- 19 L. A. Heinrich, *Green Chem.*, 2019, **21**, 1866–1888.
- 20 D. J. Hayes, S. W. Fitzpatrick, M. H. B. Hayes and J. R. H. Ross, in *Biorefineries - Industrial Processes and Products: Status Quo and Future Directions*, ed. B. Kamm, P. R. Gruber and M. Kamm, Wiley-VCH, Weinheim, 2008, vol. 1, pp. 139–164.
- 21 F. D. Pileidis and M.-M. Titirici, *ChemSusChem*, 2016, **9**, 562–582.
- 22 F. Yu, J. Thomas, M. Smet, W. Dehaen and B. F. Sels, *Green Chem.*, 2016, **18**, 1694–1705.
- 23 J. J. Bozell, L. Moens, D. C. Elliott, Y. Wang, G. G. Neuenschwander, S. W. Fitzpatrick, R. J. Bilski and J. L. Jarnefeld, *Resour., Conserv. Recycl.*, 2000, **28**, 227–239.
- 24 A. T. Adeleye, H. Louis, O. U. Akakuru, I. Joseph, O. C. Enudi and D. P. Michael, *AIMS Energy*, 2019, **7**, 165–185.
- 25 D. F. Aycock, *Org. Process Res. Dev.*, 2007, **11**, 156–159.
- 26 V. Pace, P. Hoyos, L. Castoldi, P. Dominguez de Maria and A. R. Alcantara, *ChemSusChem*, 2012, **5**, 1369–1379.
- 27 D. M. Alonso, S. G. Wettstein and J. A. Dumesic, *Green Chem.*, 2013, **15**, 584–595.
- 28 P. Bloom, To Archer-Daniels-Midland Company, WO2007094922A2, 2007.
- 29 A. Démolis, N. Essayem and F. Rataboul, *ACS Sustainable Chem. Eng.*, 2014, **2**, 1338–1352.
- 30 X. Yi, M. G. Al-Shaal, W. Ciptonugroho, I. Delidovich, X. Wang and R. Palkovits, *ChemSusChem*, 2017, **10**, 1494–1500.
- 31 J.-P. Lange, J. Z. Vestering and R. J. Haan, *Chem. Commun.*, 2007, 3488–3490.
- 32 J. G. de Vries, N. Sereinig, E. W. M. van de Vondervoort and M. C. C. Janssen, To DSM IP Assets BV, WO2012131028A1, 2012.
- 33 P. K. Wong, C. Li, L. Stubbs, M. van Meurs, D. G. Anak Kumbang, S. C. Y. Lim and E. Drent, To Agency for Science, Technology and Research, WO2012134397A1, 2012.
- 34 Y. Yang, X. R. Wei, F. X. Zeng and L. Deng, *Green Chem.*, 2016, **18**, 691–694.
- 35 J. D. Nobbs, N. Z. B. Zainal, J. Tan, E. Drent, L. P. Stubbs, C. Li, S. C. Y. Lim, D. G. A. Kumbang and M. van Meurs, *ChemistrySelect*, 2016, **1**, 539–544.
- 36 A. Marckwordt, F. El Ouahabi, H. Amani, S. Tin, N. V. Kalevaru, P. C. J. Kamer, S. Wohlrab and J. G. de Vries, *Angew. Chem., Int. Ed.*, 2019, **58**, 3486–3490.
- 37 J. Lin, H. Song, X. Shen, B. Wang, S. Xie, W. Deng, D. Wu, Q. Zhang and Y. Wang, *Chem. Commun.*, 2019, **55**, 11017–11020.
- 38 Y. Gong, L. Lin and B. Zhang, *Chin. J. Chem.*, 2012, **30**, 327–332.
- 39 J. A. Dumesic and R. M. West, To Wisconsin Alumni Research Foundation, WO002011087962A1, 2011.
- 40 W. Skorjanetz and G. Ohloff, *Helv. Chim. Acta*, 1975, **58**, 1272–1275.



- 41 J. H. Helberger, S. Ulubay and H. C. Civelekoglu, *Justus Liebigs Ann. Chem.*, 1949, **561**, 215–220.
- 42 D. Sun, Y. Takahashi, Y. Yamada and S. Sato, *Appl. Catal., A*, 2016, **526**, 62–69.
- 43 C. G. S. Lima, J. L. Monteiro, T. de Melo Lima, M. Weber Paixao and A. G. Correa, *ChemSusChem*, 2018, **11**, 25–47.
- 44 V. E. Tarabanko and K. L. Kaygorodov, *Chem. Sustainable Dev.*, 2010, 321–328.
- 45 C. S. Marvel and C. L. Levesque, *J. Am. Chem. Soc.*, 1939, **61**, 1682–1684.
- 46 Y. Yokoyama, M. Okada and H. Sumitomo, *Makromol. Chem.*, 1975, **176**, 3537–3550.
- 47 K. L. Kaygorodov, V. E. Tarabanko and N. Tarabanko, *Cogent Chem.*, 2018, **4**, 1443689.
- 48 N. Adam, G. Avar, H. Blankenheim, W. Friederichs, M. Giersig, E. Weigand, M. Halfmann, F.-W. Wittbecker, D. Larimer, U. Maier, S. Meyer-Ahrens, K.-L. Noble and H.-G. Wussow, in *Ullmann's Encyclopedia of Industrial Chemistry*, 2005, DOI: 10.1002/14356007.a21_665.pub2.
- 49 E. Gubbels, T. Heitz, M. Yamamoto, V. Chilekar, S. Zorbakhsh, M. Gepraegs, H. Köpnick, M. Schmidt, W. Brüggling, J. Rüter and W. Kaminsky, in *Ullmann's Encyclopedia of Industrial Chemistry*, 2018, pp. 1–30, DOI: 10.1002/14356007.a21_227.pub2.
- 50 M. Mascal, S. Dutta and I. Gandarias, *Angew. Chem.*, 2014, **126**, 1885–1888.
- 51 J. Xu, N. Li, X. Yang, G. Li, A. Wang, Y. Cong, X. Wang and T. Zhang, *ACS Catal.*, 2017, **7**, 5880–5886.
- 52 X.-J. Wang and M. Hong, *Angew. Chem., Int. Ed.*, 2020, **59**, 2664–2668.
- 53 A. D. Pehere, S. Xu, S. K. Thompson, M. A. Hillmyer and T. R. Hoye, *Org. Lett.*, 2016, **18**, 2584–2587.
- 54 Y. Bai, M. De Bruyn, J. H. Clark, J. R. Dodson, T. J. Farmer, M. Honoré, I. D. V. Ingram, M. Naguib, A. C. Whitwood and M. North, *Green Chem.*, 2016, **18**, 3945–3948.
- 55 M. Iqbal, R. A. Knigge, H. J. Heeres, A. A. Broekhuis and F. Picchioni, *Polymers*, 2018, **10**, 1177.
- 56 A. Blanpain, J. H. Clark, T. J. Farmer, Y. Guo, I. D. V. Ingram, J. E. Kendrick, S. B. Lawrenson, M. North, G. Rodgers and A. C. Whitwood, *ChemSusChem*, 2019, **12**, 2393–2401.
- 57 N. R. Grove, P. A. Kohl, S. A. Bidstrup Allen, S. Jayaraman and R. Shick, *J. Polym. Sci., Part B: Polym. Phys.*, 1999, **37**, 3003–3010.
- 58 D. Yang, W. Huang, J. Yu, J. Jiang, L. Zhang and M. Xie, *Polymer*, 2010, **51**, 5100–5106.
- 59 D. Rosenbach, N. Mödl, M. Hahn, J. Petry, M. A. Danzer and M. Thelakkat, *ACS Appl. Energy Mater.*, 2019, **2**, 3373–3388.
- 60 Z. Chen and R. M. Ortuño, *Tetrahedron: Asymmetry*, 1994, **5**, 371–376.
- 61 T. Řezanka and K. Sigler, *Eur. J. Org. Chem.*, 2006, 4277–4284.
- 62 H. Yanai, A. Takahashi and T. Taguchi, *Tetrahedron*, 2007, **63**, 12149–12159.
- 63 M. Chalid, H. J. Heeres and A. A. Broekhuis, *J. Appl. Polym. Sci.*, 2012, **123**, 3556–3564.
- 64 Y. Wu, R. P. Singh and L. Deng, *J. Am. Chem. Soc.*, 2011, **133**, 12458–12461.
- 65 L. Zhou, L. Lin, J. Ji, M. Xie, X. Liu and X. Feng, *Org. Lett.*, 2011, **13**, 3056–3059.
- 66 C. R. Jones, M. D. Greenhalgh, J. R. Bame, T. J. Simpson, R. J. Cox, J. W. Marshall and C. P. Butts, *Chem. Commun.*, 2016, **52**, 2920–2923.
- 67 B. Lu, J. Li, G. Lv, Y. Qi, Y. Wang, T. Deng, X. Hou and Y. Yang, *RSC Adv.*, 2016, **6**, 93956–93962.
- 68 I. Choinopoulos, *Polymers*, 2019, **11**, 298.
- 69 A. K. Pearce, J. C. Foster and R. K. O'Reilly, *J. Polym. Sci., Part A: Polym. Chem.*, 2019, **57**, 1621–1634.
- 70 J.-A. Song, B. Park, S. Kim, C. Kang, D. Lee, M.-H. Baik, R. H. Grubbs and T.-L. Choi, *J. Am. Chem. Soc.*, 2019, **141**, 10039–10047.
- 71 V. Antonucci, J. Coleman, J. B. Ferry, N. Johnson, M. Mathe, J. P. Scott and J. Xu, *Org. Process Res. Dev.*, 2011, **15**, 939–941.
- 72 F. P. Byrne, S. Jin, G. Paggiola, T. H. M. Petchey, J. H. Clark, T. J. Farmer, A. J. Hunt, C. R. McElroy and J. Sherwood, *Sustainable Chem. Processes*, 2016, **4**, 7.
- 73 C. M. Alder, J. D. Hayler, R. K. Henderson, A. M. Redman, L. Shukla, L. E. Shuster and H. F. Sneddon, *Green Chem.*, 2016, **18**, 3879–3890.
- 74 M. Singh and K. Weidner, in *Optical Interconnects for Data Centers*, ed. T. Tekin, R. Pitwon, A. Håkansson and N. Pleros, Woodhead Publishing, 2017, pp. 157–170, DOI: 10.1016/B978-0-08-100512-5.00006-1.
- 75 G. Sung, M.-C. Choi, S. Nagappan, W.-K. Lee, M. Han and C.-S. Ha, *Polym. Bull.*, 2012, **70**, 619–630.
- 76 M.-C. Choi, J.-C. Hwang, C. Kim, S. Ando and C.-S. Ha, *J. Polym. Sci., Part A: Polym. Chem.*, 2010, **48**, 1806–1814.




 Cite this: *Chem. Commun.*, 2021, 57, 10524

 Received 14th July 2021,
Accepted 11th September 2021

DOI: 10.1039/d1cc03820f

rsc.li/chemcomm

Ozonolysis of α -angelica lactone: a renewable route to malonates†‡

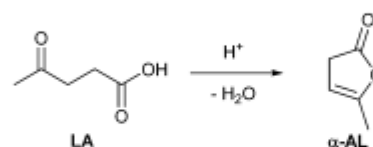
 Andrea Dell'Acqua,[†] Lukas Wille,[†] Bernhard M. Stadler,[†] Sergey Tin[†] and Johannes G. de Vries^{†*}

Industrially relevant intermediates such as malonic acid, malonates and 3-oxopropionates can be easily accessed by ozonolysis of α -angelica lactone, derived from the platform chemical levulinic acid. The roles of the solvent and of the quenching conditions are of key importance for the outcome of the reaction.

In order to become climate neutral by the year 2050, the chemical industry will have to abandon the use of fossil raw materials and thus, future chemical production processes will have to be based on renewable raw materials.¹ Although it would be possible to completely strip the biomass from oxygen to obtain a raw material that is similar to the current, it would be much better to leave at least some oxygen atoms in place since the first functionalisation of hydrocarbons is oxygenation anyway. Based on this, the concept of “platform chemicals”, was developed. These are small functional molecules, produced in a straightforward manner and in high yields from renewable sources such as sugars or lignocellulose.^{2,3} Further modifications of platform chemicals allow the synthesis of a broad scope of fine and bulk chemicals,^{4–7} monomers,^{8,9} and fuels.^{10,11} Levulinic acid (**LA**) is a C5 platform chemical that can be obtained in good yields from C6 sugars, even directly from lignocellulose by treatment with acid at higher temperatures. It can also be obtained from furfural.^{2,12–15} **LA** has been converted into a number of useful chemicals, *e.g.* solvents, monomers, fuels and fine chemicals.^{16–26} α -Angelica lactone (**α -AL**) can be obtained by reactive distillation of **LA** from phosphoric acid (Scheme 1).^{27–29} The reaction is high yielding and atom economic. **AL** can be used as a precursor for jet-fuel,^{30–32} as a monomer or precursor in different polymerizations (including anionic, cationic, UV-induced and ROMP).^{33–38} In our previous report, the C=C bond was used as reactive

handle to further functionalize **AL**.³⁸ Another possible way to upgrade α -**AL** to useful chemicals is the cleavage of the double bond under oxidative conditions. Ozonolysis represents an atom economic, relatively cheap, and easy-to-scale procedure to access carboxylic acids, ketones, aldehydes and alcohols. It has been widely applied on both lab- and industrial scale.^{39,40} The reaction has been used for the cleavage of unsaturated fatty acids, *e.g.* oleic acid to pelargonic and azelaic acid.^{41–44} Concerning biomass conversion, Heeres and co-workers efficiently applied ozonolysis in a continuous flow approach for the depolymerization of lignin.⁴⁵ Ozonolysis of α -**AL** under oxidative conditions should result in the formation of malonic acid (**MA**) and acetic acid. **MA** and its esters are widely employed in fine chemical synthesis, *e.g.* in pharmaceutical intermediates, cosmetics, agrochemicals *etc.*, with an annual estimated market of more than 20.000 t a⁻¹. They are produced on industrial scale from the petrochemical chloroacetic acid, either by cyanation followed by hydrolysis or by alkoxyacylation.⁴⁶ The fermentative production of **MA** and its esters has been reported, however, productivity of these processes is low and in addition two equivalents of salt waste are produced as a result of the need for neutralisation during the fermentation.^{47,48} Catalytic oxidation of fermentative hydroxypropionic acid has also been reported but not implemented.⁴⁹ Hence, the ozonolysis of α -**AL** could provide an atom economic pathway to produce **MA** without the usage of toxic and corrosive chemicals such as chloroacetic acid or HCN.

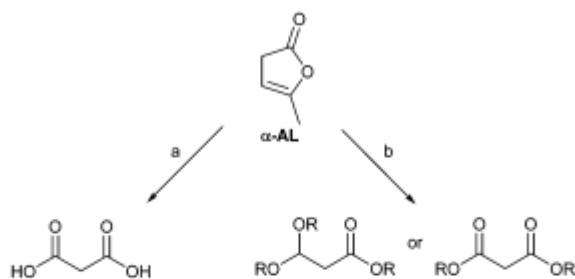
Reductive workup of the ozonolysis reaction on the other hand should yield 3-oxopropionates, that could be valuable precursors to 3-hydroxy propionates. These compounds are


 Scheme 1 Synthesis of α -AL from levulinic acid.

Leibniz Institut für Katalyse, e. V. Albert-Einstein-Strasse 29a, 18059 Rostock, Germany. E-mail: johannes.devries@katalyse.de

† Dedicated to Prof. Christian Bruneau for his outstanding contributions to catalysis.

‡ Electronic supplementary information (ESI) available: Procedures and spectra. See DOI: 10.1039/d1cc03820f



Scheme 2 Synthesis of malonates and oxo-propanoates by ozonolysis of α -AL. (a) Ozonolysis in aprotic media; (b) ozonolysis in protic media (R = H, alkyl).

starting materials for the preparation of bio-based acrylonitrile and acrylic acid.^{50,51} However, to the best of our knowledge, the ozonolysis of angelica lactones has not yet been reported in literature. Herein, we report on the ozonolysis of α -AL under different experimental conditions, obtaining either malonates or 3-oxopropionates depending on the reaction conditions (Scheme 2). It has been well-established that the choice of the solvent is crucial for controlling the outcome of the reaction.^{40,52} The use of non-participating solvents, such as hydrocarbons or halogenated solvents, affords intermediate ozonides that are then quenched by an additional oxidising or reducing agent. On the other hand, in alcoholic or aqueous medium, the ozonide immediately reacts with the solvent producing 1 equivalent of hydrogen peroxide and the carbonyl compound (or its acetal).

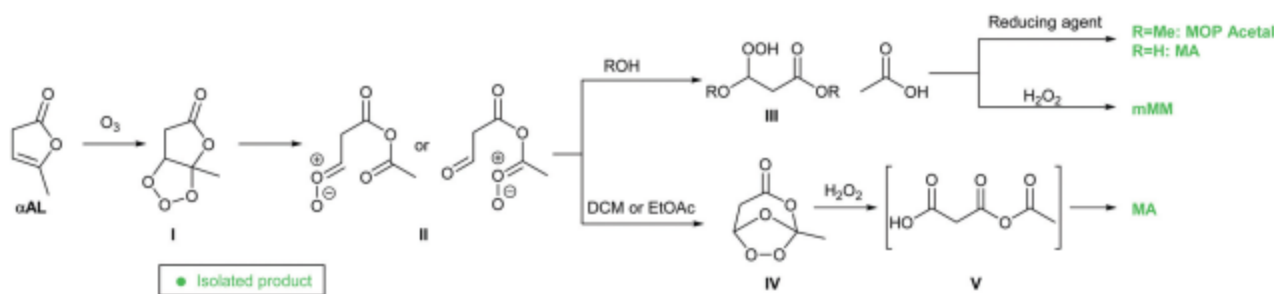
Initial screening was conducted at -78 °C using dichloromethane as non-participating solvent (Table 1, entry 1) and quenching with $\text{H}_2\text{O}_2/\text{H}_2\text{O}$. Due to the high polarity of MA, its extraction from the water phase was problematic. Thus, the solvent was changed to the more polar ethyl acetate (Table 1, entry 2). Gratifyingly, MA could be extracted in high yield (up to 90%). The intermediate anhydride V (Scheme 3) was anticipated to be too unstable to be isolated after exposing the

reaction to aqueous conditions. Indeed, the NMR signal accounting for acetic acid was detected after solvent removal. Separation of acetic acid from the malonic acid can be achieved by extensive drying *in vacuo*, until a white fine powder is obtained. As shown by Kula,⁵³ the reaction can be safely and efficiently performed between -20 and $+10$ °C. Increasing the temperature to 0 °C afforded MA in similar yields (Table 1, entry 3). Reductive quenching (with dimethyl sulfide or sodium borohydride) was attempted, aiming respectively to 3-oxo- or 3-hydroxypropionic acid, which are also useful building blocks in organic and polymer chemistry.⁵⁴ In contrast to the oxidative quenching, the desired aldehyde (Table 1, entries 4–6) or alcohol (Table 1, entry 7) was never detected, possibly due to the poor stability of the aldehyde under acidic conditions. The optimized reaction conditions were successfully scaled up to 25 g (Table 1, entry 8). Participating solvents were then investigated, as shown in Table 2. Using methanol at -78 °C afforded a mixture in which the dimethyl acetal ester was the major product (entry 1). Increasing the temperature to 0 °C resulted in a cleaner reaction: no aldehyde signal was detected by NMR (entry 2). The MOP-acetal can be conveniently obtained in a pure form by extracting the water phase with ethyl acetate. Aiming to prepare dimethyl malonate, the reaction was quenched with hydrogen peroxide solution, which combined with the acetic acid produced by hydrolysis of the anhydride was expected to oxidize the acetal. Indeed, monomethyl malonate (mMM, resulting from hydrolytic cleavage of the anhydride) was isolated in 52% yield. MM can be subsequently obtained in high yield by stirring the crude in acidic methanol. Switching the solvent to ethanol leads to the more valuable ethyl acetate as by-product, even though the yield is somewhat lower (entry 4). Water can be used as solvent as well (Table 2, entries 5 and 6). Surprisingly, the oxidation product MA was obtained, in contrast with the expected aldehyde (or its corresponding hydrate). The yield of MA obtained in water was somewhat lower than observed with non-participating solvents. This is caused by the hydrolysis of the lactone to LA, which was observed by GC-MS. The use of a co-solvent was shown to be important to prevent this side reaction, and MA was obtained in 91% isolated yield by using an acetonitrile/water mixture (Table 2, entry 8). To further investigate this unexpected behaviour, the reaction was performed in D_2O and a ^{13}C NMR spectrum was measured directly after the ozonolysis step. The resulting spectrum (ESI†, pp. S7–S8) shows signals compatible with the expected hydrated aldehyde (MOP-H) and acetic acid. After workup of the reaction mixture (excess of dimethyl sulphide, as in Table 2 entry 6), NMR shows malonic acid as the sole product (p. S8, ESI†). This observation seems to corroborate the hypothesis that MOP has low stability under the reaction and work-up conditions, leading to its oxidation to MA. According to the established mechanism for the ozonolysis reaction,^{39,40} possible pathways that account for the observed products are proposed in Scheme 3 (p. S9 for further details, ESI†). Molozonide I readily breaks down in carbonyl oxides II. The use of nucleophilic solvents affords hydroperoxide III that can be effectively quenched under reductive or oxidative

Table 1 Ozonolysis of α -AL in non-participating solvents

Entry ^a	Solvent	Temperature (°C)	Work-up	Product	MA (%)
1	DCM	-78	$\text{H}_2\text{O}_2/\text{H}_2\text{O}$	MA	89
2	EA	-78	$\text{H}_2\text{O}_2/\text{H}_2\text{O}$	MA	90
3	EA	0	$\text{H}_2\text{O}_2/\text{H}_2\text{O}$	MA	90
4	DCM	-78	Me_2S	—	—
5	EA	-78	Me_2S	—	—
6	EA	0	Me_2S	—	—
7	EA	0	NaBH_4	—	—
8 ^b	EA	0	$\text{H}_2\text{O}_2/\text{H}_2\text{O}$	MA	86

^a Reaction conditions: α -AL 25.5 mmol, $2 \text{ mL min}^{-1} \text{ O}_3$ bubbled through the solution; reaction times 30–60 min (titration with KI); quenched with 10 eq. of quenching agent. ^b Reaction performed on 25 g scale.



Scheme 3 Proposed mechanism.

Table 2 Ozonolysis of α -AL in participating solvents

Entry ^a	Solvent	Temperature (°C)	Work-up	Product		Yield (%)
				R = H: MA R = Me: MM	R = Me: MOP-Acetal R = Et: EOP-Acetal	
1	MeOH	-78	Me ₂ S	MOP-acetal		43
2	MeOH	0	Me ₂ S	MOP-acetal		46
3	MeOH	0	H ₂ O ₂ /H ₂ O	mMM		52
4	EtOH	0	Me ₂ S	EOP-acetal		21
5	H ₂ O	0	NaHSO ₃	MA		67
6	H ₂ O	0	Me ₂ S	MA		77
7	EA + 10% H ₂ O	0	NaHSO ₃	MA		63
8	ACN + 5% H ₂ O	0	NaHSO ₃	MA		91

^a Reaction conditions: α -AL 25.5 mmol, 2 mL min⁻¹ O₃ bubbled through the solution; reaction times 30–60 min (titration with KI); quenched with 10 eq. of quenching agent.

conditions. Highly energetic trioxolane IV is formed in non-participating solvents. Its cleavage leads to anhydride V as intermediate, which is eventually cleaved by water during the workup phase.

Malonic acid and 3-oxopropionic acid derivatives were prepared starting from levulinic acid derived α -angelicalactone in good to high yields by ozonolysis. This operationally simple, mild, and atom economic protocol represents a way to access these high value intermediates in a 100% renewable approach. The only by-products are acetic acid or acetates, which themselves have industrial value, and can be easily separated by distillation. A variety of solvents were proven to be effective, including alcohols and water.

The authors are thankful to S. Wohlrab and A. Wotzka for kindly lending the ozonizer apparatus and helping to set it up. AD is grateful to Henkel AG & Co for financial support.

Conflicts of interest

There are no conflicts to declare.

References

1 P. N. R. Vennestrøm, C. M. Osmundsen, C. H. Christensen and E. Taarning, *Angew. Chem., Int. Ed.*, 2011, **50**, 10502–10509.

- 2 *Top Value-Added Chemicals from Biomass Vol. I—Results of Screening for Potential Candidates from Sugars and Synthesis Gas*, ed. T. Werpy and G. Petersen, U. S. Department of Energy (DOE) by the National Renewable Energy Laboratory a DOE national Laboratory, 2004.
- 3 J. J. Bozell and G. R. Petersen, *Green Chem.*, 2010, **12**, 539–554.
- 4 B. Wozniak, S. Tin and J. G. de Vries, *Chem. Sci.*, 2019, **10**, 6024–6034.
- 5 C.-H. Zhou, X. Xia, C.-X. Lin, D.-S. Tong and J. Beltramini, *Chem. Soc. Rev.*, 2011, **40**, 5588–5617.
- 6 P. Gallezot, *Catal. Today*, 2007, **121**, 76–91.
- 7 P. J. Deuss, K. Barta and J. G. de Vries, *Catal. Sci. Technol.*, 2014, **4**, 1174–1196.
- 8 I. Delidovich, P. J. C. Hausoul, L. Deng, R. Pfützenreuter, M. Rose and R. Palkovits, *Chem. Rev.*, 2016, **116**, 1540–1599.
- 9 B. M. Stadler, C. Wulf, T. Werner, S. Tin and J. G. de Vries, *ACS Catal.*, 2019, **9**, 8012–8067.
- 10 K. I. Galkin and V. P. Ananikov, *ChemSusChem*, 2019, **12**, 185–189.
- 11 W. Leitner, J. Klankermayer, S. Pischinger, H. Pitsch and K. Kohse-Höinghaus, *Angew. Chem., Int. Ed.*, 2017, **56**, 5412–5452.
- 12 D. J. Hayes, S. W. Fitzpatrick, M. H. B. Hayes and J. R. H. Ross, in *Biorefineries - Industrial Processes and Products: Status Quo and Future Directions*, ed. B. Kamm, P. R. Gruber and M. Kamm, Wiley-VCH, Weinheim, 2006, vol. 1, pp. 139–163.
- 13 F. D. Pileidis and M.-M. Titirici, *ChemSusChem*, 2016, **9**, 562–582.
- 14 S.-H. Pyo, S. J. Glaser, N. Rehnberg and R. Hatti-Kaul, *ACS Omega*, 2020, **5**, 14275–14282.
- 15 M. Xiang, J. Liu, W. Fu, T. Tang and D. Wu, *ACS Sustainable Chem. Eng.*, 2017, **5**, 5800–5809.
- 16 A. T. Adeleye, H. Louis, O. U. Akakuru, I. Joseph, O. C. Enudi and D. P. Michael, *AIMS Energy*, 2019, **7**, 165–185.
- 17 D. M. Alonso, S. G. Wettstein and J. A. Dumesic, *Green Chem.*, 2013, **15**, 584–595.
- 18 P. Bloom, WO2007094922A2, 2007.

- 19 J. A. Dumesic and R. M. West, WO2011/087962A1, 2011.
- 20 B. Lu, J. Li, G. Lv, Y. Qi, Y. Wang, T. Deng, X. Hou and Y. Yang, *RSC Adv.*, 2016, **6**, 93956–93962.
- 21 A. Marckwardt, F. El Ouahabi, H. Amani, S. Tin, N. V. Kalevaru, P. C. J. Kamer, S. Wohlrab and J. G. de Vries, *Angew. Chem., Int. Ed.*, 2019, **58**, 3486–3490.
- 22 V. Pace, P. Hoyos, L. Castoldi, P. Dominguez de Maria and A. R. Alcantara, *ChemSusChem*, 2012, **5**, 1369–1379.
- 23 G. Pasquale, P. Vázquez, G. Romanelli and G. Baronetti, *Catal. Commun.*, 2012, **18**, 115–120.
- 24 K. Sasaki, M. Watanabe, T. Tanaka and T. Tanaka, *Appl. Microbiol. Biotechnol.*, 2002, **58**, 23–29.
- 25 J. Zhang, S. Wu, B. Li and H. Zhang, *ChemCatChem*, 2012, **4**, 1230–1237.
- 26 J. G. de Vries, *Chem. Rec.*, 2016, **16**, 2787–2800.
- 27 J. H. Helberger, S. Ulubay and H. C. Civelekoglu, *Liebigs Ann.*, 1949, **561**, 215–220.
- 28 D. Sun, Y. Takahashi, Y. Yamada and S. Sato, *Appl. Catal., A*, 2016, **526**, 62–69.
- 29 C. G. S. Lima, J. L. Monteiro, T. de Melo Lima, M. Weber Paixao and A. G. Correa, *ChemSusChem*, 2018, **11**, 25–47.
- 30 F. Chang, S. Dutta and M. Mascal, *ChemCatChem*, 2017, **9**, 2622–2626.
- 31 M. Mascal, S. Dutta and I. Gandarias, *Angew. Chem., Int. Ed.*, 2014, **53**, 1854–1857.
- 32 J. Xu, N. Li, X. Yang, G. Li, A. Wang, Y. Cong, X. Wang and T. Zhang, *ACS Catal.*, 2017, **7**, 5880–5886.
- 33 V. E. Tarabanko and K. L. Kaygorodov, *Chem. Sustainable Dev.*, 2010, **18**, 321–328.
- 34 C. S. Marvel and C. L. Levesque, *J. Am. Chem. Soc.*, 1939, **61**, 1682–1684.
- 35 Y. Yokoyama, M. Okada and H. Sumitomo, *Macromol. Chem. Phys.*, 1975, **176**, 3537–3550.
- 36 K. L. Kaygorodov, V. E. Tarabanko and N. Tarabanko, *Cogent Chem.*, 2018, **4**, 1443689.
- 37 V. E. Tarabanko and K. L. Kaygorodov, *Macromol. Symp.*, 2015, **354**, 367–373.
- 38 A. Dell'Acqua, B. M. Stadler, S. Kirchhecker, S. Tin and J. G. de Vries, *Green Chem.*, 2020, **22**, 5267–5273.
- 39 R. Criegee, *Angew. Chem., Int. Ed. Engl.*, 1975, **14**, 745–752.
- 40 R. L. Kuczkowski, *Chem. Soc. Rev.*, 1992, **21**, 79–83.
- 41 Ullmann's Encyclopedia of Industrial Chemistry, pp. 1–18, DOI: 10.1002/14356007.a08_523.pub3.
- 42 A. C. Brown, C. G. Goebel, H. F. Oehlschlaeger and R. P. Rolfs, US2813113A, 1957.
- 43 K. Louis, L. Vivier, J.-M. Clacens, M. Brandhorst, J.-L. Dubois, K. D. O. Vigier and Y. Pouilloux, *Green Chem.*, 2014, **16**, 96–101.
- 44 R. S. Atapalkar, P. R. Athawale, D. Srinivasa Reddy and A. A. Kulkarni, *Green Chem.*, 2021, **23**, 2391–2396.
- 45 M. B. Figueirêdo, F. W. Keij, A. Hommes, P. J. Deuss, R. H. Venderbosch, J. Yue and H. J. Heeres, *ACS Sustainable Chem. Eng.*, 2019, **7**, 18384–18394.
- 46 H. Strittmatter, S. Hildbrand and P. Pollak, *Ullmann's Encyclopedia of Industrial Chemistry*, Wiley-VCH Verlag GmbH & Co, 2007, DOI: 10.1002/14356007.a16_063.pub2.
- 47 J. A. Dietrich, J. L. Fortman and E. J. Stehen, WO2013134424A1, 2013.
- 48 U. Horn, A. Siering, K. Martin, G. Krauter, P. J. Mueller, B. Bardl, J. H. Ozegowski and K. Herold, DE102005052338A1, 2007.
- 49 M. T. Haas, C. Brossmer, D. Arntz and A. Freund, US5817870, 1998.
- 50 E. M. Karp, T. R. Eaton, I. N. V. Sanchez, V. Vorotnikov, M. J. Bidy, E. C. D. Tan, D. G. Brandner, R. M. Cywar, R. Liu, L. P. Manker, W. E. Michener, M. Gilhespy, Z. Skoufa, M. J. Watson, O. S. Fruchey, D. R. Vardon, R. T. Gill, A. D. Bratis and G. T. Beckham, *Science*, 2017, **358**, 1307–1310.
- 51 F. El Ouahabi, M. Polyakov, G. P. M. van Klink, S. Wohlrab, S. Tin and J. G. de Vries, *ACS Sustainable Chem. Eng.*, 2020, **8**, 1705–1708.
- 52 R. Criegee, *Angew. Chem., Int. Ed. Engl.*, 1975, **14**, 745–752.
- 53 J. Kula, *Chem. Health Safe.*, 1999, **6**, 21–22.
- 54 L. T. Mika, E. Cséfalvay and Á. Németh, *Chem. Rev.*, 2018, **118**, 505–613.

6.3 Glycolaldehyde as a Bio-based C1 Building Block for Selective N-Formylation of Secondary Amines



M. T. Flynn†, X. Liu†, A. Dell'Acqua, J. Rabeah, A. Brückner, E. Baráth, S. Tin and J. G. de Vries

ChemSusChem. **2022**, in press

DOI: 10.1002/cssc.202201264

Electronic supporting information for this article is available under:

<https://chemistry-europe.onlinelibrary.wiley.com/doi/abs/10.1002/cssc.202201264>

RESEARCH ARTICLE

Glycolaldehyde as a Bio-based C1 Building Block for Selective N-Formylation of Secondary Amines

Matthew T. Flynn[†], Xin Liu[†], Andrea Dell'Acqua[†], Jabor Rabeah, Angelika Brückner, Eszter Baráth, Sergey Tin and Johannes G. de Vries*

[a] Dr. M. T. Flynn, Dr. X. Liu, A. Dell'Acqua, Dr. J. Rabeah, Prof. Dr. A. Brückner, Dr. Eszter Baráth, Dr. S. Tin, Prof. Dr. J. G. de Vries
 Leibniz-Institut für Katalyse e. V., Albert-Einstein-Straße 29a, 18059 Rostock, Germany
 E-mail: Johannes.deVries@catalysis.de

[†] These authors contributed equally to this work.

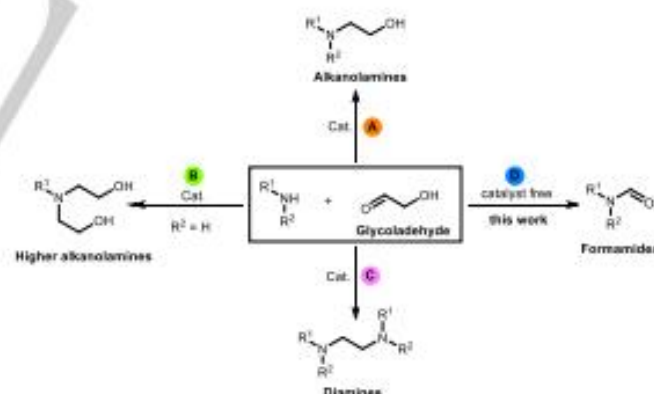
Supporting Information for this article is given via a link at the end of the document.

Abstract: Biomass derived glycolaldehyde was employed as C1 building block for the N-formylation of secondary amines using air as oxidant. The reaction is atom economic, highly selective and proceeds under catalyst free conditions. This strategy can be used for the synthesis of cyclic and acyclic formylamines, including DMF. Mechanistic studies suggest a radical oxidation pathway.

Nature generates yearly about 170 billion metric tons of biomass, 75% of which being carbohydrates.^[1] This represents the biggest source of renewable carbon on earth, and is consequently seen as the most promising alternative to fossil stocks for the production of chemicals and fuels.^[2] The addition of C1 building block represents an important strategy for the synthesis of new products. Several C1 building blocks have been used; carbon mono- and dioxide, methanol, and formic acid – all potentially obtainable from renewable resources – being the most ubiquitous examples.^[3]

N-Formamides are an important class of chemicals with widespread industrially relevant applications as solvents and raw materials for fine chemicals such as drugs, fertilizers, cosmetics and softeners.^[4] Traditionally, the C-N bond is formed by reaction of amines with C1 sources, such as formic acetic anhydride, chloral or carbon monoxide.^[5] Various routes have been reported for the synthesis of formamides employing CO₂ as carbon source and hydrogen as reducing agent.^[6] Notwithstanding the importance and applicability of the latter, we aimed to develop a practical procedure for the N-formylation of amines which avoids the use of gaseous reactants and directly utilizes biomass-derived small molecules. This approach presents some immediate limitations: 1) biomass is typically a mixture of multi-carbon compounds, and it needs to be further transformed to obtain a C1 building block; 2) transition metal catalysts are usually needed for the conversion of biomass into small chemicals, thus generating extra costs. A seminal work in this regard comes from Shi and co-workers, who reported the use of glycerol and glycerol-derived compounds (dihydroxyacetone, glyceraldehyde and glycolic acid) for the N-formylation of amines over copper-containing heterogeneous catalysts under oxidative conditions.^[7] In our attempts to prepare cleavable conjugated polymers, we serendipitously found that glycolaldehyde (GA) reacted with

secondary amines to yield the N-formylated products with very good yields. This use of glycolaldehyde as C1 building block is unprecedented and we decided to investigate this reaction in depth. GA is the smallest of the reducing sugars homologous series; it can be obtained by cracking of glucose in good yield or from biomass pyrolysis oil, where it is a major component, and it displays low toxicity.^[8] GA is widely used as a bio-based platform chemical for the addition of C2 chains on amines (Scheme 1A-C), but its use as C1 building block is, to the best of our knowledge, unprecedented.^[9] Herein, we report a highly efficient strategy for the N-formylation of secondary amines using GA as C1 source (Scheme 1D). This process offers several advantages over conventional methods. The reaction does not require a catalyst, is highly selective for secondary amine groups, and proceeds under mild conditions, using air as oxidant.



Scheme 1. Reactions of secondary amines with glycolaldehyde.

Results and Discussion

In preliminary experiments piperidine (**1a**) was chosen as the model substrate and the commercially available dimer of GA (**2a**) as the formylating agent (Table 1). Initial screening of solvents (entries 1–6) revealed that acetonitrile is the best one under the given reaction conditions. Formamide **3a** was obtained in 92% yield (entry 5). Surprisingly, when typical oxidation catalysts (entries 7 and 8) were added, lower yields of the desired product **3a** were obtained (55 and 78%

RESEARCH ARTICLE

respectively). When oxygen gas was used instead of air, the yield of **3a** was not improved (entry 9). Presence of oxygen was shown to be crucial, as the reaction does not proceed under argon (entry 10). The absence of light does not have an impact on the yield of **3a** (entry 11). Further variations in temperature and reaction time were also studied but did not lead to any improvement (See SI for details, Table S1–S2). Having optimal reaction conditions in hand, we explored the scope of the *N*-formylation of different secondary amines (Table 2). Cyclic amines afforded good to high yields (**3a–3d**, up to 92%). Remarkably, this protocol also works well for acyclic secondary amines (**1e–1l**) which are usually less reactive or not reactive at all in *N*-formylation reactions. In the case of secondary phenylamines, such as 2-(methylamino)pyridine (**1e**), *N*-methylaniline (**1f**) and diphenylamine (**1g**), the corresponding products (**3e–3g**) were obtained in good yields (up to 73%). Secondary fatty amines were also formylated obtaining **3h–3l** in

Table 1. Optimization of the reaction conditions.

entry	solvent	additive	conv./ %	3a/ %	4a/ %
1	THF	–	>99	84	31
2	CH ₂ Cl ₂	–	75	71	3
3	CHCl ₃	–	84	81	2
4	toluene	–	81	73	6
5	MeCN	–	99	92	5
6	acetone	–	81	75	5
7	MeCN	CuCl	72	55	7
8	MeCN	Pd(OAc) ₂	88	78	10
9 ^a	MeCN	–	97	92	3
10 ^b	MeCN	–	90	–	–
11 ^c	MeCN	–	99	91	4

Reaction conditions: **1a** (2.0 mmol), **2a** (0.5 mmol), solvent (5 mL), reflux, 4 h. Yields were determined by GC using mesitylene as internal standard.
^aUsing O₂ balloon with Schlenk flask. ^bUnder argon. ^cReaction in the dark.

yields up to 70%. Ephedrine was formylated to give a mixture of rotamers in 27% yield. However, the reaction does not proceed for primary amines such as aniline (**1m**), benzylamine (**1n**) and *n*-hexylamine (**1o**) (See ESI for details, Scheme S1). Given the paramount importance of dimethylformamide (DMF),^[10] we applied our protocol for the *N*-formylation of dimethylamine. Different dimethylamine solutions were tested using O₂ as oxidant at atmospheric pressure at 95 °C and 8 h (Table 3, entries 1–4). Only dimethylamine solution in THF (2.0 M) afforded DMF in low yield (24%). In previous studies, dimethylammonium dimethyl carbamate is usually chosen as starting material for the synthesis of DMF.^[6b] Under the same conditions, DMF was obtained in 21% yield (entry 5). As we assumed that the low yields were due to the low boiling point of dimethylamine, we performed the reaction in a sealed autoclave in the presence of pressurized air as oxygen source (entries 6 and 7). DMF was obtained in higher yields (57 and 45% yield). This demonstrates the potential of the shown procedure for further practical applications in DMF manufacturing. To gain

Table 2. Substrate scope of *N*-formylation of amines 1

1	2a	3
3a , 92%, 81% ^a	3b , 83%	3c , 74% ^a
3d , 80%	3e , 73%	3f , 66% ^a
3g , 65% ^a	3h , 70% ^a	3i , 62% ^b
3j , 65%	3k , 61% ^a	3l , 66% ^b
3m , 27% ^{a,c}	3n , 0%	3o , traces
		3p , 0%

Reaction conditions: **1** (2.0 mmol), **2a** (0.5 mmol), MeCN (5.0 mL), reflux, 4 h. Yields were determined by GC using mesitylene as internal standard.
^aIsolated yields. ^b**1** (1.0 mmol), **2a** (0.5 mmol), 12 h. ^c16 hours, O₂ (1 atm).

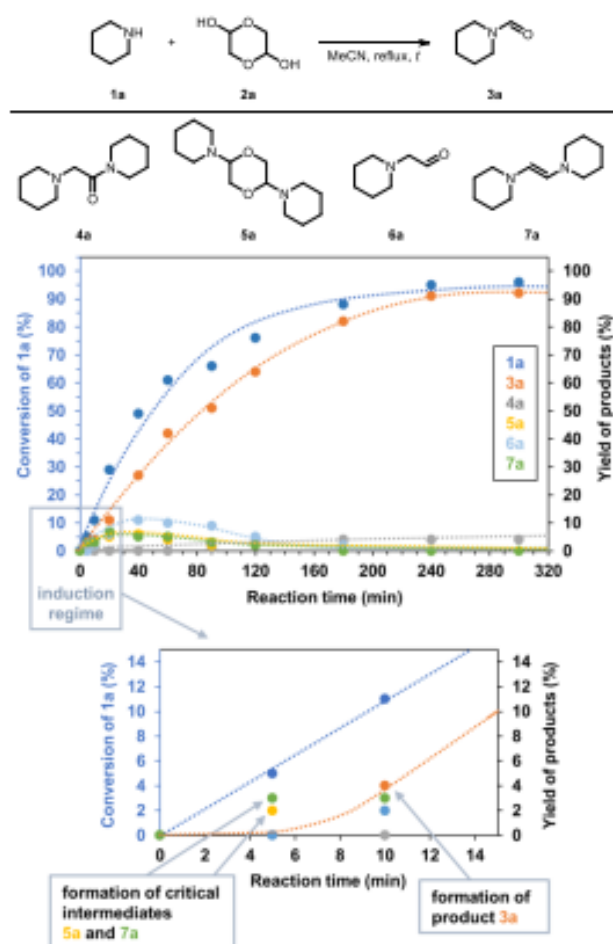
mechanistic insights, the reaction between **1a** and **2a** was monitored over time (Scheme 2). When piperidine **1a** and glycolaldehyde dimer were reacted under standard reaction conditions, four types of compounds were detected. As early as after 5 minutes the desired product starts to form. Amide **4a** is detected only after 90 minutes. Its concentration increases with time, reaching a plateau after 180 minutes. This suggests that **4a** is not an intermediate towards the desired product, but more likely a by-product coming from another reaction path. The compounds **5a**, **6a** and **7a** are all produced at the initial stage of the reaction, but their concentration stays low (< 15%) and they get eventually consumed in the later stage of the reaction. After 4 hours all

Table 3. Synthesis of DMF from dimethylamine and glycolaldehyde.

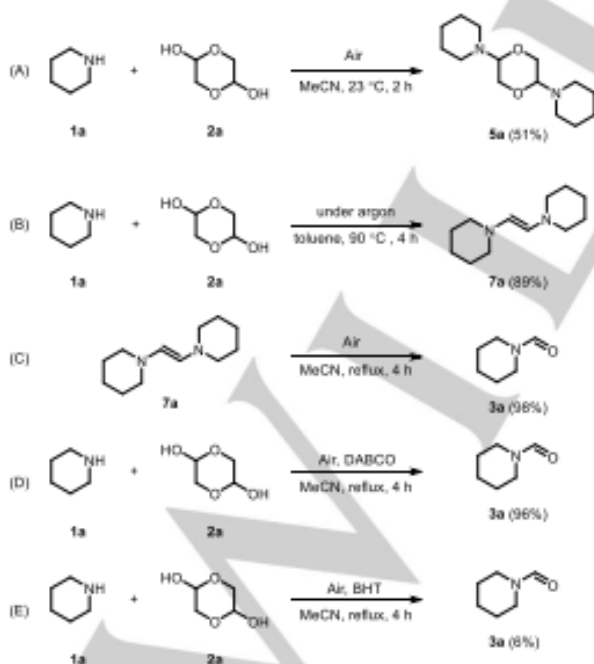
entry	dimethylamine solution 4	oxygen source	5a/ %
1	2.0 M in THF	O ₂ balloon	24
2	40 wt. % in H ₂ O	O ₂ balloon	0
3	2.0 M in methanol	O ₂ balloon	0
4	5.6 M in ethanol	O ₂ balloon	0
5	(CH ₃) ₂ NH · (CH ₃) ₂ NCOOH	O ₂ balloon	21
6	2.0 M in THF	air (10 bar) ^a	57
7	(CH ₃) ₂ NH · (CH ₃) ₂ NCOOH	air (10 bar) ^a	45

Reaction conditions: **1a** (1.0 mmol), **2a** (0.5 mmol), MeCN (5 mL), 95 °C, 8 h. Yields were determined by GC using mesitylene as the internal standard.
^aAutoclave instead of Schlenk flask.

RESEARCH ARTICLE



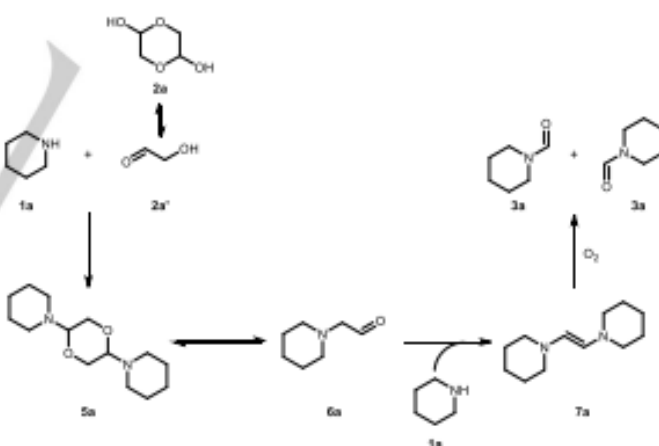
Scheme 2. Reaction profile of the *N*-formylation from amine with glycolaldehyde.



Scheme 3. Control experiments.

intermediates are converted to either **3a** or **4a**. From this observation it can be postulated that **5a**, **6a** and **7a** are all

intermediates to the product as well as to the unwanted **4a**. In order to get a conclusive mechanistic picture, several control experiments were performed (Scheme 3). Firstly, piperidine **1a** and glycolaldehyde dimer **2a** were stirred at room temperature until a homogeneous solution was formed. Colourless crystals were formed after stirring was halted. They were collected by filtration and washed with ice-cold acetonitrile, and **5a** was obtained in 51% yield (Scheme 3A). Notably, **5a** monomerises over time in CDCl_3 (even faster in C_6D_6), to form 2-(piperidin-1-yl) acetaldehyde **6a** (Supporting Information, Figure S1 and S2). As mentioned before (Table 1, entry 10 and Scheme 3B), the reaction under inert conditions does not lead to the formylated product, but the enamine **7a** could be obtained in 89% yield as a low-melting solid that gradually turned yellow over the course of the next 2 days (Figure S3). This suggests that oxygen is the actual oxidizing agent in the reaction. In addition, using isolated **7a** as starting materials under our standard conditions, the corresponding product **3a** can be obtained in excellent yield (Scheme 3C). This is a further indication that the oxygen atom on the formyl group does not come from water (that is produced upon condensation between the aldehyde and the amine), but rather from oxygen itself. To exclude the involvement of singlet oxygen the reaction was performed in the presence of an excess (5 eq with respect to piperidine) of 1,4-diazabicyclo[2.2.2]octane (DABCO, Scheme 3D), which is a known quencher for $^1\text{O}_2$.^[11] The reaction proceeded to full conversion to the desired product, thus excluding that $^1\text{O}_2$ has an active role. Considering these results and previous reports, we propose the reaction pathway shown in Scheme 4. Initially, glycolaldehyde dimer **2a** and glycolaldehyde **2a'** rapidly interconvert in solution. Then, piperidine **1a** quickly



Scheme 4. Putative reaction pathway.

reacts with glycolaldehyde **2a'** forming **5a**. Compounds **5a** and **6a** exist in equilibrium in solution. The latter undergoes a second amination reaction with **1a** to form **7a**. The actual oxidation should then take place via a radical mechanism. To prove this hypothesis the formylation of **1a** was run in the presence of 2 equivalents of butylated hydroxytoluene (BHT), a common quenching agent for radical species. Indeed, the yield of the reaction dropped to 6%, which indicates that the reaction was effectively inhibited by BHT. To further support this assumption, *in situ* EPR experiments

RESEARCH ARTICLE

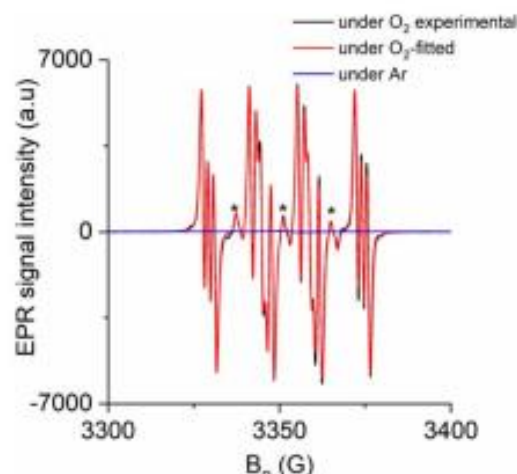
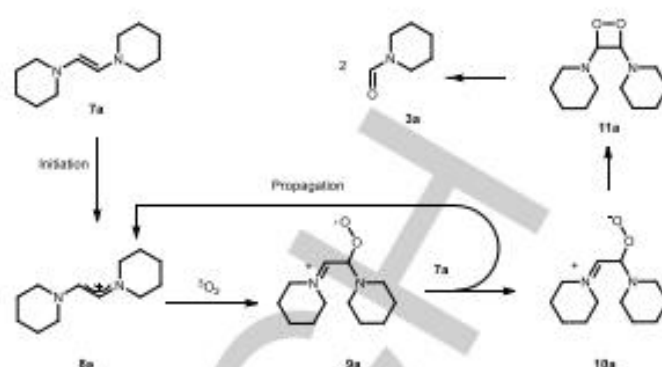


Figure 1. EPR spectra of 0.2 M dienamine **7a** + 10 μL DMPO measured at 20 $^{\circ}\text{C}$ after heating 4 h at 80 $^{\circ}\text{C}$ under a) Ar (blue-line); b) O_2 (black-line); c) Fitted spectrum of (b) using Bruker SpinFit package program (red line). *EPR signal of DMPOX due to the oxidation of DMPO.

using **7a** and the spin trap 5,5-dimethyl-1-pyrroline N-oxide (DMPO) were conducted in the presence and absence of O_2 . No radical intermediates have been detected under Ar at the reaction temperature (80 $^{\circ}\text{C}$). However, in the presence of O_2 , a multi-line EPR signal (triplet-of-sextets) appeared at $g = 2.006$. This signal can be fitted (Bruker-SpinFit package) by assuming the coupling to $A_N = 14.0$, $A_H = 16.7$, and $A_{N_2} = 1.7$ G (Figure 1) indicating the formation of a DMPO- $\cdot\text{N}$ spin adduct.^[12] This suggests that a nitrogen-centered radical is formed upon interaction of **7a** with O_2 . Additionally, there is a weak three-line signal (1:1:1) at $g = 2.006$ with $A_N = 13.8$ G attributed to the formation of aminoxyl radical (DMPOX),



Scheme 5 Proposed mechanism for the radical oxidation of **7a**.

indicating small extent of degradation of DMPO. We propose the following radical mechanism based on Scheme 5. As initiation step we assume the enediamine **7a** is oxidised to the radical cation **8a** by oxygen. This most likely is the species that is trapped by the spin trap. This type of reactivity is well-precedented from the work of Wiberg who showed that reaction of tetra-(dimethylamino)ethylene with oxygen leads to the formation of a radical cation.^[13] Reaction of **8a** with oxygen leads to formation of the peroxo radical **9a**. This compound may abstract an electron from **7a** in the propagating step leading to the species **10a** and the regeneration of **8a**. Ring-closure of **10a** to the dioxetane **11a** is well-precedented from earlier work of Foote and others on the reaction between enamines and singlet oxygen.^[14] Thermal decomposition of the dioxetane to 2 equivalents of formamide is again well-precedented. To obtain more information about the structure of the spin trap adduct we subjected the reaction mixture to ESI-MS (see Supporting

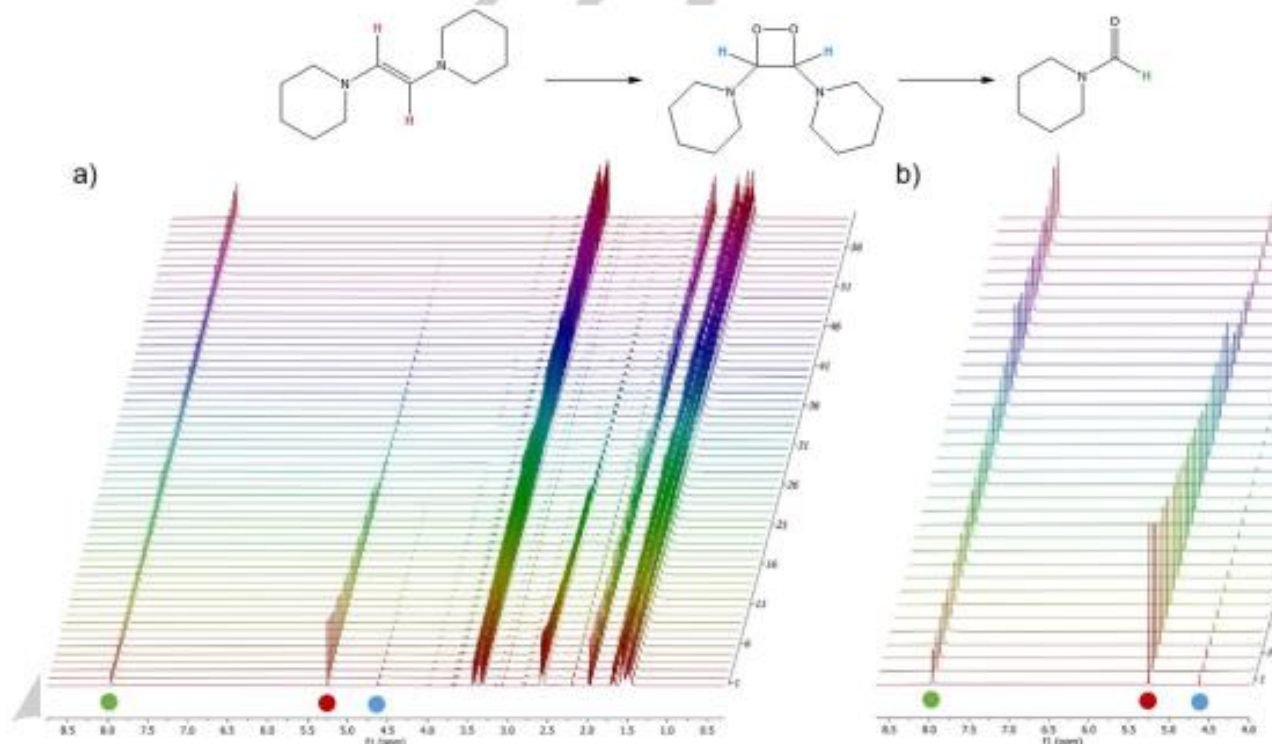


Figure 2. Reaction monitoring by ^1H NMR in CD_3CN over 16 h: a) full spectrum; b) characteristic region between 4.0 and 8.5 ppm. Reaction conditions: **7a** in CD_3CN , room temperature, 1 atm O_2 .

RESEARCH ARTICLE

Information for details). Although a signal for the spin trapped **8a** ($m/z = 307$) was not visible, we found a small signal at $m/z = 309$, possibly due to reduction by the formic acid that was used in the MS sample preparation. More interesting, a signal at $m/z = 339$ fits very well with the spin-trapped intermediate **9a** (Scheme 5, Figure 2). Dioxetanes are not very long-lived intermediates, certainly not at the temperature of the reaction. For that reason, we followed the reaction of **7a** in CD_3CN at room temperature over 16 h. In the 1H NMR (Fig. 2) we see the signal of the olefinic proton of **7a** and slowly over time the formation of the formamide **3a** with the characteristic formyl proton at 7.92 ppm. Interestingly in the first 9 hours of the reaction, we also see a small peak at 4.92 ppm which fits very well with the anticipated adsorption of the dioxetane protons.

Conclusions

Bio-based glycolaldehyde was used for the first time as a C1 building block for the selective catalyst-free N-formylation of secondary amines to formamides under mild experimental conditions. The protocol is highly selective for secondary amines, with several aromatic and aliphatic (both cyclic and linear) being N-formylated. Based on control experiments, a spin trap experiment, MS and 1H NMR we propose a radical oxidation mechanism that leads to formation of a dioxetane that splits in two formamide molecules.

Experimental Section

All experiments were performed under argon atmosphere by using standard Schlenk technique or in a glove box, if not stated otherwise. For further details, see Supporting Information.

Synthesis of intermediate 5a. Glycolaldehyde dimer **2a** (60 mg, 0.5 mmol) was suspended in MeCN (2 mL) to make an 0.5 M solution. Then **1a** (0.1 mL, 1.0 mmol) was added, and the mixture stirred at room temperature until a homogeneous solution formed. The reaction was then left without stirring at room temperature, depositing colourless crystals after 1 h. The reaction was left standing overnight and cooled to 0 °C for 1 h. The crystals were collected by filtration and washed with ice-cold MeCN, and **5a** was obtained in 51% yield. 1H -NMR (300 MHz, $CDCl_3$) δ = 3.99 (dd, $J = 9.8, 2.5$ Hz, 1H), 3.86 – 3.76 (m, 1H), 3.70 (dd, $J = 11.3, 9.8$ Hz, 1H), 2.83 – 2.73 (m, 2H), 2.64 – 2.52 (m, 2H), 1.59 – 1.50 (m, 4H), 1.48 – 1.40 (m, 2H) ppm.

Synthesis of intermediate 7a. Glycolaldehyde dimer **2a** (300 mg, 2.5 mmol) was suspended in anhydrous toluene (50 mL) under argon. The toluene was degassed by bubbling argon for 30 minutes, and then **1a** (1.0 mL, 10.1 mmol) was added. The reaction mixture was heated to 90 °C for 2 h. Removal of the solvent under high vacuum gave a pale-yellow crystalline residue **7a** in 89% yield. This residue could be distilled under vacuum to yield a colourless oil, which crystallized to a low-melting solid at room temperature and turned yellow over the course of 1-2 days while standing at room temperature under argon. 1H -NMR (300 MHz, Toluene- d_8) δ = 5.31 (s, 2H), 2.61 – 2.52 (m, 8H), 1.59 – 1.48 (m, 8H), 1.39 – 1.33 (m, 4H) ppm.

General Procedure for the N-formylation of amines. In a Schlenk tube (20 mL), glycolaldehyde dimer **2a** (60 mg, 0.5 mmol) was suspended in acetonitrile (5 mL), and secondary amine **1** (2.0 mmol) was added. The reaction mixture was heated to reflux under air for 4 h. After removal of all volatiles *in vacuo* the crude mixture was purified by column chromatography on silica gel to afford the isolated yield of products.

Acknowledgements

XL is grateful for the financial support of the China Scholarship Council (CSC, 201708530236). MF and AD are grateful to the Fachagentur Nachwachsende Rohstoffe e. V. (FNR) for funding the project BIOVIN as part of the funding program "Nachwachsende Rohstoffe" (FNR, promotional reference n° 2219NR171). We thank Drs. Horst Beck, Adrian Brandt, Andreas Taden and Kenji Ito (all Henkel AG) for helpful discussions. Dr. Marcus Klahn and the analytical department of LIKAT are acknowledged for the help with the ESI-MS and NMR experiments.

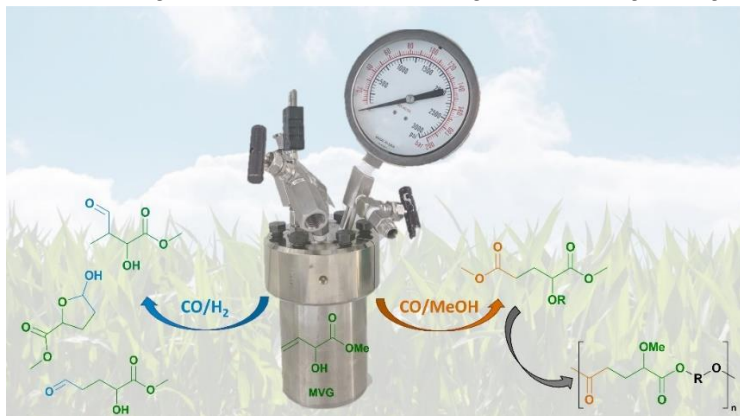
Keywords: Glycolaldehyde • Platform chemicals • N-formylation • Oxidation • Secondary amines

- [1] a) A. Corma, S. Iborra, A. Velty, *Chem. Rev.* **2007**, *107*, 2411-2502; b) H. Kopetz, *Nature* **2013**, *494*, 29-31; c) L. T. Mika, E. Csefalvay, A. Nemeth, *Chem. Rev.* **2018**, *118*, 505-613; d) M.-A. Perea-Moreno, E. Samerón-Manzano, A.-J. Perea-Moreno, *Sustainability* **2019**, *11*, 863.
- [2] a) P. N. R. Vennestrom, C. M. Osmundsen, C. H. Christensen, E. Taarning, *Angew. Chem. Int. Ed.* **2011**, *50*, 10502-10509; b) R. S. Varma, *ACS Sustain. Chem. Eng.* **2019**, *7*, 6458-6470; c) Y.-K. Chen, C.-H. Lin, W.-C. Wang, *Energy* **2020**, *201*, 117855.
- [3] a) J. Daniell, M. Köpke, S. D. Simpson, *Energies* **2012**, *5*, 5372-5417; b) J. Albert, R. Wölfel, A. Bösmann, P. Wasserscheid, *Energy Environ. Sci.* **2012**, *5*, 7956-7962; c) Q. Liu, L. Wu, R. Jackstell, M. Beller, *Nat. Commun.* **2015**, *6*, 1-15; d) Y. Li, X. Cui, K. Dong, K. Junge, M. Beller, *ACS Catal.* **2017**, *7*, 1077-1086; e) Q. Zou, G. Long, T. Zhao, X. Hu, *Green Chem.* **2020**, *22*, 1134-1138; f) K. Hua, X. Liu, B. Wei, Z. Shao, Y. Deng, L. Zhong, H. Wang, Y. Sun, *Green Chem.* **2021**; g) K. Natte, H. Neumann, M. Beller, R. V. Jagadeesh, *Angew. Chem. Int. Ed.* **2017**, *56*, 6384-6394; h) M.-C. Fu, in *Studies on Green Synthetic Reactions Based on Formic Acid from Biomass*, Springer Singapore, Singapore, **2020**, pp. 1-26.
- [4] a) H. Bipp, H. Kieczka, in *Ullmann's Encyclopedia of Industrial Chemistry*, **2011** https://onlinelibrary.wiley.com/doi/abs/10.1002/14356007.a12_001.pub2; b) J. R. Dunetz, J. Magano, G. A. Weisenburger, *Org. Process Res. Dev.* **2016**, *20*, 140-177.
- [5] G. A. Olah, L. Ohannesian, M. Arvanaghi, *Chem. Rev.* **1987**, *87*, 671-686.
- [6] a) N. Ortega, C. Richter, F. Glorius, *Org. Lett.* **2013**, *15*, 1776-1779; b) L. Zhang, Z. Han, X. Zhao, Z. Wang, K. Ding, *Angew. Chem. Int. Ed.* **2015**, *127*, 6284-6287; c) M. Hulla, G. Laurenczy, P. J. Dyson, *ACS Catal.* **2018**, *8*, 10619-10630; d) M. Nasrollahzadeh, N. Motahharifar, M. Sajjadi, A. M. Aghbolagh, M. Shokouhimehr, R. S. Varma, *Green Chem.* **2019**, *21*, 5144-5167.
- [7] a) X. Dai, J. Rabeah, H. Yuan, A. Brückner, X. Cui, F. Shi, *ChemSusChem* **2016**, *9*, 3133-3138; b) X. Dai, S. Adomeit, J. Rabeah, C. Kreyenschulte, A. Brückner, H. Wang, F. Shi, *Angew. Chem. Int. Ed.* **2019**, *58*, 5251-

RESEARCH ARTICLE

- 5255; c) X. Dai, X. Wang, J. Rabeah, C. Kreyenschulte, A. Brückner, F. Shi, *Chem. Eur. J.* **2021**, *27*, 16889-16895.
- [8] C. B. Schandel, M. Høj, C. M. Osmundsen, A. D. Jensen, E. Taarning, *ChemSusChem* **2020**, *13*, 688-692.
- [9] a) G. Liang, A. Wang, L. Li, G. Xu, N. Yan, T. Zhang, *Angew. Chem. Int. Ed.* **2017**, *129*, 3096-3100; b) W. Faveere, T. Mihaylov, M. Pelckmans, K. Moonen, F. Gillis-D'Hamers, R. Bosschaerts, K. Pierloot, B. F. Sels, *ACS Catal* **2019**, *10*, 391-404; c) W. H. Faveere, S. Van Praet, B. Vermeeren, K. N. Dumoleijn, K. Moonen, E. Taarning, B. F. Sels, *Angew. Chem. Int. Ed.* **2021**, *133*, 12312-12331.
- [10] a) J. Muzart, *Tetrahedron* **2009**, *65*, 8313-8323; b) S. Ding, N. Jiao, *Angew. Chem. Int. Ed.* **2012**, *51*, 9226-9237.
- [11] C. Ouannes, T. Wilson, *J. Am. Chem. Soc.* **1968**, *90*, 6527-6528.
- [12] F. Li, L. Xiao, L. Liu, *Sci. Rep.* **2016**, *6*, 22876.
- [13] N. Wiberg, *Angew. Chem. Int. Ed. Engl.* **1968**, *7*, 766-779.
- [14] a) C. S. Foote, J. W.-P. Lin, *Tetrahedron Lett.* **1968**, 3267-3270; b) J. E. Huber, *Tetrahedron Lett.* **1968**, 3271-3272; c) H. H. Wasserman, S. Terao, *Tetrahedron Lett.* **1975**, 1735-1738.

6.4 New Bifunctional Monomers from Methyl Vinyl Glycolate.



A. Dell'Acqua, C. Schünemann, E. Baráth, S. Tin, J. G. de Vries

Manuscript under revision

ARTICLE

New Bifunctional Monomers from Methyl Vinyl Glycolate.

Andrea Dell'Acqua,^a Claas Schünemann,^a Eszter Baráth,^a Sergey Tin^a and Johannes G. de Vries^{a*}Received 00th January 20xx,
Accepted 00th January 20xx

DOI: 10.1039/x0xx00000x

Methyl Vinyl Glycolate (MVG) can be obtained by acid-catalyzed conversion of C4 and C6 sugars. Applications of MVG in polymers are so far limited to its use as co-monomer for poly(lactic acid) and as crosslinking agent. In this work, hydroformylation and methoxycarbonylation of MVG were investigated to produce novel bifunctional monomers. Polyesters with high renewable-atom content were successfully prepared and characterized.

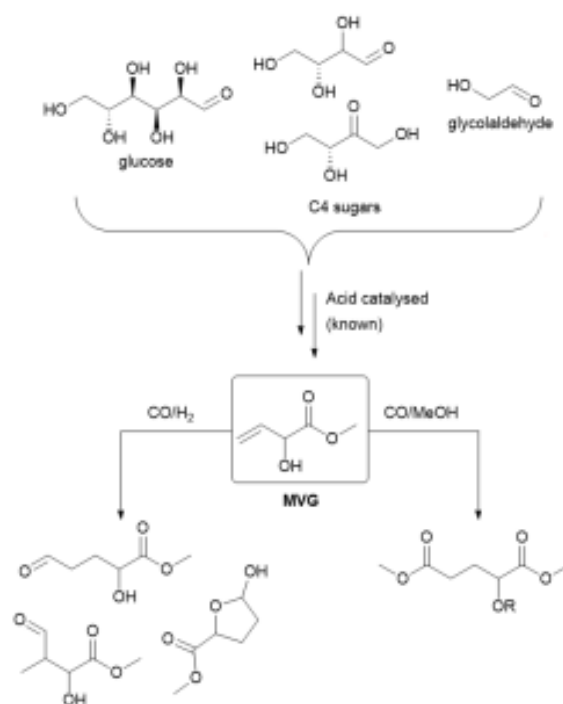
Introduction

The Paris Agreement has set the ambitious goal to achieve carbon neutrality by 2050. This, together with increasing awareness of environmental issues and the depletion of fossil resources, will fuel a progressive switch to a fully renewable based chemical industry.^{1–3} Due to the disastrous environmental impact caused by the ubiquitous use of plastics, the demand for eco-friendlier polymers, based on renewable resources and/or easily degradable in the environment is growing rapidly.⁴ In view of their wide range of applications in many technical fields, polyesters are a prominent target when it comes to the development of bio-based alternatives.^{5–7} The largest amount of nature generated biomass is composed of sugars. They can be easily converted into a plethora of platform molecules rich in functional groups, whose reactivity can be used to prepare different bulk and fine chemicals, fuels, solvents etc.^{8–11}

Methyl vinyl glycolate (MVG) was obtained for the first time by Taarning and co-workers as a by-product in the synthesis of methyl lactate from C6 sugars and methanol employing Sn- β zeolites as catalyst.¹² The group of Sels extensively studied the mechanism of MVG formation,¹³ showing the key role of the intermediate tetrose sugars and glycolaldehyde formed by retro-aldol reaction (Scheme 1). In fact, by starting from tetroses or glycolaldehyde the yield of MVG can be increased.^{12, 14, 15} MVG is a highly functionalised small molecule, bearing three different reactive moieties (*i.e.*, vinyl, hydroxy and ester groups) that can be further transformed. Reported reactions of MVG include its dimerization to maple furanone, thiol-ene reaction, cyclization to a lactide-like dimer, Claisen rearrangement, homo and cross metathesis of the C=C group, allylic rearrangement and transesterification.^{16, 17} α -Hydroxy acids such as lactic and glycolic acid are of interest for their application in the production of biocompatible, biodegradable and renewable polyesters.^{18–21} MVG, being itself an α -hydroxy acid ester, has been incorporated as a co-monomer into poly(L-lactic acid) (PLLA).²² This represents a valuable approach not only to tune PLLA's properties such as hydrophilicity, but also to introduce cross-linkable groups that can extend the range of

applications of poly(hydroxy acids). On the other hand, MVG's double bond could also be used as a handle to introduce new functional groups. In this work, we investigate well-established and atom economic hydroformylation and alkoxy carbonylation chemistry towards new and bio-based bifunctional monomers.

Hydroformylation of olefins is of paramount importance since its discovery in the late 1930's, and it is currently one of the biggest homogeneous catalysed processes in industry.²³ Syngas can be obtained from renewable resources, for example by biomass gasification, thus bringing hydroformylation into the realm of bio-based production of chemicals.^{24–26} Likewise, alkoxy carbonylation has also been applied in several industrial processes, such as the synthesis of methyl propionate from ethylene or the functionalization of methyl oleate.^{5, 27}



Scheme 1. Synthesis of MVG from sugars (top) and synthesis of new (bifunctional) monomers from MVG (bottom, this work).

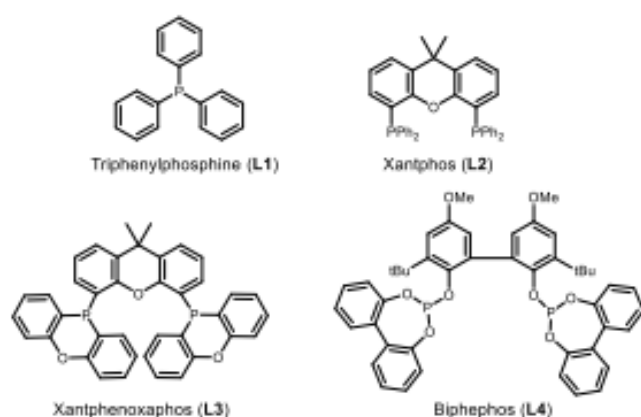


Figure 1 Ligands tested in the hydroformylation of MVG.

Herein, we report the synthesis of new monomers derived from MVG and their application in the production of novel polyesters.

Results and discussion

Hydroformylation of MVG.

Due to their superior activities and general ability to operate under milder conditions, rhodium complexes with phosphorus containing ligands are often the catalysts of choice when hydroformylation of olefins is explored.²³ Different commercially available phosphine and phosphite ligands were selected for an initial screening of the reaction conditions (Figure 1). Table 1 shows the initial attempts in hydroformylating MVG using $\text{Rh}(\text{CO})_2(\text{acac})$ (dicarbonyl(acetylacetonato)rhodium(I)) as metal source in the presence of an excess of phosphine or phosphite ligand (20:1 to the metal) and 10 bar of syngas at 80 °C. The reaction can in principle afford a linear (1) and a branched (2) isomer. Due to MVG's OH group, cyclization of the linear product to 5-membered cyclic hemiacetal (3) can take place. Using simple triphenylphosphine (L1) resulted in full conversion of MVG in

both toluene and THF (Table 1, entries 1 and 2), though no significant prevalence of either the linear or branched aldehyde was observed. Notably, most of the linear isomer cyclized to the acetal. Switching to the bidentate ligand L2 dramatically increased the linear to branched ratio, again with no appreciable difference in toluene or THF (Table 1, entries 3 and 4). Increasing the steric hindrance seemed to hamper the activity (L3, entry 5), while the use of the bisphosphite L4 afforded the same results as L2 (entry 6). In most of the industrial processes, aldehydes are only intermediates that are typically further transformed by reduction or oxidation to the corresponding alcohols or carboxylic acids, respectively. By this approach we envisage that hydroformylation could be effectively applied to upgrade MVG to novel useful monomers for polymers, for example as diester or diacid, hydroxyester, diols or triols that can have several applications, for example as monomers and crosslinker for polyesters.¹⁷

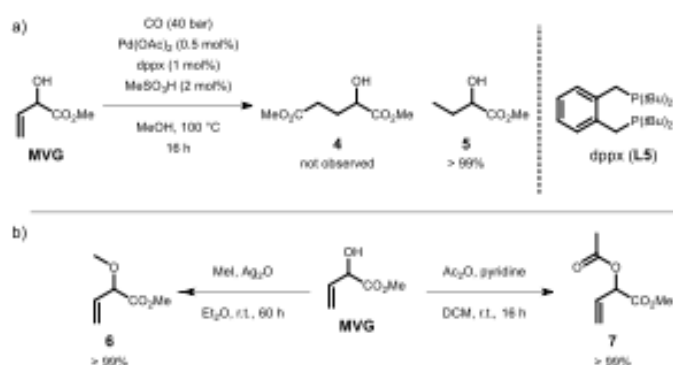
Methoxycarbonylation of MVG.

We first attempted the methoxycarbonylation of MVG applying the well-established combination of palladium(II) acetate, α, α' -bis(di-*t*-butylphosphino)-*o*-xylene (Lucite Alpha ligand, dppx) and methylsulfonic acid.^{28, 29} However, the desired product (Scheme 2a, 4) could not be detected: reduction of the double bond took place, affording the saturated methyl 2-hydroxybutyrate (5) which was isolated in quantitative yield. Protection of the OH might help in slowing down the hydrogenation both by steric factors and due to the competing C=C isomerization to the internal position, that should be faster than in the case of the unprotected alcohol. For this reason, methylation and acetylation of MVG were attempted (Scheme 2b, 6 and 7 respectively). Methylation of MVG turned out to be a rather slow reaction, and only in the presence of silver(I) oxide and after 60 hours the desired product could be isolated in quantitative yield (see Supporting Information for details). Acetylation on the other hand proceeded faster, but when tertiary amines such as triethylamine or diisopropylethylamine are employed, isomerization of the C=C bond to the internal

Table 1 Hydroformylation of MVG.

Entry	Ligand	Solvent	MVG Conversion [%] ^[a]	1 [%] ^[a]	2 [%] ^[a]	3 [%] ^[a]	L/B ^[b]
1	L1	Toluene	>99	6	39	55	61:39
2	L1	THF	>99	6	33	61	67:33
3	L2	Toluene	>99	10	3	87	97:3
4	L2	THF	>99	9	2	89	98:2
5	L3	Toluene	71	17	6	48	91:9
6	L4	Toluene	>99	11	5	84	95:5

^[a]NMR conversion; ^[b]Linear to branched ratio = $\{[\text{conc.}(1) + \text{conc.}(3)] / \text{conc.}(2)\} * 100\%$.



Scheme 2 a) attempt in direct methoxycarbonylation of MVG; b) functionalization of the hydroxyl group of MVG.

position occurred. To suppress this undesired reaction, a milder base such as pyridine had to be used (see Supporting Information).¹⁶ With the two functionalized MVGs in hand, we explored the methoxycarbonylation reaction (Table 2). Other than the previously mentioned dppx ligand, ligands with smaller and larger bite angles were tried (dppe and dppe respectively). For methoxy-MVG (**6**) dppx showed the highest conversion (entry 1), but only 30% of that was the desired product **8**, the rest being the product of C=C isomerization to the internal olefin. Increasing the catalyst loading had a positive effect on the conversion, but the yield of **8** did not improve. By considering the well-established mechanisms of

methoxycarbonylation on the one hand, and the possible Pd-catalysed allylic isomerization pattern on the other hand (see Supporting Information), we tried to vary the pressure and the acid concentration to prevent the (reversible) side reaction. Indeed, by increasing the pressure of CO to 40 bar the yield of the desired product more than doubled compared to the previous attempt (entry 6). On the other hand, higher acid concentration led to partial degradation of the starting material and products (entry 7). Since **8** is the only irreversible product, we also tried increasing the temperature aiming to achieve better selectivity. Gratefully, full selectivity to the desired product was achieved at 120 °C (entry 9). The acetylated analogue **7** turned out more challenging. None of the ligands afforded appreciable amount of product **9** (entries 10–12). In this case the prevailing side reaction was found to be allylic substitution, as previously reported by the group of Madsen.³⁰ Both the methanol from the solvent and the acetate from the substrate can in theory act as nucleophilic partner, and the corresponding products were detected in high amounts by GC and isolated by column chromatography (Supporting Information). The same considerations previously discussed for **6** also apply in this case: higher temperatures and pressures had a positive effect on selectivity. However, no more than 21% of the desired product could ever be obtained. The acetyl group is also prone to be cleaved by methanol giving back MVG, that can be reduced to **5** and undergo oligomerization under the acidic

Table 2. Methoxycarbonylation of protected MVG.

Entry	Substr.	[Pd] [mol%]	Ligand	Pressure [bar]	Conv. [%] ^[a]	Product (8 or 9) [%] ^[a]	Isomerization (10) [%] ^[a]	Allylic rearrangement 11 [%] ^[a]	12 [%] ^[a]
1	6	0.5	L5	20	67	30	32	0	0
2	6	0.5	L6	20	<2	Traces	Traces	0	0
3	6	0.5	L7	20	<2	Traces	Traces	0	0
4	6	1.0	L5	20	86	31	28	0	0
5	6	2.0	L5	20	>99	33	24	0	0
6	6	1.0	L5	40	>99	71	27	0	0
7 ^[b]	6	1.0	L5	40	>99	47	31	0	0
8 ^[c]	6	1.0	L5	40	>99	63	32	0	0
9 ^[d]	6	1.0	L5	40	>99	>99 (77) ^[e]	0	0	0
10	7	0.5	L5	20	56	Traces	0	36	Traces
11	7	0.5	L6	20	44	0	0	Traces	Traces
12	7	0.5	L7	20	83	Traces	0	20	55
13	7	1.0	L5	20	54	9	0	21	0
14	7	2.0	L5	20	>99	18	0	17	Traces
15	7	1.0	L5	40	47	6	0	14	0
16 ^[b]	7	1.0	L5	40	82	21	0	0	0
17 ^[c]	7	1.0	L5	40	>99	Traces	0	27	Traces

^[a]GC yields; *n*-dodecane as internal standard. ^[b]20 mol% of MeSO₃H. ^[c]100 °C. ^[d]120 °C. ^[e]isolated yield.

Table 3. Polycondensation of **9** with different aliphatic diols.


Entry	Diol	Yield [%]	M_n^{GPC} [kg/mol]	M_w^{GPC} [kg/mol]	\bar{D}	T_g [°C] ^[a]
1	1,4-butanediol	91	20.6	45.4	2.2	-37
2	1,6-hexanediol	82	11.3	18.1	1.6	-43
3	1,12-dodecanediol	93	22.1	41.8	1.9	-20
4	1,4-pentanediol	87	28.5	61.7	2.1	-22

^[a] Measured by DSC.

reaction conditions. For this reason, we selected product **8** as the more promising alternative potential novel monomer for the preparation of polyesters.

Synthesis of MVG-derived polyesters.

Polycondensation of **8** and different diols in the presence of catalytic titanium(IV) isopropoxide was investigated. The reaction was run under solvent-free conditions at 150 °C for 6 hours, then vacuum was applied to drive the reaction to completion. Aliphatic linear diols, namely C4, C6 and C12, were tested (Table 3, entries 1-3). Additionally, 1,4-pentanediol, that could be obtained from levulinic acid and represents a promising new building block for polyesters,⁶ was tried (entry 4). Isolated yields up to 93% were obtained (Table 3), with molecular weight in the range of 10 to 20 kg/mol. The polymers were extensively characterized by ¹H and ¹³C NMR, IR, GPC, and DSC. All the materials were amorphous, elastic solids, with glass transitions (T_g) below room temperature. Applications of such materials might be found, for example, in the field of hot-melt adhesives or thermoplastic elastomers, where low T_g s are required.^{31, 32}

Conclusions

Sugar-derived methyl vinyl glycolate can be envisioned as a new building block for polymers. In this contribution, its reactivity in hydroformylation and methoxycarbonylation reactions was explored to afford new bifunctional monomers. Novel polyesters could be prepared in a straight-forward manner from MVG-derived diesters.

Experimental section

Hydroformylation of MVG In a glovebox, dicarbonyl(acetylacetonato)rhodium(I) (1.2 mg, 0.005 mmol, 0.5 mol%) and the desired ligand (0.095 mmol, 0.1 eq) were weighed into a vial. The vial was sealed, equipped with a magnetic stirrer and transferred out of the glovebox. The desired solvent (toluene or THF, 1.35 mL, 0.7 mol/L with respect

to MVG) and MVG (110 mg, 0.95 mmol, 1 eq) were added under argon atmosphere. The vials were placed into a 300 mL Parr stainless steel autoclave and pierced with a needle. The autoclave was flushed three times with nitrogen, then pressurized with 10 bar of syngas and heated to 80 °C. After stirring overnight, the reaction was cooled down to room temperature, the crude mixtures were filtered over celite, and the volatiles evaporated under reduced pressure. The crude residue was dissolved in CDCl₃ and analysed by ¹H NMR and GC-MS (Supporting Information).

Methyl 2-methoxybut-3-enoate (6) In a 250 mL Schlenk flask Ag₂O (19.6 g, 84.4 mmol, 2 eq) was suspended in 60 mL of diethyl ether (0.7 mol/L with respect to MVG). MVG (4.90 g, 42.2 mmol, 1 eq) was added under argon atmosphere. To the stirred suspension, methyl iodide (13.0 g, 84.4 mmol, 2 eq) was slowly added via syringe. The reaction was stirred at room temperature while monitoring the conversion by GC. After 60 hours, MVG was fully converted. The reaction was filtered to remove the solids, then the solvent and the excess of methylating agent removed by carefully distilling under vacuum, affording a colourless liquid (5.51 g, quantitative yield). ¹H NMR (300 MHz, CDCl₃) δ 5.85 (ddd, *J* = 17.2, 10.4, 6.4 Hz, 1H), 5.46 (dt, *J* = 17.2, 1.3 Hz, 1H), 5.34 (dt, *J* = 10.4, 1.3 Hz, 1H), 4.26 (dt, *J* = 6.4, 1.3 Hz, 1H), 3.76 (s, 3H), 3.40 (s, 3H). ¹³C NMR (75 MHz, CDCl₃) δ 171.1, 132.7, 119.6, 81.7, 57.5, 52.4.

Methyl 2-acetoxybut-3-enoate (7) In a 50 mL Schlenk flask, MVG (550 mg, 4.74 mmol, 1 eq) and pyridine (750 mg, 9.47 mmol, 2 eq) were dissolved in dichloromethane (16 mL, 0.3 mol/L with respect to MVG). To the stirred mixture, acetic anhydride (967 mg, 9.47 mmol, 2 eq) was slowly added via syringe. The reaction was stirred at room temperature overnight, then poured into ice-cold water and extracted three times with DCM. The organic phase was washed with 1M HCl, water and brine, then dried over Na₂SO₄ and concentrated in vacuum, affording 746 mg of colourless liquid (quantitative yield). ¹H NMR (400 MHz, CDCl₃) δ 5.87 – 5.77 (m, 1H), 5.41 – 5.31 (m, 2H), 5.24 (ddd, *J* = 10.5, 1.4, 0.9 Hz, 1H), 3.63 (s, 3H), 2.04 (s, 3H). ¹³C NMR (101 MHz, CDCl₃) δ 169.7, 168.7, 129.9, 119.5, 72.8, 52.3, 20.3.

Methoxycarbonylation reactions In a glovebox, palladium(II) diacetate (1.7 mg, 0.01 mmol, 1.0 mol%) and the desired ligand (0.02 mmol, 2.0 mol%) were weighed into a vial. The vial was sealed, equipped with a magnetic stirrer, and transferred out of the glovebox. Methanol (1.5 mL, 0.5 mol/L with respect to the substrate), methanesulfonic acid (2.2 mg, 0.02 mmol, 2 mol%) and the desired MVG derivative (see Table 2 main text; 0.80 mmol, 1 eq) were added under argon atmosphere. The vials were placed into a 300 mL Parr stainless steel autoclave and pierced with a needle. The autoclave was flushed three times with nitrogen, then pressurized with the desired pressure of carbon monoxide and heated to the required temperature. After stirring for the desired time, the reaction was cooled down to room temperature, the crude mixtures filtered over celite, and volatiles evaporated under reduced pressure. The crude

was purified by flash column chromatography (gradient elution, from 100% *n*-hexane to 100% ethyl acetate), affording the diester as a yellowish liquid.

Dimethyl 2-methoxypentanedioate (8) The general procedure described above was applied using **6** as substrate. **8** was obtained in 77% isolated yield as a clear colourless liquid. ¹H NMR (300 MHz, CDCl₃) δ 3.82 (dd, *J* = 7.8, 4.7 Hz, 1H), 3.75 (s, 3H), 3.67 (s, 3H), 3.38 (s, 3H), 2.44 (ddd, *J* = 7.7, 7.0, 3.6 Hz, 2H), 2.18 – 1.92 (m, 2H). ¹³C NMR (75 MHz, CDCl₃) δ 173.4, 172.7, 79.3, 58.4, 52.1, 51.8, 29.6, 27.9. ESI-MS (ES⁺): calculated for C₈H₁₄O₅: 191.0919; found: 213.0737 [M-Na]⁺.

Polycondensation reactions A 5 mL vial equipped with a stirring bar was charged with the desired diol (2.0 mmol, 1 eq) and **9** (380 mg, 2.0 mmol, 1 eq). The starting materials were extensively dried via vacuum-argon cycles, then titanium(IV) isopropoxide (3.2 mg, 0.01 mmol, 1 mol%) was added via syringe and the reaction heated up to 150 °C. After stirring under argon atmosphere for 6 hours, vacuum was applied for 1 hour. Viscosity visibly increased up to the point that the mixture wasn't stirred. Temperature was then increased to 190 °C and the reaction kept in vacuum another hour. After cooling down to room temperature, the solid products were analysed by NMR and GPC (Supporting Information).

Author Contributions

AD, ST and JdV developed the project and designed the reactions. AD performed the practical work including reactions and hydroformylations and wrote the manuscript. CS prepared and scaled up functionalized MVG and helped in the characterization of the polymers. ST, JdV and EB supervised the overall progresses.

Conflicts of interest

There are no conflicts to declare.

Acknowledgements

The German Federal Ministry of Food and Agriculture (BMEL) and the project sponsor Fachagentur Nachwachsende Rohstoffe e. V. (FNR) are acknowledged for financing the project »BIOVIN« as part of the funding program "Nachwachsende Rohstoffe"FPNR, promotional reference n° 2219NR171. The authors are grateful to Brian Spiegelberg, Andreas Taden, Adrian Brandt and Horst Beck (Henkel AG & Co) for the useful discussions. Haldor Topsøe A/S is thanked for gifting MVG.

Notes and references

1. A. Corma, S. Iborra and A. Velty, *Chemical Reviews*, 2007, **107**, 2411-2502.
2. P. N. R. Vennestrøm, C. M. Osmundsen, C. H. Christensen and E. Taarning, *Angewandte Chemie International Edition*, 2011, **50**, 10502-10509.
3. C. O. Tuck, E. Pérez, I. T. Horváth, R. A. Sheldon and M. Poliakoff, *Science*, 2012, **337**, 695-699.
4. *Bioplastics market data*, <https://www.european-bioplastics.org/market/>, (accessed 24/06/2022).
5. Y. Liu and S. Mecking, *Angewandte Chemie International Edition*, 2019, **58**, 3346-3350.
6. B. M. Stadler, A. Brandt, A. Kux, H. Beck and J. G. de Vries, *ChemSusChem*, 2020, **13**, 556-563.
7. H. Sardon, D. Mecerreyes, A. Basterretxea, L. Avérous and C. Jehanno, *ACS Sustainable Chemistry & Engineering*, 2021, **9**, 10664-10677.
8. L. T. Mika, E. Cséfalvay and Á. Németh, *Chemical Reviews*, 2018, **118**, 505-613.
9. K. I. Galkin and V. P. Ananikov, *ChemSusChem*, 2019, **12**, 185-189.
10. I. Bodachivskyj, U. Kuzhiumparambil and D. B. G. Williams, *ChemSusChem*, 2018, **11**, 642-660.
11. P. J. Deuss, K. Barta and J. G. de Vries, *Catalysis Science & Technology*, 2014, **4**, 1174-1196.
12. M. S. Holm, S. Saravanamurugan and E. Taarning, *Science*, 2010, **328**, 602-605.
13. M. Dusselier, P. Van Wouwe, F. de Clippel, J. Dijkmans, D. W. Gammon and B. F. Sels, *ChemCatChem*, 2013, **5**, 569-575.
14. R. De Clercq, M. Dusselier, C. Christiaens, J. Dijkmans, R. I. Iacobescu, Y. Pontikes and B. F. Sels, *ACS Catalysis*, 2015, **5**, 5803-5811.
15. S. Tolborg, S. Meier, I. Sádaba, S. G. Elliot, S. K. Kristensen, S. Saravanamurugan, A. Riisager, P. Fristrup, T. Skrydstrup and E. Taarning, *Green Chemistry*, 2016, **18**, 3360-3369.
16. A. Sølvhøj, E. Taarning and R. Madsen, *Green Chemistry*, 2016, **18**, 5448-5455.
17. M. B. Buendia, A. E. Daugaard and A. Riisager, *Catalysis Letters*, 2021, **151**, 8-16.
18. I. Delidovich, P. J. C. Hausoul, L. Deng, R. Pfützenreuter, M. Rose and R. Palkovits, *Chemical Reviews*, 2016, **116**, 1540-1599.
19. B. M. Stadler, C. Wulf, T. Werner, S. Tin and J. G. de Vries, *ACS Catalysis*, 2019, **9**, 8012-8067.
20. H. Li, R. M. Shakaroun, S. M. Guillaume and J.-F. Carpentier, *Chemistry – A European Journal*, 2020, **26**, 128-138.
21. E. Gubbels, T. Heitz, M. Yamamoto, V. Chilekar, S. Zorbakhsh, M. Gepraegs, H. Köpnick, M. Schmidt, W. Brüggling, J. Rüter and W. Kaminsky, in *Ullmann's Encyclopedia of Industrial Chemistry*, DOI: https://doi.org/10.1002/14356007.a21_227.pub2, pp. 1-30.
22. M. Dusselier, P. Van Wouwe, S. De Smet, R. De Clercq, L. Verbelen, P. Van Puyvelde, F. E. Du Prez and B. F. Sels, *ACS Catalysis*, 2013, **3**, 1786-1800.
23. R. Franke, D. Selent and A. Börner, *Chemical Reviews*, 2012, **112**, 5675-5732.
24. V. S. Sikarwar, M. Zhao, P. Clough, J. Yao, X. Zhong, M. Z. Memon, N. Shah, E. J. Anthony and P. S. Fennell, *Energy & Environmental Science*, 2016, **9**, 2939-2977.
25. M. B. Figueirêdo, I. Hita, P. J. Deuss, R. H. Venderbosch and H. J. Heeres, *Green Chemistry*, 2022, **24**, 4680-4702.
26. S. Püschel, S. Störtte, J. Topphoff, A. J. Vorholt and W. Leitner, *ChemSusChem*, 2021, **14**, 5226-5234.
27. K. Dong, X. Fang, S. Gülak, R. Franke, A. Spannenberg, H. Neumann, R. Jackstell and M. Beller, *Nature Communications*, 2017, **8**, 14117.

28. W. Clegg, M. R. J. Elsegood, G. R. Eastham, R. P. Tooze, X. Lan Wang and K. Whiston, *Chemical Communications*, 1999, DOI: 10.1039/A905521E, 1877-1878.
29. P. A. C. Graham Ronald Eastham, Robert Paul Tooze, Kingsley John Cavell, Peter Gerald Edwards, Dennis Lee Coleman, 2004.
30. B. M. Jessen, J. M. Onozabal, C. M. Pedersen, A. Sølvhøj, E. Taarning and R. Madsen, *ChemistrySelect*, 2020, 5, 2559-2563.
31. A. Plichta, T. Jaskulski, P. Lisowska, K. Macios and A. Kundys, *Polymer*, 2015, 72, 307-316.
32. A. R. Kim, M. S. Park, S. Lee, M. Ra, J. Shin and Y.-W. Kim, *Journal of Applied Polymer Science*, 2020, 137, 48474.

7. Appendix

7.1 Contributions to the Individual Publications

“Scalable synthesis and polymerisation of a β -angelica lactone derived monomer”

A. Dell’Acqua, † B. M. Stadler, † S. Kirchhecker, S. Tin, J. G. de Vries (†equal contributions), *Green Chem.* **2020**, *22*, 5267–5273.

Scale-up and optimization of the reaction conditions for the isomerization α to β AL. Scope of different dienes in the Diels-Alder and scale-up of the reaction with cyclopentadiene. Polymerization using different solvents and characterization of the polymers by DSC and GPC. Around half of the manuscript preparation.

Overall contribution about 40%

“Ozonolysis of α -angelica lactone: a renewable route to malonates”

A. Dell’Acqua, L. Wille, B. M. Stadler, S. Tin, J. G. de Vries, *Chem. Commun.* **2021**, *57*, 10524-10527.

Design of the reaction setup. Screening of solvents and quenching conditions. Scale-up of the production of malonic acid. Mechanistic investigations. Preparation of the manuscript.

Overall contribution about 70%

“Glycolaldehyde as a Bio-based C1 Building Block for Selective N-Formylation of Secondary Amines”

M. T. Flynn[†], X. Liu[†], A. Dell’Acqua, J. Rabeah, A. Brückner, E. Baráth, S. Tin, J. G. de Vries (†equal contributions), *ChemSusChem.* **2022**, in press.

Mechanistic investigations and control experiments. Help with the substrate scope and in writing the manuscript.

Overall contribution about 30%

“New Bifunctional Monomers from Methyl Vinyl Glycolate”

A. Dell’Acqua, C. Schünemann, E. Baráth, S. Tin, J. G. de Vries, *manuscript under revision.*

Design of the concept of the project and of the experiments. Synthesis of MVG derivatives, hydroformylations and methoxycarbonylations. Polycondensations and full characterizations of the polymers. Redaction of the manuscript.

Overall contribution about 85%.

7.2 Supporting Information

Scalable synthesis and polymerisation of an α -angelica lactone derived monomer

Andrea Dell'Acqua,^{a,†} Bernhard M. Stadler,^{a,†} Sahra Kirchecker,^a Sergey Tin^a and Johannes G. de Vries^{a,*}

^aLeibniz Institut für Katalyse e. V. an der Universität Rostock

Albert-Einstein-Strasse 29a, 18055 Rostock

E-mail: johannes.devries@catalysis.de

Experimental Procedures

1. General information

Reagents: α -angelica lactone (98%, Sigma Aldrich) was used as received, triethylamine (99% Acros) was distilled over KOH and stored under argon atmosphere, aluminium triflate (98%, Sigma Aldrich) and zinc chloride (99%, abcr) were stored under argon in a glove box. Cyclopentadiene (CPD) was prepared by thermal cracking of dicyclopentadiene (TCI) over iron(0) at 180°C.

NMR-Spectroscopy: ¹H-NMR and ¹³C-NMR were recorded at ambient temperature on 300 MHz spectrometers (Avance 300 respectively Fourier 300) or a 400 MHz spectrometer (Avance 400) from Bruker. The chemical shifts δ are given in ppm and referenced to the residual proton signal of the deuterated solvent used.

Gel permeation chromatography (GPC): Gel permeation chromatograms were recorded with 1260 Infinity GPC/SEC System from Agilent Technologies. The setup consisted of a SECcurity Isocratic Pump, SECcurity 2-Canal-Inline-Degaser, SECcurity GPC-Column thermostat TCC6000, SECcurity Fraction Collector and SECcurity Differential Refractometer detector. The measurements were performed at a constant temperature of 50 °C using three columns with a polyester co-polymer network as the stationary phase (PSS GRAM 30 Å, 10 μ m particle size, 8.0 \times 50 mm; PSS GRAM 30 Å, 10 μ m particle size, 8.0 \times 300 mm; PSS GRAM 1000 Å particle size, 8.0 \times 300 mm). THF was applied as the mobile phase with a flow rate of 1 mL·min⁻¹. Polystyrene standards from ReadyCal (PSS-pskitr1I-10, M_p = 370–252000 g·mol⁻¹) were used for calibration purposes.

Differential scanning calorimetry (DSC): Melting points and glass transition temperatures of polymers were measured with a Star-SW DSC from Mettler Toledo using the following temperature program: -90.00 °C isothermal 5.00 min; Ramp 10.00 °C min⁻¹ to 200.00 °C; Ramp 10.00 °C/min to -90.00 °C; -90.00 °C isothermal 5.00 min; Ramp 10.00 °C min to 200.00 °C; Ramp 10.00 °C/min to -90.00 °C.

TGA measurements were conducted with an STA-499-Jupiter DSC/TGA device from Netzsch using a heating rate of 10.00°C from 25°C to 600°C under a nitrogen atmosphere.

2. Preparation of a mixture of angelica lactones with 90 mol-% content of the β -isomer

α -angelica lactone (98%, 120 g, 1.2 mol) was added to a 250 ml two neck flask equipped with a condenser and a magnetic stirrer followed by the addition of triethyl amine (5 mol-%, 8.5 ml). The mixture was heated to 100 °C under an argon atmosphere and monitored by ¹H-NMR. After 1.5 hours a ratio of β / α -angelica lactone of 90-95/10-5 was reached and the condenser exchanged with a distillation head. Subsequent vacuum distillation at 6 \times 10⁻² mbar yielded two fractions: 38-42°C containing mainly the α -isomer. 45-50°C yielded a mixture of angelica lactones with 90 mol-% content of the β -isomer (106 g, 88% of theory).

^1H NMR (400 MHz, CD_2Cl_2 , signals of β -isomer are reported) δ 7.46 (dd, $J = 5.7, 1.5$ Hz, 1H), 6.04 (dd, $J = 5.7, 2.0$ Hz, 1H), 5.11 (qt, $J = 6.9, 2.0, 1.5$ Hz, 1H), 1.41 (d, $J = 6.9$ Hz, 3H). ^{13}C NMR (101 MHz, CD_2Cl_2) δ 173.3, 158.0, 121.3, 80.0, 19.0.

3. Screening procedure of the DA-reaction with β -Angelica lactone and CPD

In a dry and argon purged 10 ml reaction tube the angelica lactone mixture (β -AL=90%, 10 mmol, 900 μl) and the desired catalyst were mixed. Freshly prepared CPD (3.0-10 eq. 2.5-8.3 ml) was added, the tube was sealed and heated with a microwave oven to the desired reaction temperature where it is kept for the indicated time.

The 2 diastereoisomers of the product were separated by flash column chromatography (heptane/ethyl acetate 8:2), affording the *endo* and *exo* isomers (each of them is a racemic mixture of 4 stereoisomers) adduct as colourless oils (*endo*: 949 mg, 5.9 mmol, 30%; *exo*: 119 mg, 0.7 mmol, 7%; *endo/exo* 89/11).

exo ^1H NMR (300 MHz, CD_2Cl_2) δ 6.21 – 6.04 (m, 2H), 4.17 (qd, $J = 6.4, 3.2$ Hz, 1H), 3.24 – 3.03 (m, 1H), 2.82 (dtq, $J = 3.1, 1.5, 0.8$ Hz, 1H), 2.59 (dt, $J = 8.3, 1.3$ Hz, 1H), 2.08 – 1.97 (m, 1H), 1.50 – 1.35 (m, 7H), 1.30 (d, $J = 6.4$ Hz, 3H). ^{13}C NMR (75 MHz, CD_2Cl_2) δ 177.4, 136.4, 134.9, 78.9, 51.6, 48.5, 48.2, 46.0, 45.6, 22.8.

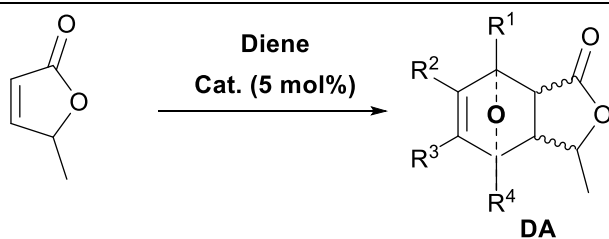
endo ^1H NMR (300 MHz, CD_2Cl_2) δ 6.22 – 6.09 (m, 2H), 3.95 (qd, $J = 6.5, 3.1$ Hz, 1H), 3.26 – 2.97 (m, 3H), 2.67 – 2.54 (m, 1H), 1.57 – 1.46 (m, 1H), 1.39 – 1.29 (m, 1H), 1.25 (d, $J = 6.5$ Hz, 3H). ^{13}C NMR (75 MHz, CDCl_3) δ 177.3, 137.6, 137.5, 80.7, 50.0, 48.9, 47.6, 46.3, 43.1, 23.2.

4. Semi continuous synthesis of the β -Angelica lactone CPD adduct

A 500 mL 2-neck round bottom flask was filled with dicyclopentadiene (100 mL) and iron(0) powder and equipped with a distillation setup. Cyclopentadiene was obtained by thermal cracking of its corresponding dimer at 180 °C and then condensed into a dropping funnel. 2 equivalents (84 mL, 67 g, 1.0 mol) were dropped over 10 hours into a 1 liter 3-necks round bottom flask containing the angelica lactone mixture (β -AL=90%; 50 g, 0.5 mol) and zinc(II) chloride (3.5 g, 0.03 mol, 0.05 eq) while heating up to 70 °C. Once the addition was complete, the reaction was stirred for another 10 hours and monitored by GC. After cooling down to room temperature, acetone (80-150 ml) was added to precipitate the Lewis acid catalyst. The liquid phase was concentrated *in vacuo* and the remaining AL dimers were eventually precipitated by addition of ice cold methanol (100 ml) followed by filtration. Solvent removal afforded the product as an orange liquid (69 g, 0.4 mol, 82% yield, *endo:exo* 89/11).

5. Screening of the DA-reaction with other dienes

Microwave-assisted reactions. In an oven-dried 10 mL reaction tube the angelica lactones mixture (β -AL=90%; 98 mg, 1 mmol), the desired solvent (if used, 2 mL) and catalyst (5 mol%) were added under argon. The diene (10 eq) was added subsequently while stirring the mixture, then the tube was placed in a microwave oven and heated at the desired temperature for the indicated time (Table S1).

Table S1 Screening of the reaction conditions for the DA-reaction between β -AL and different dienes

Entry	Substrate	Lewis Acid	Solvent	Temperature	Time	DA ^a
				[°C]	[min]	[%]
1	2,5-DMF ^b	-	-	60	30	0
2	2,5-DMF	ZnCl ₂	-	60	30	0
3	2,5-DMF	Et ₃ Al / AlCl ₃	-	90	30	0
4	β -Farnesene	ZnCl ₂	-	60	30	0
5	β -Farnesene	AlCl ₃	-	60	30	0
6	β -Farnesene	Et ₃ Al / AlCl ₃	-	90	30	0
7	β -Farnesene	Et ₃ Al / AlCl ₃	Toluene	110	90	0
8	Myrcene	ZnCl ₂	-	60	30	< 2%
9	Myrcene	Et ₃ Al / AlCl ₃	-	90	30	< 2%
10	Myrcene	Et ₃ Al / AlCl ₃	Toluene	110	90	0
11	Myrcene	In(OTf) ₃	-	70	60	0
12	Myrcene	Sm(OTf) ₃	-	70	60	0
13	Furane	ZnCl ₂	-	60	30	0
14	Furane	Et ₃ Al / AlCl ₃	-	90	30	0
15	Furane	Et ₃ Al / AlCl ₃	Toluene	110	90	0
16	Furane	Yb(OTf) ₃	-	70	30	0
17	Furane	Yb(OTf) ₃	-	130	30	0
18	Furfuryl alcohol	ZnCl ₂	-	70	30	0
19	Furfuryl alcohol	ZnCl ₂	-	130	30	0
20	Furfuryl alcohol	AlCl ₃	-	70	30	0
21	Furfuryl alcohol	AlCl ₃	-	130	30	0
22	Isoprene	ZnCl ₂	-	70	30	0
23	Isoprene	ZnCl ₂	-	130	30	0
24	Isoprene	AlCl ₃	-	70	30	0
25	Isoprene	AlCl ₃	-	130	30	0

^aGC conversion. ^b2,5-DMF = 2,5-dimethylfuran.

High temperature reactions. 4 mL glass vials equipped with magnetic stirring bar and PTFE septum were filled with the angelica lactones mixture (β -AL=90%; 98 mg, 1 mmol) and the diene (10 eq) under argon. The vials were then pierced with needles and placed in a 300 mL stainless steel autoclave, which was pressurised with 20 bar of nitrogen and heated up to 200 °C. The reaction was stirred for 16 hours, then cooled down to room temperature and the reaction mixture was filtered over a short path of silica and directly analysed by GC.

Isoprene/ β AL. β -Angelica lactone (0.1 mL, 1.0 mmol, 1 eq) and isoprene (2.0 mL, 20 mmol, 20 eq) were added to a stainless steel autoclave and pressurized with 30 bar of nitrogen (to prevent isoprene evaporation). The reaction was stirred at 200 °C for 24 hours. The crude was purified by flash column chromatography (heptane/EtOAc 8:2). The desired product (as mixture of 2 regioisomers, each of them containing 2 diastereoisomers and 2 enantiomers) was obtained as a yellow oil (99.5 mg, 0.6 mmol, 60%).

^1H NMR (300 MHz, CDCl_3) δ 5.45 – 5.32 (m, 1H), 4.25 – 4.15 (m, 1H), 2.85 – 2.67 (m, 1H), 2.37 – 2.04 (m, 4H), 1.91 – 1.70 (m, 1H), 1.62 (dddt, $J = 3.8, 2.4, 1.9, 0.9$ Hz, 3H), 1.32 (dd, $J = 6.4, 3.8$ Hz, 3H). ^{13}C NMR (75 MHz, CDCl_3) δ 179.2, 179.1, 132.9, 132.4, 119.1, 118.8, 80.9, 80.9, 39.7, 38.6, 37.3, 36.3, 29.3, 26.9, 25.0, 23.7, 23.4, 22.6, 19.3, 19.2.

MS (EI): m/z calcd. for $[\text{C}_{10}\text{H}_{14}\text{O}_2]^+$: 166.1; found: 166.

Myrcene/ β AL. β -Angelica lactone (0.1 mL, 1.0 mmol, 1 eq) and myrcene (1.7 mL, 20 mmol, 20 eq) were added to a SS autoclave and pressurized with 30 bar of nitrogen (to prevent isoprene evaporation). The reaction was stirred at 200 °C for 24 hours. The crude was purified by flash column chromatography (heptane/EtOAc 8:2). The desired product (as mixture of 2 regioisomers, each of them containing 2 diastereoisomers and 2 enantiomers) was obtained as a yellow oil (127 mg, 0.54 mmol, 54%).

MS (EI): m/z calcd. for $[\text{C}_{15}\text{H}_{22}\text{O}_2]^+$: 234.3; found: 234.

Farnesene/ β AL. β -Angelica lactone (0.1 mL, 1.0 mmol, 1 eq) and β -farnesene (2.4 mL, 20 mmol, 20 eq) were added to a SS autoclave and pressurized with 30 bar of nitrogen (to prevent isoprene evaporation). The reaction was stirred at 200 °C for 24 hours. The crude was purified by flash-column chromatography (heptane/EtOAc 8:2). The desired product (as mixture of 2 regioisomers, each of them

containing 2 diastereoisomers and 2 enantiomers) was obtained as a yellow oil (41.3 mg, 0.18 mmol, 18%).

MS (EI): m/z calcd. for $[C_{20}H_{30}O_2]^+$: 302.5; found: 302.

Table S2 Screening of the reaction conditions for the DA-reaction between β -AL and different dienes

Entry	Diene	Conversion ^a [%]
1	2,5-DMF	-
2	β -Farnesene	64 (18) ^b
3	Myrcene	> 99 (54)
4	Furane	-
5	Furfuryl alcohol	-
6	Isoprene	> 99 (60)

^aGC Conversion. ^bIsolated yields after column chromatography (Heptane/Ethyl acetate 8:2) are reported in brackets.

6. Ring-opening metathesis polymerization of Cp/ β AL adduct

Solvent screening. To a stirred solution of Grubbs II catalyst (4.7 mg, 0.006 mmol, 0.25 mol%) in the desired solvent (Table 3) the Cp/ β AL adduct (0.2 mL, 2.2 mmol, 1 eq) was added under argon atmosphere. The reaction was stirred overnight. In few minutes after the addition, all the solutions turned opalescent and a white'ish precipitate appeared, except for the reaction in DCM. The reaction mixtures were then concentrated *in vacuo* and washed several times with methanol (using DCM to re-dissolve the polymer). All the reaction afforded a white'ish, gummy solid. A small portion of each sample was dissolved in a DMF/LiBr solution and analyzed by GPC.

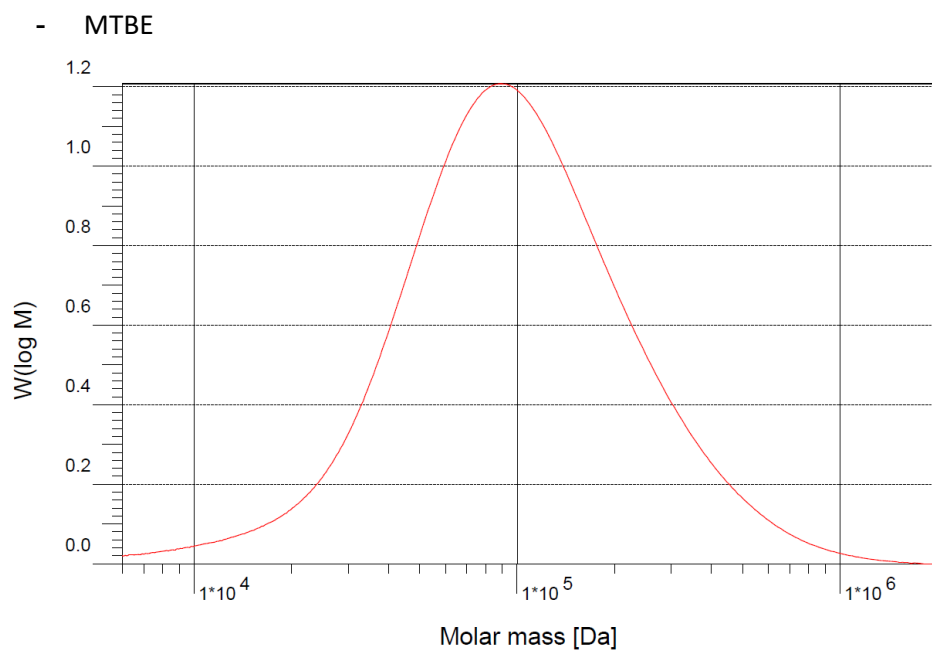


Figure S1. GPC chromatogram of poly-Cp/ β AL; polymerization performed in MTBE.

$$\overline{M}_n = 67.8 \text{ kDa}; \overline{M}_w = 138 \text{ kDa}; \mathcal{D} = 2.04$$

- 2-Methyl-THF

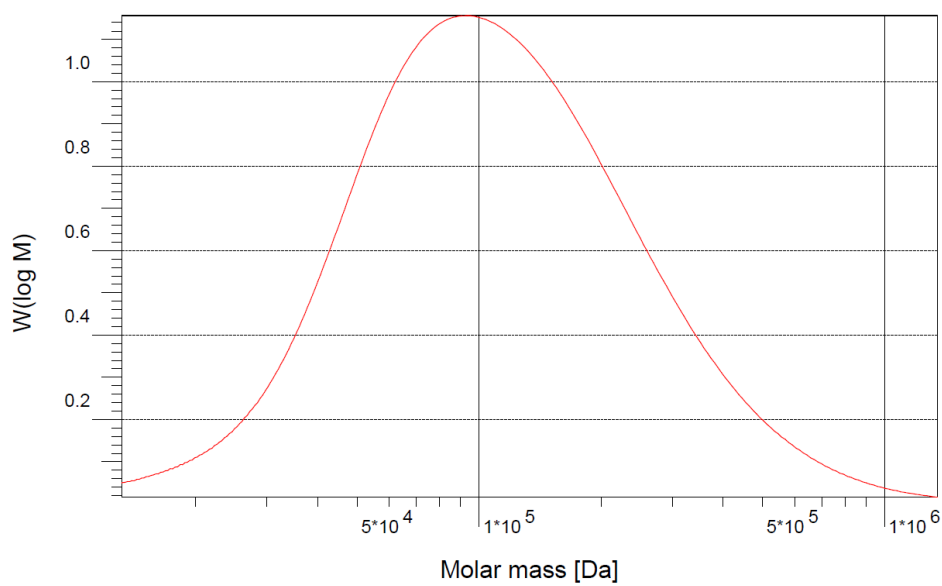


Figure S2. GPC chromatogram of poly-Cp/ β AL; polymerization performed in 2-Me-THF.

$$\overline{M}_n = 80.6 \text{ kDa}; \overline{M}_w = 154 \text{ kDa}; \mathcal{D} = 1.91$$

- EtOAc

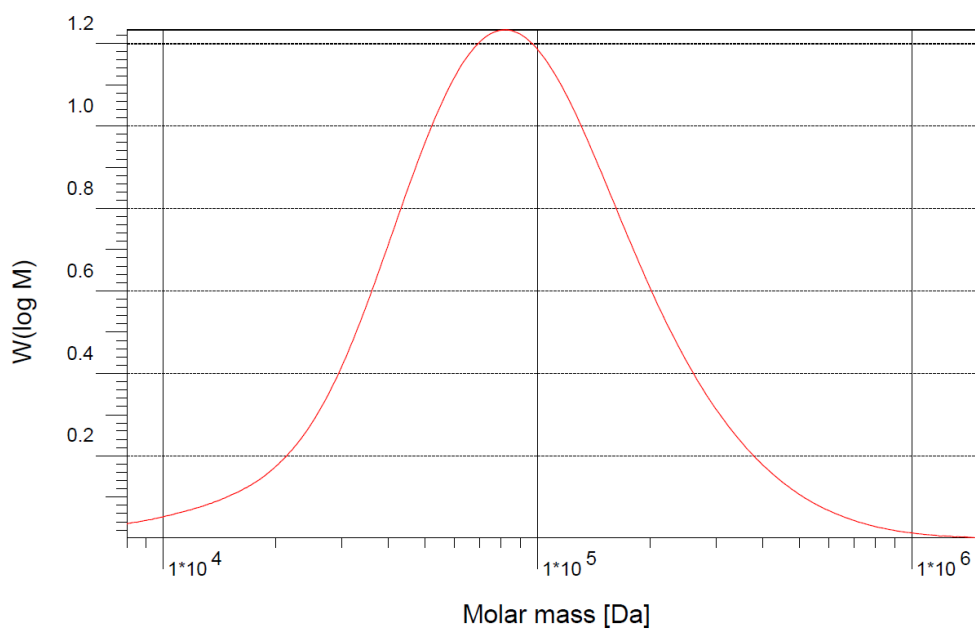


Figure S3. GPC chromatogram of poly-Cp/ β AL; polymerization performed in EtOAc.

$\bar{M}_n = 64.1$ kDa; $\bar{M}_w = 118$ kDa; $\mathcal{D} = 1.85$

- MIBK

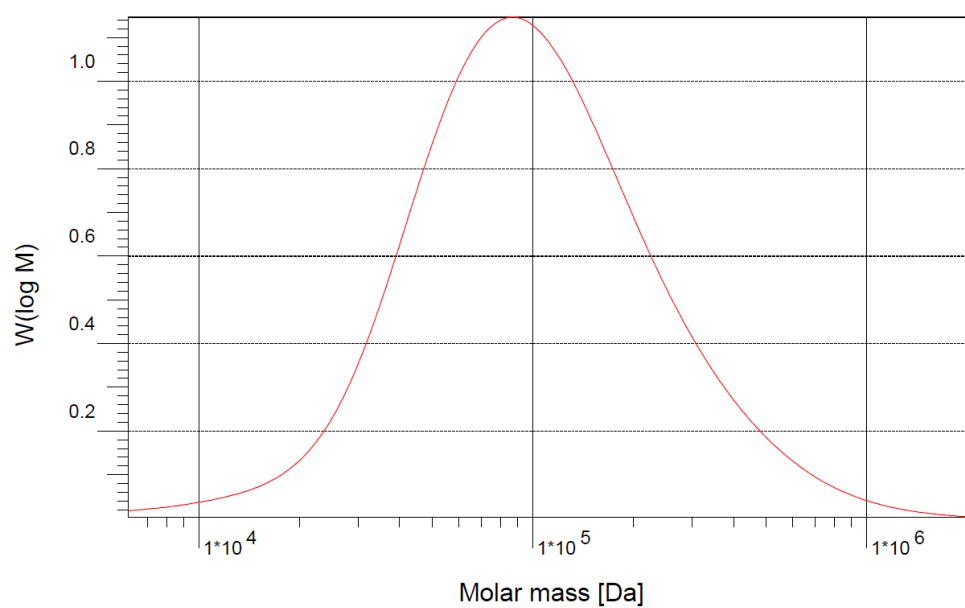


Figure S4. GPC chromatogram of poly-Cp/ β AL; polymerization performed in MIBK.

$\overline{M}_n = 70.9 \text{ kDa}$; $\overline{M}_w = 146 \text{ kDa}$; $\mathcal{D} = 2.06$

- DCM

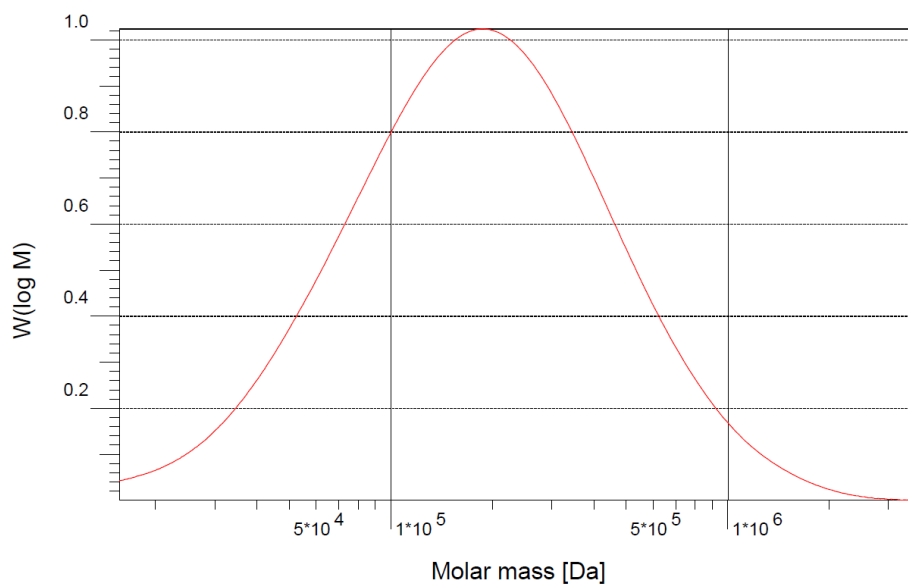


Figure S5. GPC chromatogram of poly-Cp/ β AL; polymerization performed in DCM.

$\overline{M}_n = 122 \text{ kDa}$; $\overline{M}_w = 264 \text{ kDa}$; $\mathcal{D} = 2.17$

Poly-norbornene. To a stirred solution of Grubbs II catalyst (4.7 mg, 0.006 mmol, 0.25 mol%) in 2 mL of dichloromethane, norbornene (207 mg, 2.2 mmol, 1 eq) was added under argon atmosphere. The reaction was stirred for 5 hours. The reaction mixtures were then concentrated *in vacuo* and washed several times with methanol (using DCM to re-dissolve the polymer). All the reaction afforded a white'ish, gummy solid. A small portion of each sample was dissolved in a THF and analyzed by GPC.

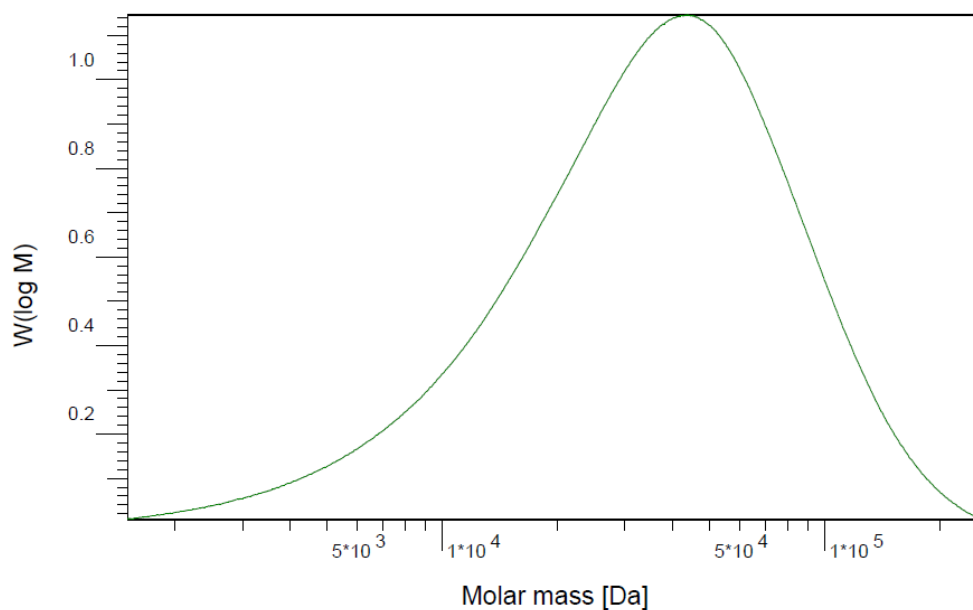


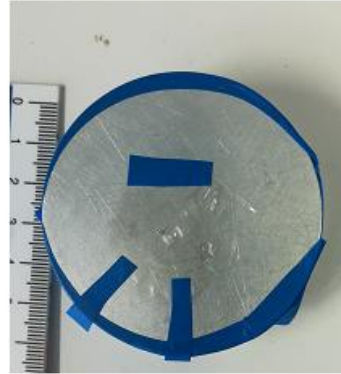
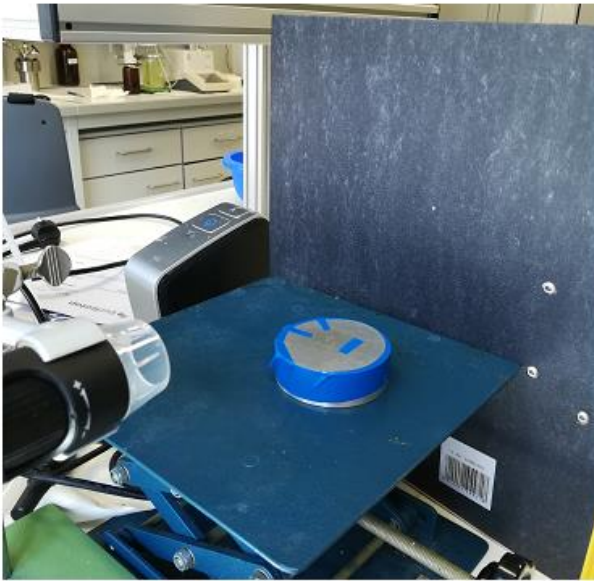
Figure S6. GPC chromatogram of poly-norbornene.

$$\overline{M}_n = 21.8 \text{ kDa}; \overline{M}_w = 45.9 \text{ kDa}; \mathcal{D} = 2.11$$

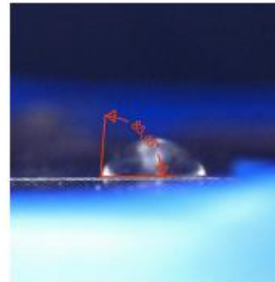
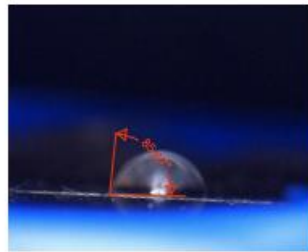
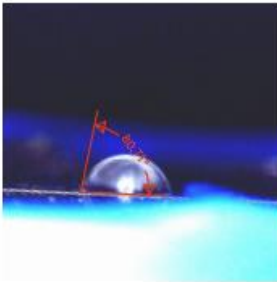
7. Contact angle measurements

A film of the desired polymer (obtained by casting a solution of the polymer in dichloromethane on a Teflon mold and letting the solvent evaporate over 4 hours) was anchored to a stainless-steel flat surface (Figure S7-a). 10 μL of distilled water were dropped on the polymer film using a Hamilton syringe. A picture of the drop was recorded using a DNT DigiMicro Profi digital microscope. Contact angles were determined by measuring the angle using CorrelDraw software. The reported values are the average between 3 different measurements.

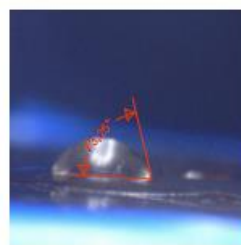
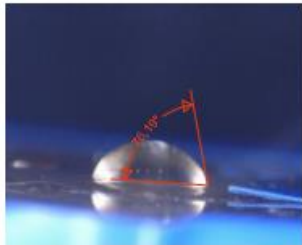
a)



b)



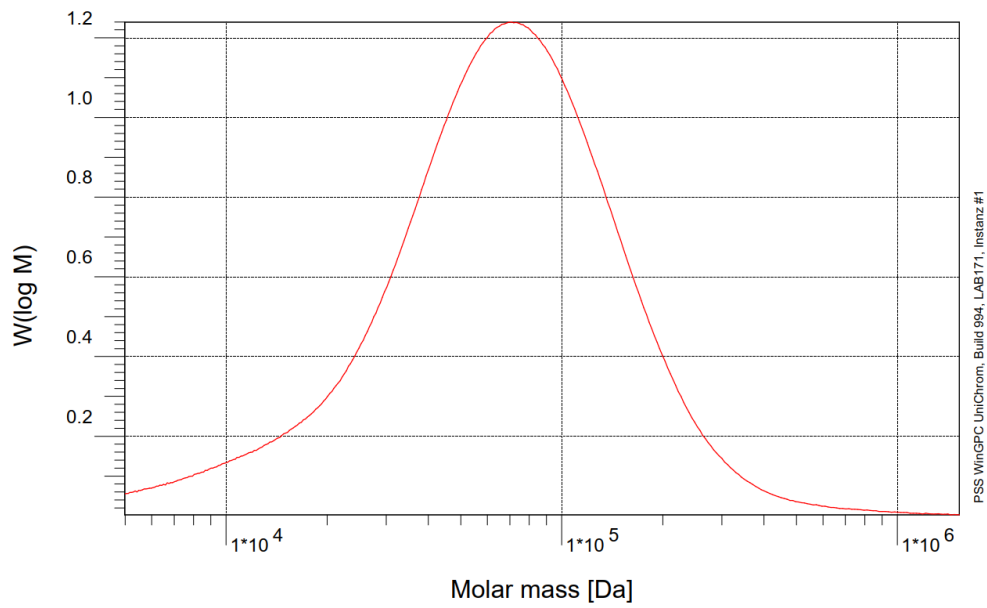
c)



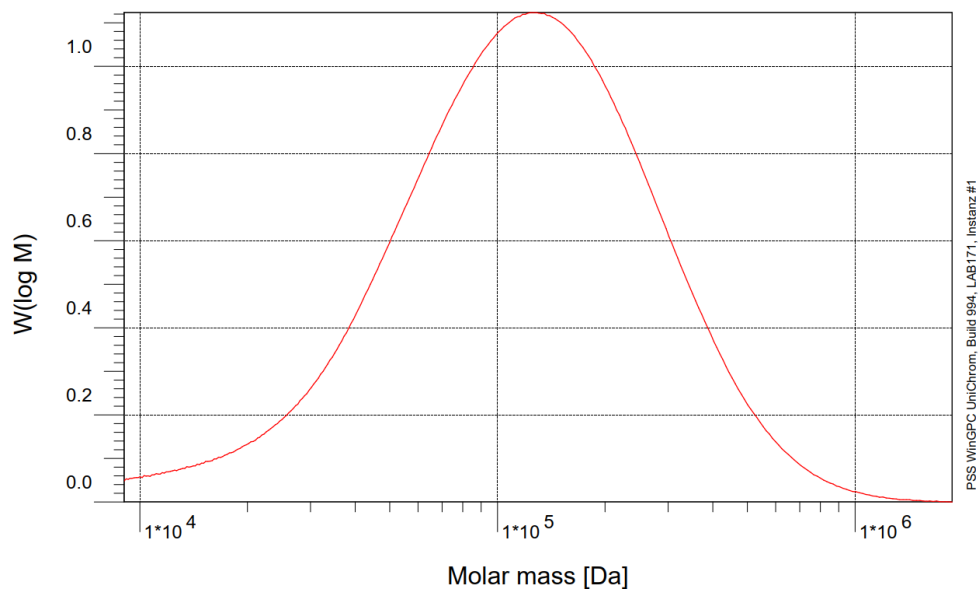
Average contact angle: *poly*-Norbornene: $\theta = 83.9^\circ$; *poly*-Cp/ β AL: $\theta = 75.7^\circ$

8. Experiments at different monomer / initiator ratios.

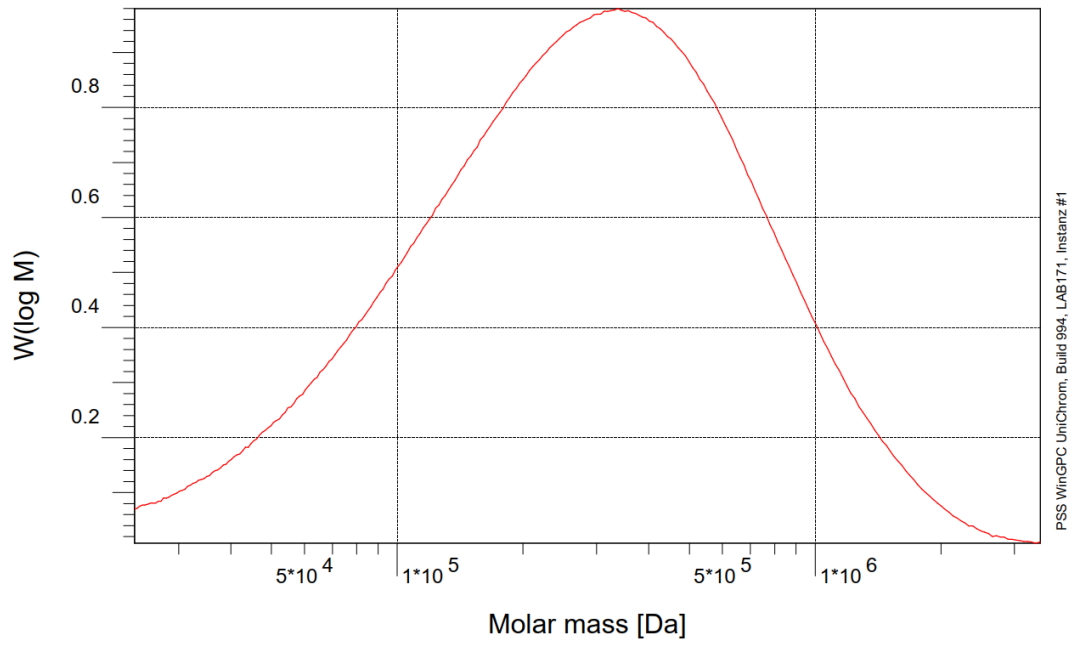
100:1



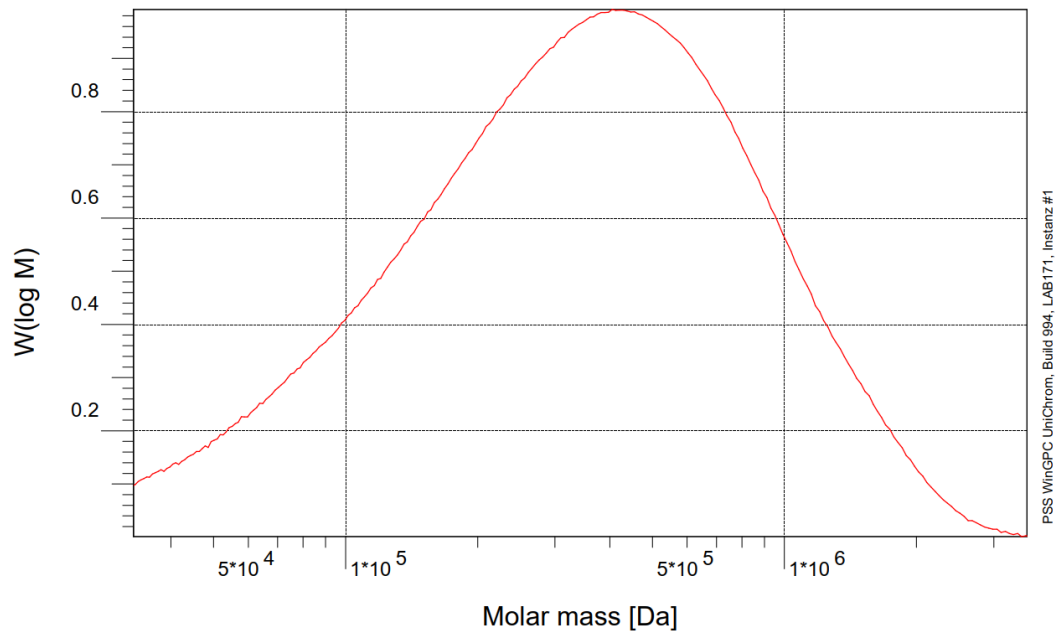
200:1



400:1

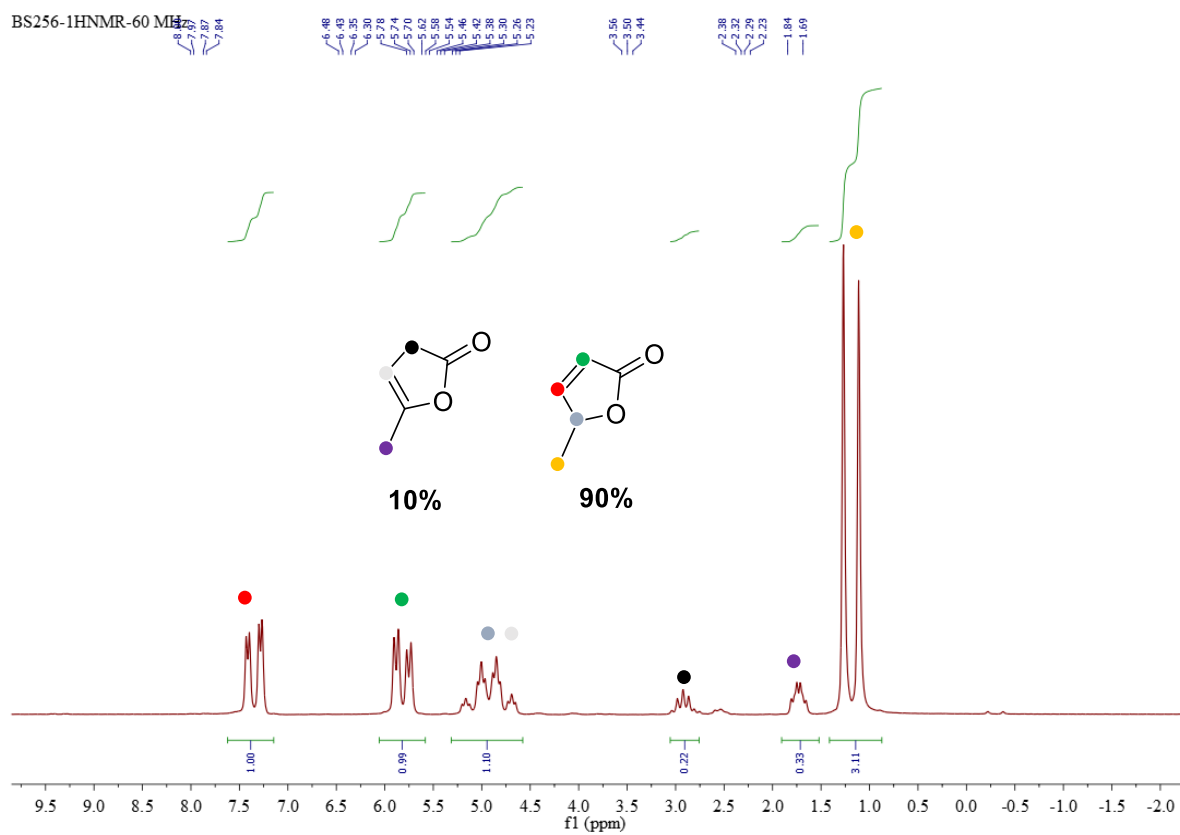


600:1



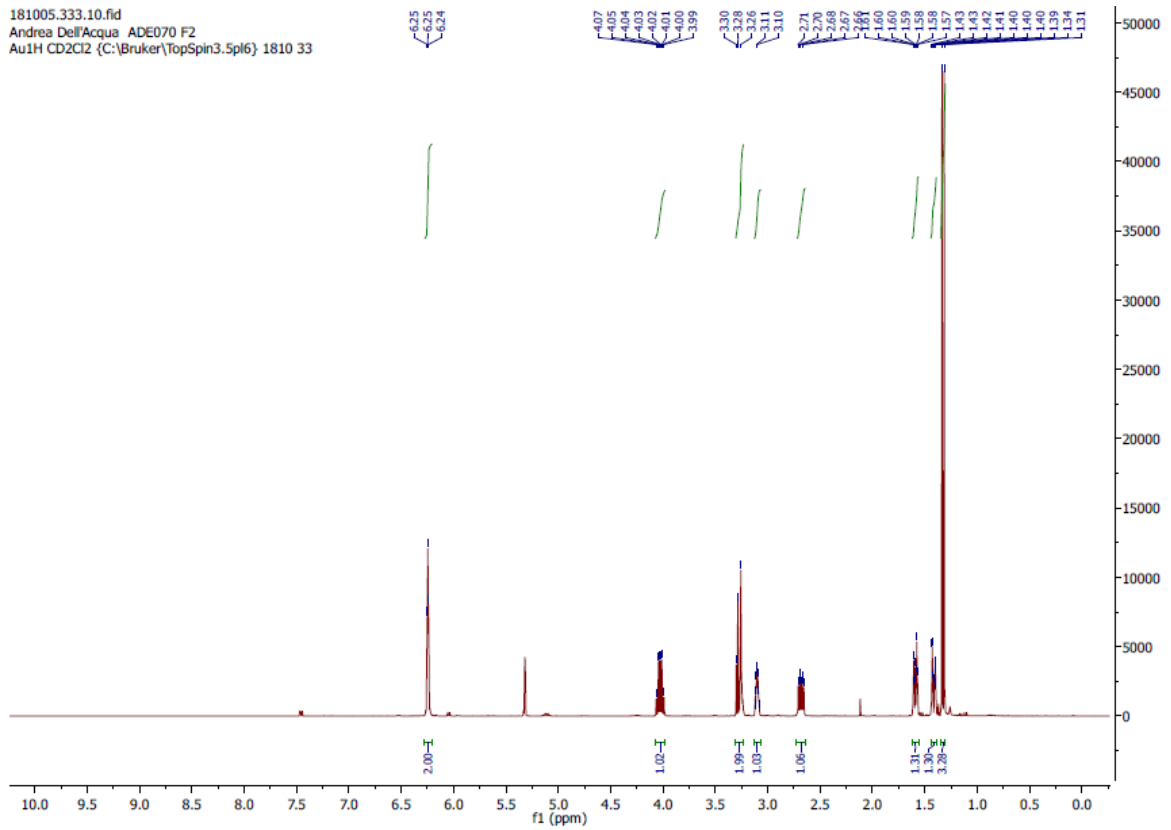
9. Spectral data

$^1\text{H-NMR}$ of the angelica lactone product mixture

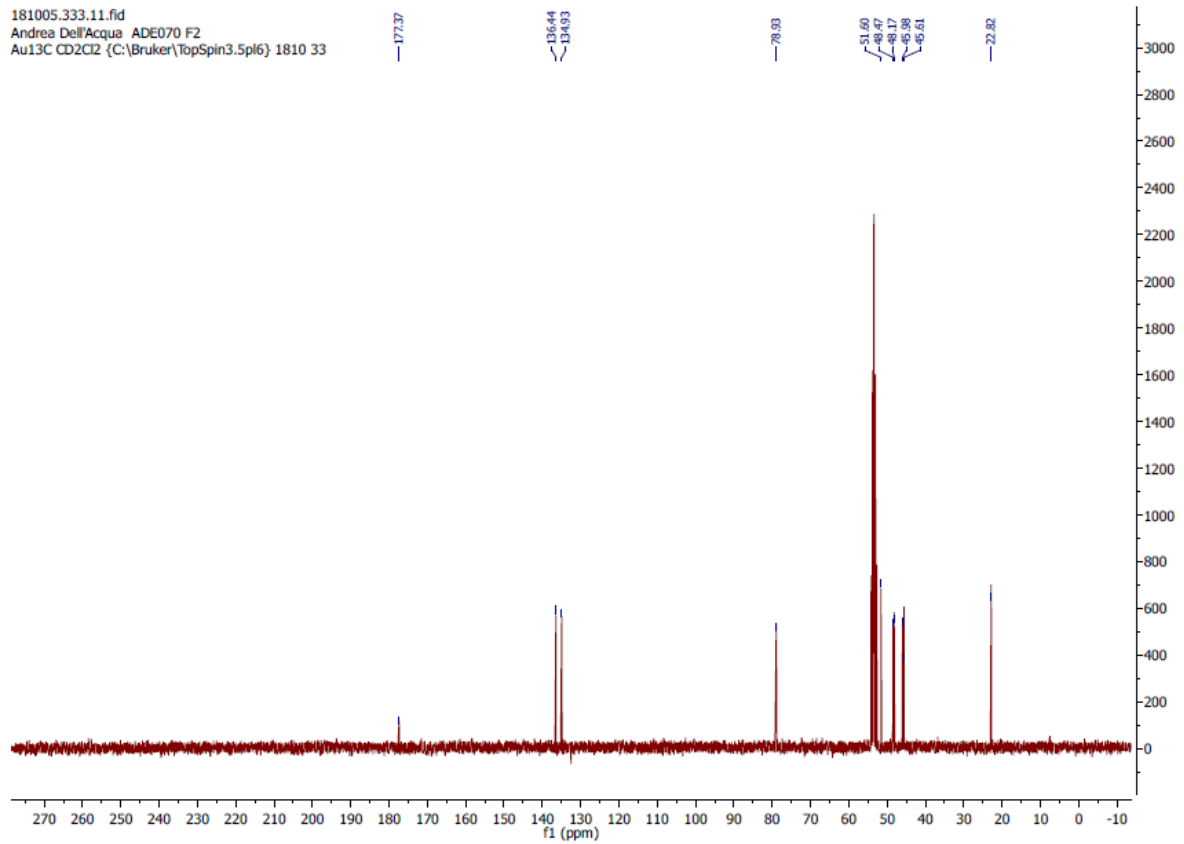


endo-Cp/ β AL

181005.333.10.fid
 Andrea Dell'Acqua ADE070 F2
 Au1H CD2Cl2 (C:\Bruker\TopSpin3.5pl6) 1810 33

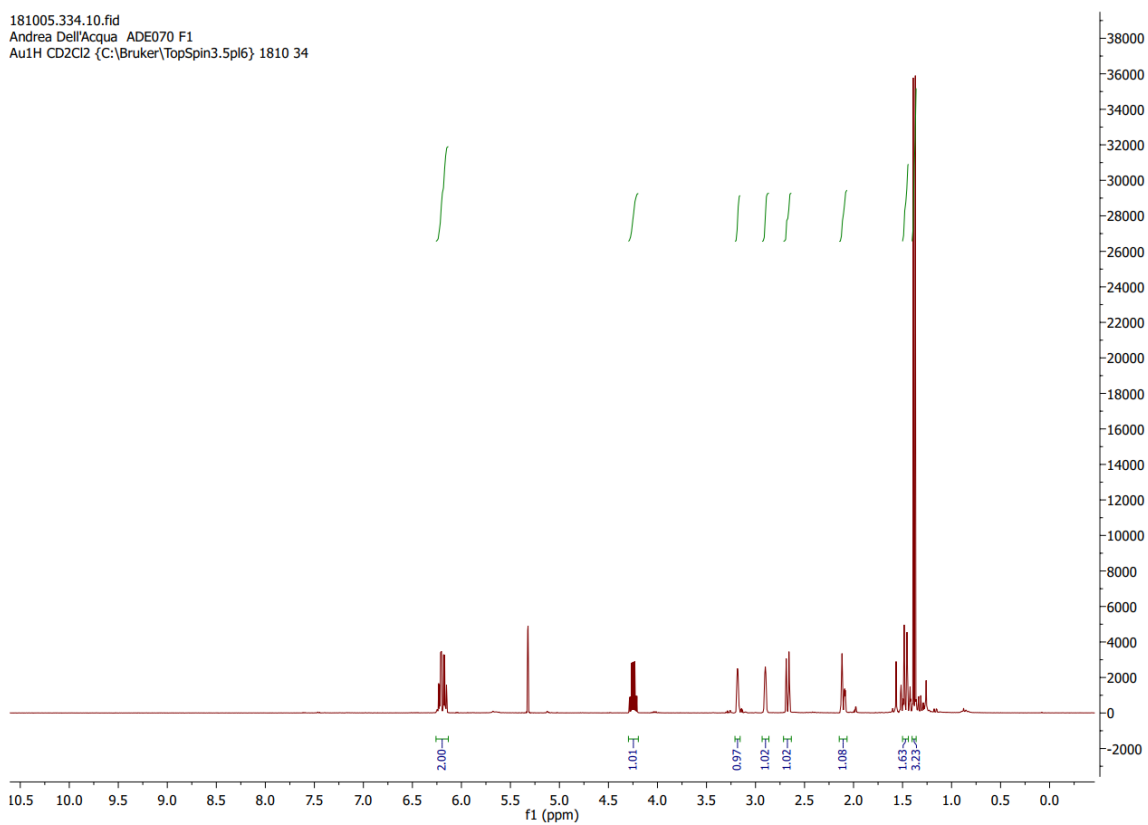


181005.333.11.fid
 Andrea Dell'Acqua ADE070 F2
 Au13C CD2Cl2 (C:\Bruker\TopSpin3.5pl6) 1810 33

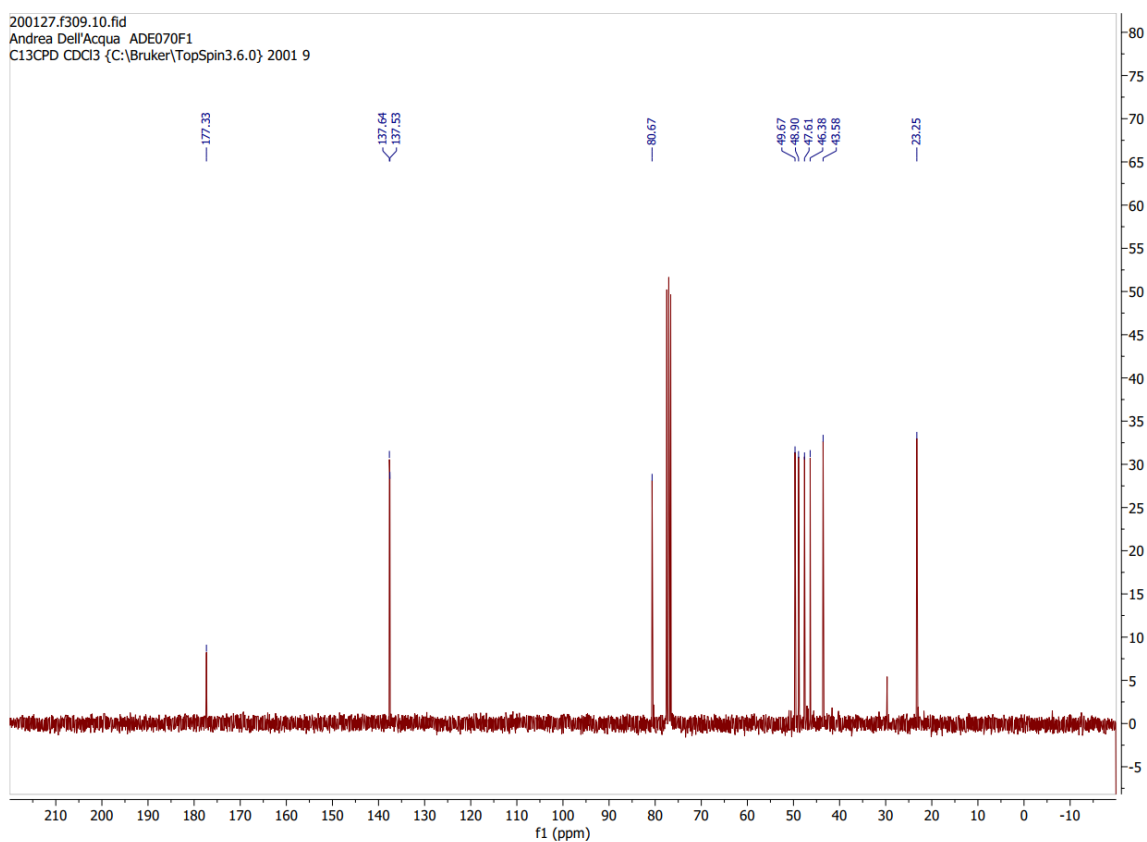


exo-Cp/ β AL

181005.334.10.fid
Andrea Dell'Acqua ADE070 F1
Au1H CD2Cl2 {C:\Bruker\TopSpin3.5pl6} 1810 34

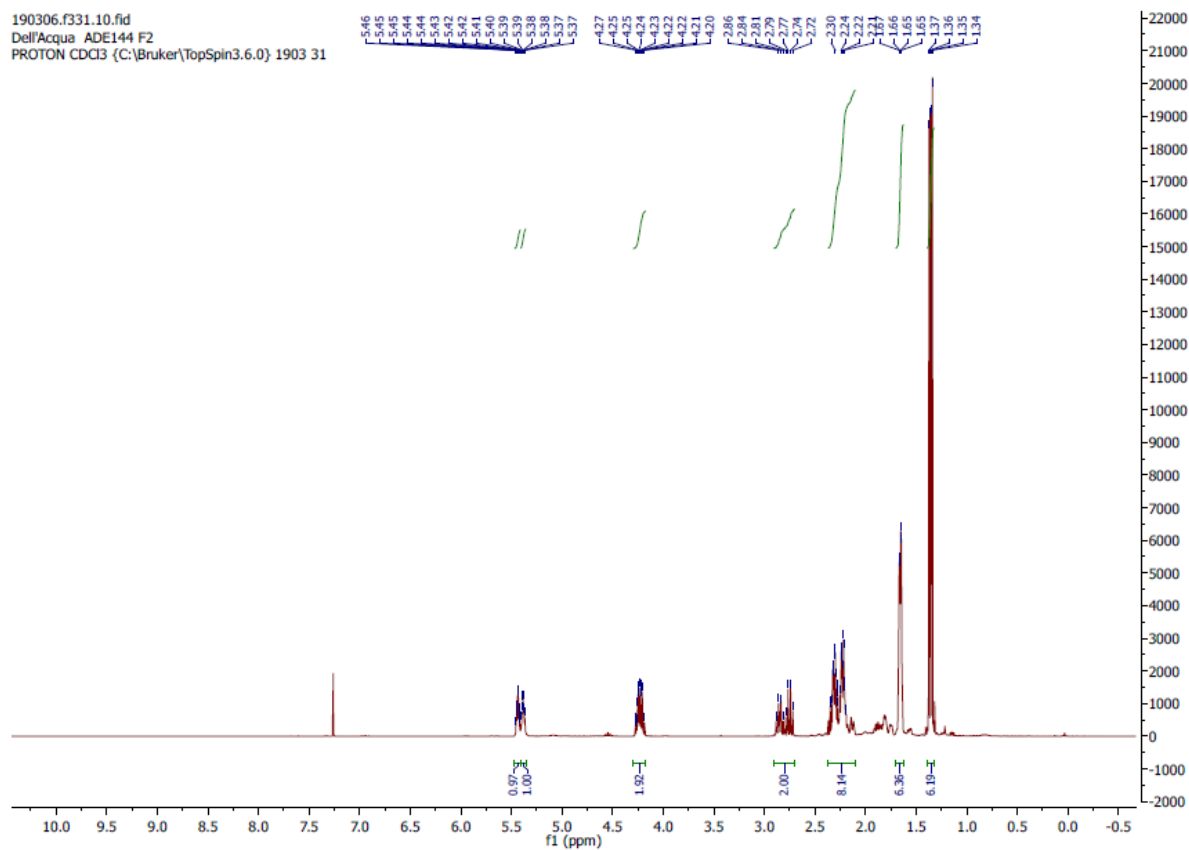


200127.f309.10.fid
Andrea Dell'Acqua ADE070F1
C13CPD CDCl3 {C:\Bruker\TopSpin3.6.0} 2001 9

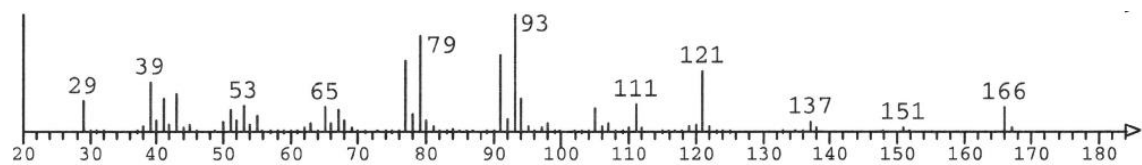
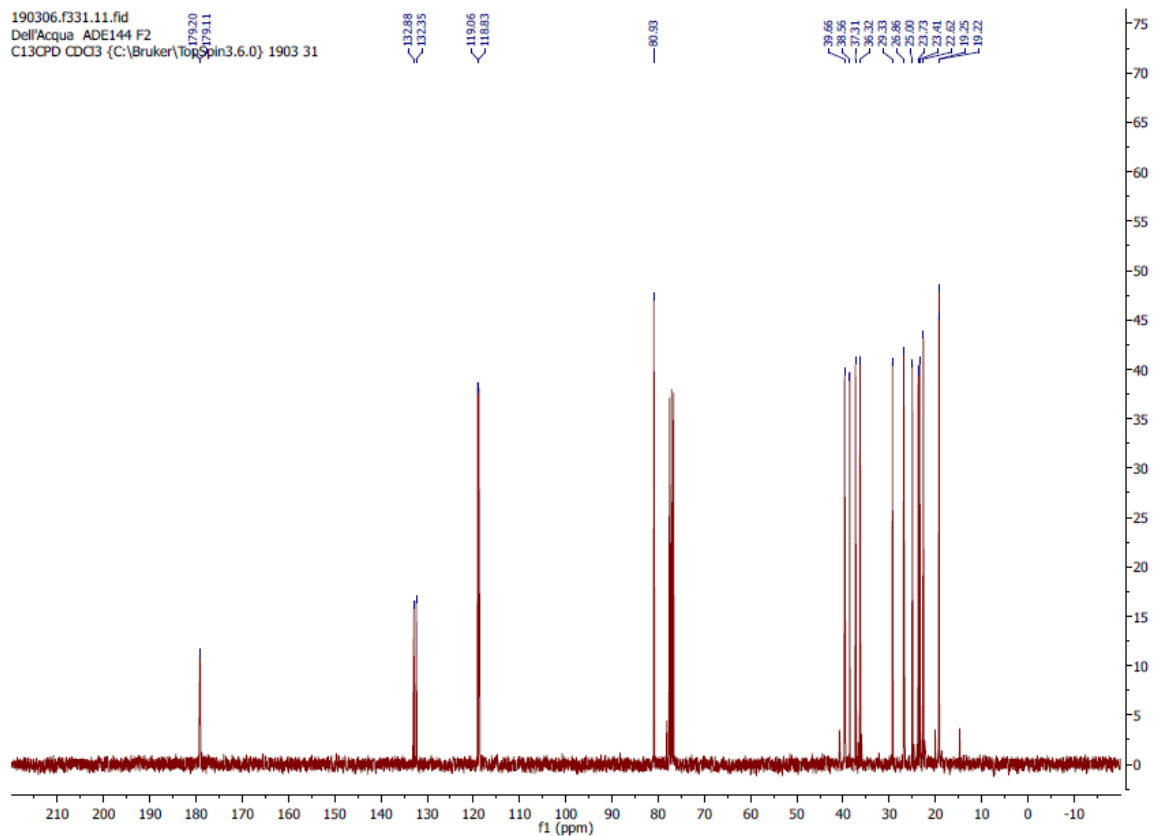


Isoprene/ β AL

Due to the co-presence of different regio- and stereoisomers, NMR data for the other DA adducts are not easily intelligible. NMR was used mainly to confirm the absence of the β AL (C=C signal), while ESI to confirm the product structure.

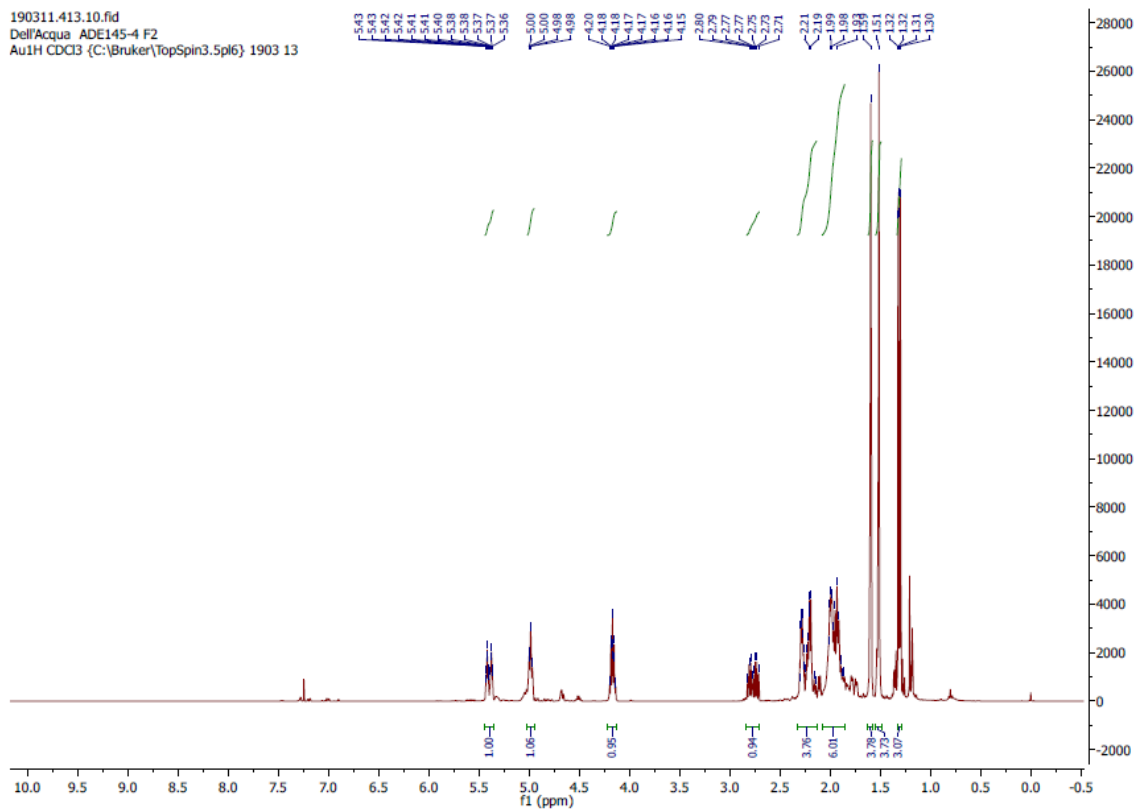


190306.f331.11.fid
Dell'Acqua ADE144 F2
C13CPD CDCl3 {C:\Bruker\TopSpin3.6.0} 1903 31

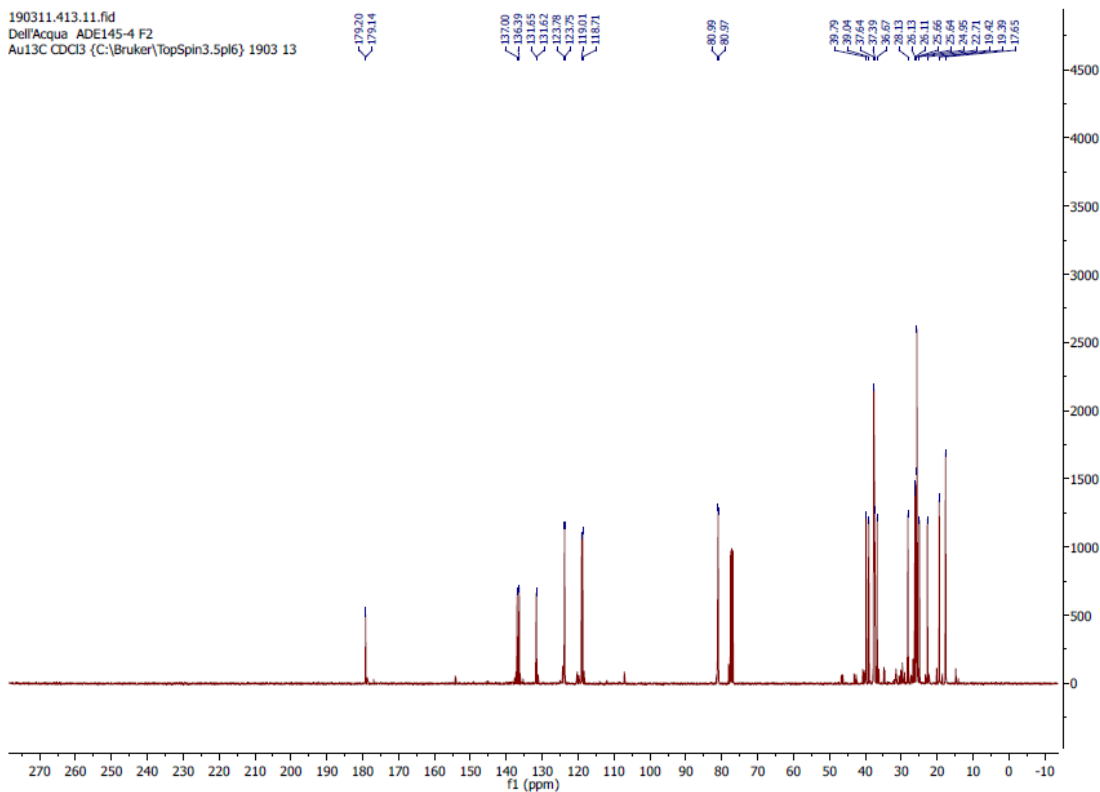


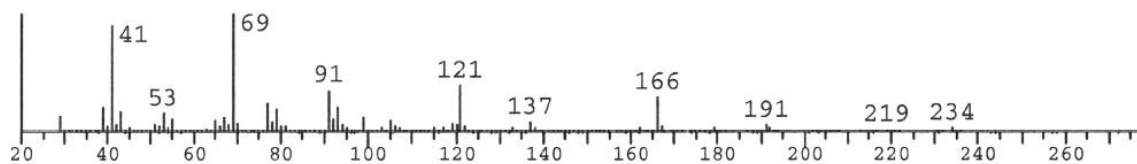
Myrcene/ β AL

190311.413.10.fid
 Dell'Acqua ADE145-4 F2
 Au1H CDCl3 (C:\Bruker\TopSpin3.5pl6) 1903 13



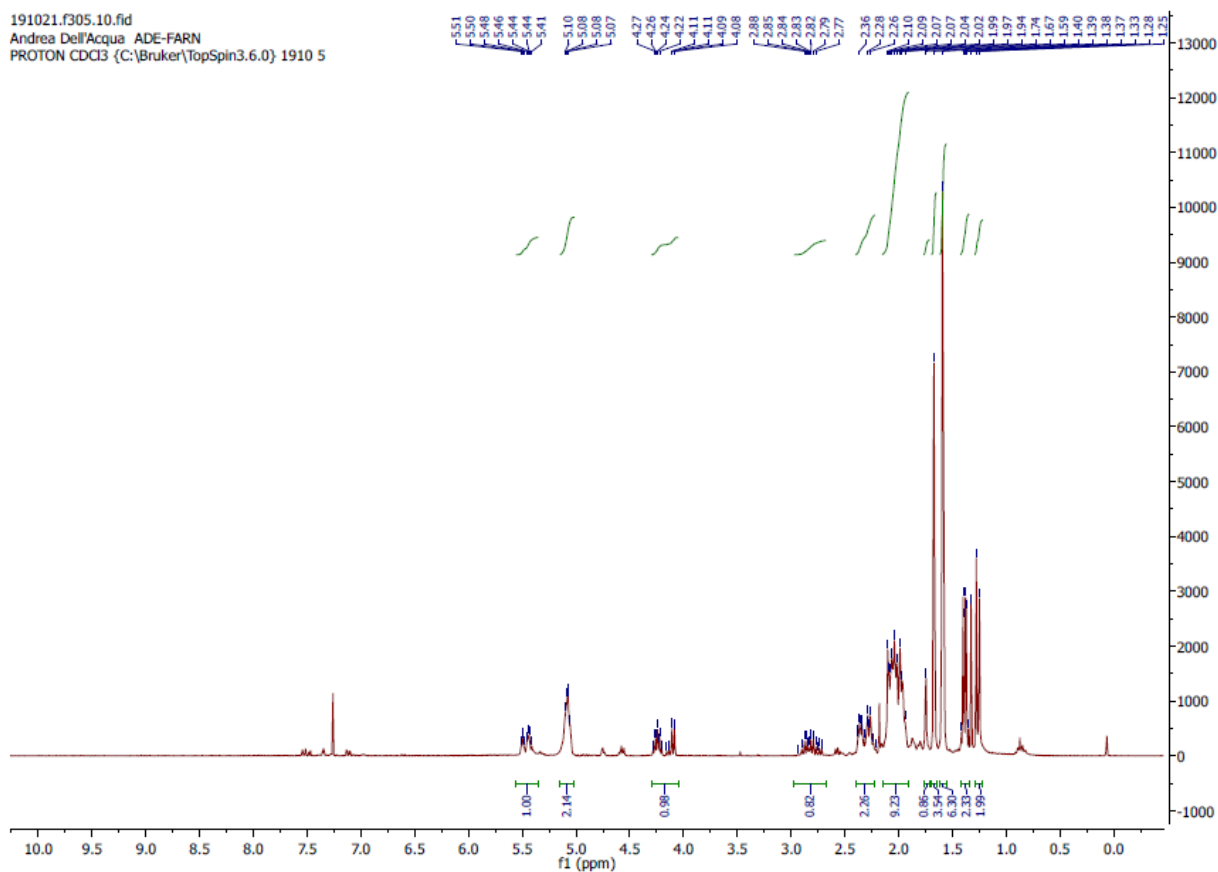
190311.413.11.fid
 Dell'Acqua ADE145-4 F2
 Au13C CDCl3 (C:\Bruker\TopSpin3.5pl6) 1903 13



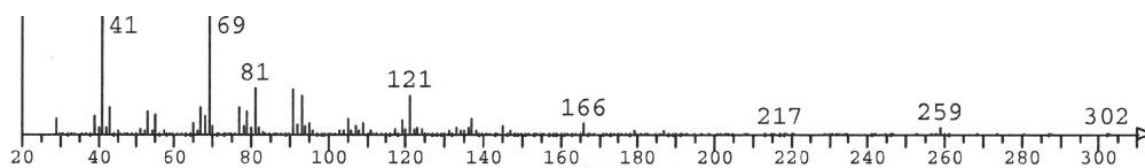
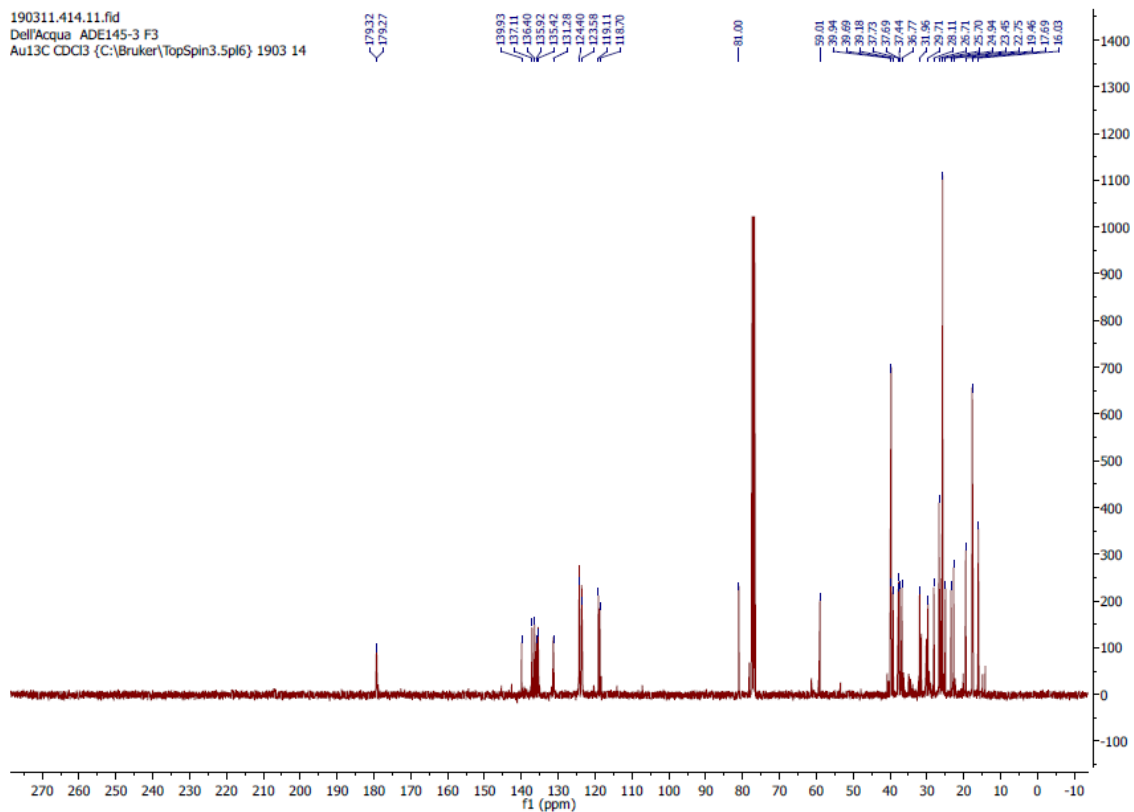


- Farnesene/βAL

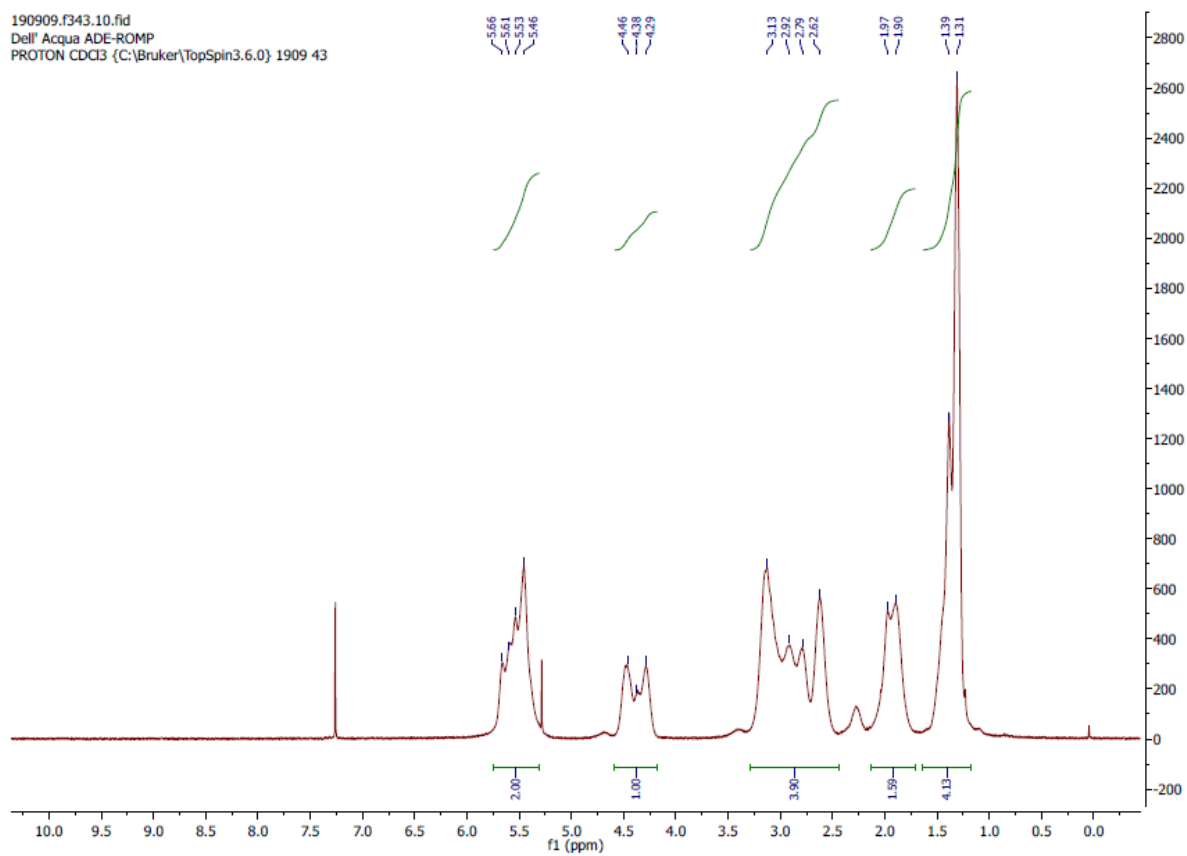
191021.f305.10.fid
 Andrea Dell'Acqua ADE-FARN
 PROTON CDCl3 (C:\Bruker\TopSpin3.6.0) 1910 5



190311.414.11.fid
DellAcqua ADE145-3 F3
Au13C CDCl3 (C:\Bruker\TopSpin3.Spl6) 1903 14



- poly-Cp/ β AL



10. TGA/DSC analysis

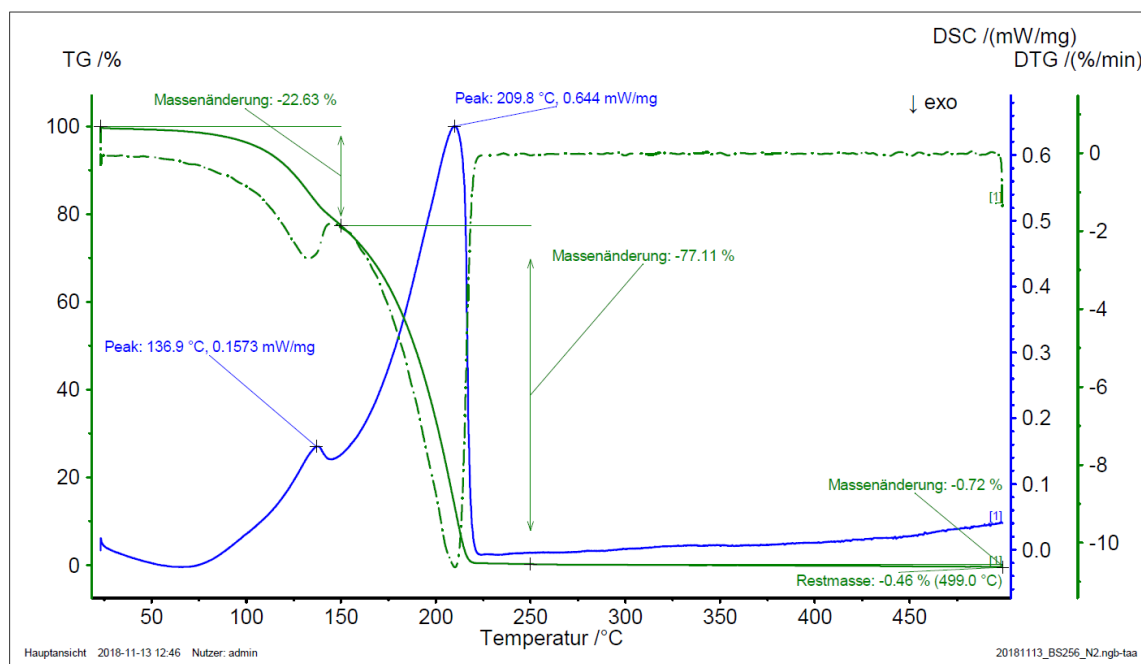


Figure S7 DSC-TG of the Cp/ β AL Diels-Alder adduct.

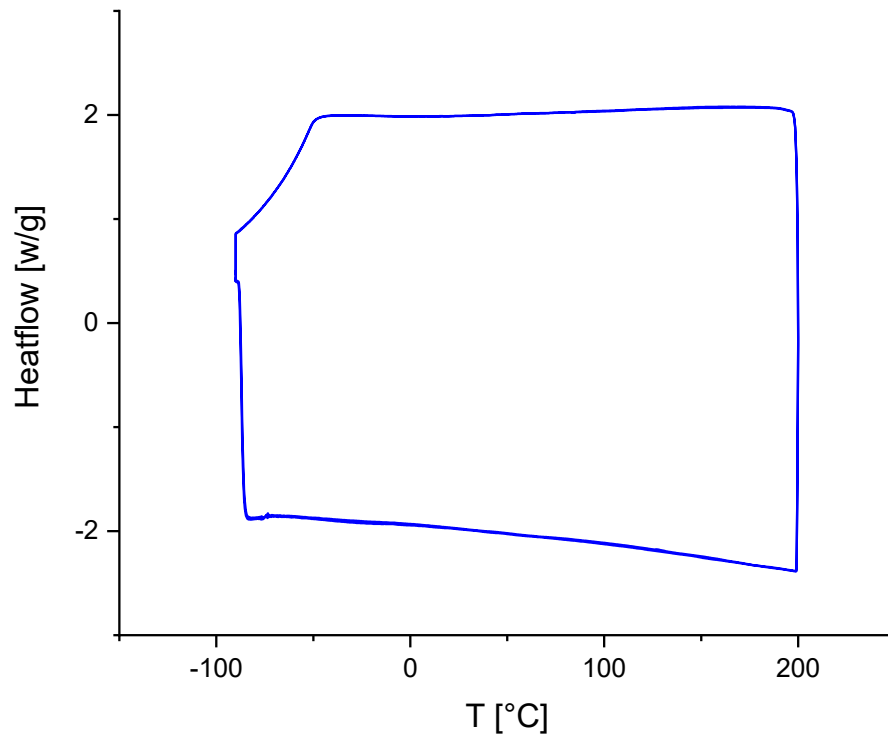


Figure S8 DSC of poly-Cp/ β AL recorded. Two heating and cooling cycles from -90°C to 200°C are shown. Acquisition was carried out with a Star-SW DSC from Mettler Toledo.

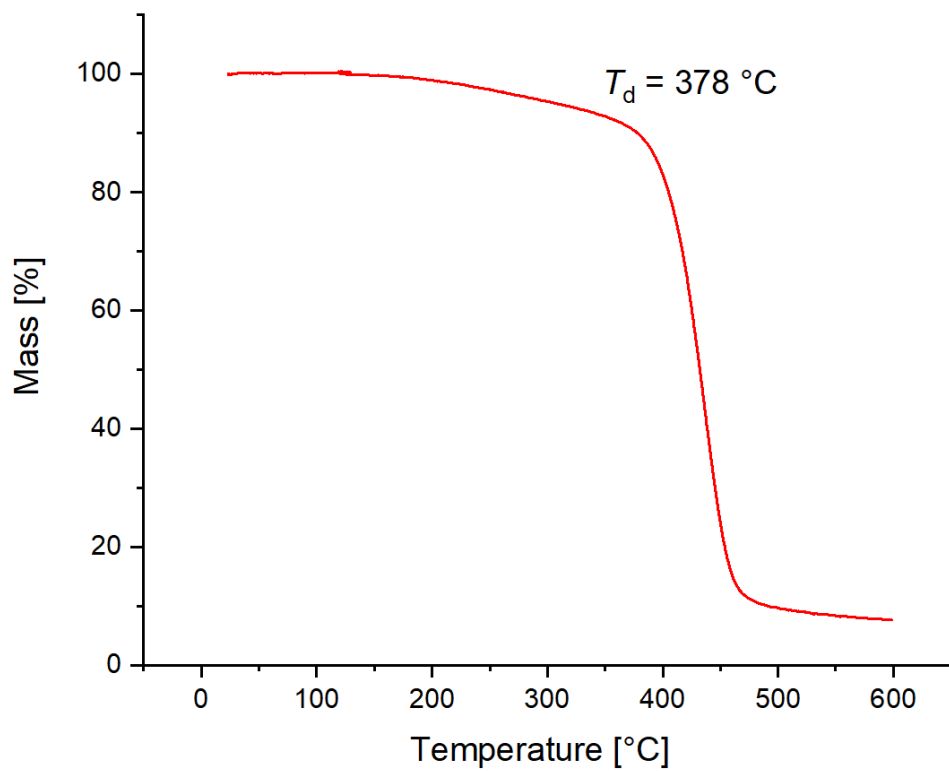


Figure S9 TGA of poly-Cp/βAL. The onset of decomposition (T_d) was taken at 10% of mass loss.

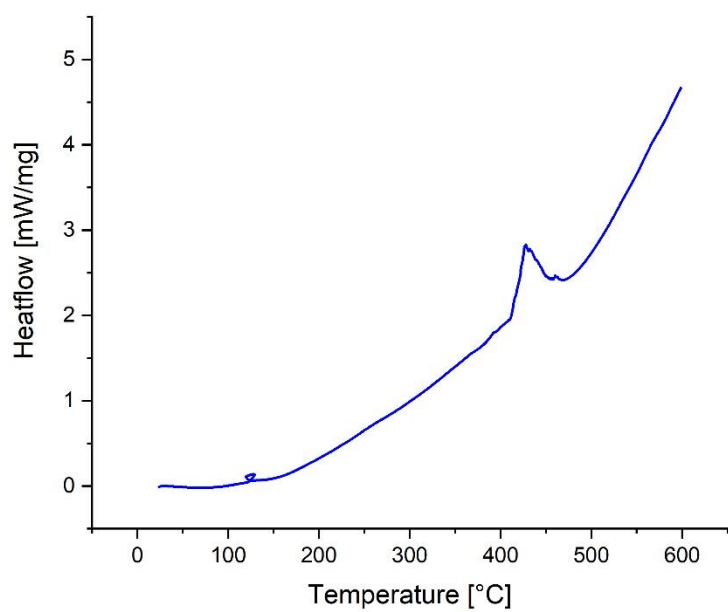


Figure S10 Corresponding DSC trace to Figure S8

Ozonolysis of α -angelica lactone: a renewable route to malonates

Andrea Dell'Acqua, Lukas Wille, Bernhard M. Stadler, Sergey Tin and Johannes G. de Vries*

^aLeibniz Institut für Katalyse e. V. an der Universität Rostock

Albert-Einstein-Strasse 29a, 18055 Rostock

E-mail: johannes.devries@catalysis.de

Supporting Information

1. General information

Reagents: α -angelica lactone (98%, Sigma Aldrich), hydrogen peroxide (30% aqueous solution, Sigma Aldrich), dimethyl sulfide (>99%, Sigma Aldrich), sodium borohydride (98%, ABCR), palladium on activated charcoal (10% Pd, Fluka) and all the solvents (>99%, Walter) were used as received.

NMR Spectroscopy: ^1H -NMR and ^{13}C -NMR were recorded at ambient temperature on 300 MHz spectrometers (Avance 300 or Fourier 300) or a 400 MHz spectrometer (Avance 400) from Bruker. The chemical shifts δ are given in ppm and referenced to the residual proton signal of the deuterated solvent used.

Mass spectroscopy: measurements were recorded on an Agilent 6210 time-of-flight LC/MS (ESI) or on a Thermo Electron MAT 95-XP (EI, 70 eV). Peaks as listed correspond to the highest abundant peak and are of the expected isotope pattern.

Ozonolysis: reactions were performed with a Sander model 301.19 ozonizer employing dry compressed air (Figure S1).



Figure S8. Typical set-up for ozonolysis reactions.

2. Synthetic procedures

Malonic acid (MA): α -AL (2.50 g, 25.5 mmol) was dissolved in 50 mL of the required solvent (see Table 1 in the main text). The solution was cooled down to the desired temperature (dry ice-acetone or ice-water) and ozone was bubbled through the solution ($2 \text{ g}\cdot\text{h}^{-1}$) until titration with KI showed an excess of ozone. Argon was bubbled through the reaction mixture for 30 minutes, the contents were carefully poured into hydrogen peroxide cooled at $0 \text{ }^\circ\text{C}$ (25 mL, 30% aq. solution, 255 mmol, 10 eq) and the resulting solution was stirred for further 20 hours at room temperature. After negative peroxide test, the aqueous layer was extracted with ethyl acetate (4x50 mL), the organic layer was concentrated under reduced pressure and dried *in vacuo* for 6 h. **MA** was obtained as a fine white powder in up to 91% isolated yield (see Tables 1 and 2 in the main text).

^1H NMR (300 MHz, Acetone-*d*6) δ 10.71 (s, 2H), 3.39 (s, 2H). ^{13}C NMR (300 MHz, Acetone-*d*6) δ 168.6, 41.3.¹

ESI-MS (ES^-): calculated for $\text{C}_3\text{H}_4\text{O}_4$: 104.01; found: 103.00 [$\text{M}-\text{H}$] $^-$.

Methyl 3,3-dimethoxypropanoate (MOP Acetal): α -AL (2.50 g, 25.5 mmol) was dissolved in 50 mL of methanol (see Table 1 in the main text). The solution was cooled down to the desired temperature (dry ice-acetone or ice-water) and ozone was bubbled through the solution ($2 \text{ g}\cdot\text{h}^{-1}$) until titration with KI showed an excess of ozone. Argon was bubbled through the reaction mixture for 30 minutes, the contents were carefully poured into 19 mL of dimethyl sulfide (255 mmol, 10 eq) and stirred for a further 20 hours. The crude was concentrated to about half of the initial volume, then partitioned between water and ethyl acetate and the water phase extracted (4x50 mL EtOAc). The collected organic phases were washed with saturated aqueous NaHCO_3 (100 mL) and brine to remove the residual acetic acid, the volatiles concentrated under reduced pressure affording pure **MOP acetal** as a colourless liquid in up to 46% isolated yield (see Tables 1 and 2 in the main text).

^1H NMR (300 MHz, Chloroform-*d*) δ 4.82 (t, $J = 5.6 \text{ Hz}$, 1H), 3.68 (s, 3H), 3.35 (s, 6H), 2.64 (d, $J = 5.9 \text{ Hz}$, 2H). ^{13}C NMR (300 MHz, CDCl_3) δ 170.4, 101.4, 53.6, 51.9, 38.8.²

ESI-MS (ES^-): calculated for $\text{C}_6\text{H}_{12}\text{O}_4$: 148.07; found: 147.05 [$\text{M}-\text{H}$] $^-$.

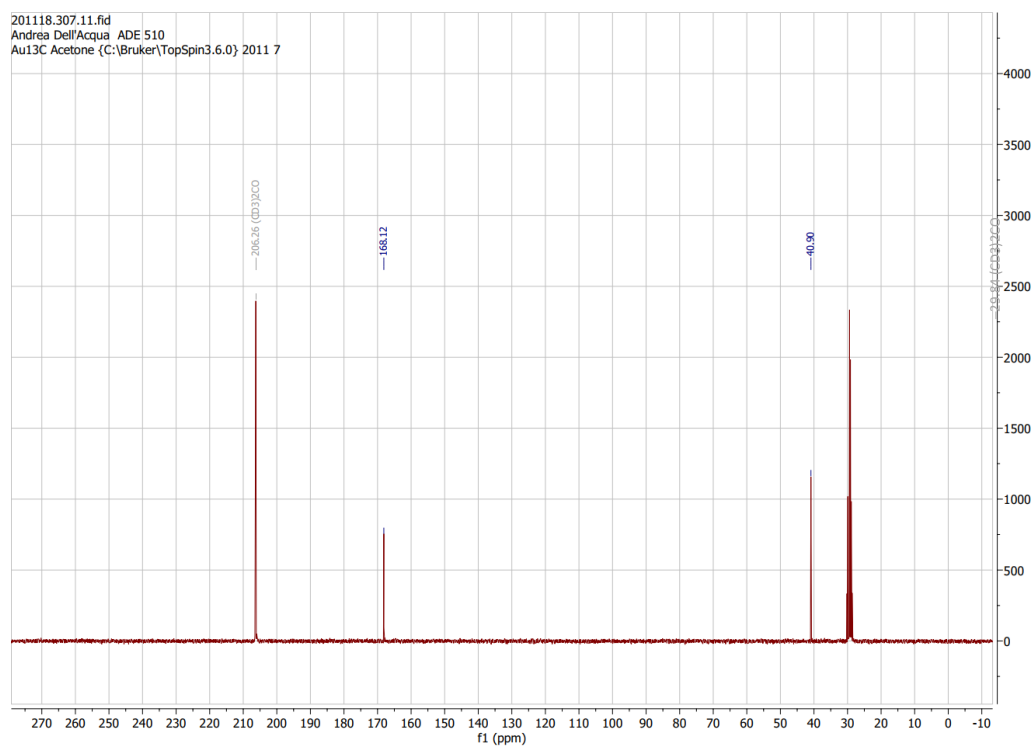
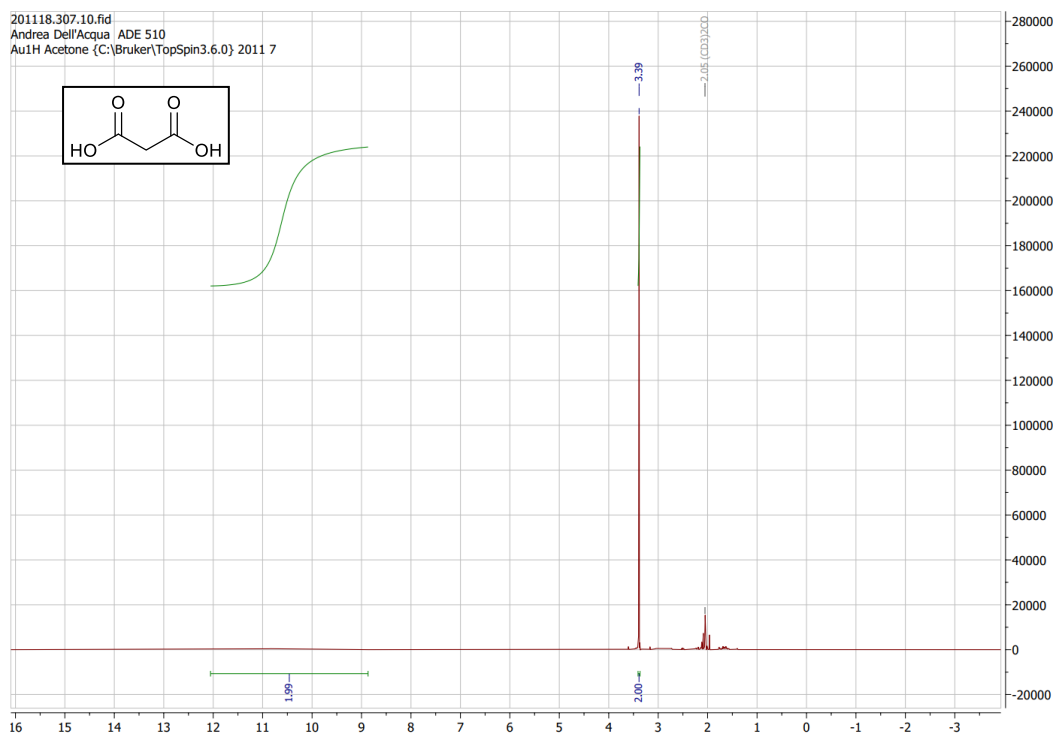
Monomethyl malonate (mMM): The general procedure described for the synthesis of **MA** was repeated using methanol as solvent. **mMM** was obtained after extraction with ethyl acetate and concentration in vacuum as colourless liquid (1.58 g, 52% yield).

^1H NMR (300 MHz, Chloroform-*d*) δ 3.78 (s, 3H), 3.45 (s, 2H). ^{13}C NMR (75 MHz, CDCl_3) δ 171.7, 167.4, 53.1, 41.3.¹

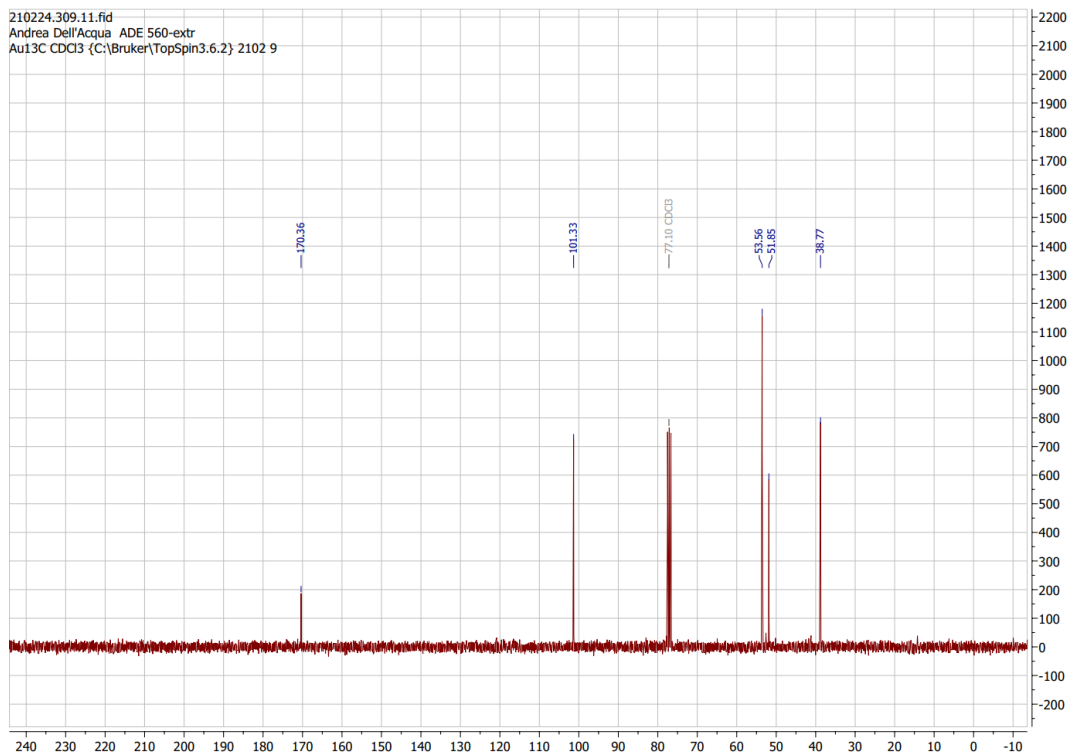
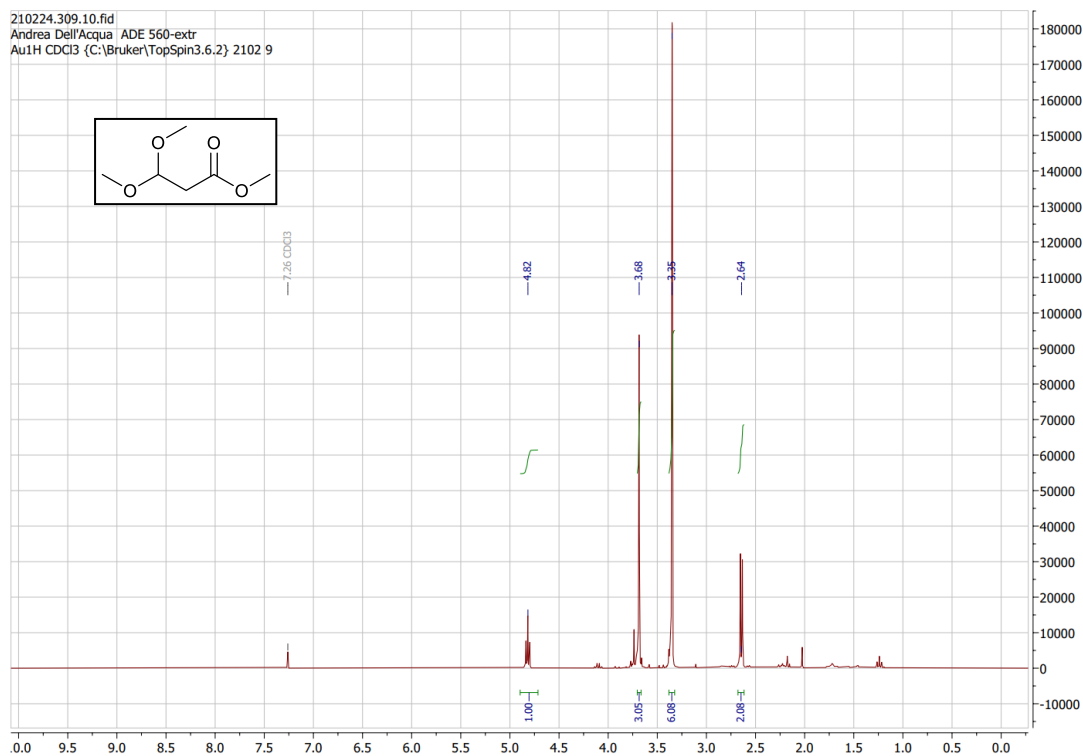
ESI-MS (ES^-): calculated for $\text{C}_4\text{H}_6\text{O}_4$: 118.03; found: 117.05 [$\text{M}-\text{H}$] $^-$.

Scale-up synthesis of MA: The procedure described for MA synthesis was repeated using 25 g (0.26 mol) of α AL in 500 mL of ethyl acetate. The organic phase was concentrated after negative peroxide test, affording a colourless liquid. **MA** (22.71 g, 86% yield) was obtained as a white solid after extensive drying in vacuum.

MA

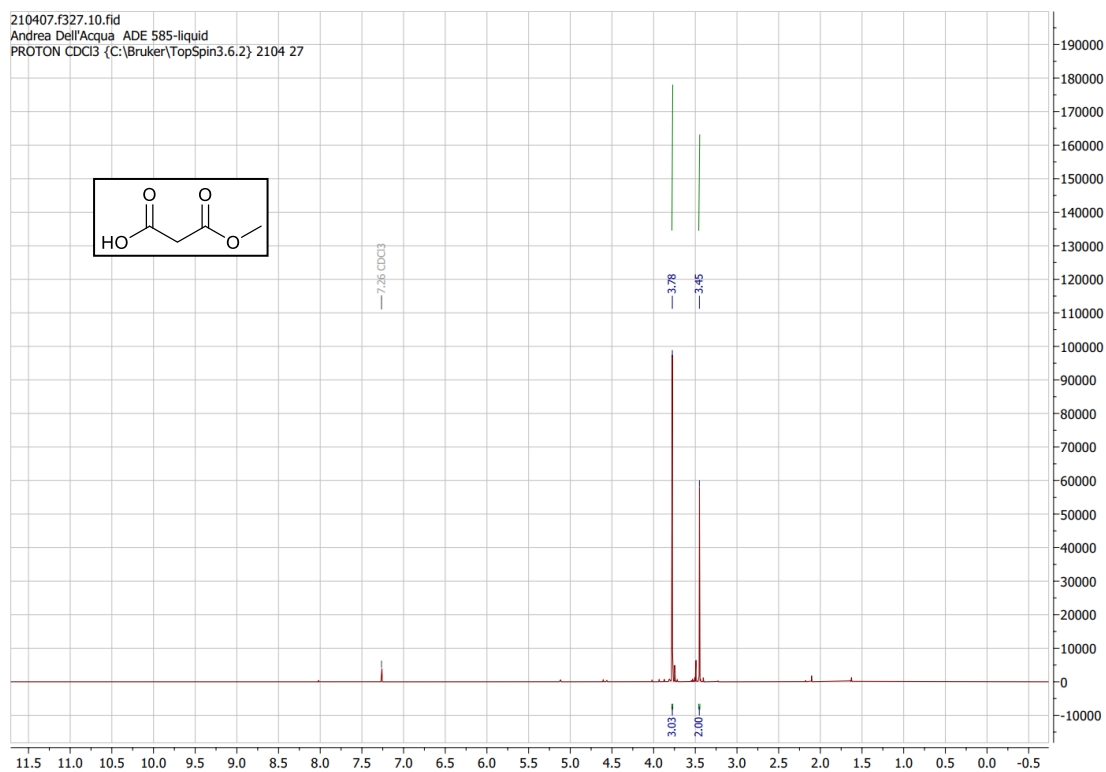
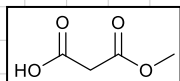


MOP-acetal

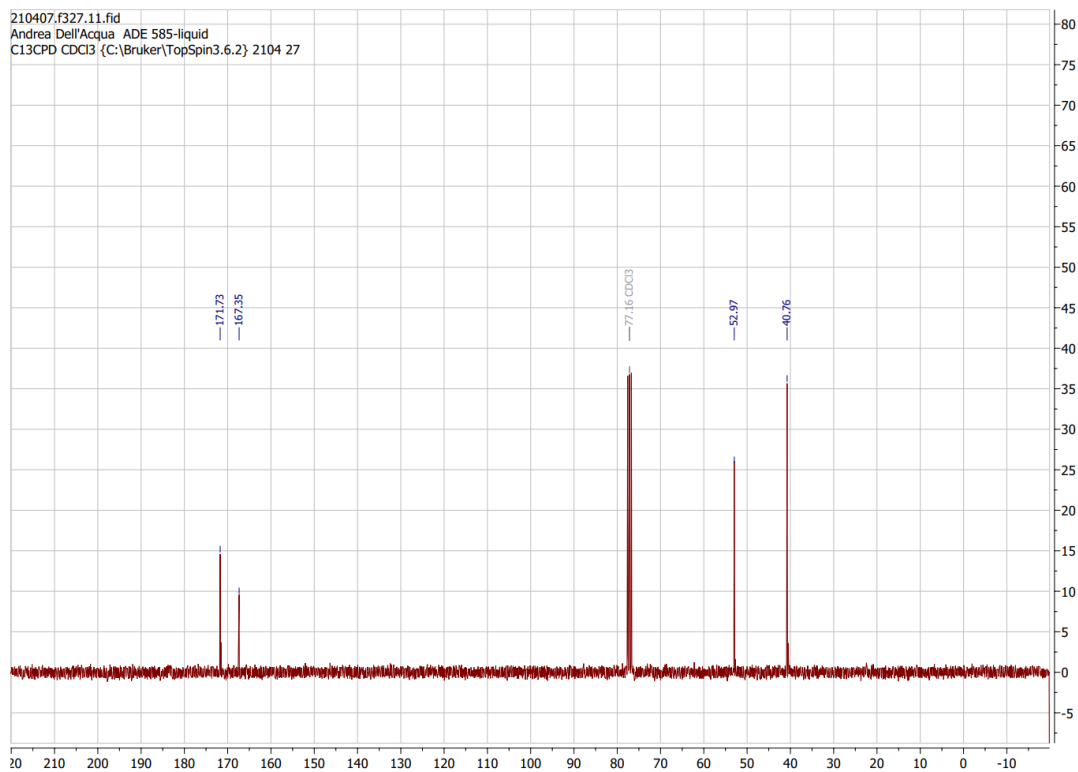


mMM

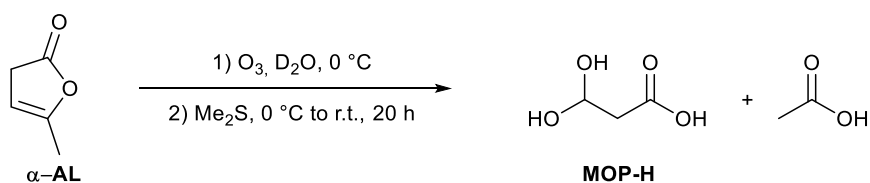
210407.f327.10.fid
Andrea Dell'Acqua ADE 585-liquid
PROTON CDCl₃ {C:\Bruker\TopSpin3.6.2} 2104 27



210407.f327.11.fid
Andrea Dell'Acqua ADE 585-liquid
C13CPD CDCl₃ {C:\Bruker\TopSpin3.6.2} 2104 27

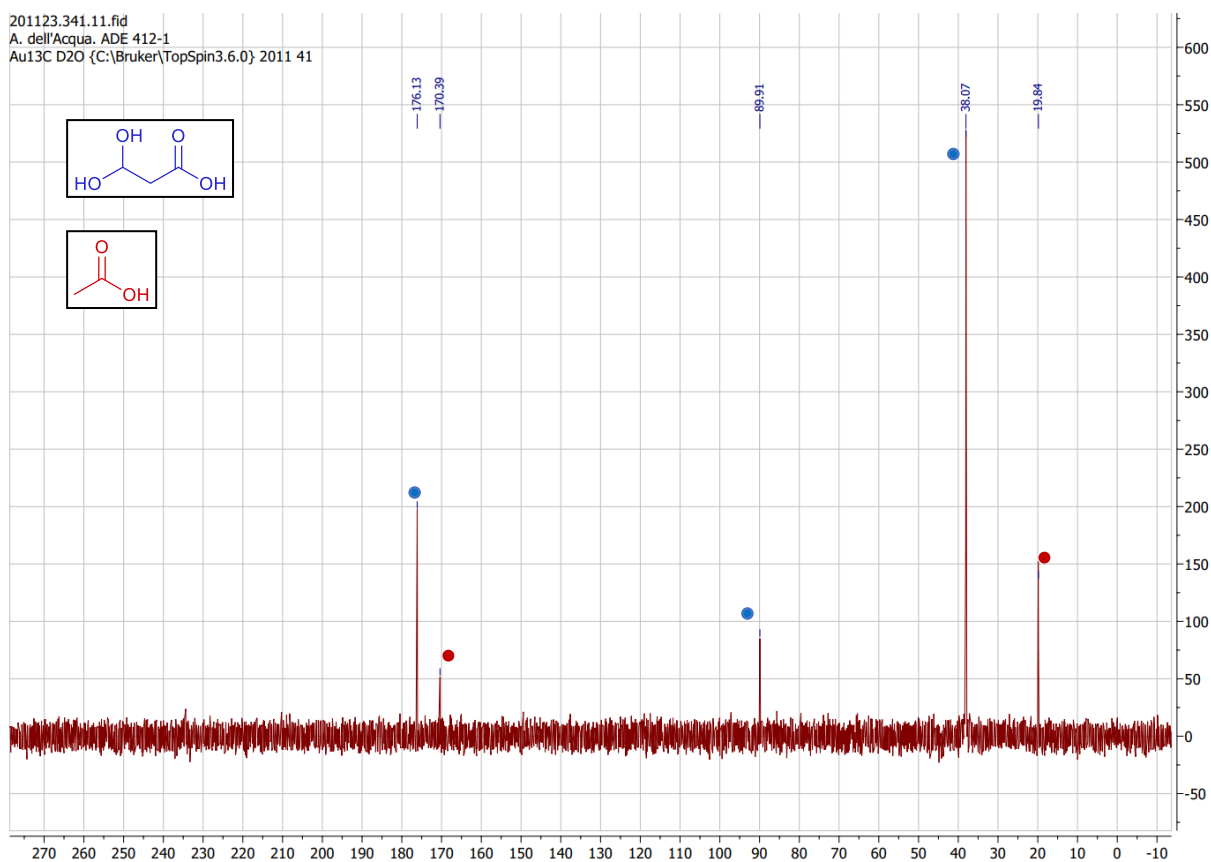


3. Aldehyde trapping experiments

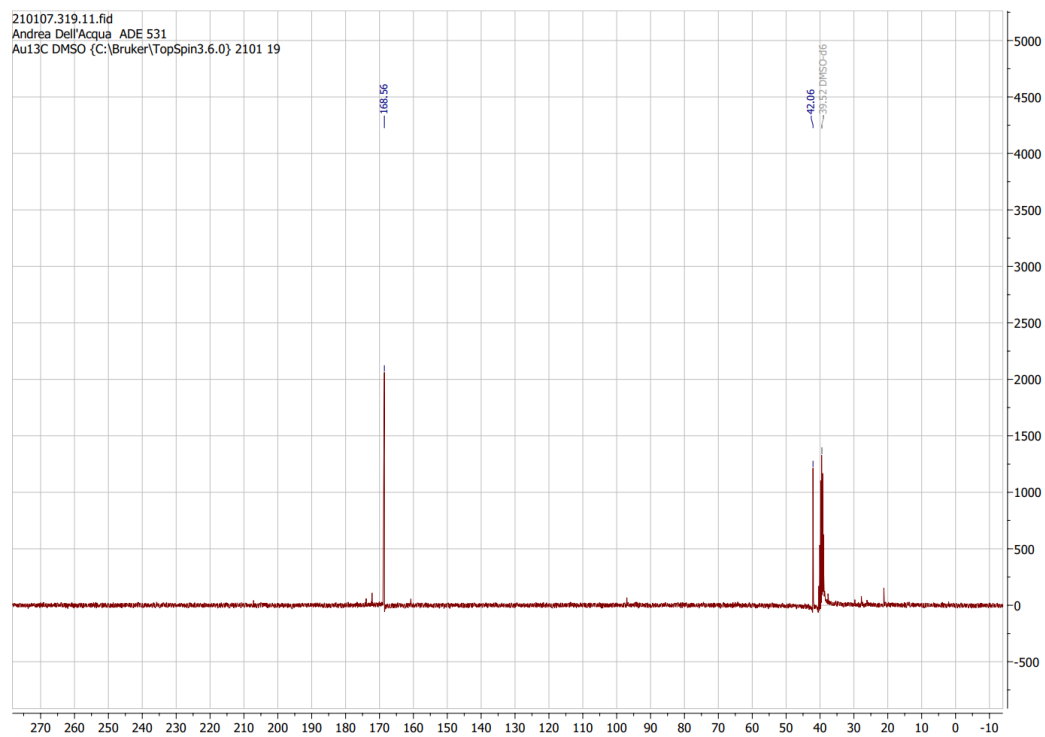
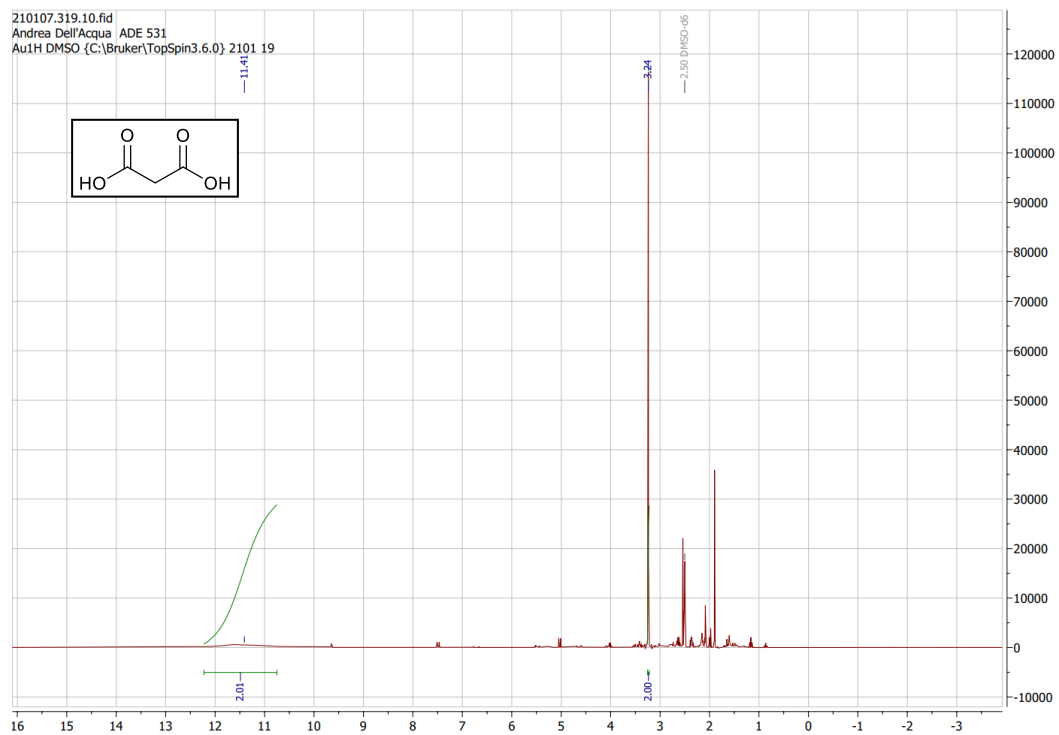


The general procedure described in 2. was repeated, performing the reaction in D₂O (250 mg of α -AL in 5.0 mL of D₂O). A ¹³C NMR sample was measured after purging the reaction mixture with argon for 20 minutes, and the remaining solution worked-up following the procedure described above (1.0 mL Me₂S as quenching agent, followed by water-acetate extraction).

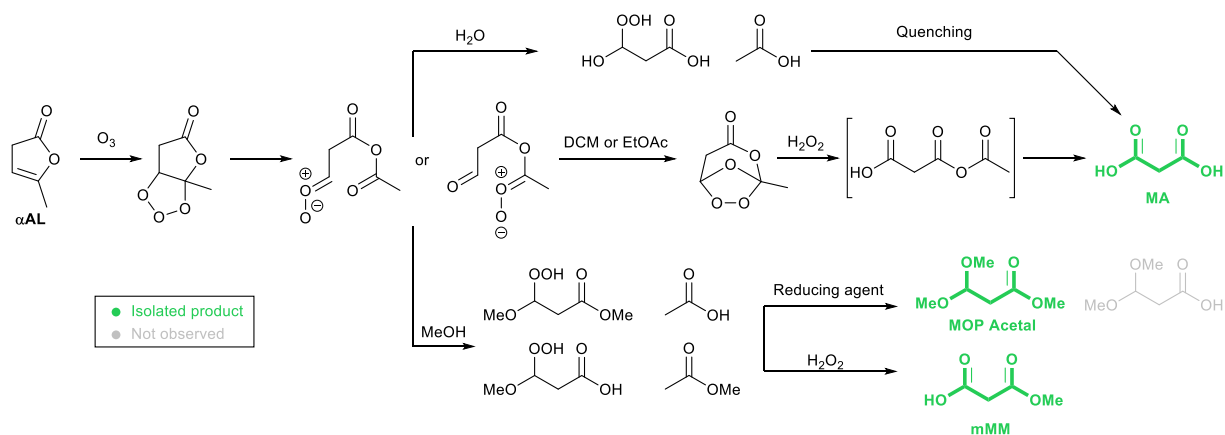
Before quenching (¹³C in D₂O)



After quenching with Me₂S and extraction



5. Proposed mechanism^{3,4}



4. References

1. F. Rajabi, C. Wilhelm and W. R. Thiel, *Green Chem.*, 2020, **22**, 4438-4444.
2. M. Limbach, S. Dalai and A. de Meijere, *Advanced Synthesis & Catalysis*, 2004, **346**, 760-766.
3. R. Criegee, *Angew. Chem. Int. Ed.*, 1975, **14**, 745-752.
4. R. L. Kuczkowski, *Chem. Soc. Rev.*, 1992, **21**, 79-83.

Glycolaldehyde as a Bio-based C1 Building Block for Selective N-Formylation of Secondary Amines

Matthew T. Flynn[†], Xin Liu[†], Andrea Dell'Acqua, Jabor Rabeah, Angelika Brückner, Eszter Baráth, Sergey Tin and Johannes G. de Vries*

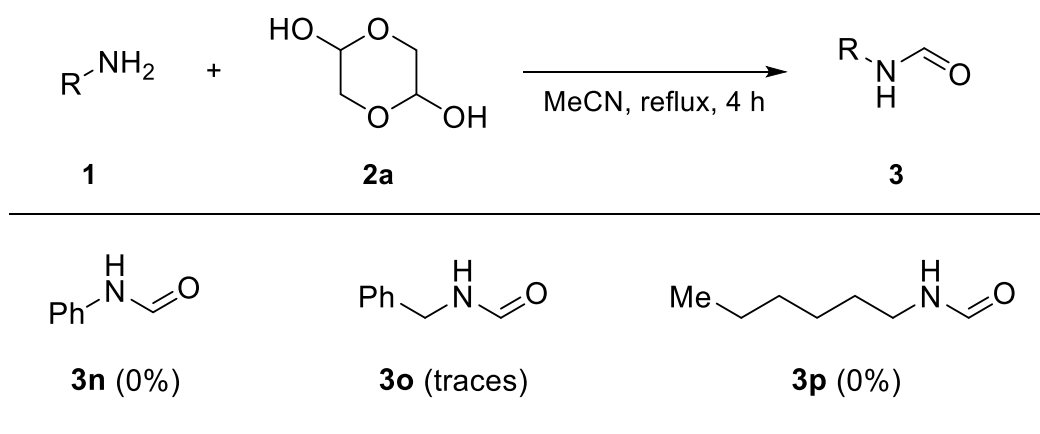
Leibniz-Institute für Katalyse, Albert-Einstein-Straße 29a, 18059 Rostock, Germany

E-mail: Johannes.deVries@catalysis.de

1. General considerations

All experiments were performed under argon atmosphere by using standard Schlenk technique or in a glove box, if not stated otherwise. Dry THF, MeCN, toluene, CH₂Cl₂ and CHCl₃ were purchased from *Acros Organics*, degassed and purged with argon prior to use. Chemicals were purchased from *Sigma*, *Alfa*, *Strem*, *Abcr*, *Acros* and *TCl*. Deuterated solvents were ordered from *Deutero GmbH* and stored over molecular sieves. NMR spectra were recorded using *Bruker 300 Fourier*, *Bruker AV 300* and *Bruker AV 400* spectrometers. Chemical shifts are reported in ppm relative to the deuterated solvent. Coupling constants are expressed in Hertz (Hz). The following abbreviations are used: s = singlet, d = doublet, t = triplet and m = multiplet. Analytical thin layer chromatography (TLC) was carried out using commercial silica-gel plates, spots were detected with UV light and revealed with KMnO₄. GC analyses were performed on a Trace 1310 chromatograph with a 30 m HP column. The reported gas chromatography (GC) yields and conversions are based on a calibrated area of mesitylene as internal standard. HR-MS measurements were recorded on an Agilent 6210 time-of-flight LC/MS (ESI) or on a Thermo Electron MAT 95-XP (EI, 70 eV). Peaks as listed correspond to the highest abundant peak and are of the expected isotope pattern. EPR spectra were recorded on an X-band Bruker EMX CW-micro EPR spectrometer equipped with an ER4119HS high-sensitivity resonator using a microwave power of Ca 6.9 mW, modulation frequency of 100 kHz and modulation amplitude up to 5 G. The $h\nu = g\beta B_0$ equation was used to calculate g values with ν and B_0 being the frequency and resonance field, respectively. EPR spectrum was simulated using SpinFit (Bruker).

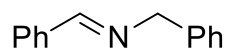
2. Additional reactions



Reaction conditions: **1** (2.0 mmol), **2a** (0.5 mmol), MeCN (5.0 mL), reflux, 4 h. Yield were determined by GC using mesitylene as the internal standard.

Scheme S1. Substrate scope of *N*-formylation of primary amines **1**

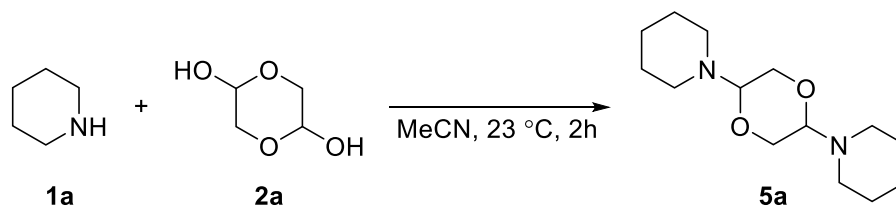
Note: A small amount of the desired product **3o** was observed in this reaction. The major by-product is *N*-benzylidenebenzylamine **8o** which is the result of oxidative cross-coupling.



8o

3. Mechanistic experiments

3.1 Synthesis intermediate 5a from piperidine 1a and glycolaldehyde dimer 2a.



General Procedure: Glycolaldehyde dimer **2a** (60 mg, 0.50 mmol) was suspended in MeCN (2 mL) to make an 0.5 M solution. Then **1a** (0.1 mL, 1.01 mmol) was added, and the mixture stirred at room temperature until a homogeneous solution formed. The reaction was then left without stirring at room temperature, depositing colourless crystals after 1 h. The reaction was left standing overnight and cooled to 0 °C for 1 h. The crystals were collected by filtration and washed with ice-cold MeCN, and **5a** was obtained in 51% yield.

The $^1\text{H-NMR}$ of **5a** was shown in Figure S1.

$^1\text{H-NMR}$ (300 MHz, CDCl_3) δ = 3.99 (dd, J = 9.6, 2.5 Hz, 1H), 3.86 – 3.76 (m, 1H), 3.70 (dd, J = 11.3, 9.6 Hz, 1H), 2.83 – 2.73 (m, 2H), 2.64 – 2.52 (m, 2H), 1.59 – 1.50 (m, 4H), 1.48 – 1.40 (m, 2H) ppm.

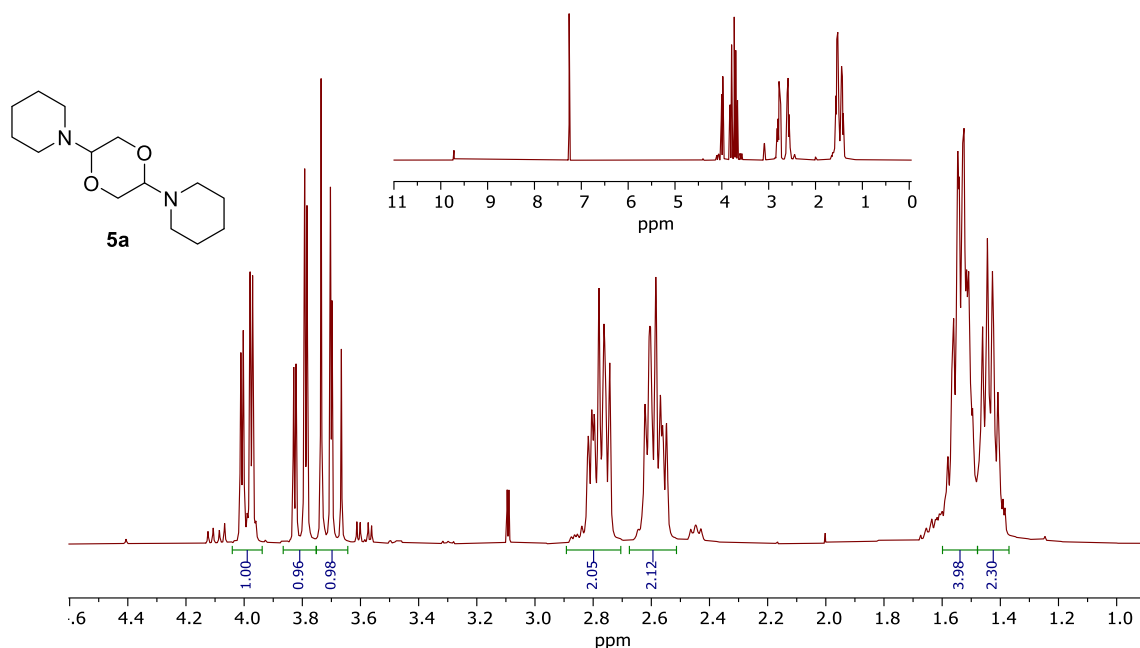
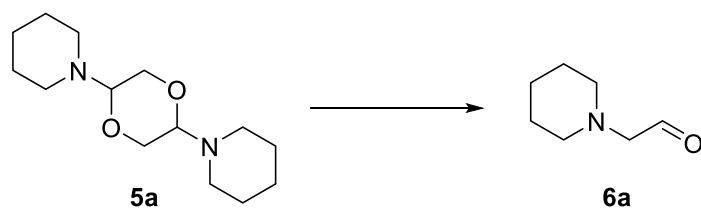


Figure S1. $^1\text{H-NMR}$ of **5a** in CDCl_3

3.2 Obtained intermediate 6a from 5a.



General Procedure: 5a which from 3.1 was easy monomerizes to 6a over time in CDCl_3 .

The $^1\text{H-NMR}$ of 6a was shown in Figure S2.

$^1\text{H-NMR}$ (300 MHz, CDCl_3) δ = 9.52 – 9.45 (m, 1H), 2.60 – 2.52 (m, 3H), 2.09 – 1.99 (m, 4H), 1.42 – 1.31 (m, 5H), 1.21 – 1.10 (m, 2H) ppm.

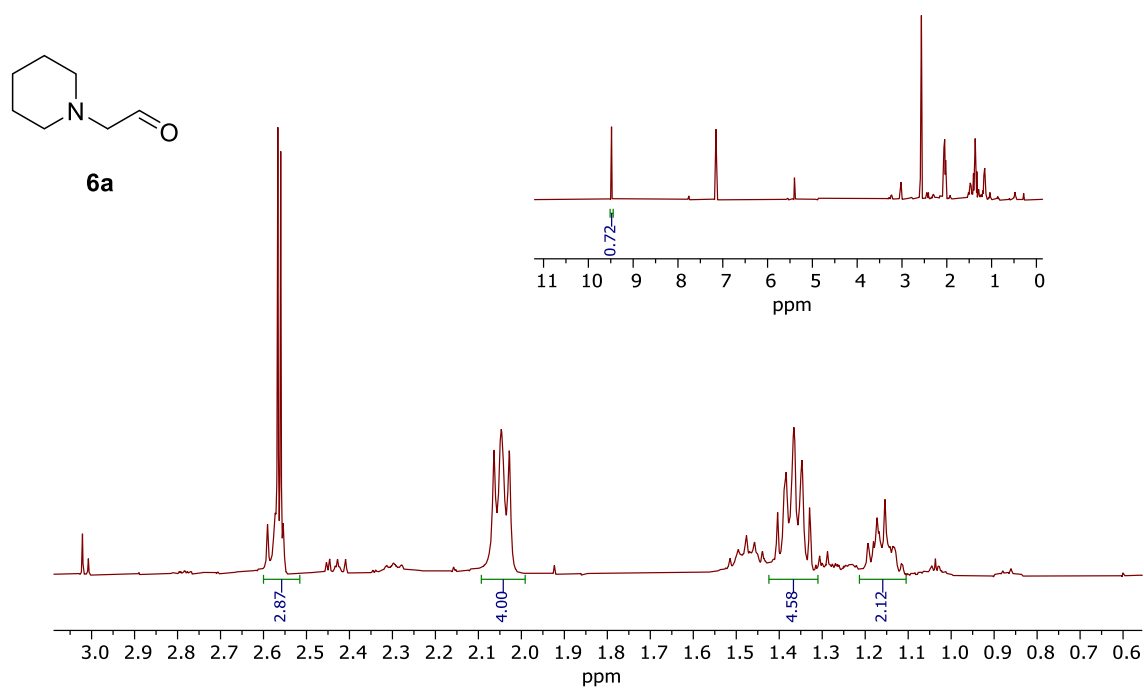
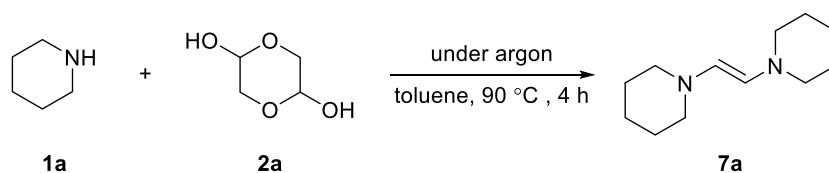


Figure S2. $^1\text{H-NMR}$ of 6a in CDCl_3

3.3 Synthesis of intermediate 7a



General Procedure: Glycolaldehyde dimer **2a** (300 mg, 2.50 mmol) was suspended in anhydrous toluene (50 mL) under argon. The toluene was degassed by bubbling argon for 30 minutes, and then **1a** (1.0 mL, 10.1 mmol) was added. The reaction mixture was heated to 90 °C for 2 h. Removal of the solvent under high vacuum gave a pale-yellow crystalline residue **7a** in 89% yield. This residue could be distilled under vacuum to yield a colourless oil, which crystallized to a low-melting solid at room temperature and turned yellow over the course of 1-2 days while standing at room temperature under argon.

The $^1\text{H-NMR}$ of **7a** was shown in Figure S3.

$^1\text{H-NMR}$ (300 MHz, Toluene- d_8) δ = 5.31 (s, 2H), 2.61 – 2.52 (m, 8H), 1.59 – 1.48 (m, 8H), 1.39 – 1.33 (m, 4H) ppm.

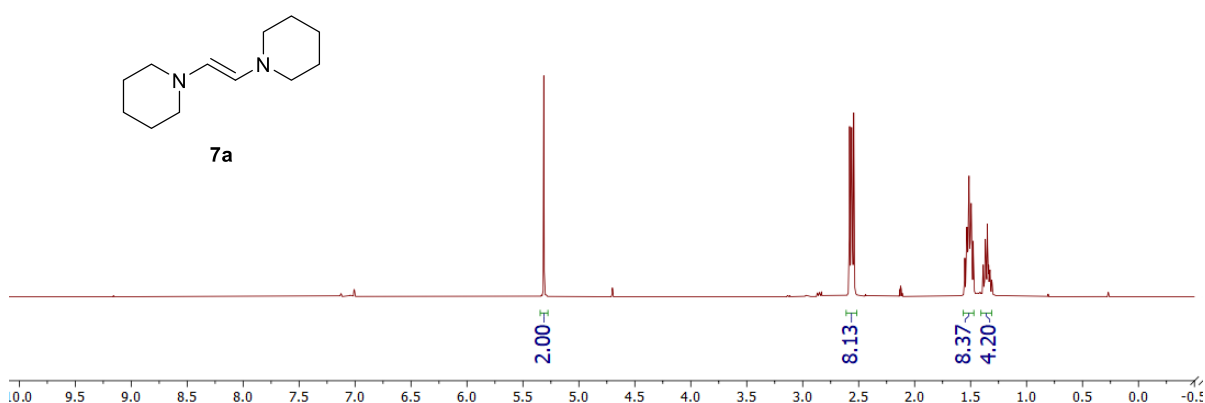


Figure S3. $^1\text{H-NMR}$ of **7a** in Toluene- d_8

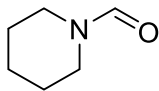
4. Selective *N*-formylation of secondary amines

4.1 General method of this reaction system

General Procedure: In a Schlenk tube (20 mL), glycolaldehyde dimer **2a** (60 mg, 0.5 mmol) was suspended in acetonitrile (5 mL), and secondary amine **1** (2.0 mmol) were added. The reaction mixture was heated to reflux under air for 4 h. After removal of all volatiles in vacuo the crude mixture was purified by column chromatography on silica gel to afford the isolated yield of products.

4.2 Characterization data of products

N-formylpiperidine (**3a**)



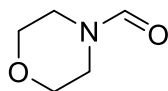
According to the GP: The compound **3a** was obtained by column chromatography (SiO₂, pentane:ethyl acetate = 5:1 and 3% of Et₃N) as colourless solid (91.5 mg, 0.811 mmol, 81 %)

¹H-NMR (300 MHz, CDCl₃, 25 °C) δ = 7.89 (s, 1H), 3.47 – 3.28 (m, 2H), 3.28 – 3.13 (m, 2H), 1.66 – 1.52 (m, 2H), 1.52 – 1.37 (m, 4H) ppm.

¹³C-NMR (75 MHz, CDCl₃, 25 °C) δ = 160.65, 46.68, 40.45, 26.45, 24.96, 24.57 ppm.

The spectroscopic data correspond to those reported in the literature.¹

N-formylmorpholine (**3c**)



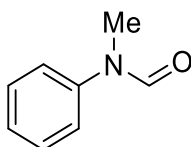
According to the GP: The compound **3c** was obtained by column chromatography (SiO₂, pentane:ethyl acetate = 50:1 and 3% of Et₃N) as colourless solid (85.3 mg, 0.741 mmol, 74 %)

¹H-NMR (300 MHz, CDCl₃, 25 °C) δ = 8.15 – 7.87 (m, 1H), 3.71 – 3.63 (m, 4H), 3.59 – 3.54 (m, 2H), 3.39 – 3.31 (m, 2H) ppm.

¹³C-NMR (75 MHz, CDCl₃, 25 °C) δ = 160.92, 67.30, 66.50, 45.86, 40.67 ppm.

The spectroscopic data correspond to those reported in the literature.¹

N-methyl-*N*-phenylformamide (**3f**)



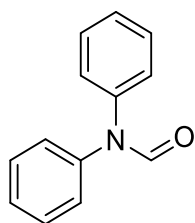
According to the GP: The compound **3f** was obtained by column chromatography (SiO₂, pentane:ethyl acetate = 5:1 and 3% of Et₃N) as yellow oil (91.7 mg, 0.680 mmol, 68%)

¹H-NMR (300 MHz, CDCl₃, 25 °C) δ = 8.53 – 8.42 (m, 1H), 7.45 – 7.36 (m, 2H), 7.31 – 7.22 (m, 1H), 7.19 – 7.14 (m, 2H), 3.30 (s, 3H) ppm.

¹³C-NMR (75 MHz, CDCl₃, 25 °C) δ = 162.31, 142.15, 129.61, 126.37, 122.32, 32.01 ppm.

The spectroscopic data correspond to those reported in the literature.²

diphenylformamide (**3g**)



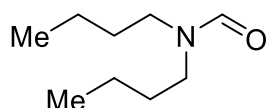
According to the GP: The compound **3g** was obtained by column chromatography (SiO₂, pentane:ethyl acetate = 5:1 and 3% of Et₃N) as yellow oil (118 mg, 0.599 mmol, 60%)

¹H-NMR (300 MHz, CDCl₃, 25 °C) δ = 8.70 (s, 1H), 7.48 – 7.38 (m, 4H), 7.37 – 7.28 (m, 4H), 7.24 – 7.16 (m, 2H) ppm.

¹³C-NMR (75 MHz, CDCl₃, 25 °C) δ = 161.46, 141.50, 139.33, 129.41, 128.90, 126.76, 126.59, 125.83, 124.79 ppm.

The spectroscopic data correspond to those reported in the literature.³

N,N-dibutylformamide (**3k**)



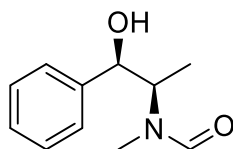
According to the GP: The compound **3k** was obtained by column chromatography (SiO₂, pentane:ethyl acetate = 10:1 and 3% of Et₃N) as colourless solid (110 mg, 0.702 mmol, 70%)

¹H-NMR (300 MHz, CDCl₃, 25 °C) δ = 8.02 (s, 1H), 3.33 – 3.22 (m, 2H), 3.17 (t, *J* = 7.1 Hz, 2H), 1.57 – 1.43 (m, 4H), 1.38 – 1.18 (m, 4H), 0.91 (td, *J* = 7.2, 2.1 Hz, 6H) ppm.

¹³C-NMR (75 MHz, CDCl₃, 25 °C) δ = 162.74, 47.21, 41.89, 30.77, 29.43, 20.20, 19.67, 13.83, 13.67 ppm.

The spectroscopic data correspond to those reported in the literature.⁴

(1*R*, 2*S*)-(-)-Ephedrine (**3m**)



Full conversion was achieved after 16 hours under 1 atm of oxygen. Compound **3m** was obtained by column chromatography (SiO₂, hexane:ethyl acetate = 6:4) as a viscous yellow oil (102 mg, 0.273 mmol, 27%). Mixture of diastereoisomers (*cis* : *trans* = 4:6).

¹H-NMR (300 MHz, CDCl₃, 25 °C) δ = 7.83 (s, 1H), 7.67 (s, 1H), 7.40 – 7.19 (m, 5+5H), 4.85 (d, J = 4.2 Hz, 1H), 4.59 (d, J = 6.7 Hz, 1H), 4.06 – 3.68 (bs, 1+1H), 3.60 (p, J = 6.9 Hz, 1H), 2.78 (s, 3H), 2.67 (s, 3H), 1.32 (d, J = 6.9 Hz, 3H), 1.19 (d, J = 7.1 Hz, 3H).

¹³C-NMR (75 MHz, CDCl₃, 25 °C) δ = 163.73, 163.24, 141.74, 141.63, 128.59, 128.27, 128.14, 127.64, 126.26, 126.21, 76.22, 75.82, 60.10, 55.71, 33.18, 27.33, 14.39, 11.05.

The spectroscopic data correspond to those reported in the literature.⁵

5. NMR spectra

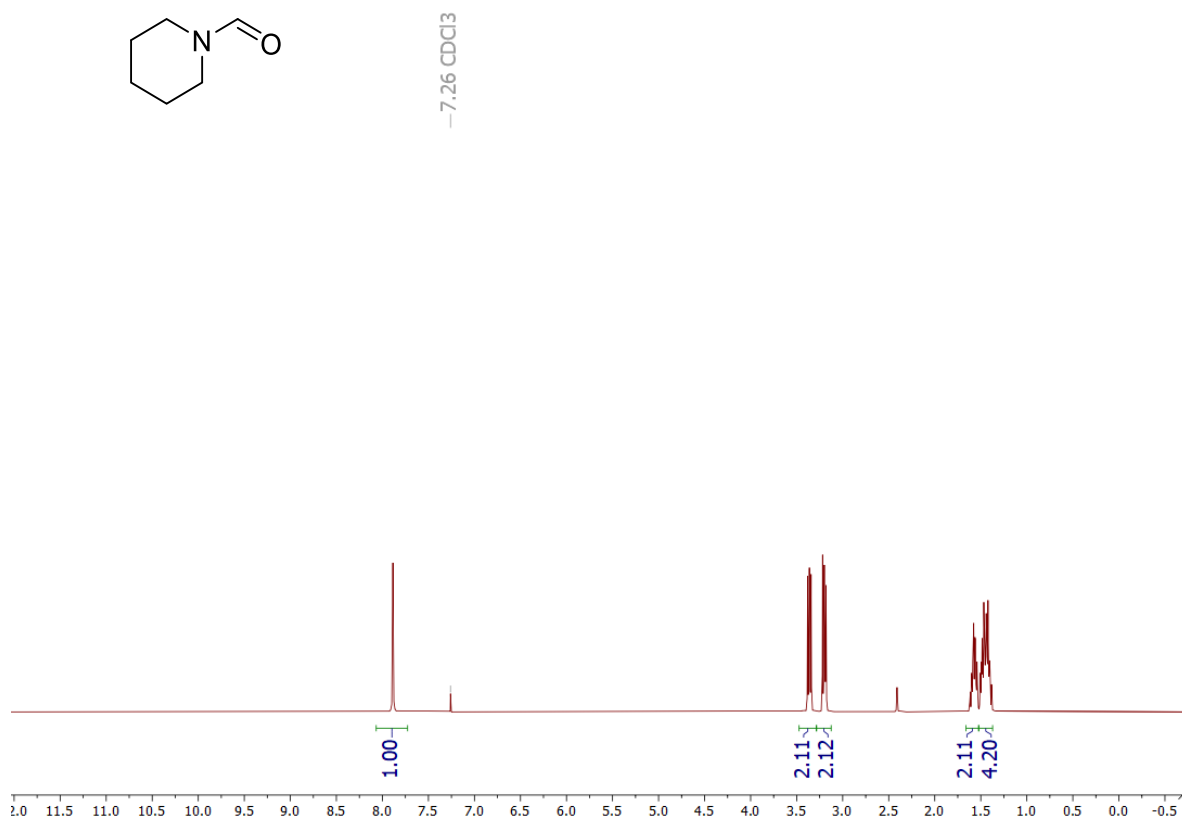


Figure S4. ¹H-NMR of 3a in CDCl₃

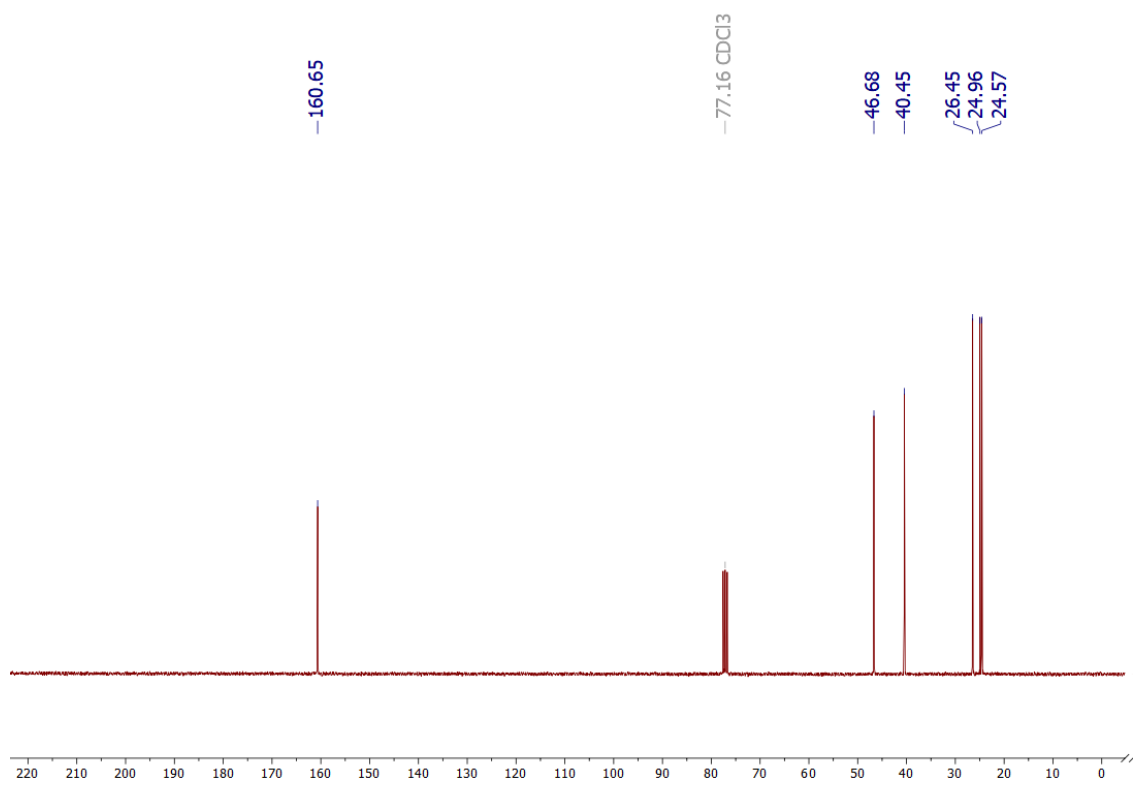


Figure S5. ¹³C-NMR of **3a** in CDCl₃

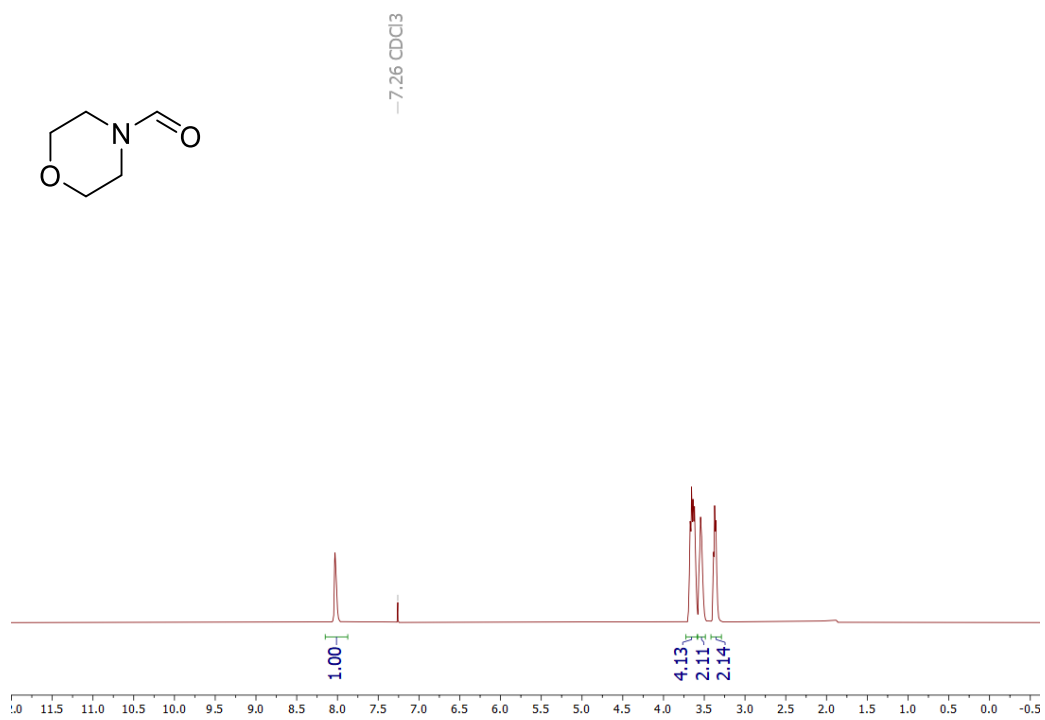


Figure S6. ¹H-NMR of **3c** in CDCl₃

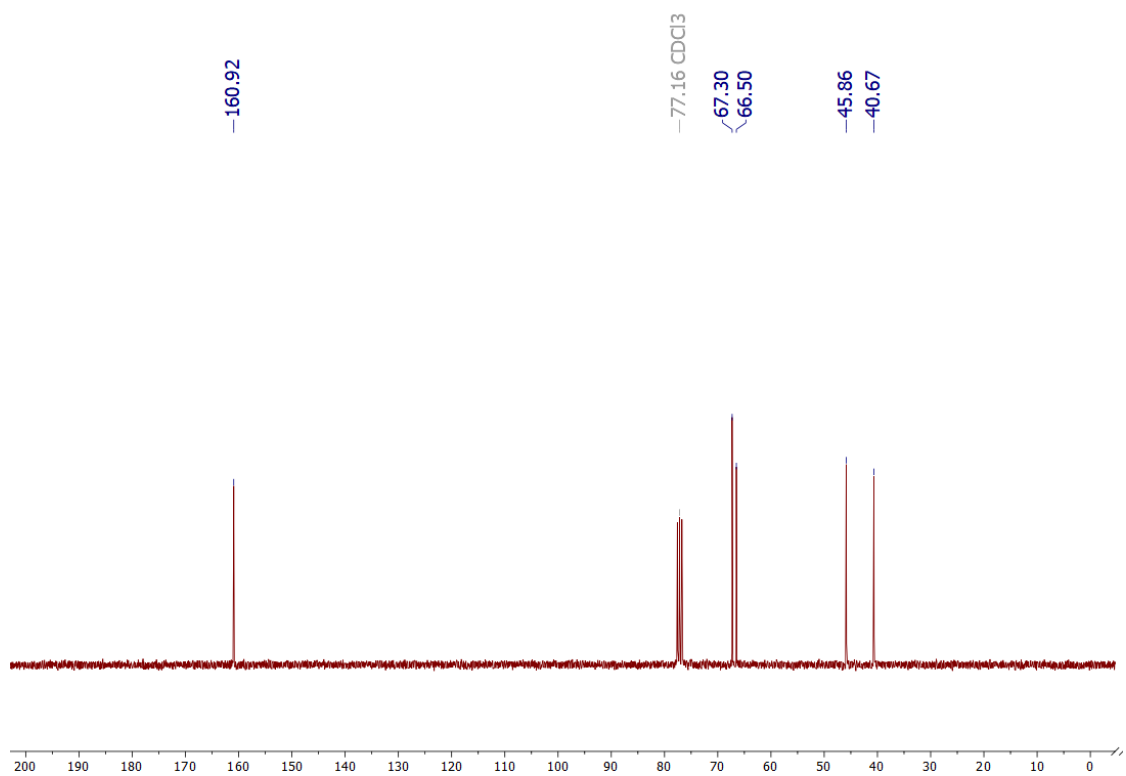


Figure S7. ¹³C-NMR of **3c** in CDCl₃

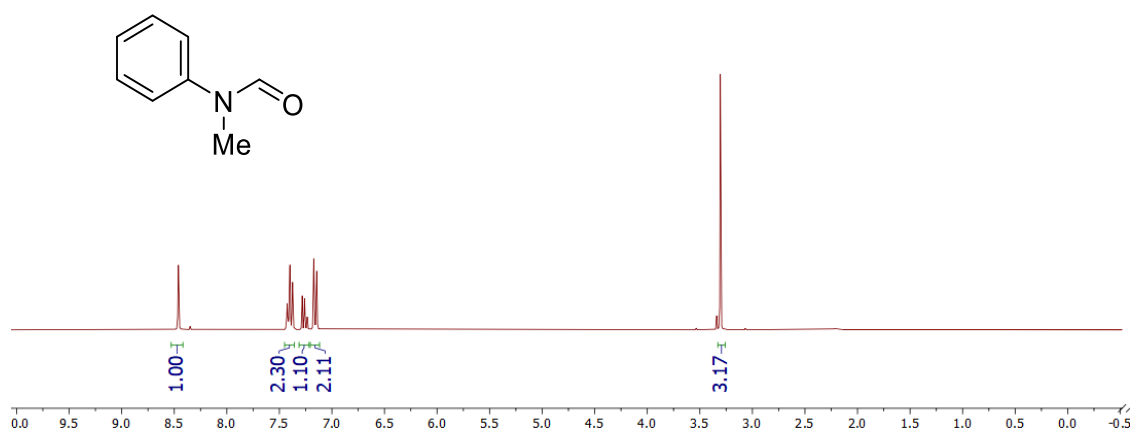


Figure S8. ¹H-NMR of **3f** in CDCl₃

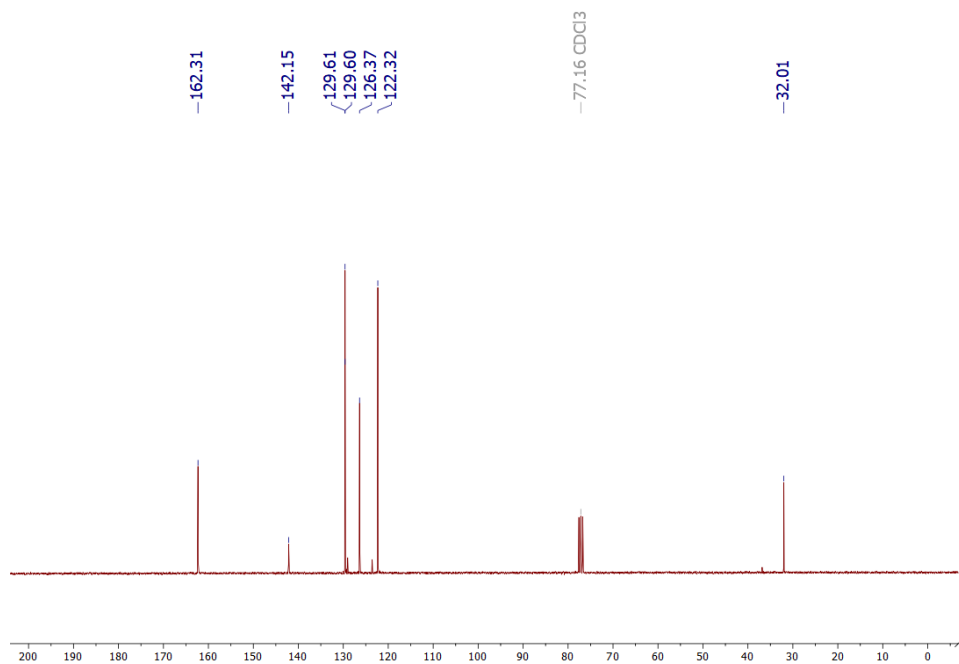


Figure S9. ¹³C-NMR of **3f** in CDCl₃

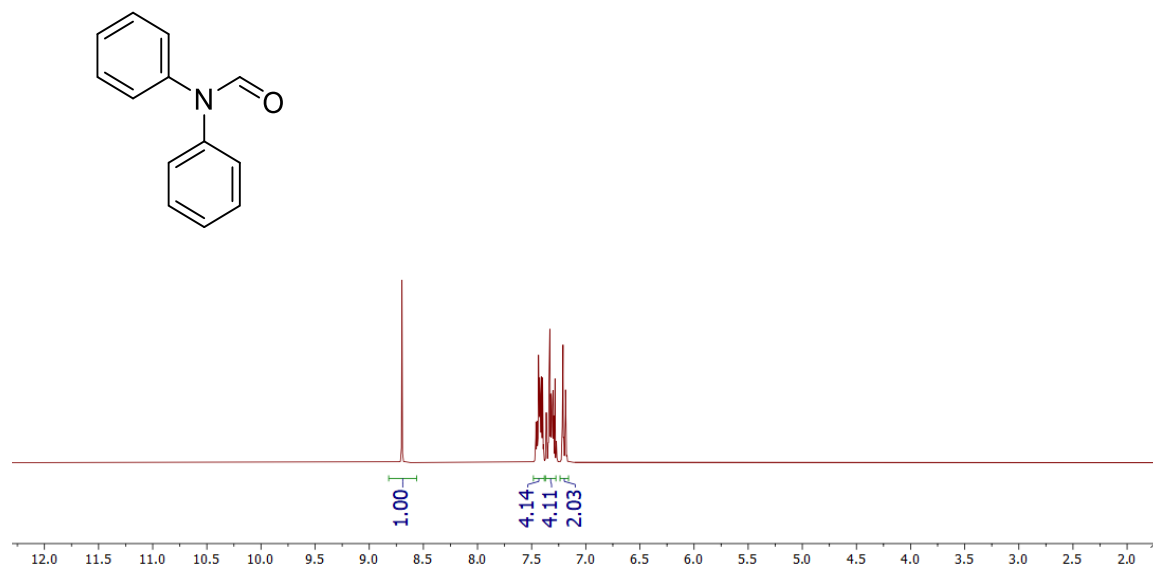


Figure S10. ¹H-NMR of **3g** in CDCl₃

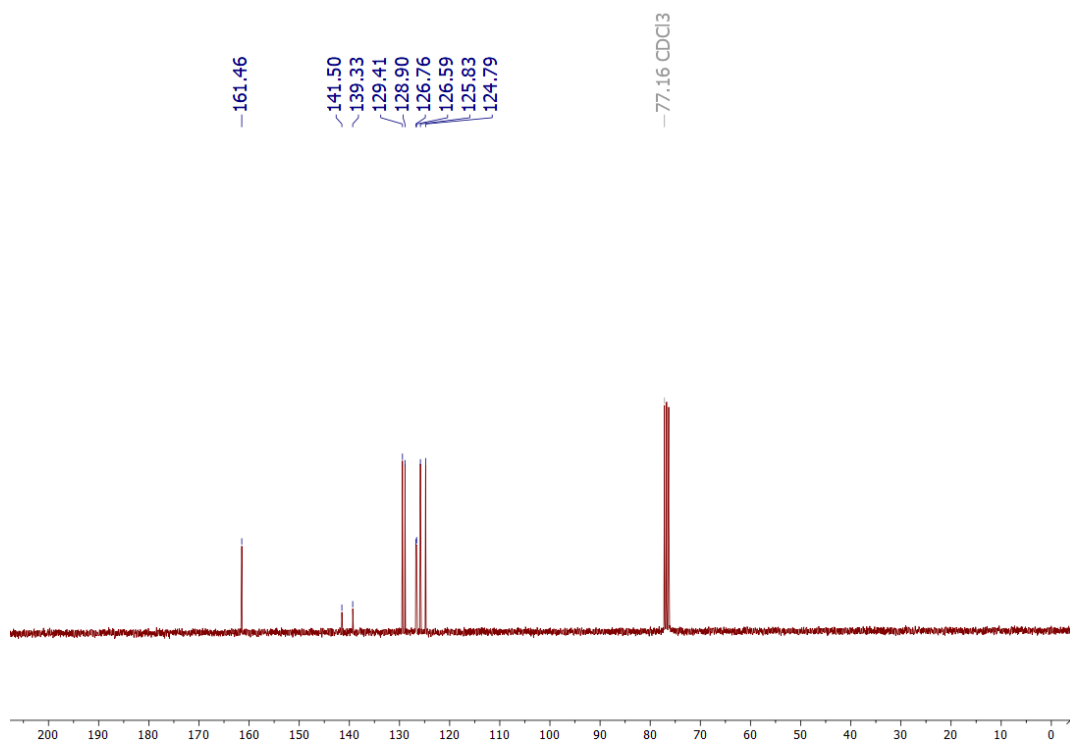


Figure S11. ¹³C-NMR of **3g** in CDCl₃

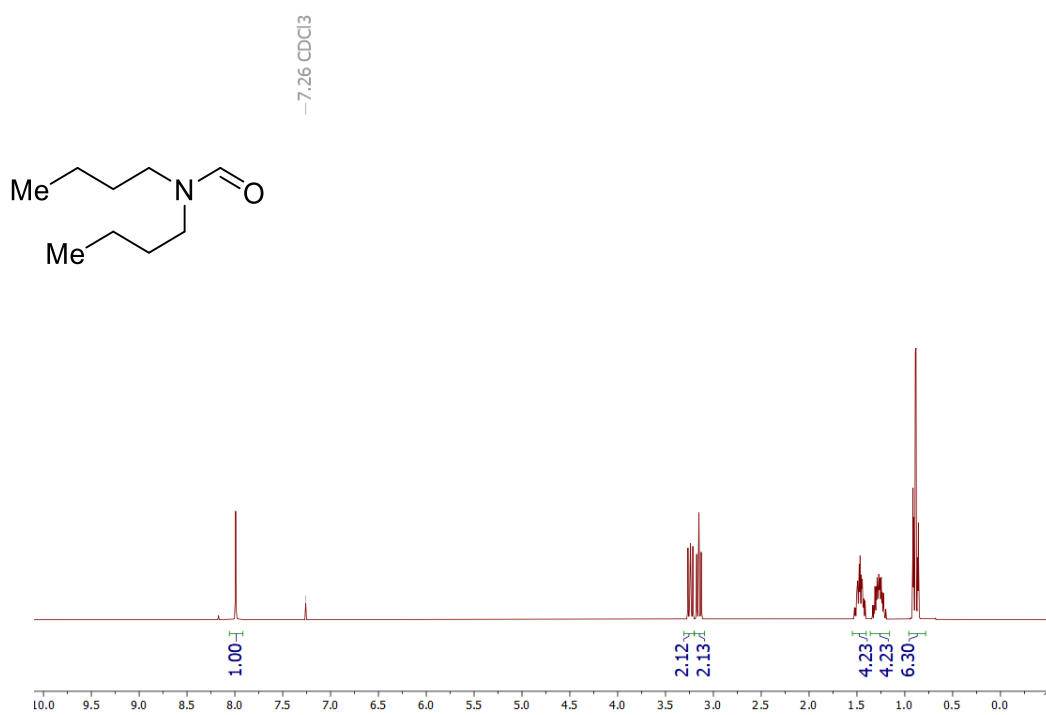


Figure S12. ¹H-NMR of **3h** in CDCl₃

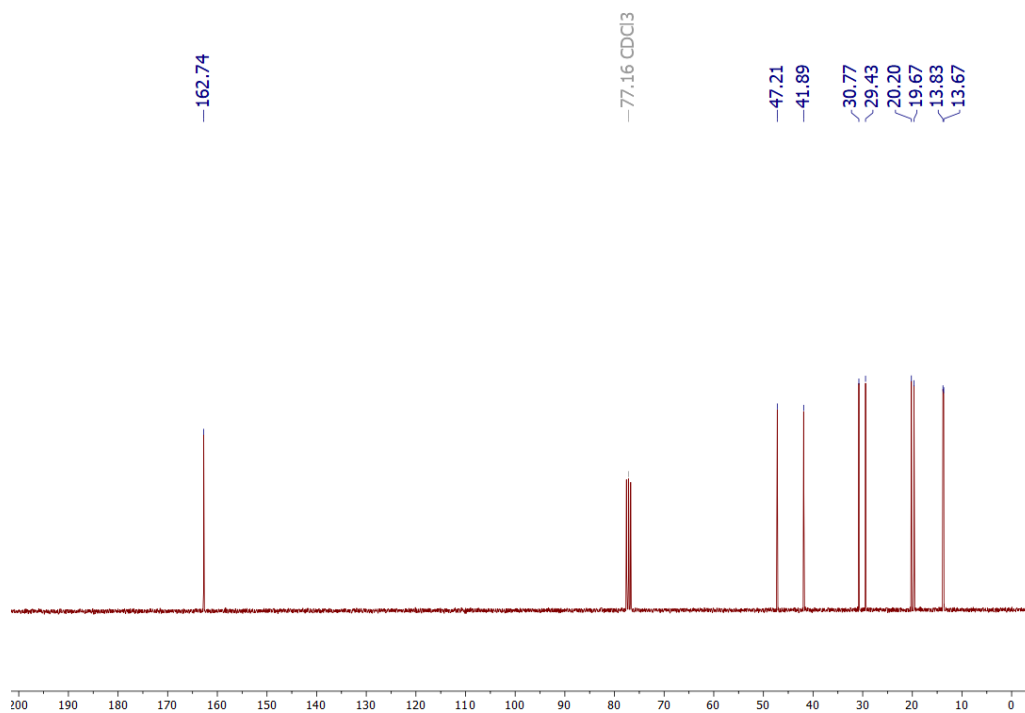


Figure S13. ¹³C-NMR of **3h** in CDCl₃

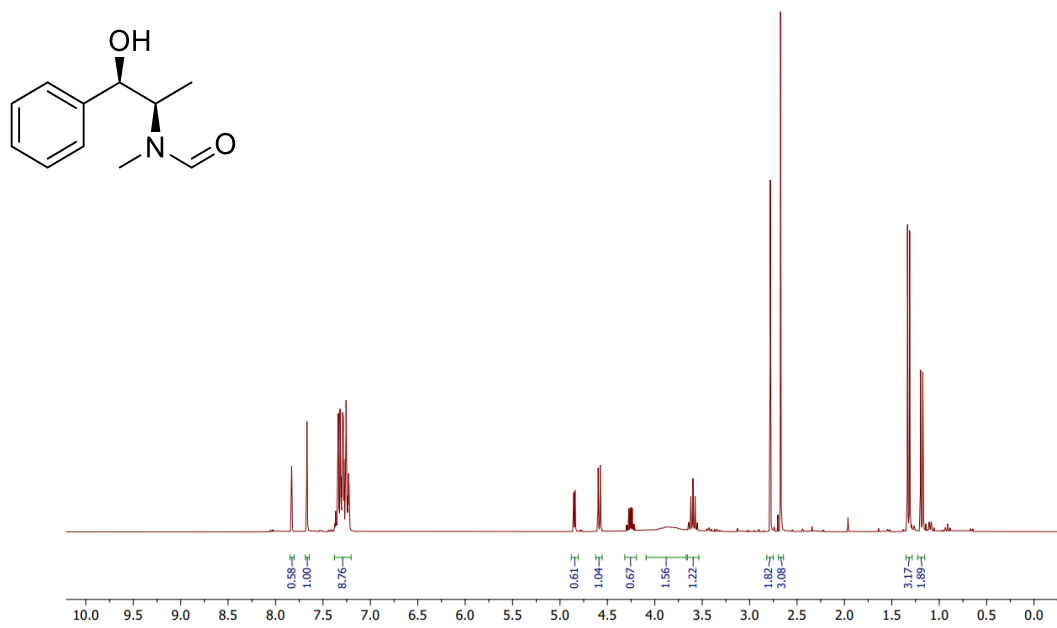


Figure S14. ¹H-NMR of **3m** in CDCl₃

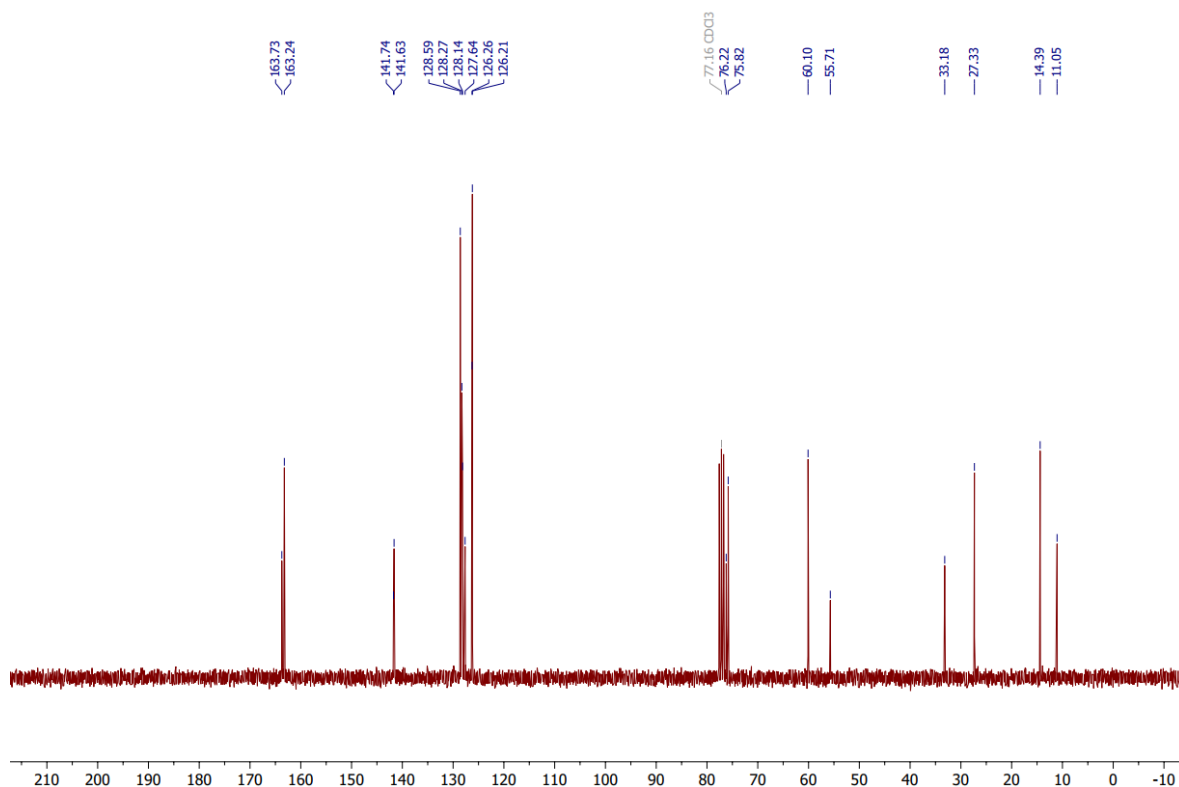


Figure S15. ^{13}C -NMR of **3m** in CDCl_3

6. EPR experiments

In a 5 mL vial, piperidine (67 mg, 0.78 mmol, 2 eq) and glycolaldehyde dimer (47 mg, 0.39 mmol, 1 eq) were dissolved in 2 mL of acetonitrile. The vials were sealed with a septum, then bubbled either with argon or oxygen and heated at 90 °C for 4 hours. EPR spectra were recorded on a Bruker cw ELEXSYS 500-10/12 spectrometer (X-band, 9.7 GHz) with a microwave power of 6.3 mW, a modulation frequency of 100 kHz and modulation amplitude of up to 1G. A special home-made flat cell (ID = 0.5 mL) was filled under Ar with 0.2 mL of enamine solution and DMPO (10 μL) and measured at 20 °C.

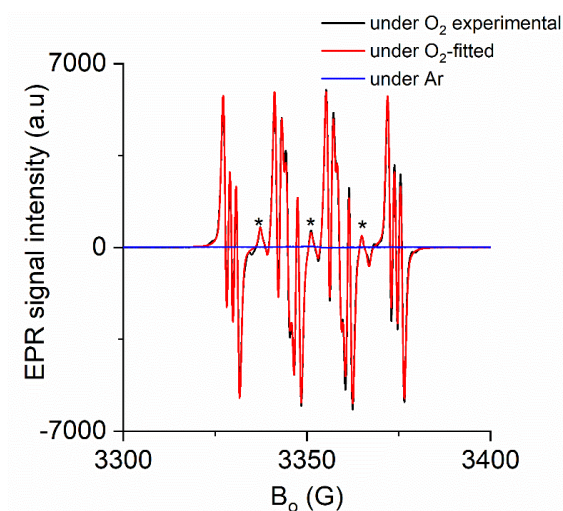


Figure S16. EPR of the reaction between **1a** and **2a**.

7. ESI-MS

In a 5 mL vial, piperidine (67 mg, 0.78 mmol, 2 eq), glycolaldehyde dimer (47 mg, 0.39 mmol, 1 eq) and DMPO (89 mg, 0.78 mmol, 2 eq) were dissolved in 2 mL of acetonitrile. The vials were sealed with a septum, then bubbled with oxygen and heated at 90 °C for 15 minutes. A sample was taken and diluted 1:10 with cold acetonitrile, then ESI-MS measured.

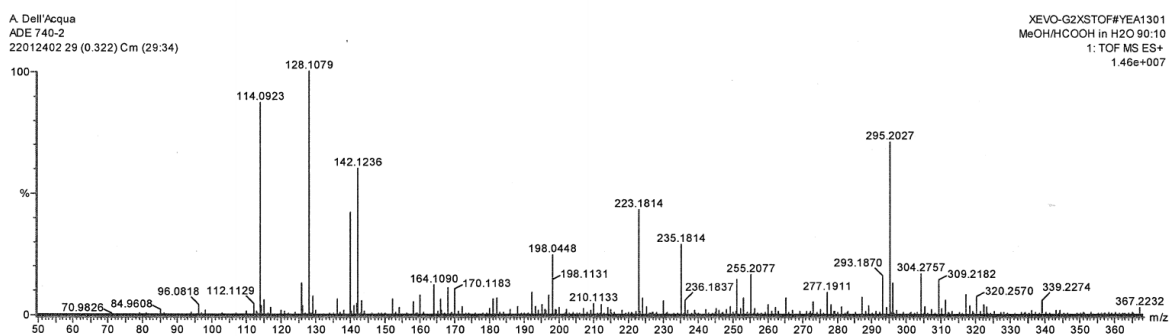


Figure S17. High-resolution ESI-MS spectrum of the reaction between **1a** and **2a** in the presence of DMPO.

8. NMR Studies

In a Young NMR tube, enamine **7a** was diluted in CD₃CN (ca. 0.1 g mol⁻¹). The solution was bubbled with 1 atm of oxygen for 15 minutes, then the tube sealed and ¹H NMR spectra (400 MHz) measured with an interval of 15 minutes.

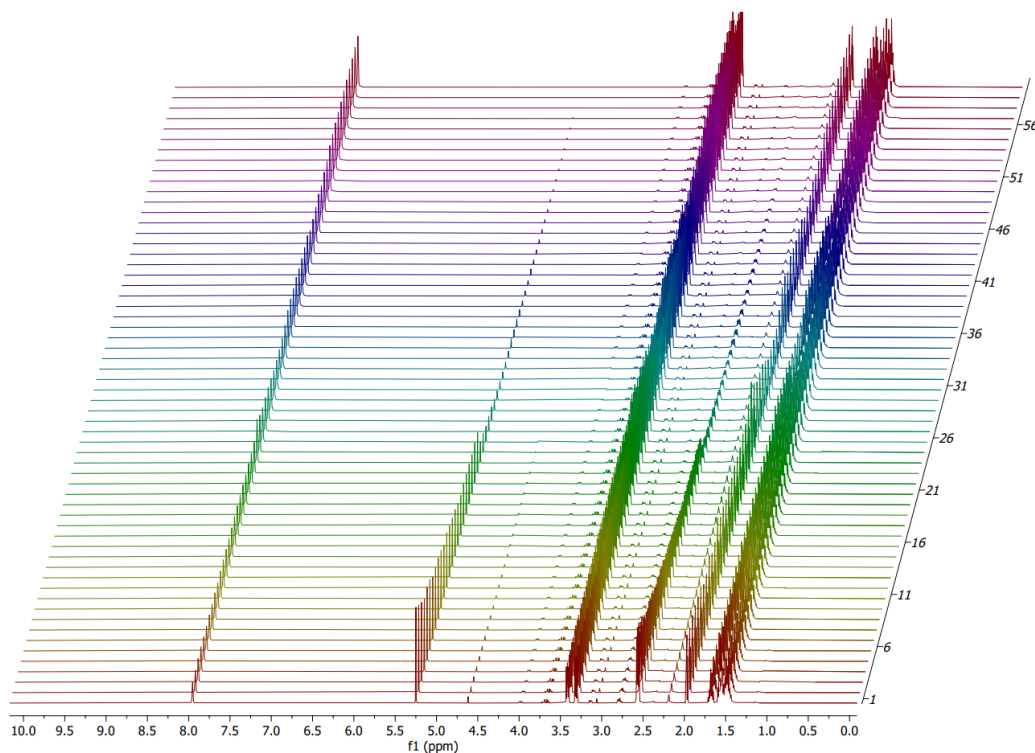


Figure S18. Stacked plot of time-resolved ¹H-NMR of **7a** in CD₃CN in the presence of 1 atm of O₂.

220208.419.4.fid
Dell'Acqua / ADE746
Au1H CD3CN {C:\Bruker\TopSpin3.5pl6} 2202 19

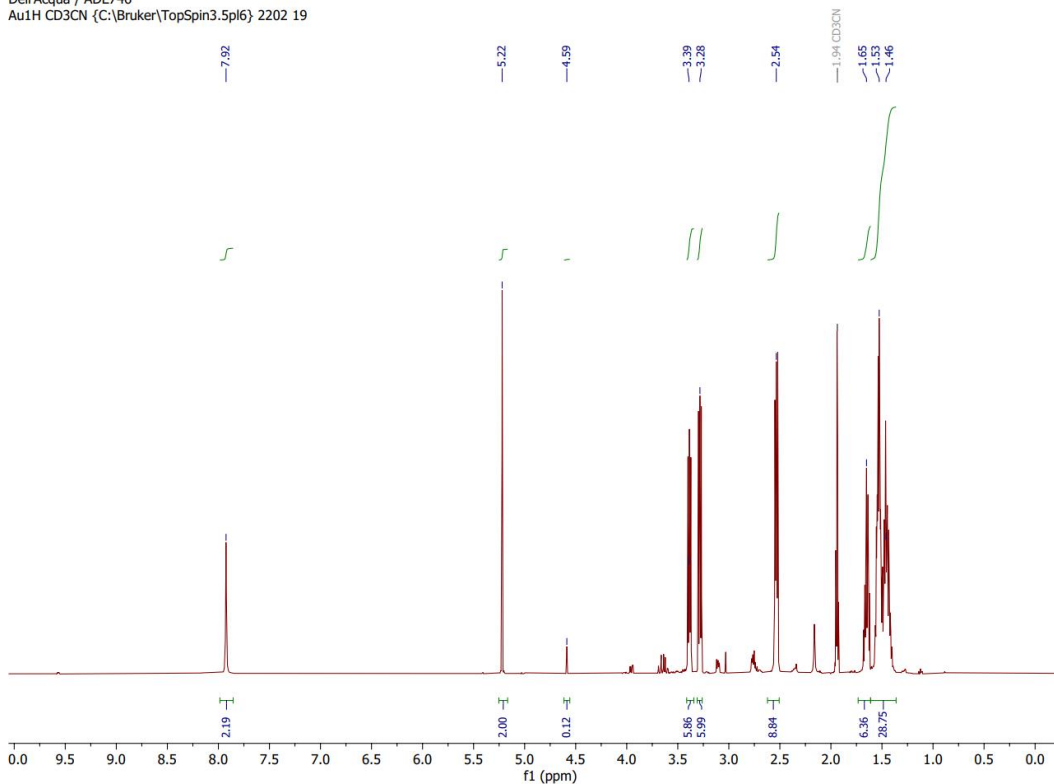


Figure S19. ¹H-NMR spectrum from S18 after 1 hour

220208.419.60.fid
Dell'Acqua / ADE746
Au1H CD3CN {C:\Bruker\TopSpin3.5pl6} 2202 19

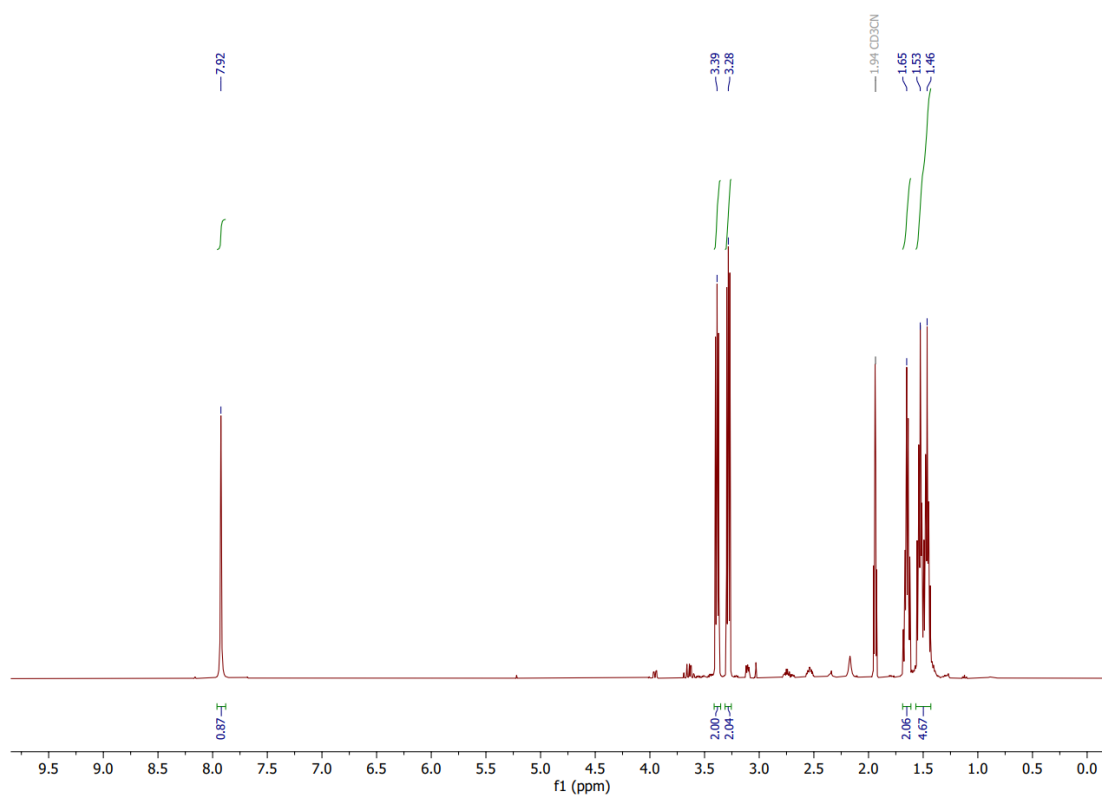


Figure S20. ¹H-NMR spectrum from S18 after 16 hours

9. References

1. S. N. Rao, D. C. Mohan and S. Adimurthy, *Organic letters*, 2013, 15, 1496-1499.
2. Q. Zou, G. Long, T. Zhao and X. Hu, *Green Chem.*, 2020, 22, 1134-1138.
3. J. Yin, J. Zhang, C. Cai, G.-J. Deng and H. Gong, *Organic letters*, 2018, 21, 387-392.
4. X. Cui, Y. Zhang, Y. Deng and F. Shi, *Chemical Communications*, 2014, 50, 189-191.
5. K. Bao, W. Zhang, X. Bu, Z. Song, L. Zhang and M. Cheng, *Chemical Communications*, 2008, 5429-5431.

New Bifunctional Monomers from Methyl Vinyl Glycolate.

Andrea Dell'Acqua,^a Claas Schünemann,^a Eszter Baráth,^a Sergey Tin^a and Johannes G. de Vries*^a

^aLeibniz Institut für Katalyse e. V. an der Universität Rostock
Albert-Einstein-Strasse 29a, 18055 Rostock
E-mail: johannes.devries@catalysis.de

Supporting Information

1. General information

Reagents: Methyl vinyl glycolate was supplied by Haldor Topsøe A/S. All the other reagents and solvents were obtained from commercial sources and used as received unless noted otherwise. Dry solvents were obtained from a solvent purification system or purchased water-free in a bottle with septum. All the reagents and solvents were handled in oven-dried glassware using standard Schlenk techniques, unless otherwise stated.

NMR-Spectroscopy: ¹H-NMR and ¹³C-NMR were recorded at ambient temperature on 300 MHz spectrometers (Avance 300 or Fourier 300) or a 400 MHz spectrometer (Avance 400) from Bruker. The chemical shifts δ are given in ppm and referenced to the residual proton signal of the deuterated solvent used.

Gas Chromatography (GC): GC analysis was carried out on an Agilent 7890B GC system with a HP-5 normal-phase silica column, using He as a carrier gas and dodecane as internal standard.

Gel permeation chromatography (GPC): Gel permeation chromatograms were recorded with 1260 Infinity GPC/SEC System from Agilent Technologies. The setup consisted of a SECcurity Isocratic Pump, SECcurity 2-Canal-Inline-Degaser, SECcurity GPC-Column thermostat TCC6000, SECcurity Fraction Collector and SECcurity Differential Refractometer detector. The measurements were performed at a constant temperature of 50 °C using three columns with a polyester co-polymer network as the stationary phase (PSS GRAM 30 Å, 10 μ m particle size, 8.0 \times 50 mm; PSS GRAM 30 Å, 10 μ m particle size, 8.0 \times 300 mm; PSS GRAM 1000 Å particle size, 8.0 \times 300 mm). THF was applied as the mobile phase with a flow rate of 1 mL·min⁻¹. Polystyrene standards from ReadyCal (PSS-pskitr1I-10, M_p = 370–2520000 g·mol⁻¹) were used for calibration purposes.

Differential scanning calorimetry (DSC): Melting points and glass transition temperatures of polyesters were measured with a Star-SW DSC from Mettler Toledo using the following temperature program: -90.00 °C isothermal 5.00 min; Ramp 10.00 °C min⁻¹ to 150.00 °C; Ramp 10.00 °C/min to -90.00 °C; -90.00 °C isothermal 5.00 min; Ramp 10.00 °C min to 150.00 °C; Ramp 10.00 °C/min to -90.00 °C.

Infrared Spectroscopy: ATR-IR measurements were recorded on a Nicolet iS5 FT-IR (ThermoFisher) device calibrated on 1.5 mil polystyrene and equipped with a GladiATR 210 accessory from PIKE technologies.

Mass spectroscopy (ESI-MS): measurements were recorded on an Agilent 6210 time-of-flight LC/MS (ESI) or on a Thermo Electron MAT 95-XP (EI, 70 eV). Peaks as listed correspond to the highest abundant peak and are of the expected isotope pattern.

2. Experimental procedures

Hydroformylation of MVG: In a glovebox, dicarbonyl(acetylacetonato)rhodium(I) (1.2 mg, 0.005 mmol, 0.5 mol%) and the desired ligand (0.095 mmol, 0.1 eq) were weighted into a vial. The vial was sealed, equipped with a magnetic stirrer and transferred out of the glovebox. The desired solvent (toluene or THF, 1.35 mL, 0.7 mol/L with respect to MVG) and MVG (110 mg, 0.95 mmol, 1 eq) were added under argon atmosphere. The vials were placed into a 300 mL Parr stainless steel autoclave and pierced with a needle. The autoclave was flushed three times with nitrogen, then pressurized with 10 bar of syngas and heated to 80 °C. After stirring overnight, the reaction was cooled down to room temperature, the crude mixtures filtered over celite, and volatiles evaporated under reduced pressure. The crude residue was dissolved in CDCl₃ and analysed by ¹H NMR and GC-MS. Linear product (**1**) ¹H NMR (300 MHz, CDCl₃) δ 9.77 (t, *J* = 1.2 Hz, 1H), 4.23 (dd, *J* = 7.8, 4.2 Hz, 1H), 3.77 (s, 3H), 2.65 – 2.55 (m, 2H), 2.48 – 2.36 (m, 2H). Branched product (**2**), mixture of 2 diastereoisomers: ¹H NMR (300 MHz, CDCl₃) δ 9.73 (d, *J* = 0.7 Hz, 1H), 9.65 (s, 1H), 4.76 (d, *J* = 3.0 Hz, 1H), 4.42 (d, *J* = 3.9 Hz, 1H), 3.77 (s, 3H), 3.75 (s, 3H), 2.54 – 2.37 (m, 1H), 2.37 – 2.12 (m, 1H), 1.26 (d, *J* = 7.3 Hz, 3H), 1.12 (d, *J* = 7.2 Hz, 3H). ¹³C NMR (75 MHz, CDCl₃) δ 201.9, 201.7, 174.9, 70.9, 69.6, 53.1, 53.0, 49.8, 49.6, 9.9, 7.6. Hydroxyacetal (**3**), mixture of 2 diastereoisomers: ¹H NMR (300 MHz, CDCl₃) δ 5.75 – 5.71 (m, 1H), 5.60 (t, *J* = 3.2 Hz, 1H), 4.71 (dd, *J* = 8.6, 4.2 Hz, 1H), 4.55 (dd, *J* = 8.2, 7.1 Hz, 1H), 3.75 (s, 3H), 3.72 (s, 3H), 2.11 – 1.82 (m, 6H). ¹³C NMR (75 MHz, CDCl₃) δ 174.8, 173.2, 100.2, 99.7, 77.2, 76.3, 52.5, 52.3, 33.7, 32.2, 28.1, 28.0.

Methylation of MVG: In a 250 mL Schlenk flask Ag₂O (19.6 g, 84.4 mmol, 2 eq) was suspended in 60 mL of diethyl ether (0.7 mol/L with respect to MVG). MVG (4.90 g, 42.2 mmol, 1 eq) was added under argon atmosphere. To the stirred suspension, methyl iodide (13.0 g, 84.4 mmol, 2 eq) was slowly added via syringe. The reaction was stirred at room temperature while monitoring the conversion by GC. After 60 hours, MVG was fully converted. The reaction was filtered to remove the solids, then the

solvent and the excess of methylating agent removed by carefully distilling under vacuum, affording a colourless liquid (5.51 g, quantitative yield). The analytical data corresponds to the known literature.¹

¹H NMR (300 MHz, CDCl₃) δ 5.85 (ddd, *J* = 17.2, 10.4, 6.4 Hz, 1H), 5.46 (dt, *J* = 17.2, 1.3 Hz, 1H), 5.34 (dt, *J* = 10.4, 1.3 Hz, 1H), 4.26 (dt, *J* = 6.4, 1.3 Hz, 1H), 3.76 (s, 3H), 3.40 (s, 3H). ¹³C NMR (75 MHz, CDCl₃) δ 171.1, 132.7, 119.6, 81.7, 57.5, 52.4.

Acetylation of MVG: In a 50 mL Schlenk flask, MVG (550 mg, 4.74 mmol, 1 eq) and pyridine (750 mg, 9.47 mmol, 2 eq) were dissolved in dichloromethane (16 mL, 0.3 mol/L with respect to MVG). To the stirred mixture, acetic anhydride (967 mg, 9.47 mmol, 2 eq) was slowly added via syringe. The reaction was stirred at room temperature overnight, then poured into ice-cold water and extracted three times with DCM. The organic phase was washed with 1M HCl, water and brine, then dried over Na₂SO₄ and concentrated in vacuum, affording 746 mg of colourless liquid (quantitative yield). The analytical data corresponds to the known literature.²

¹H NMR (400 MHz, CDCl₃) δ 5.87 – 5.77 (m, 1H), 5.41 – 5.31 (m, 2H), 5.24 (ddd, *J* = 10.5, 1.4, 0.9 Hz, 1H), 3.63 (s, 3H), 2.04 (s, 3H). ¹³C NMR (101 MHz, CDCl₃) δ 169.7, 168.7, 129.9, 119.5, 72.8, 52.3, 20.3.

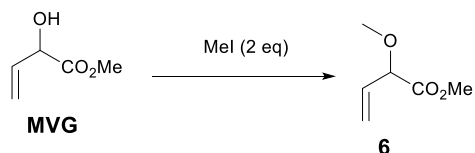
Methoxycarbonylation reactions: In a glovebox, palladium(II) diacetate (1.7 mg, 0.01 mmol, 1.0 mol%) and the desired ligand (0.02 mmol, 2.0 ml%) were weighted into a vial. The vial was sealed, equipped with a magnetic stirrer, and transferred out of the glovebox. Methanol (1.5 mL, 0.5 mol/L with respect to the substrate), methanesulfonic acid (2.2 mg, 0.02 mmol, 2 mol%) and the desired MVG derivative (see Table 2 main text; 0.80 mmol, 1 eq) were added under argon atmosphere. The vials were placed into a 300 mL Parr stainless steel autoclave and pierced with a needle. The autoclave was flushed three times with nitrogen, then pressurized with the desired pressure of carbon monoxide and heated to the required temperature. After stirring for the desired time, the reaction was cooled down to room temperature, the crude mixtures filtered over celite, and volatiles evaporated under reduced pressure. The crude was purified by flash column chromatography (gradient elution, from 100% *n*-hexane to 100% ethyl acetate), affording the diester as a yellowish liquid.

¹H NMR (300 MHz, CDCl₃) δ 3.82 (dd, *J* = 7.8, 4.7 Hz, 1H), 3.75 (s, 3H), 3.67 (s, 3H), 3.38 (s, 3H), 2.44 (ddd, *J* = 7.7, 7.0, 3.6 Hz, 2H), 2.18 – 1.92 (m, 2H). ¹³C NMR (75 MHz, CDCl₃) δ 173.4, 172.7, 79.3, 58.4, 52.1, 51.8, 29.6, 27.9. ESI-MS (ES⁺): calculated for C₈H₁₄O₅: 191.0919; found: 213.0737 [M-Na]⁺.

Polycondensation reactions: A 5 mL vial equipped with stirring bar was charged with the desired diol (2.0 mmol, 1 eq) and **8** (380 mg, 2.0 mmol, 1 eq). The starting materials were extensively dried via

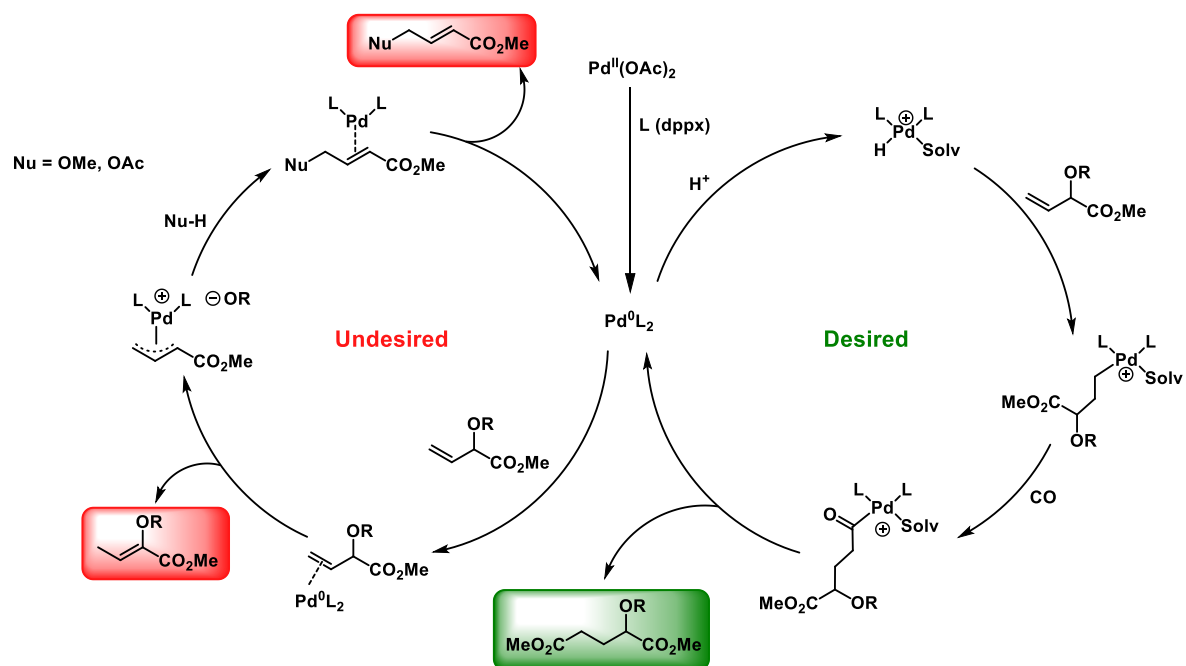
vacuum-argon cycles, then titanium(IV) isopropoxide (3.2 mg, 0.01 mmol, 1 mol%) was added via syringe and the reaction heated up to 150 °C. After stirring under argon atmosphere for 6 hours, vacuum was applied for 1 hour. Viscosity visibly increased up to the point that the mixture wasn't stirred. Temperature was then increased to 190 °C and the reaction kept in vacuum another hour. After cooling down to room temperature, the solid products were analysed by NMR and GPC.

3. Screening of reaction conditions for the methylation of MVG



Entry	Conditions	Outcome
1	NaH, THF, 0 °C – r.t., 16 h	C=C isomerization
2	Ag ₂ O, Et ₂ O, r.t., 24 h	6 (49 % after FCC)
3	K ₂ CO ₃ , THF, 80 °C, 1 h	-
4	K ₂ CO ₃ , MeOH, 80 °C, 1 h	MeOMVG dimerization
5	K ₂ CO ₃ , neat, 80 °C, 1 h	-
6	K ₂ CO ₃ , acetone, 80 °C, 1 h	-
7	NaOMe, MeOH, 80 °C, 1 h	C=C isomerization
8	DIPEA, Et ₂ O, r.t., 48 h	C=C isomerization

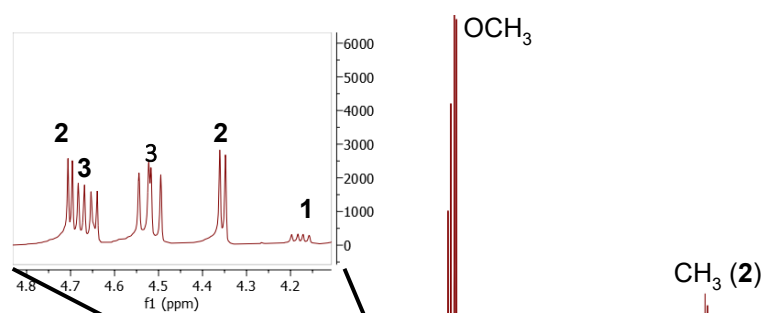
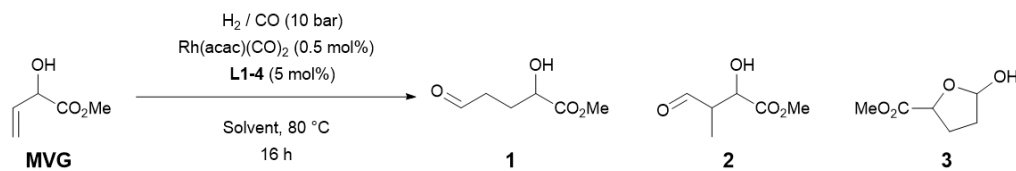
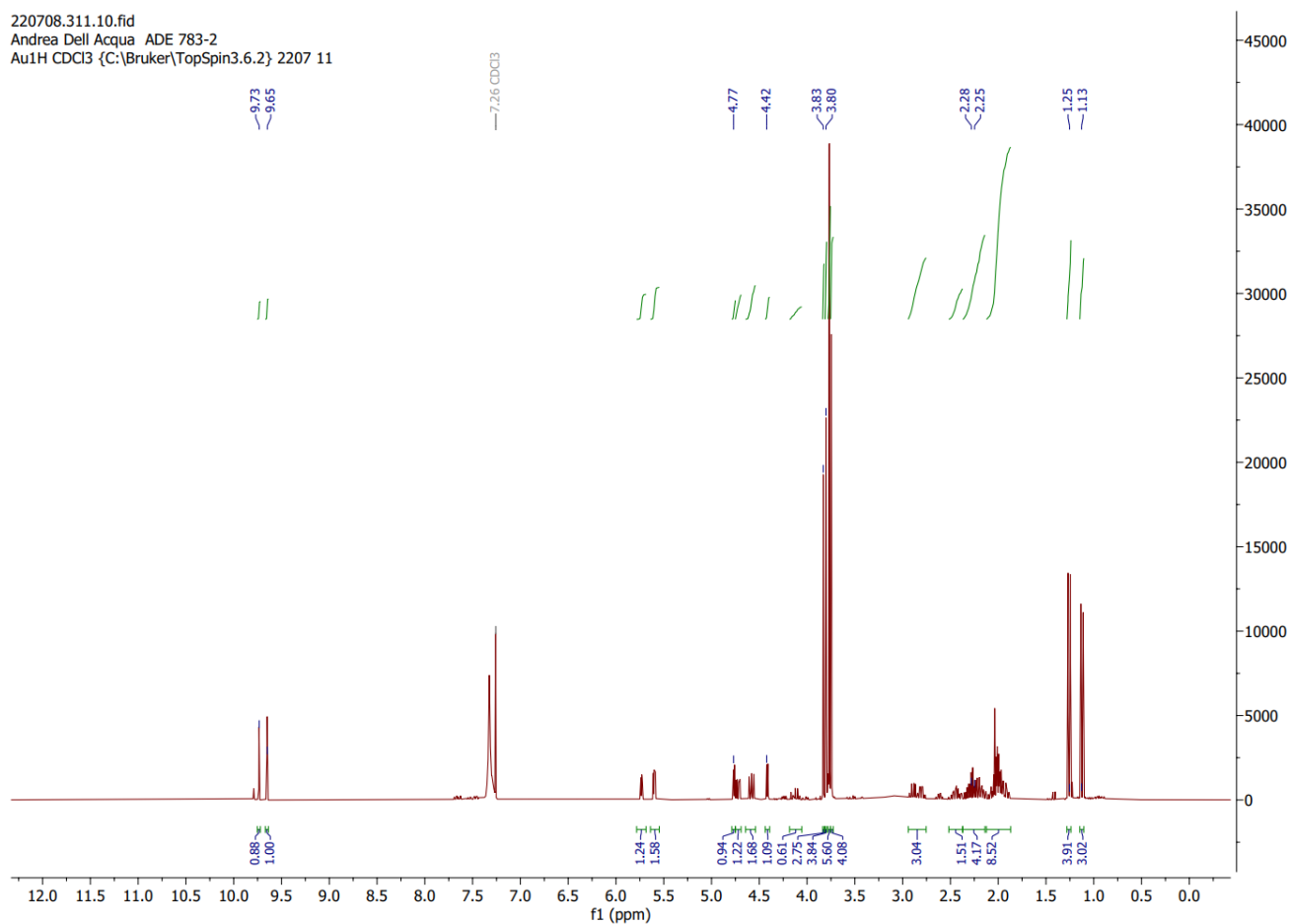
4. Mechanisms involved in the Pd-catalysed methoxycarbonylation



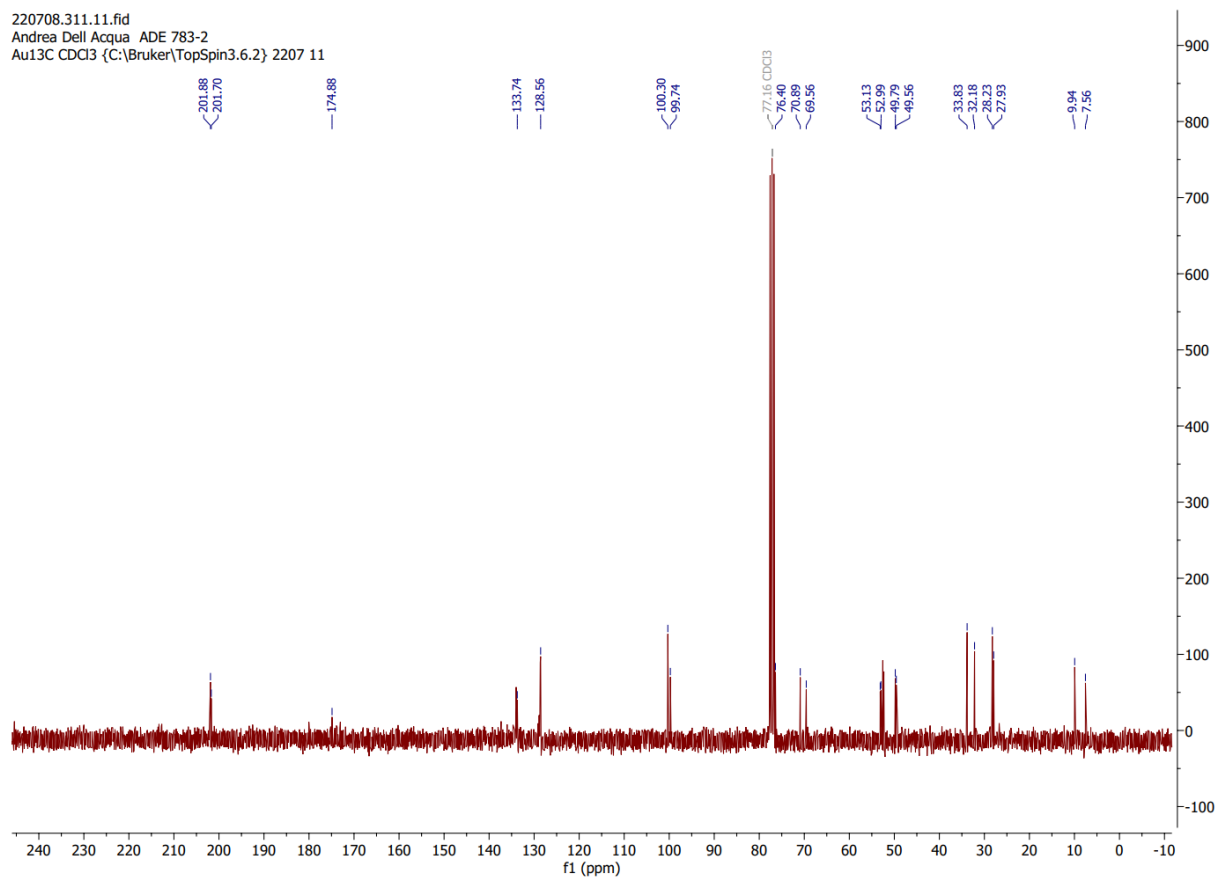
5. Characterization of products

NMR Spectra

- Representative spectra in CDCl₃ of the crude mixture after hydroformylation of MVG using PPh₃ as ligand (Table 1 main text, entry 1 and 2):

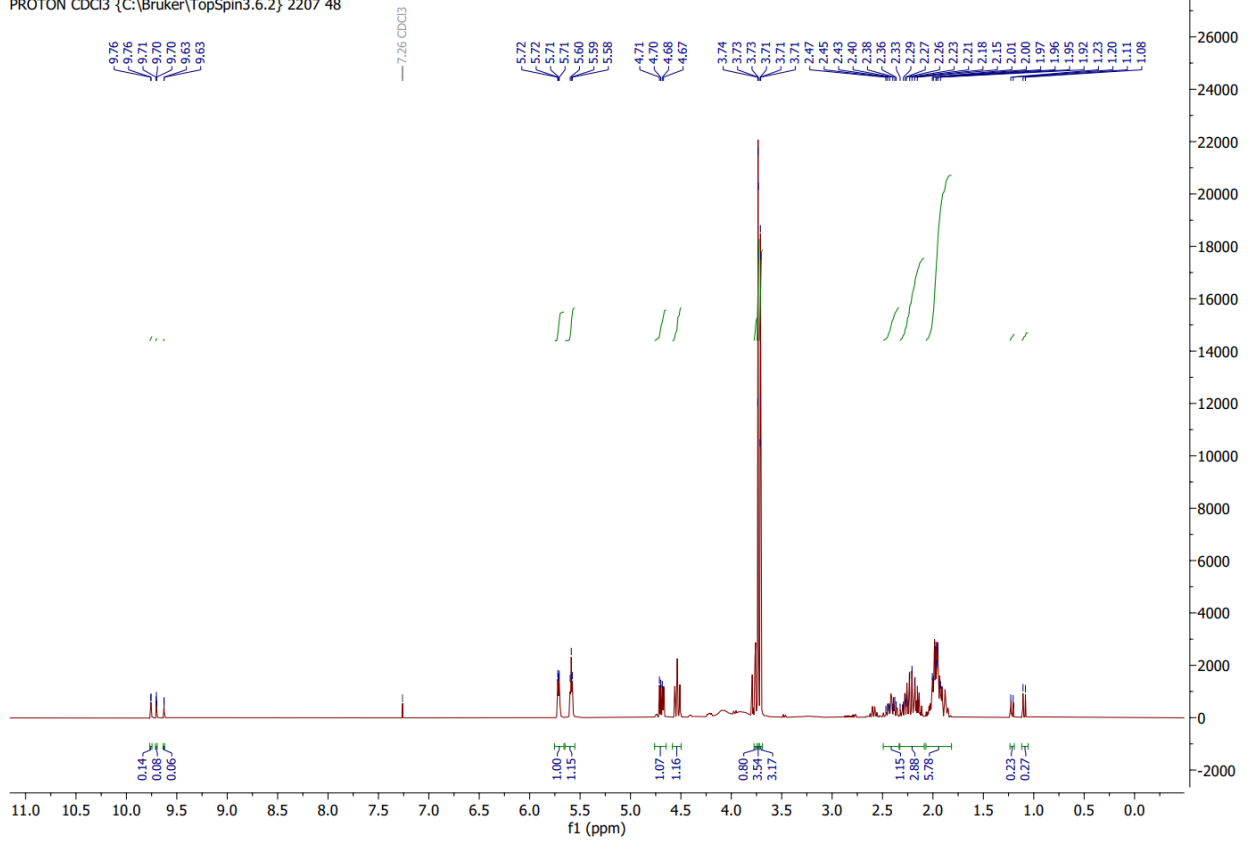


220708.311.11.fid
Andrea Dell'Acqua ADE 783-2
Au13C CDCl3 {C:\Bruker\TopSpin3.6.2} 2207 11

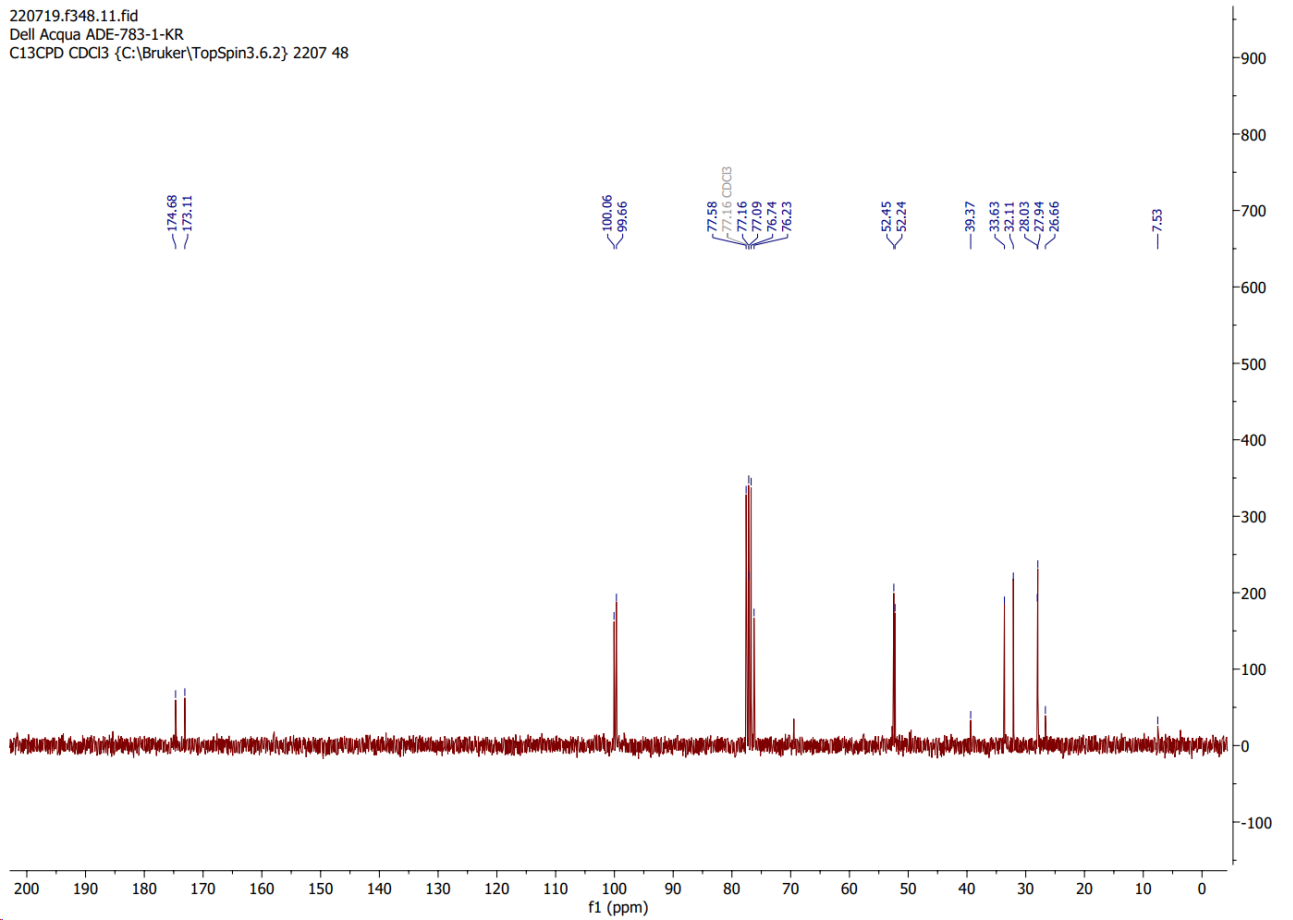


- Representative spectra in CDCl₃ of the high linear containing mixture after hydroformylation of MVG using Xantphos as ligand (Table 1 main text, entry 3 and 4):

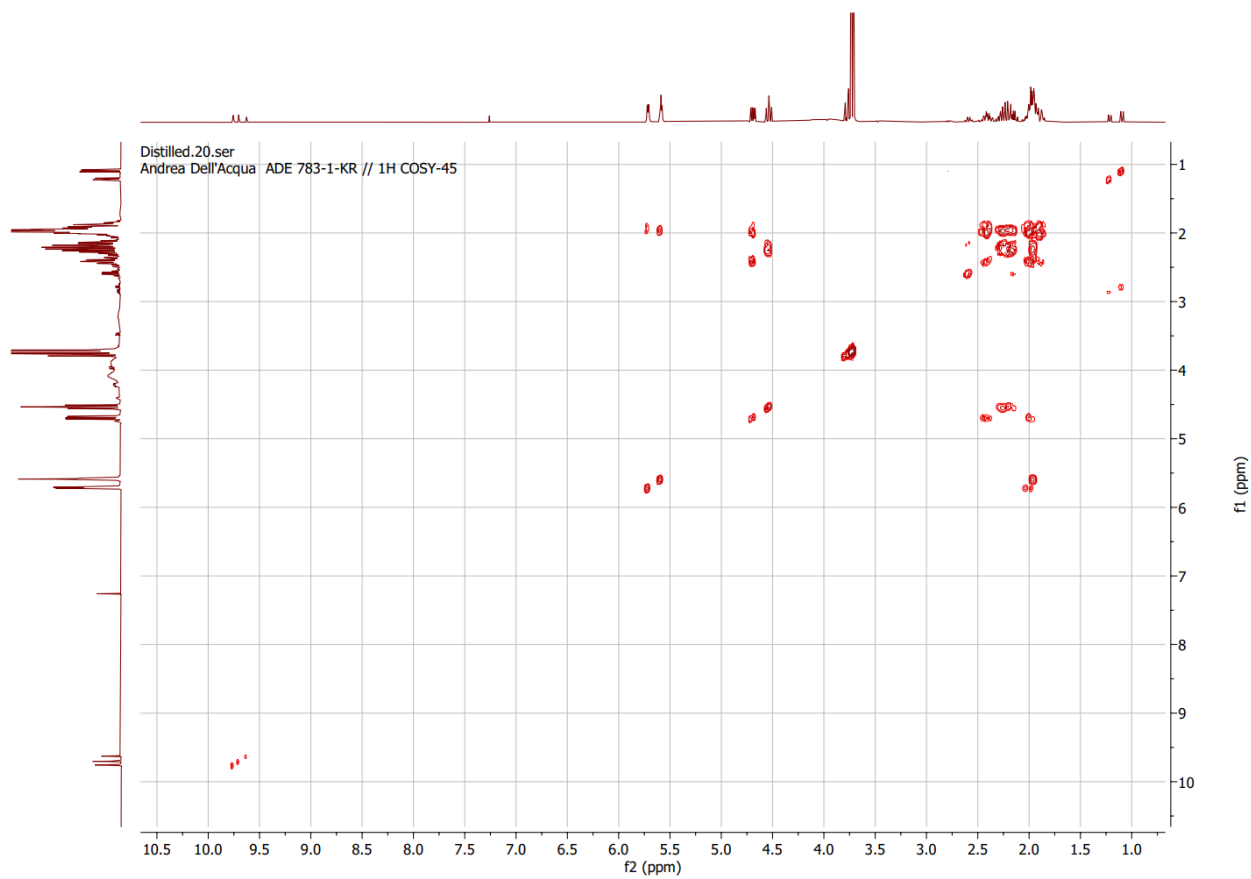
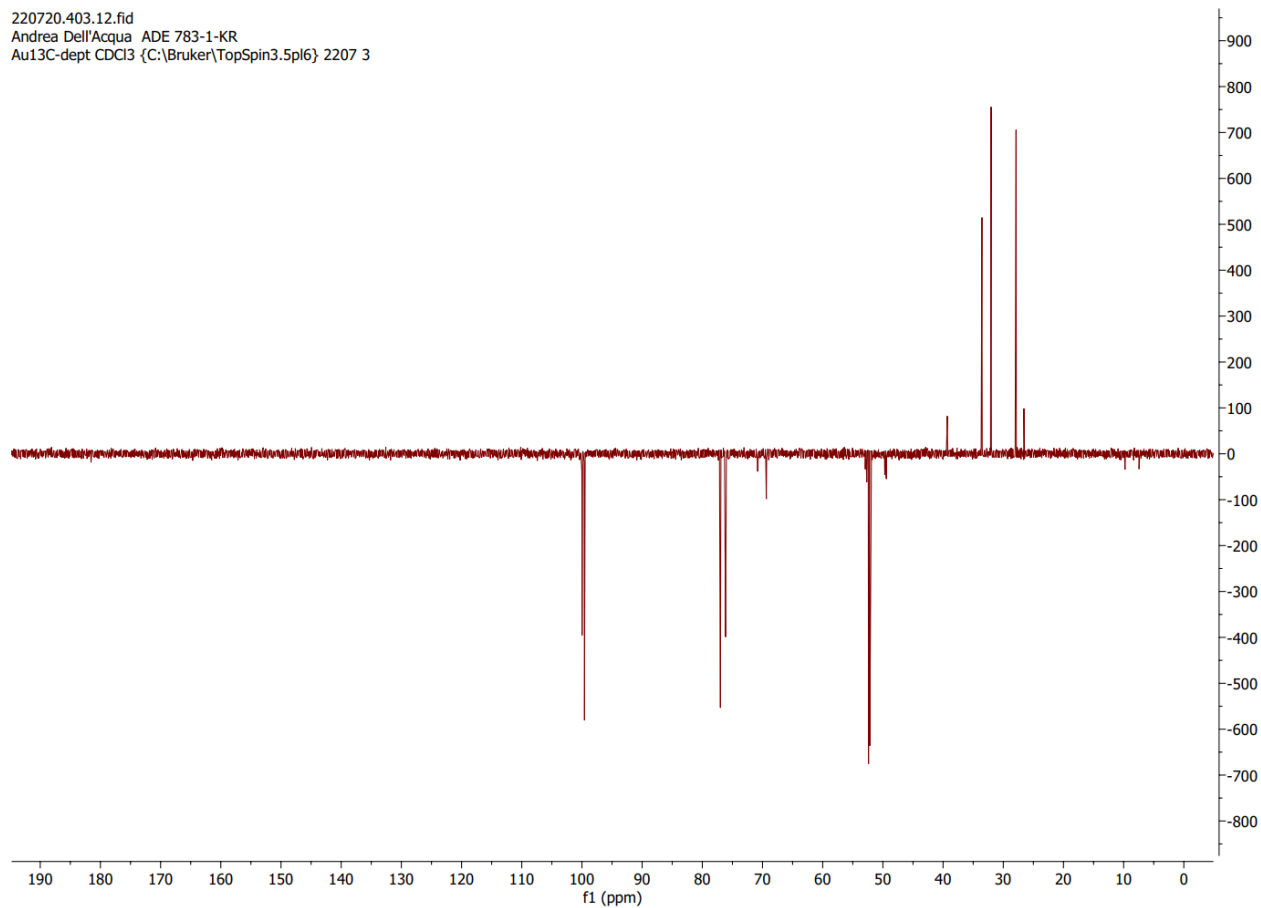
220719.f348.10.fid
 Dell Acqua ADE-783-1-KR
 PROTON CDCl3 {C:\Bruker\TopSpin3.6.2} 2207 48



220719.f348.11.fid
 Dell Acqua ADE-783-1-KR
 C13CPD CDCl3 {C:\Bruker\TopSpin3.6.2} 2207 48

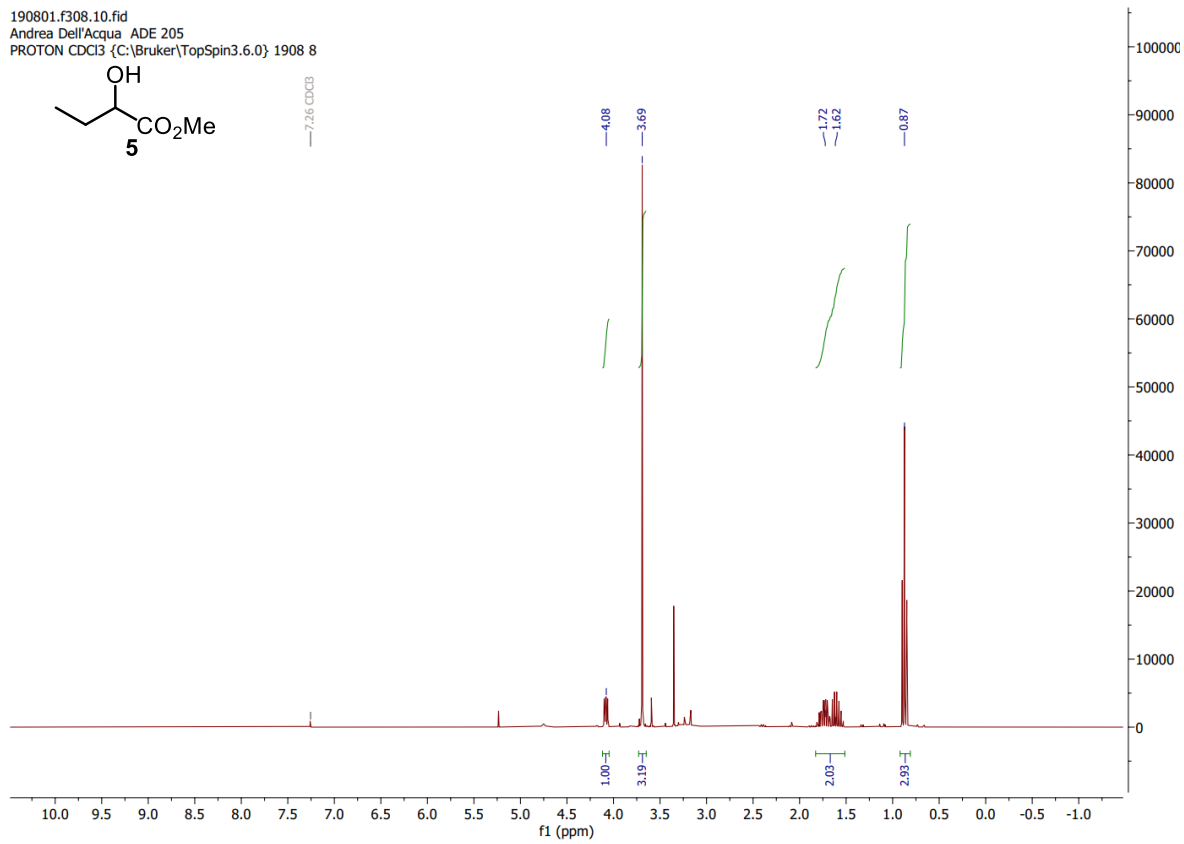
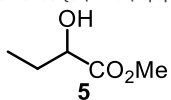


220720.403.12.fid
Andrea Dell'Acqua ADE 783-1-KR
Au13C-dept CDCl3 {C:\Bruker\TopSpin3.5pl6} 2207 3

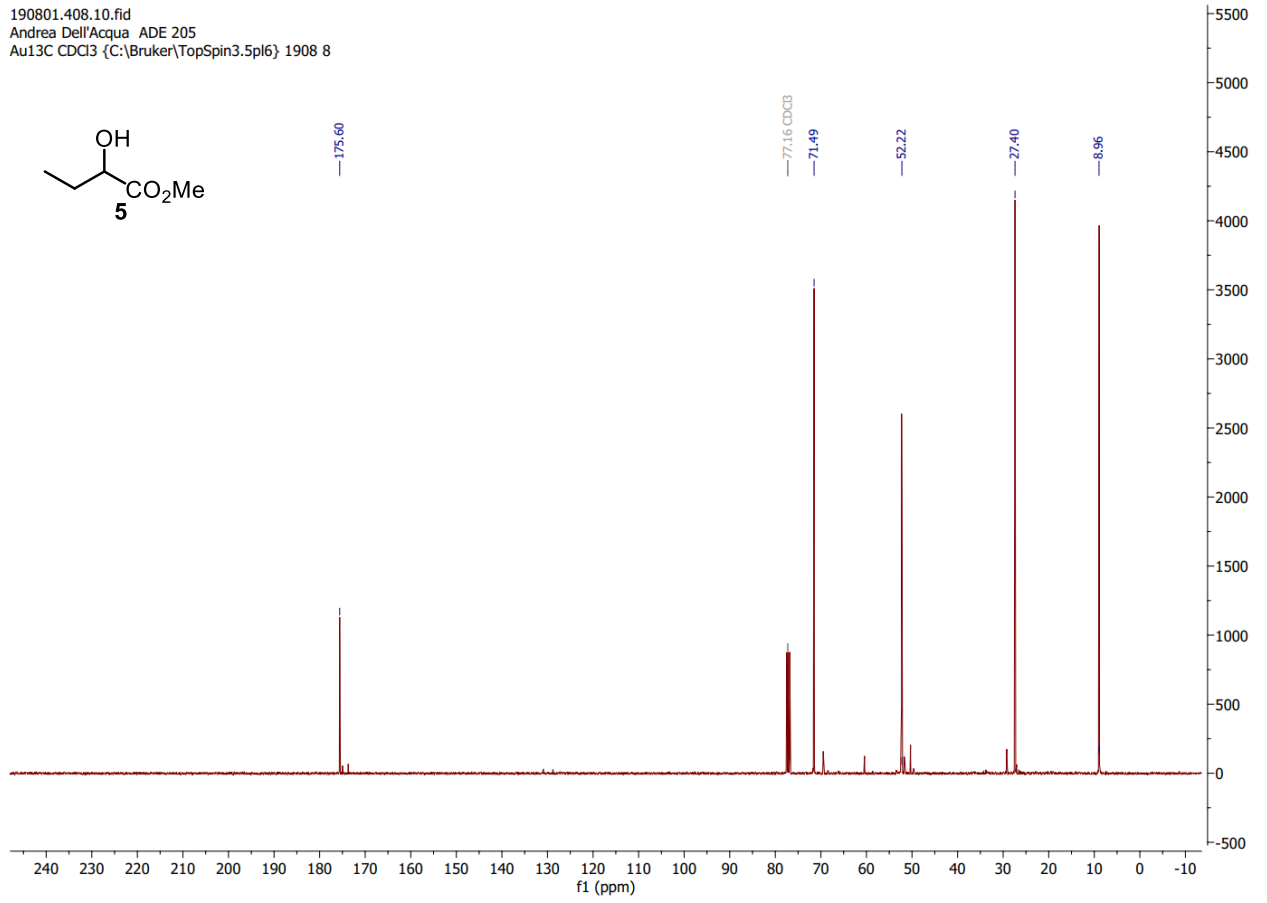
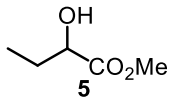


NMR spectra of isolated products:

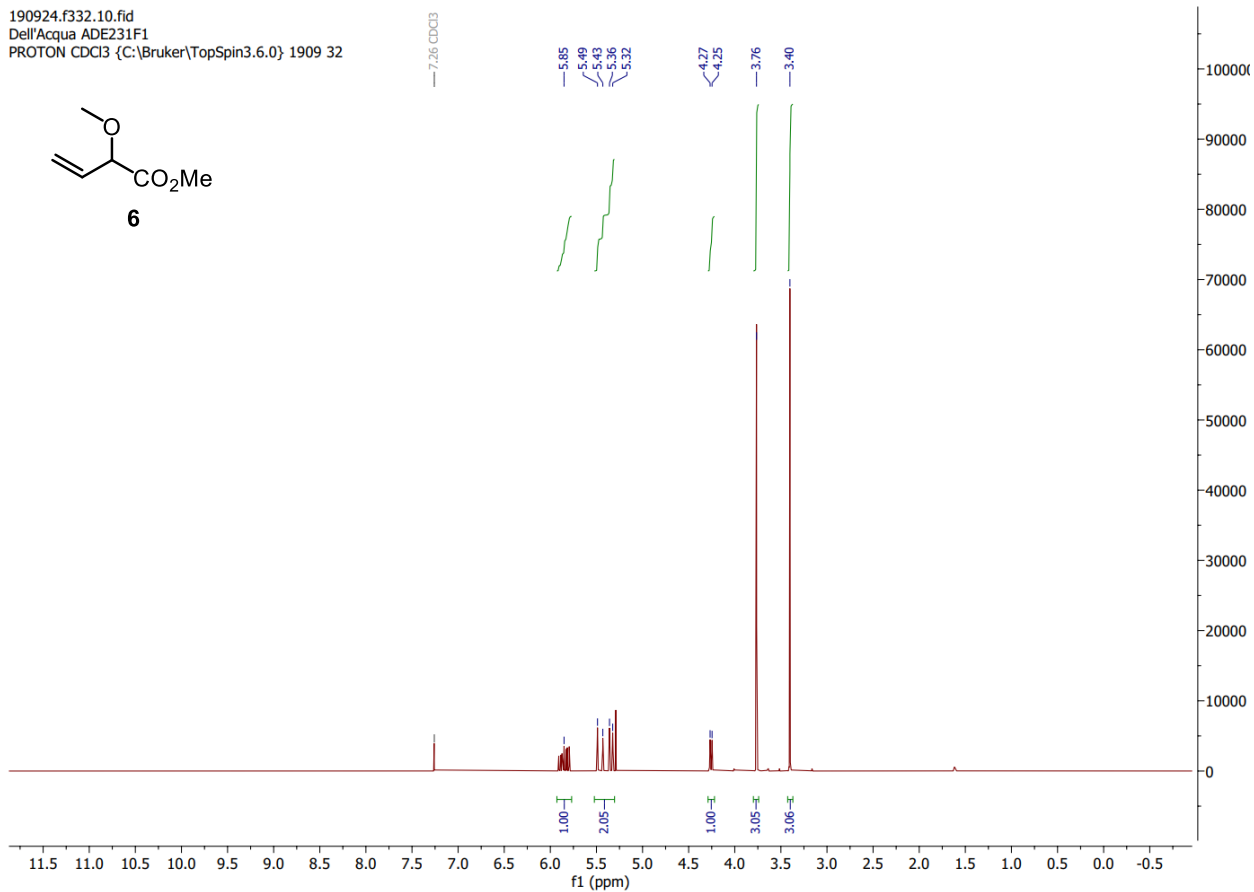
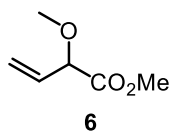
190801.f308.10.fid
Andrea Dell'Acqua ADE 205
PROTON CDCl3 {C:\Bruker\TopSpin3.6.0} 1908 8



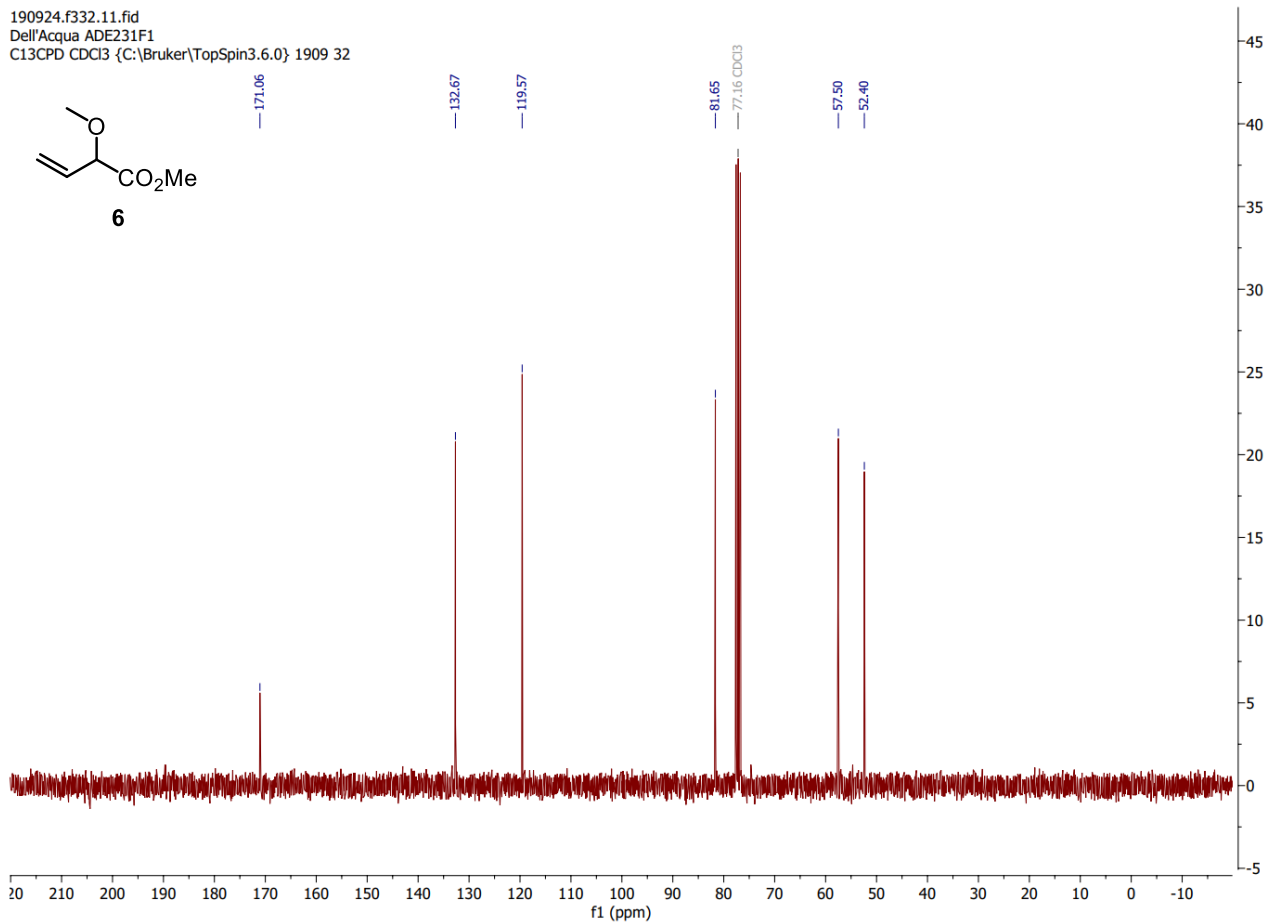
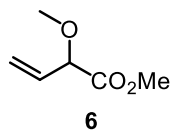
190801.408.10.fid
Andrea Dell'Acqua ADE 205
Au13C CDCl3 {C:\Bruker\TopSpin3.5pl6} 1908 8



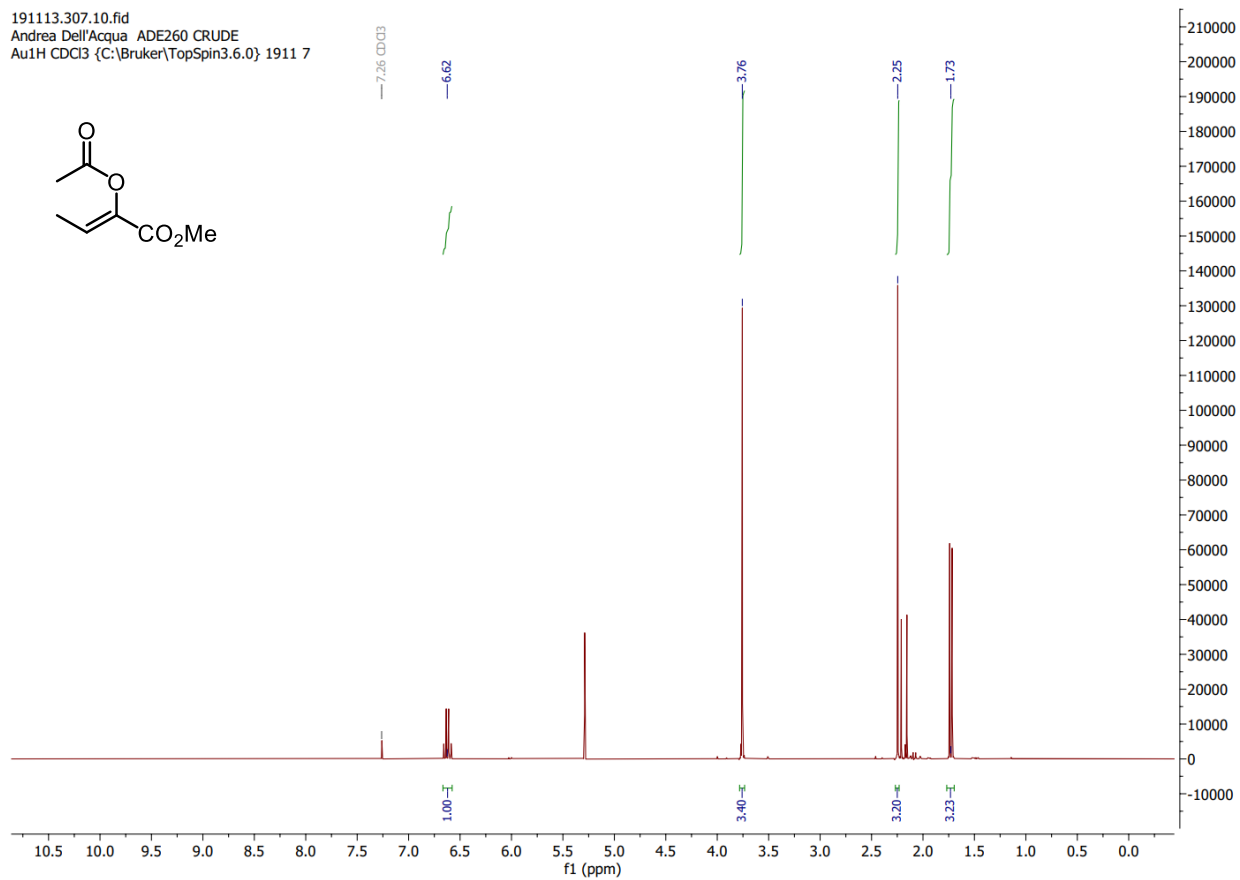
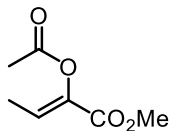
190924.f332.10.fid
Dell'Acqua ADE231F1
PROTON CDCl3 {C:\Bruker\TopSpin3.6.0} 1909 32



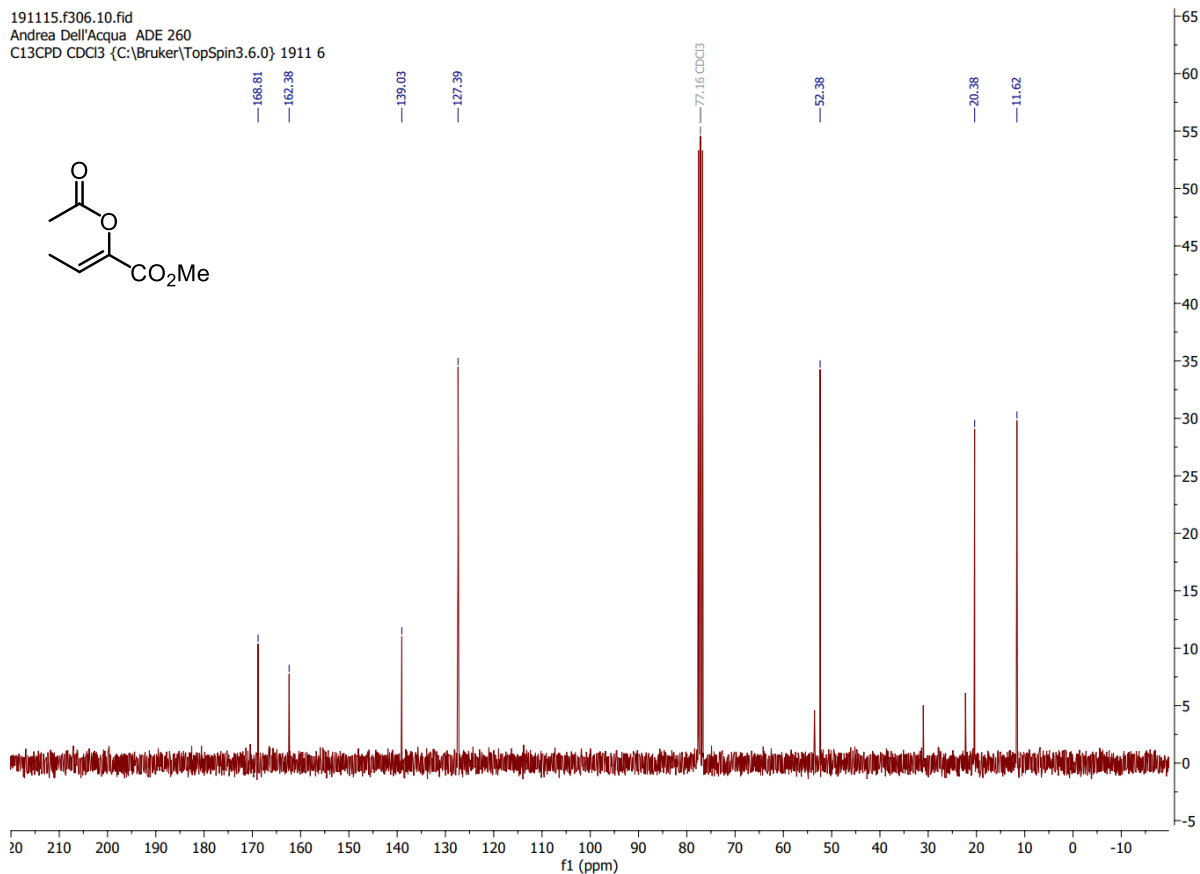
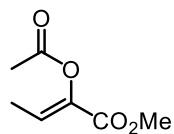
190924.f332.11.fid
Dell'Acqua ADE231F1
C13CPD CDCl3 {C:\Bruker\TopSpin3.6.0} 1909 32



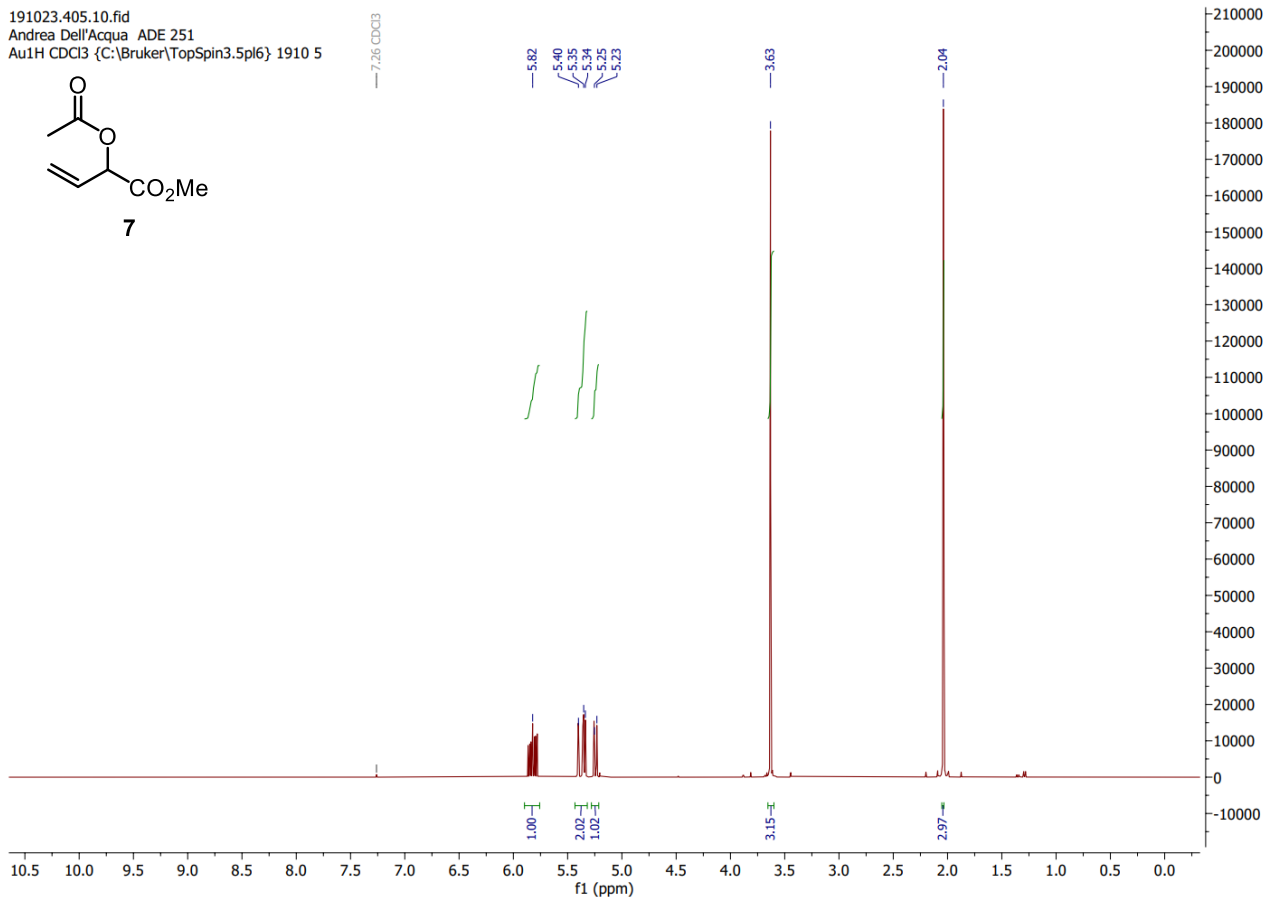
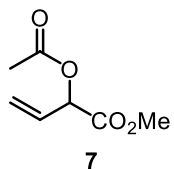
191113.307.10.fid
Andrea Dell'Acqua ADE260 CRUDE
Au1H CDCl3 {C:\Bruker\TopSpin3.6.0} 1911 7



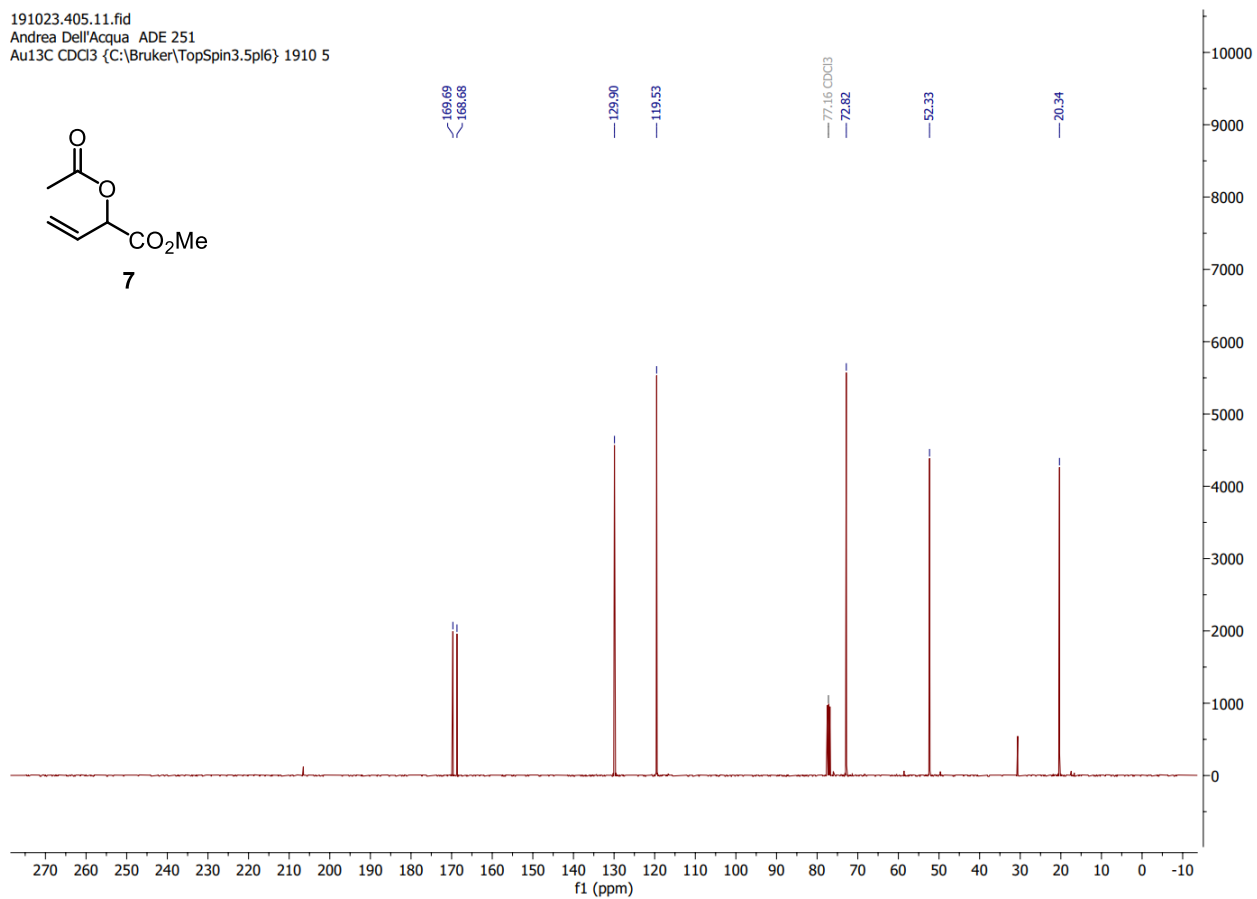
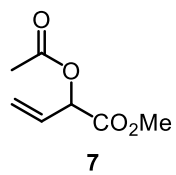
191115.f306.10.fid
 Andrea Dell'Acqua ADE 260
 C13CPD CDCl3 {C:\Bruker\TopSpin3.6.0} 1911 6



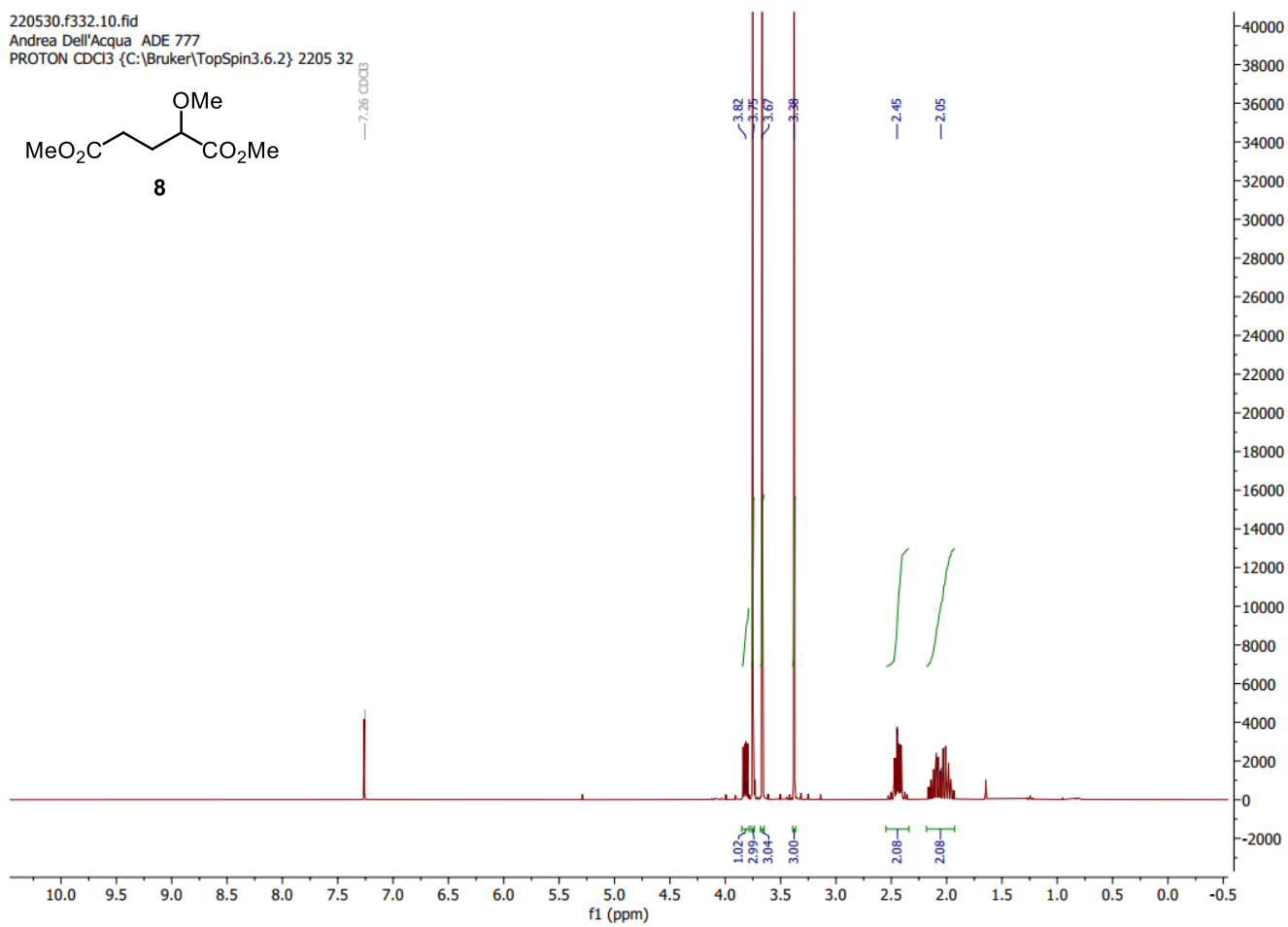
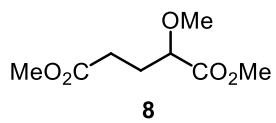
191023.405.10.fid
 Andrea Dell'Acqua ADE 251
 Au1H CDCl3 {C:\Bruker\TopSpin3.5pl6} 1910 5



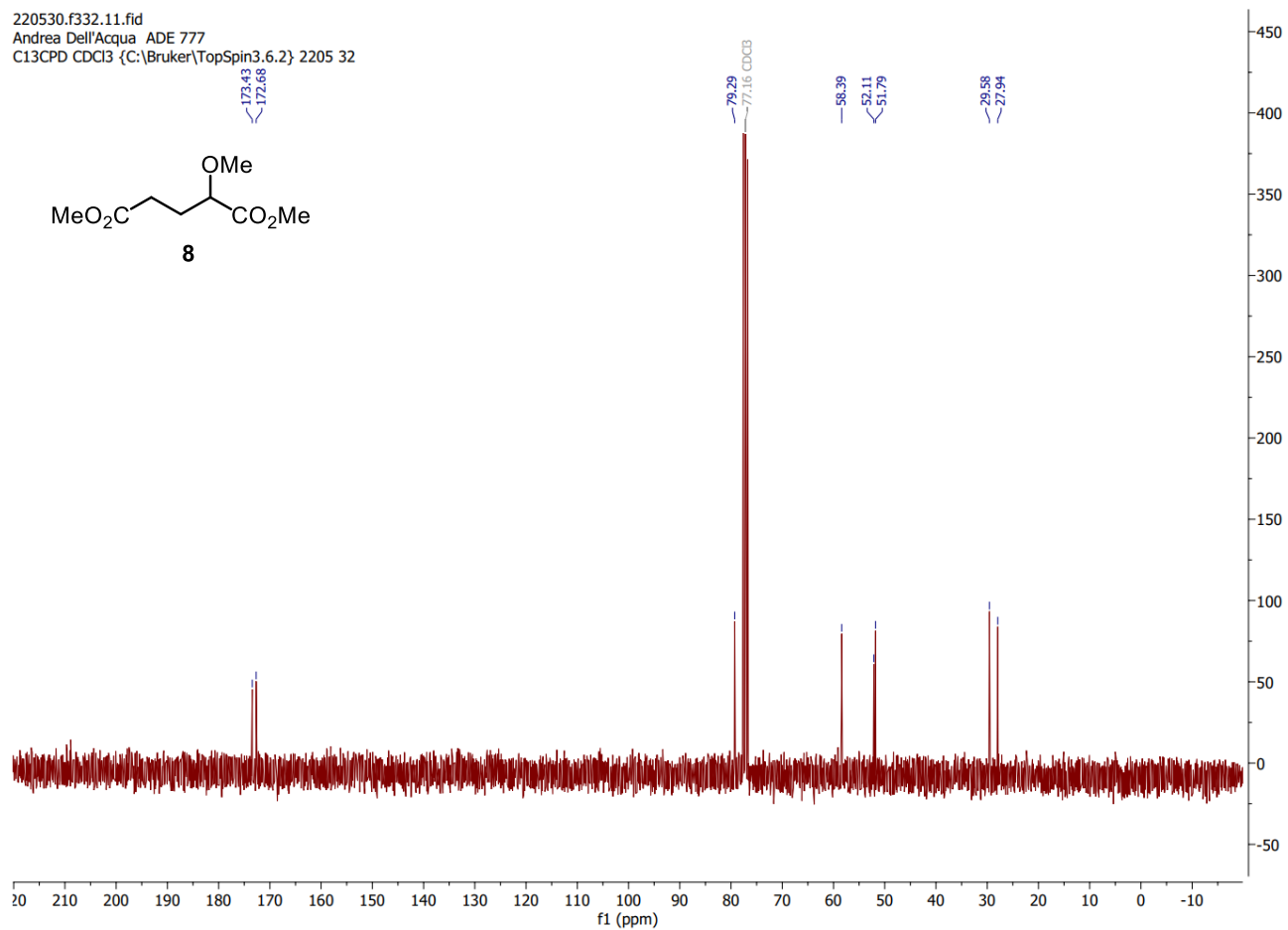
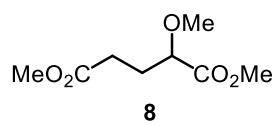
191023.405.11.fid
Andrea Dell'Acqua ADE 251
Au13C CDCl3 {C:\Bruker\TopSpin3.5pl6} 1910 5



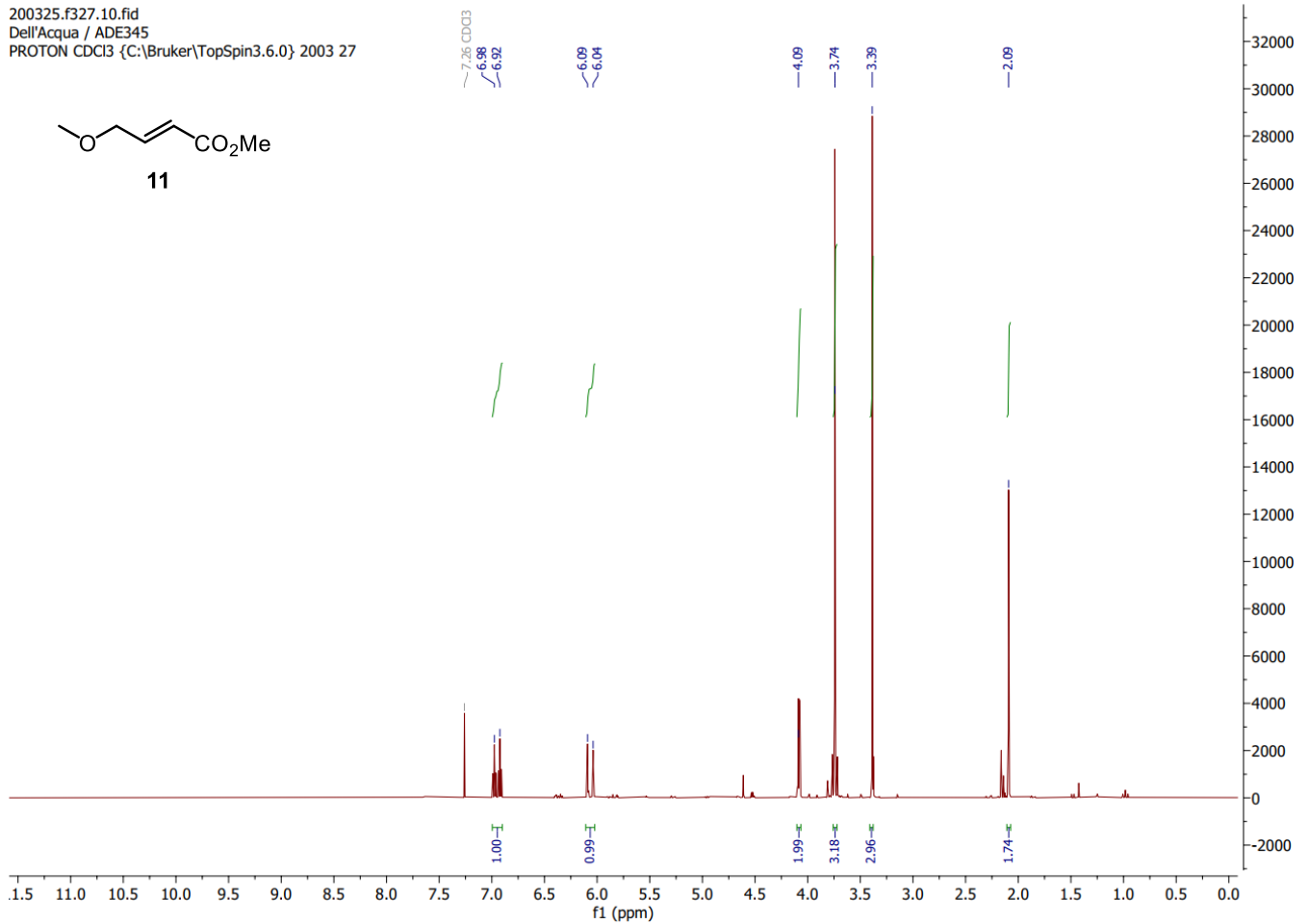
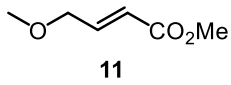
220530.f332.10.fid
Andrea Dell'Acqua ADE 777
PROTON CDCl3 {C:\Bruker\TopSpin3.6.2} 2205 32



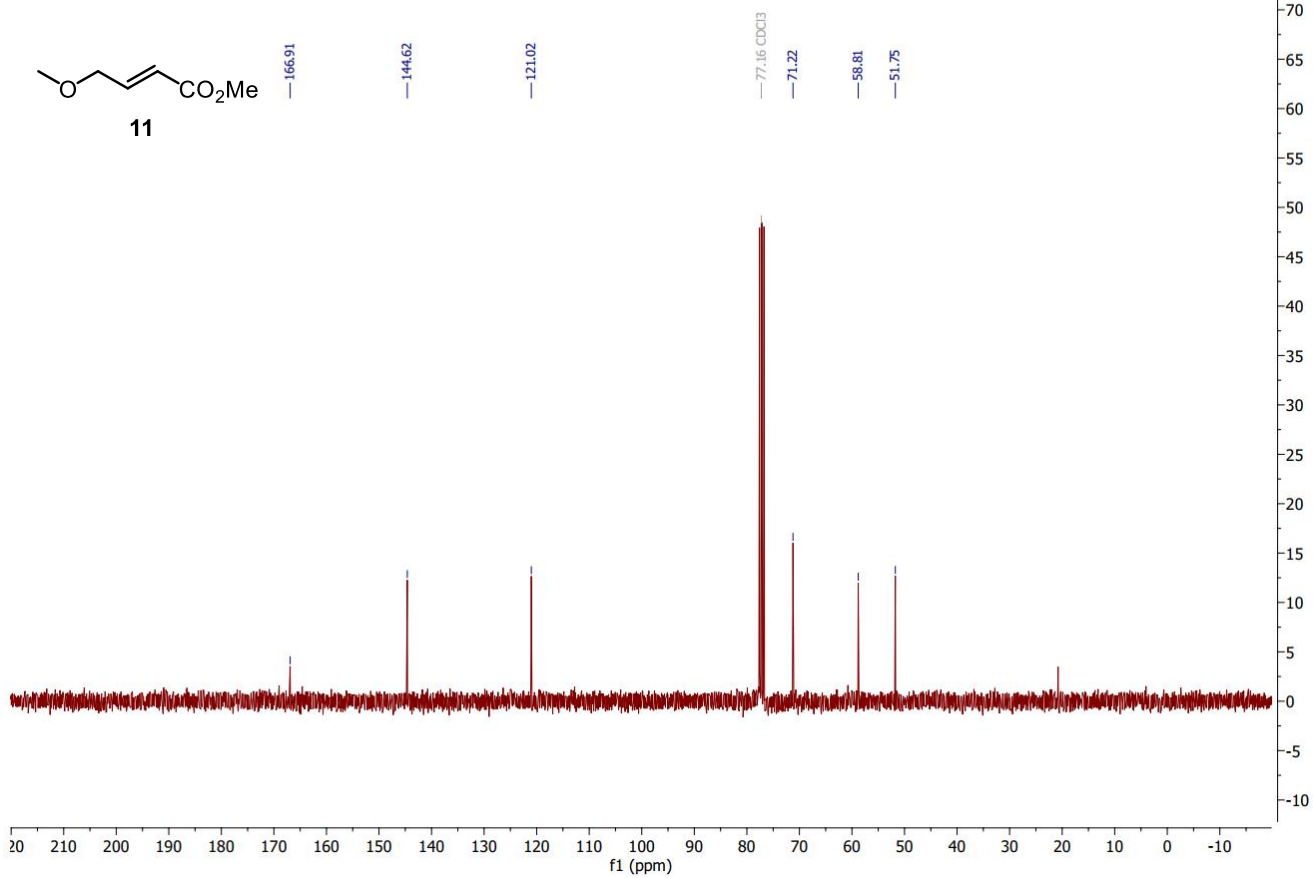
220530.f332.11.fid
Andrea Dell'Acqua ADE 777
C13CPD CDCl3 {C:\Bruker\TopSpin3.6.2} 2205 32



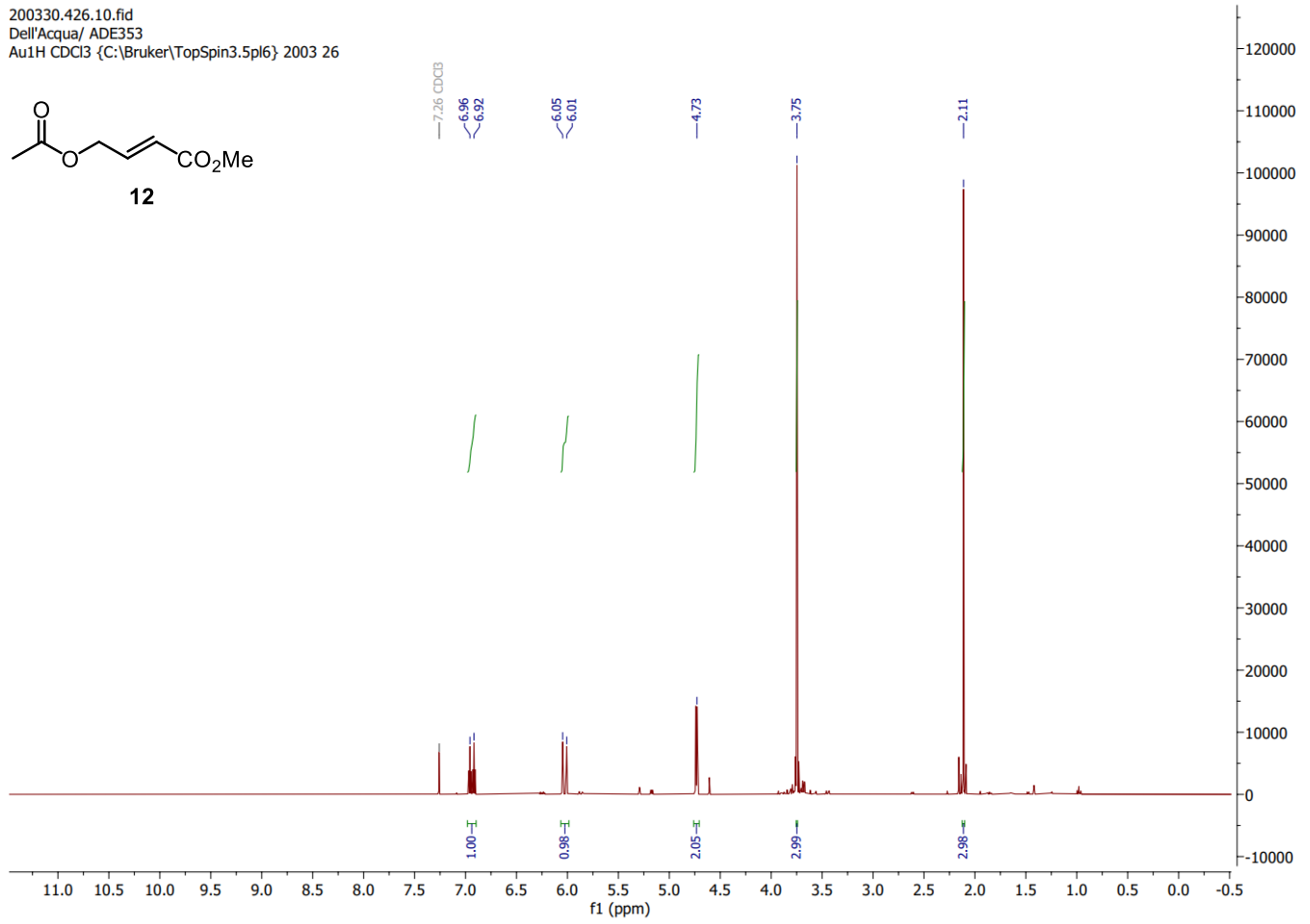
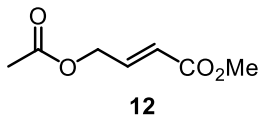
200325.f327.10.fid
Dell'Acqua / ADE345
PROTON CDCl3 {C:\Bruker\TopSpin3.6.0} 2003 27



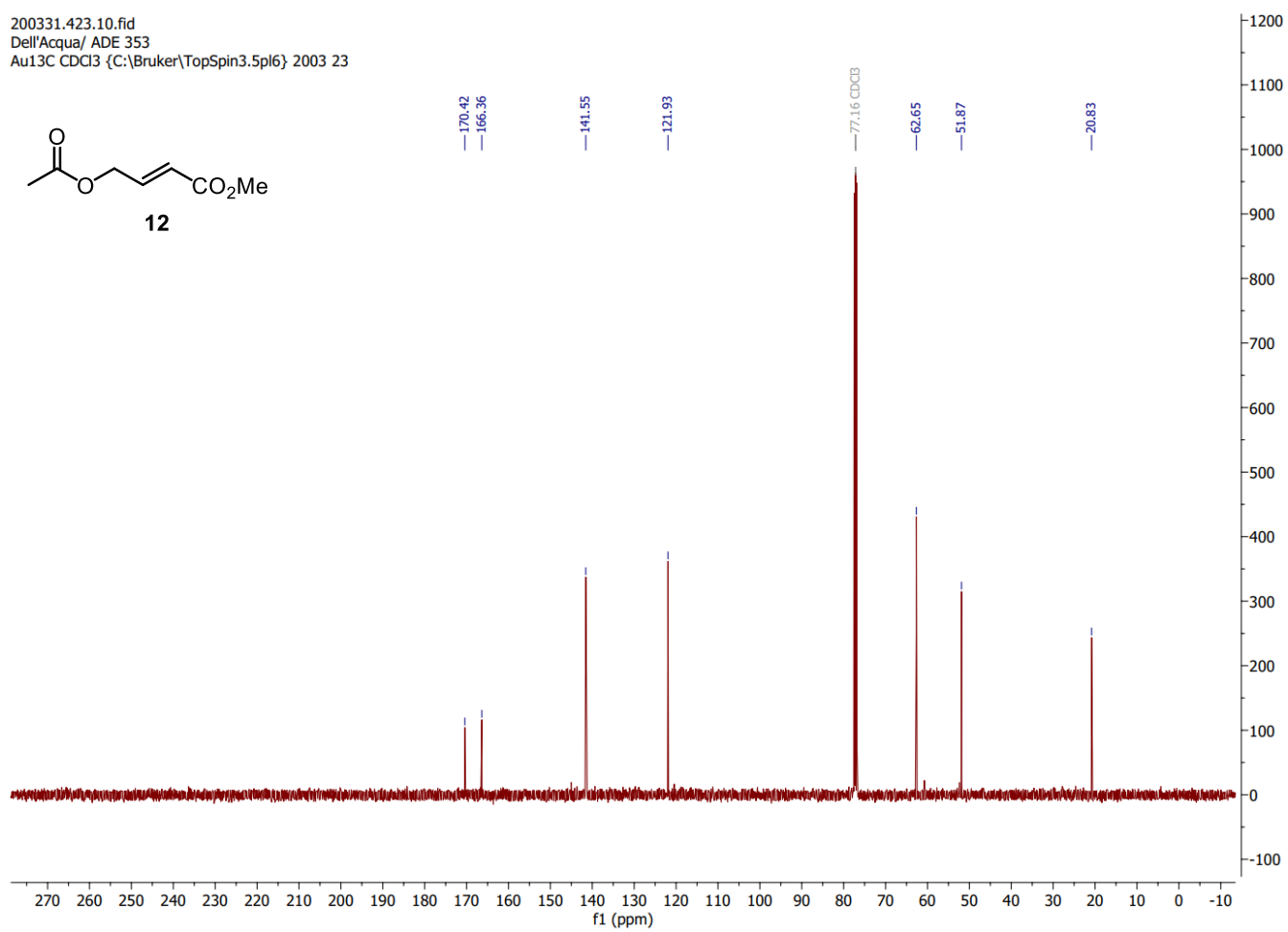
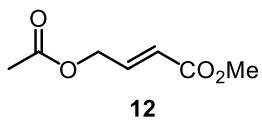
200325.f351.10.fid
Dell'Acqua / ADE345
C13CPD CDCl3 {C:\Bruker\TopSpin3.6.0} 2003 51



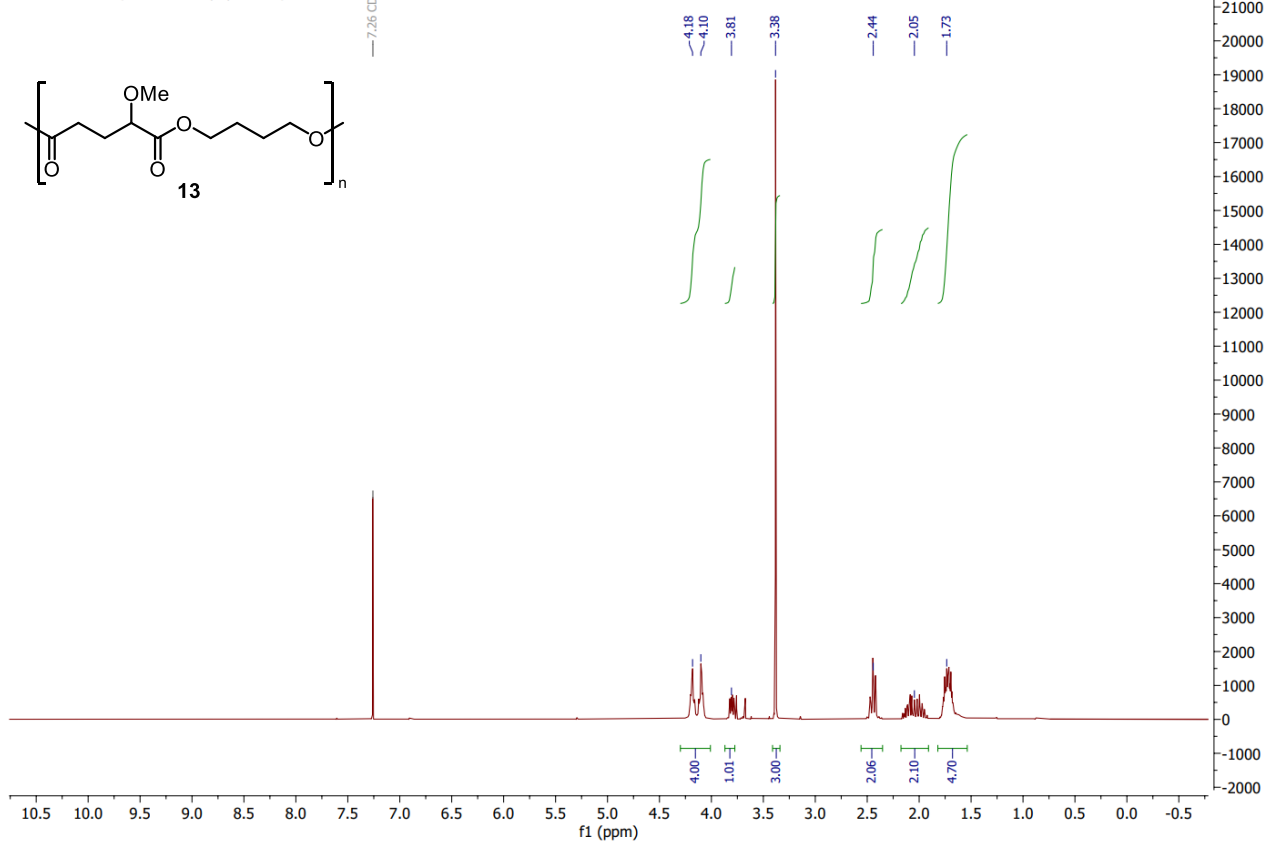
200330.426.10.fid
Dell'Acqua/ ADE353
Au1H CDCl3 {C:\Bruker\TopSpin3.5pl6} 2003 26



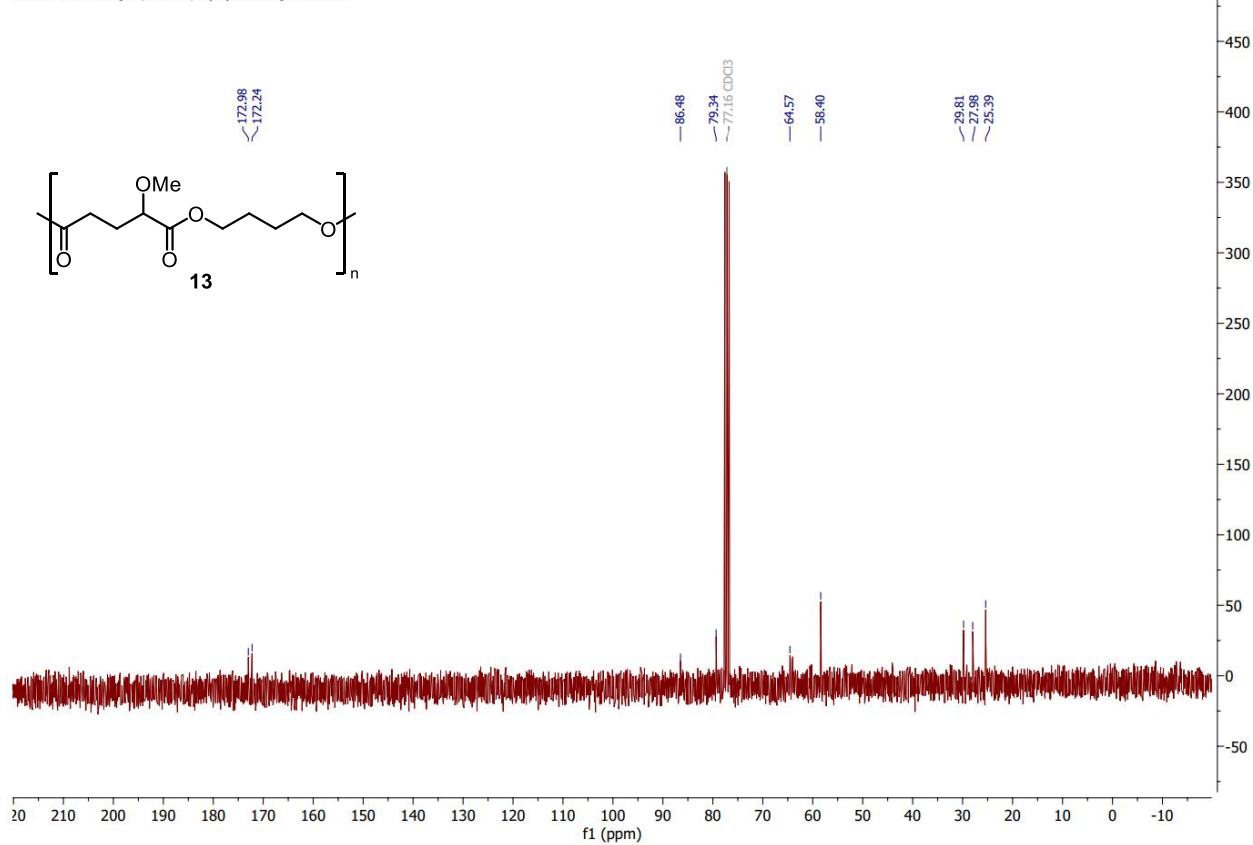
200331.423.10.fid
Dell'Acqua/ ADE 353
Au13C CDCl3 {C:\Bruker\TopSpin3.5pl6} 2003 23



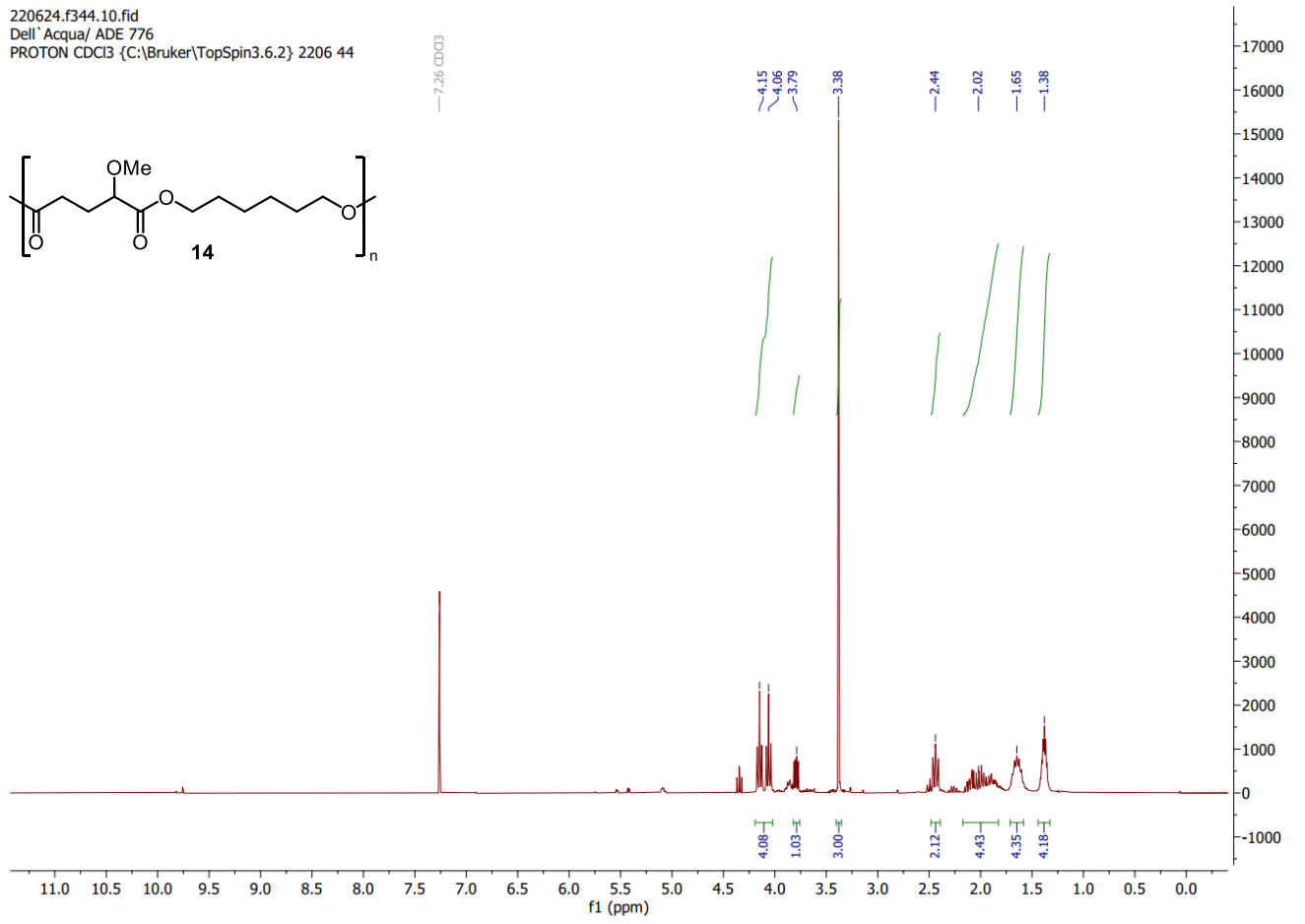
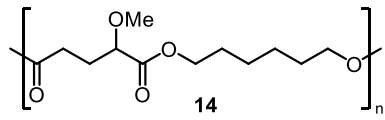
220617.f351.11.fid
Dell'Acqua/ADE 782
PROTON CDCl3 {C:\Bruker\TopSpin3.6.2} 2206 51



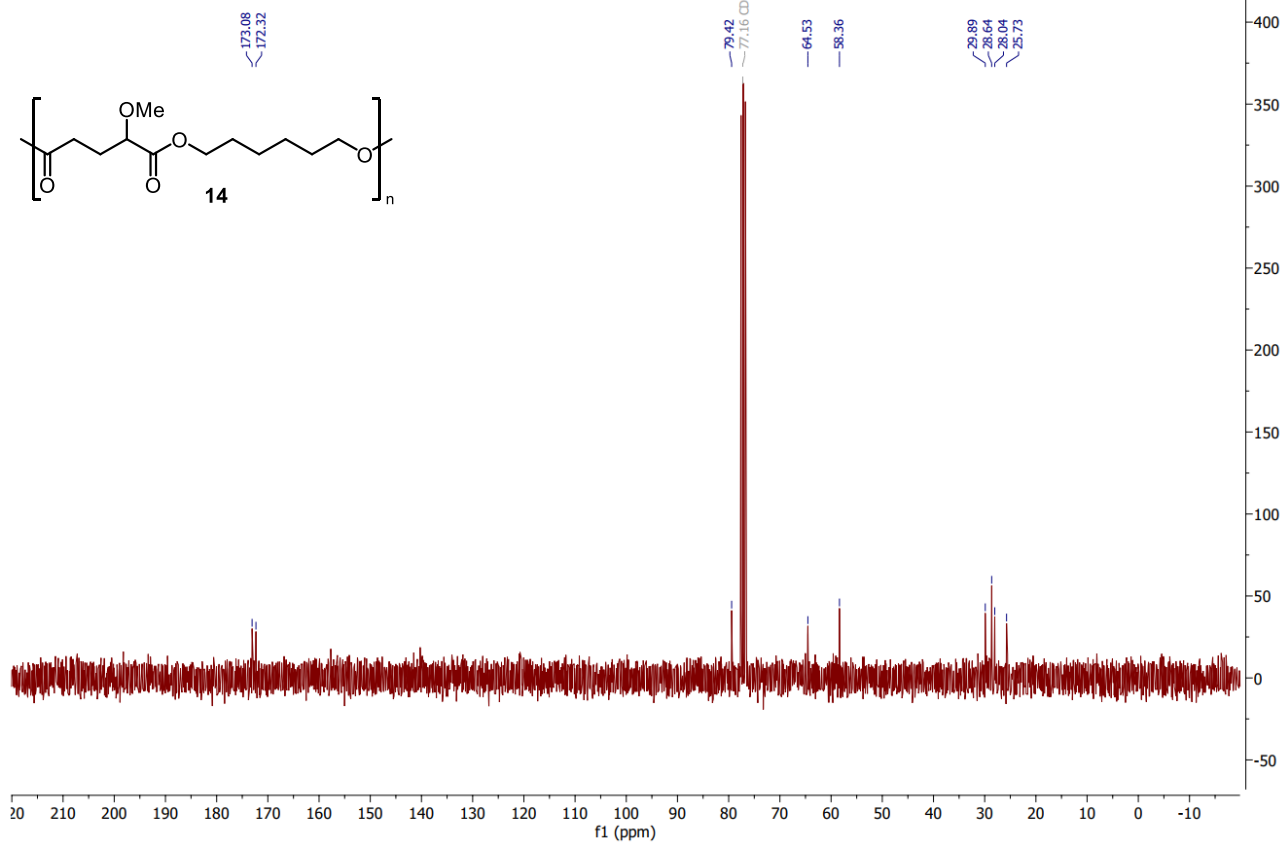
220617.f351.10.fid
Dell'Acqua/ADE 782
C13CPD CDCl3 {C:\Bruker\TopSpin3.6.2} 2206 51



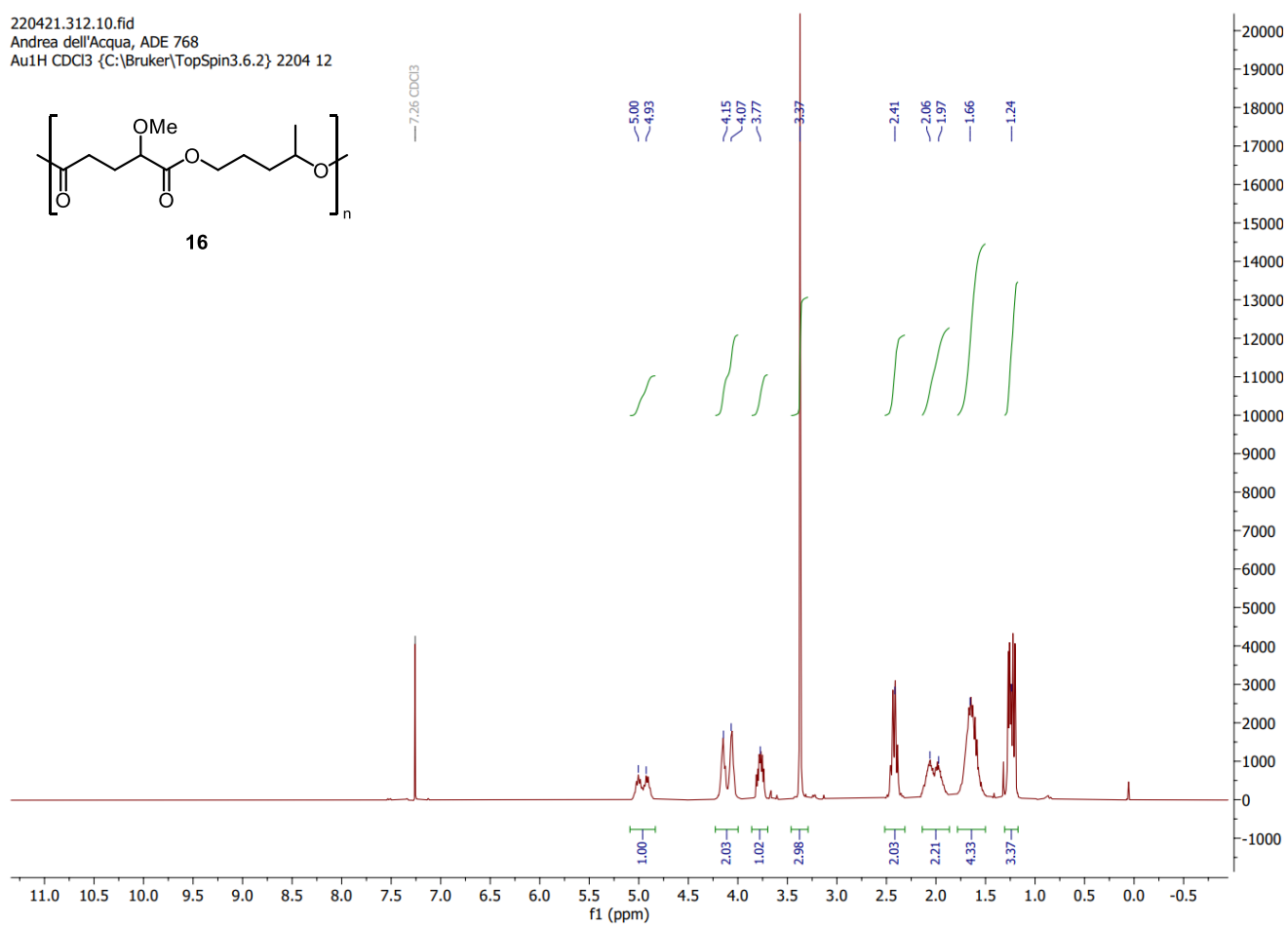
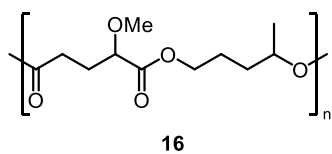
220624.f344.10.fid
Dell'Acqua/ ADE 776
PROTON CDCl3 {C:\Bruker\TopSpin3.6.2} 2206 44



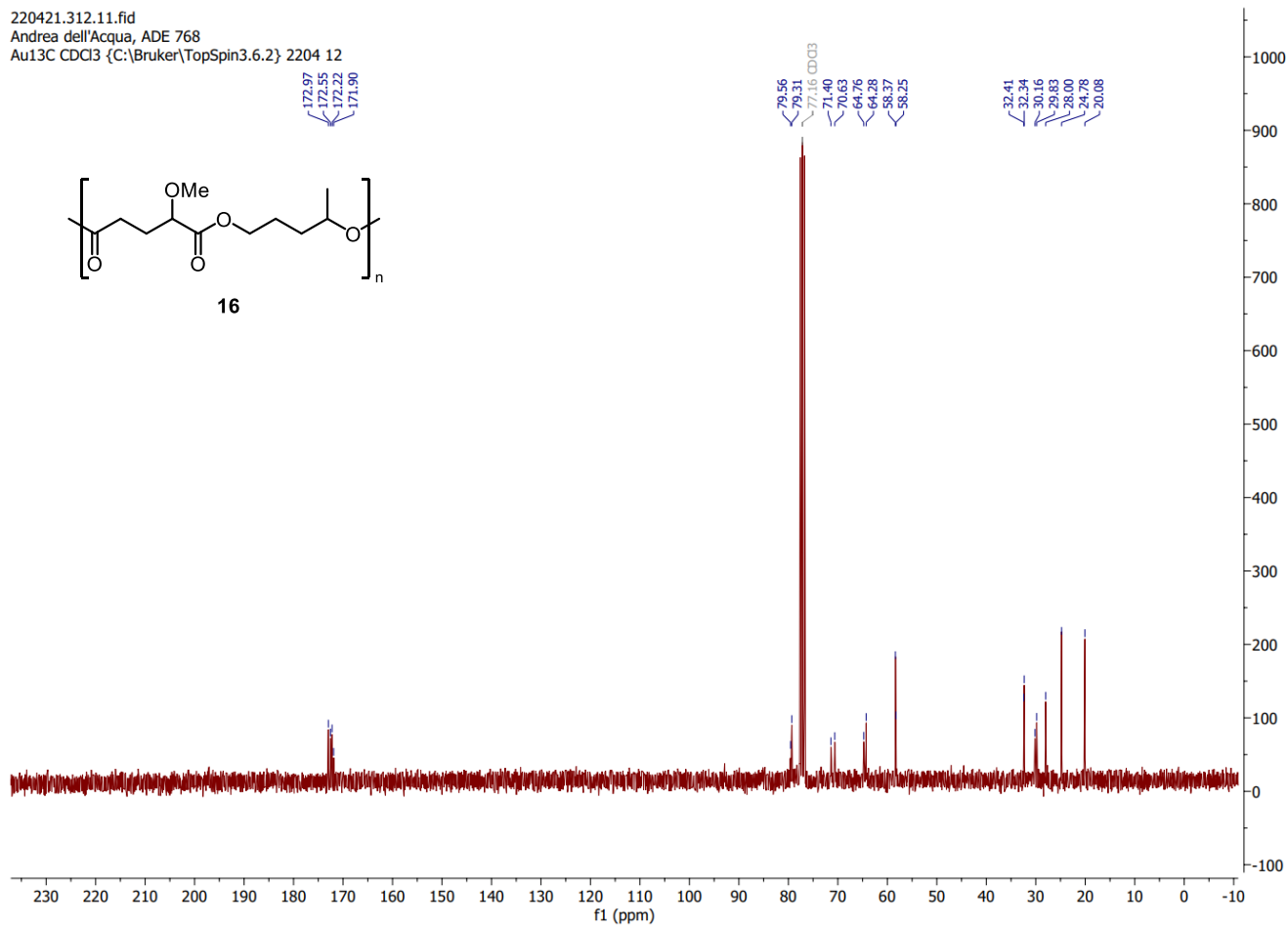
220624.f344.11.fid
Dell' Acqua/ ADE 776
C13CPD CDCl3 {C:\Bruker\TopSpin3.6.2} 2206 44



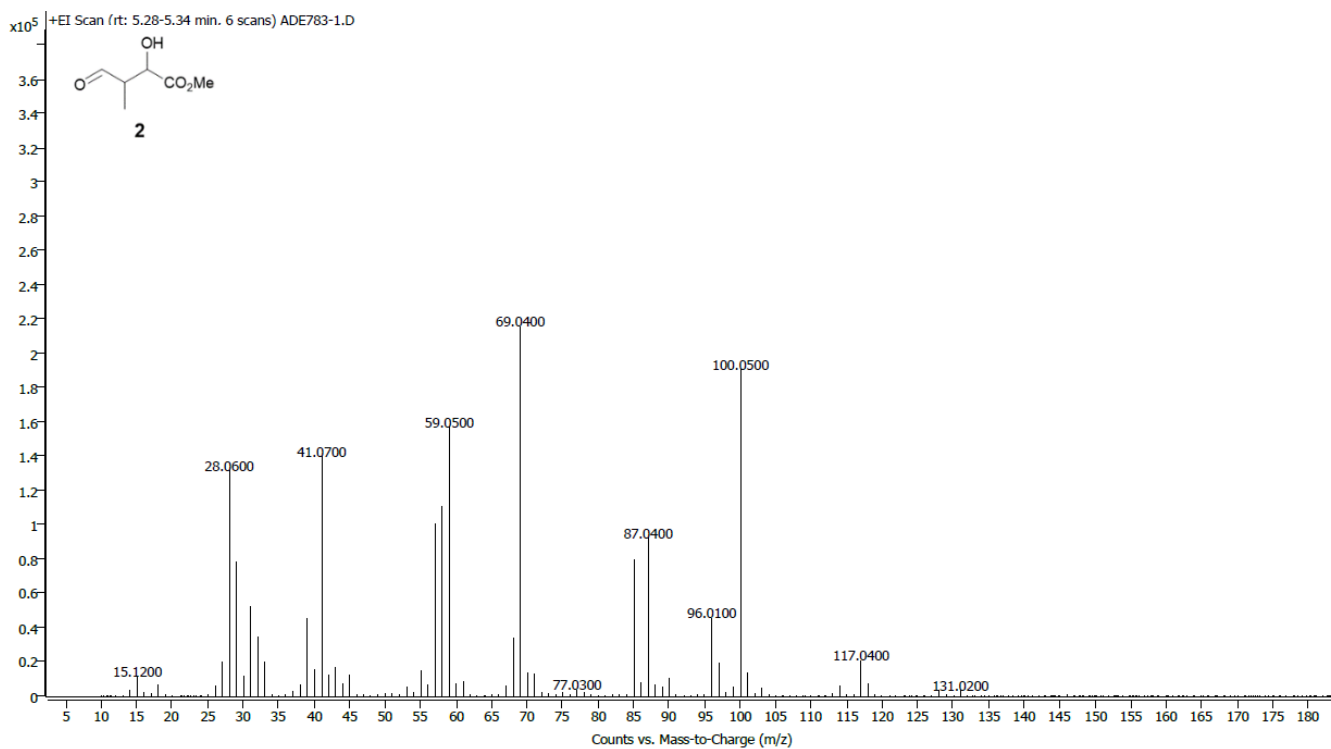
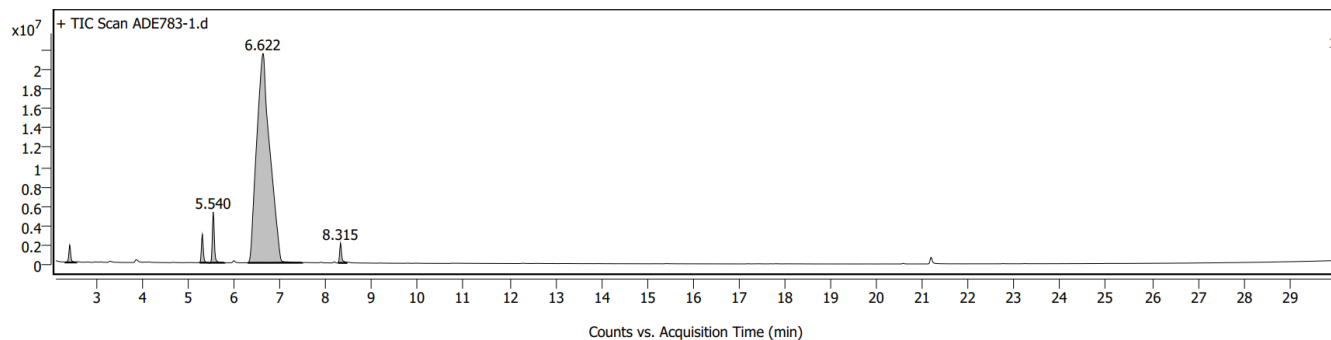
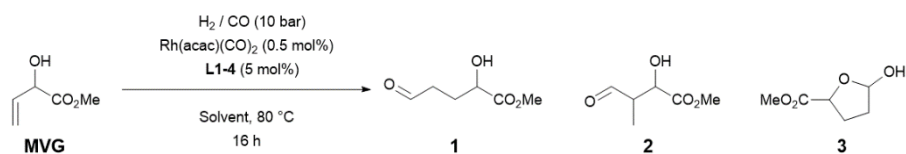
220421.312.10.fid
Andrea dell'Acqua, ADE 768
Au1H CDCl3 {C:\Bruker\TopSpin3.6.2} 2204 12

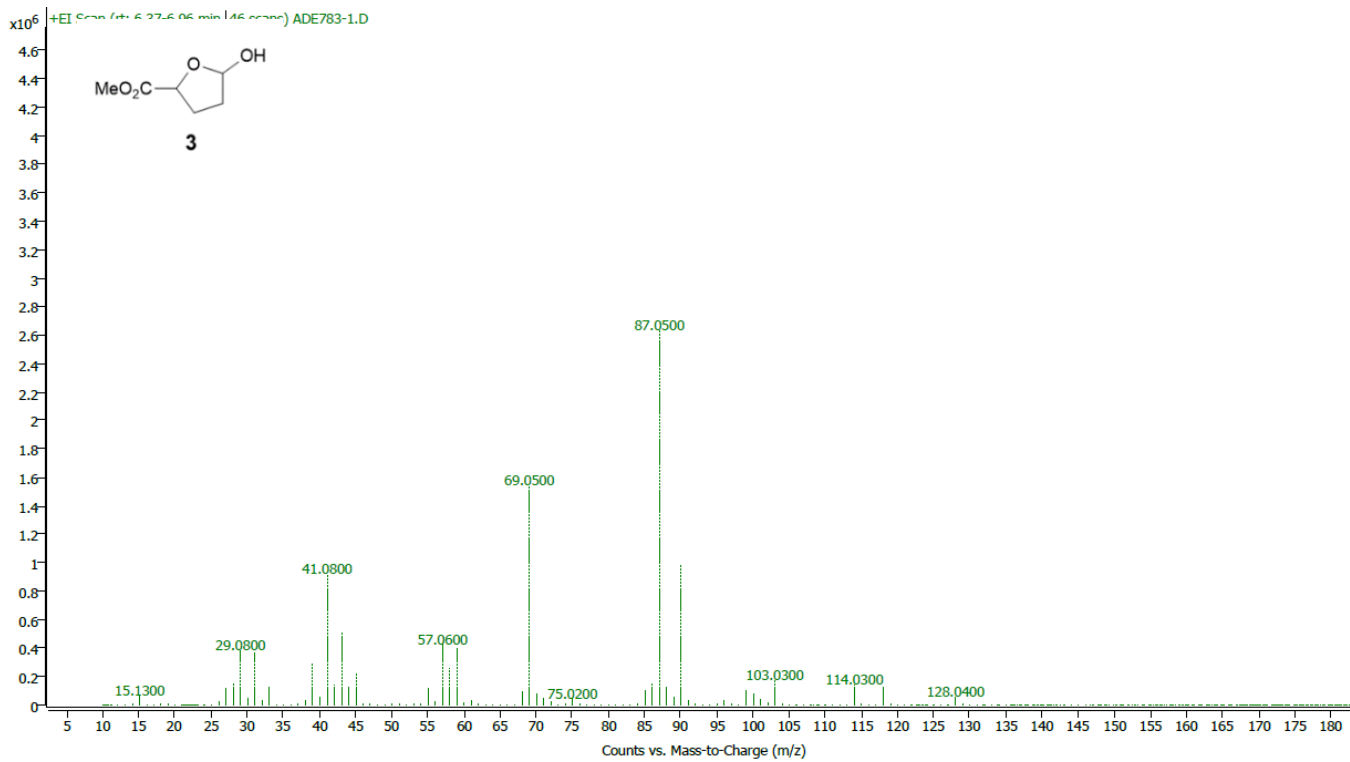
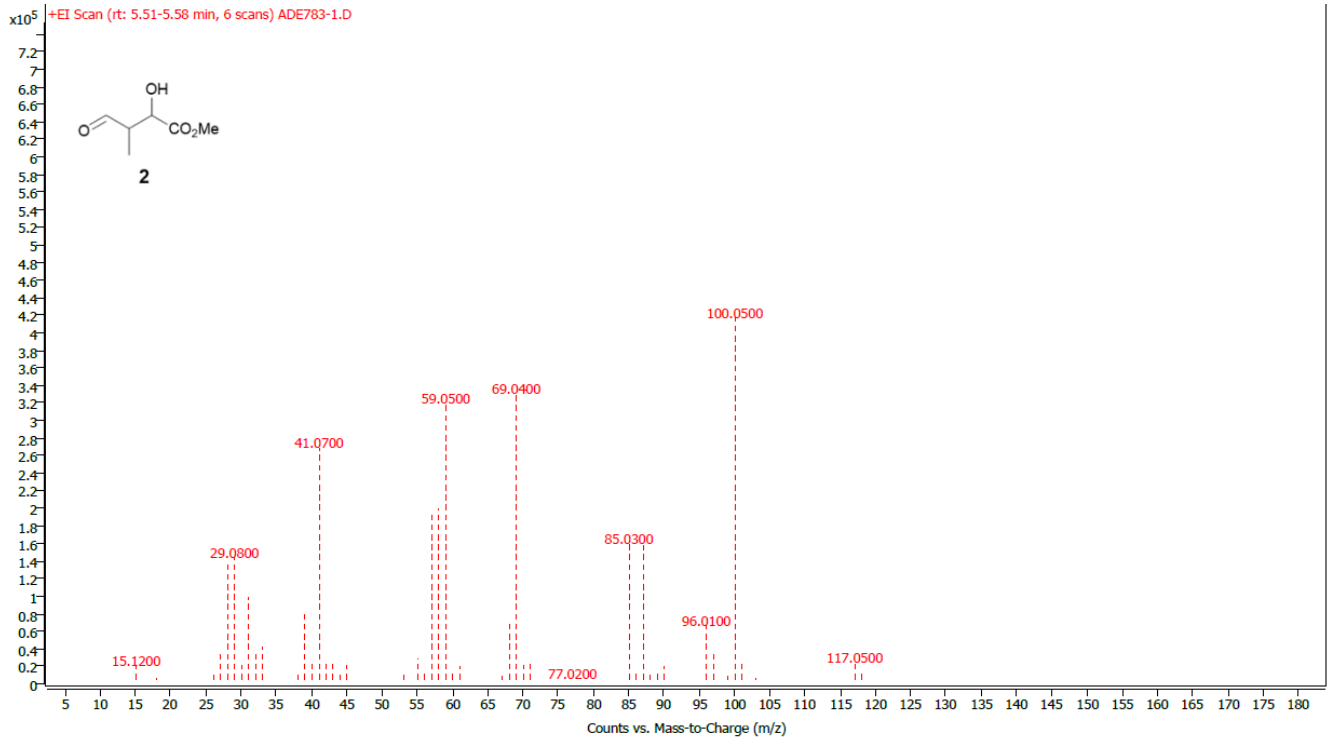


220421.312.11.fid
Andrea dell'Acqua, ADE 768
Au13C CDCl3 {C:\Bruker\TopSpin3.6.2} 2204 12



GC-MS





ESI-MS Chromatograms

ESI-TOF Accurate Mass Report

File:22062015
Vial:1:F,4
Description:MeOH/0,1%HCOOH in H2O 90:10

Sample Name:ADE777
Date:20-Jun-2022

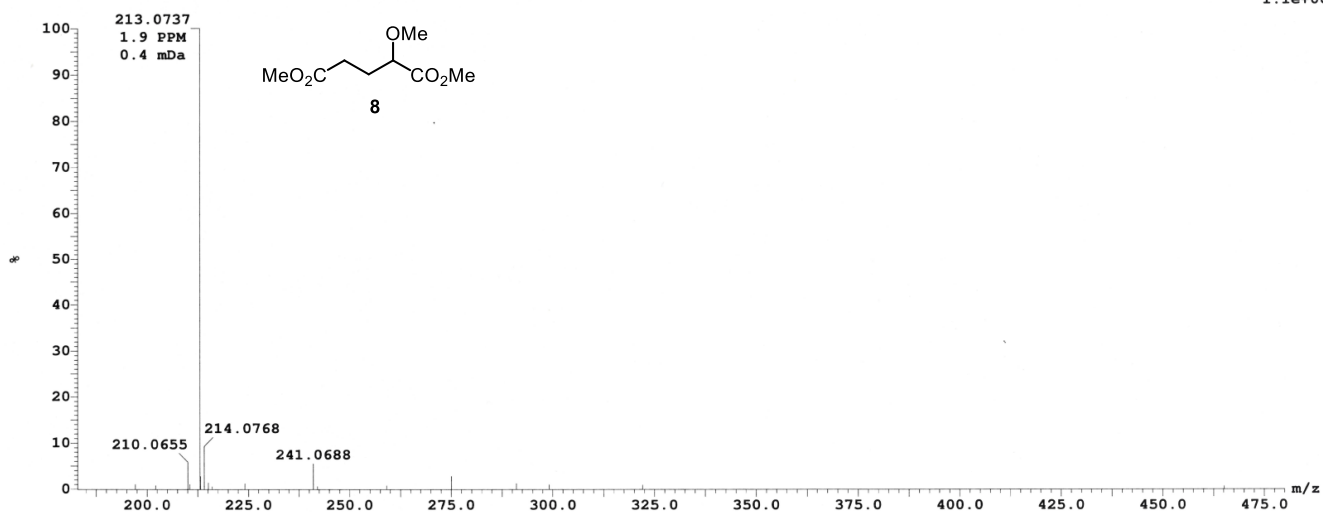
UserName:Dell'Acqua
Time:16:03:20

Page 2

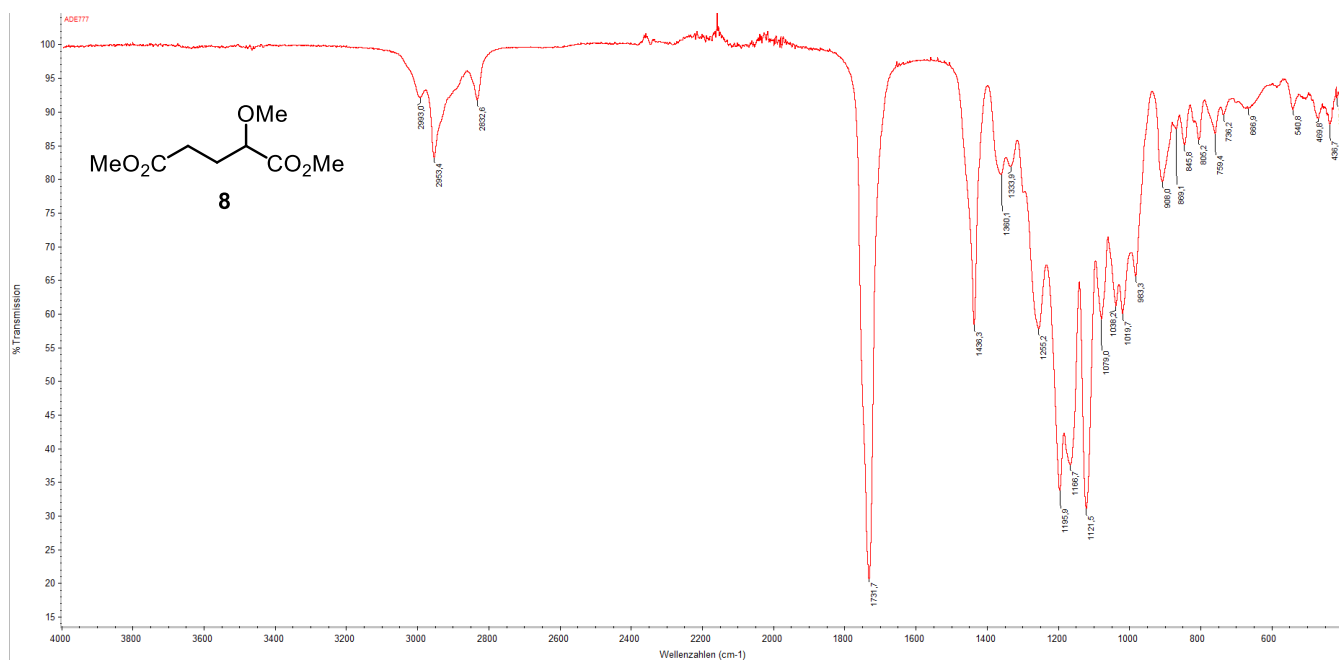
Sample Report:

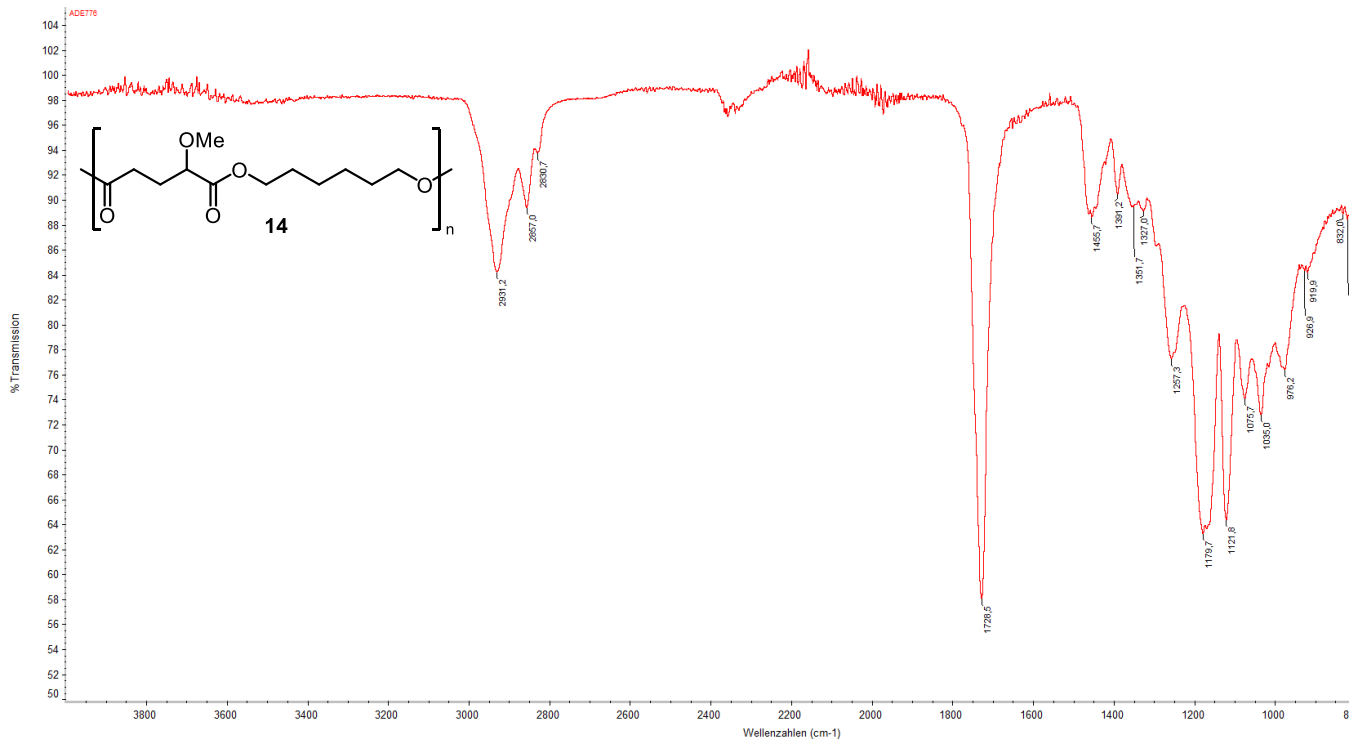
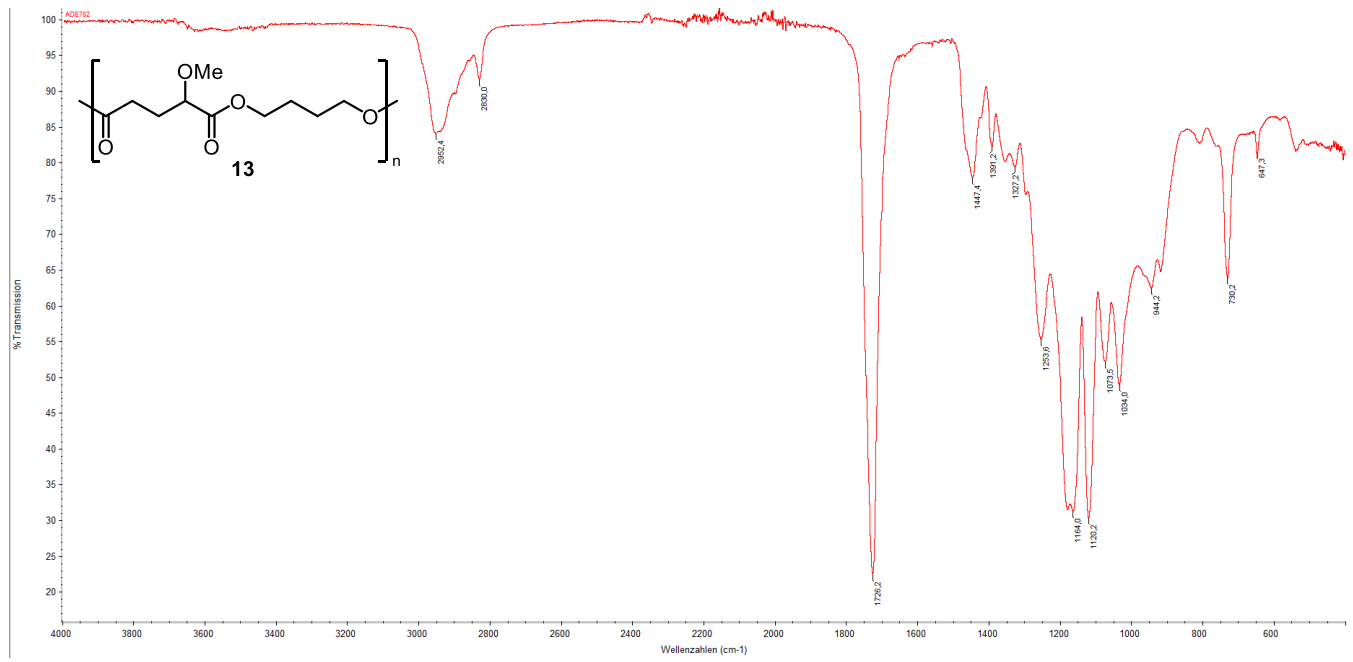
(Time: 0.31) Combine ((23:26+31)-112:117) - Dead time test passed

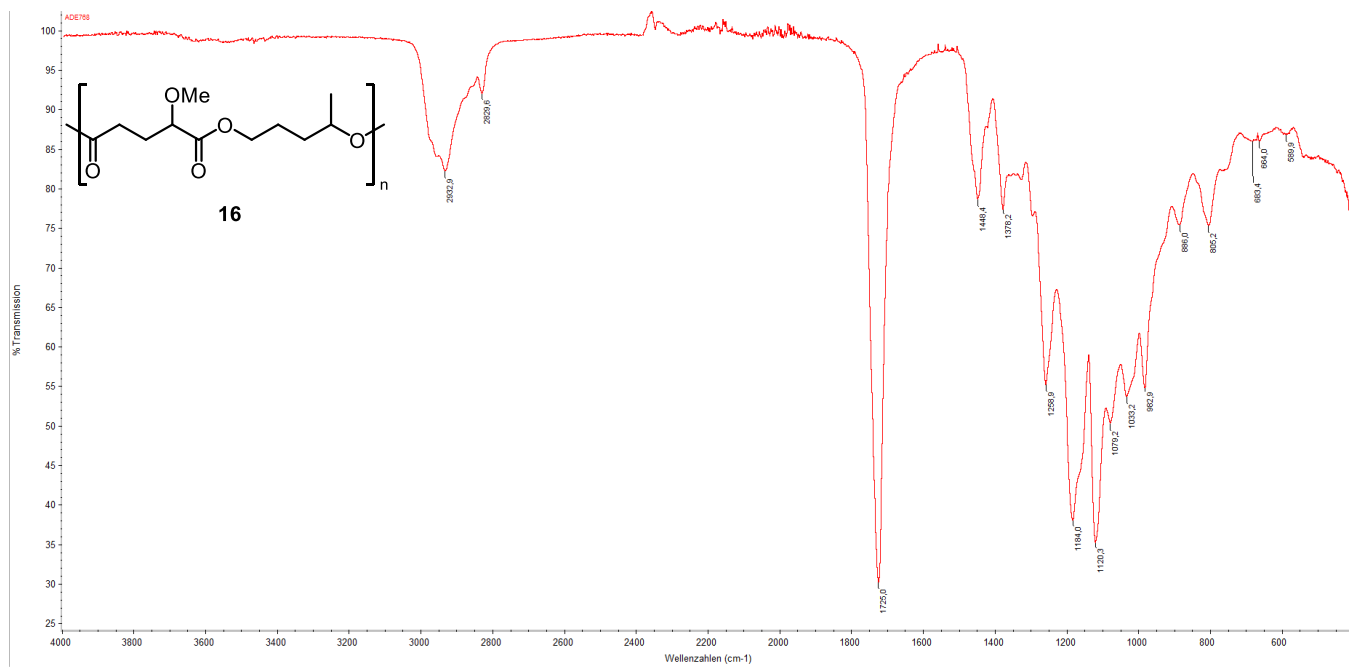
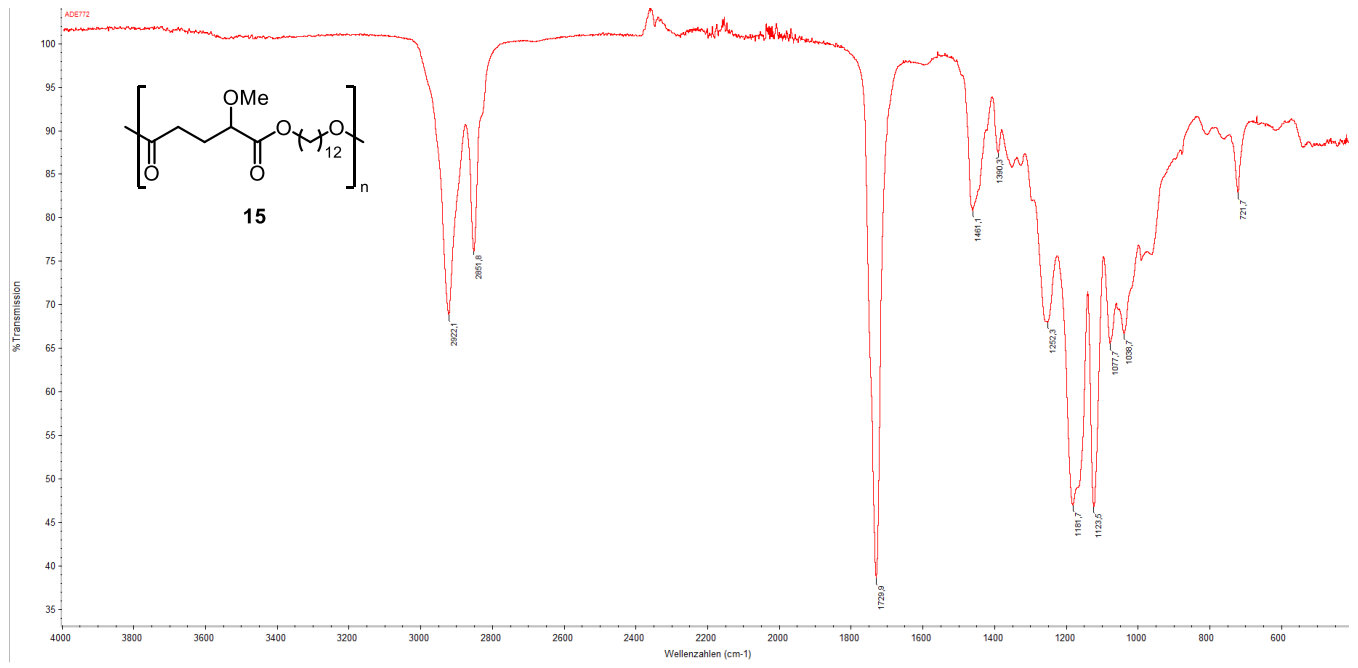
1:TOF MS ES+
1.1e+008



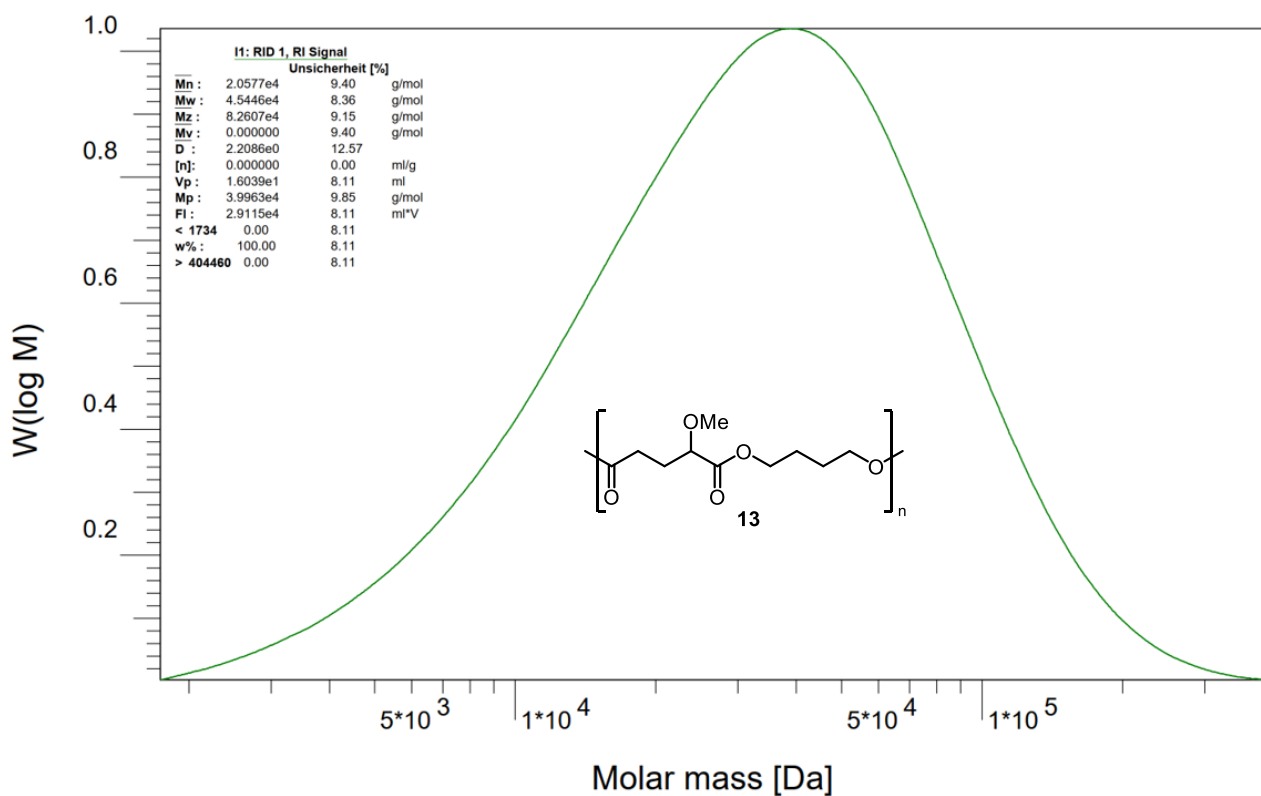
ATR-IR



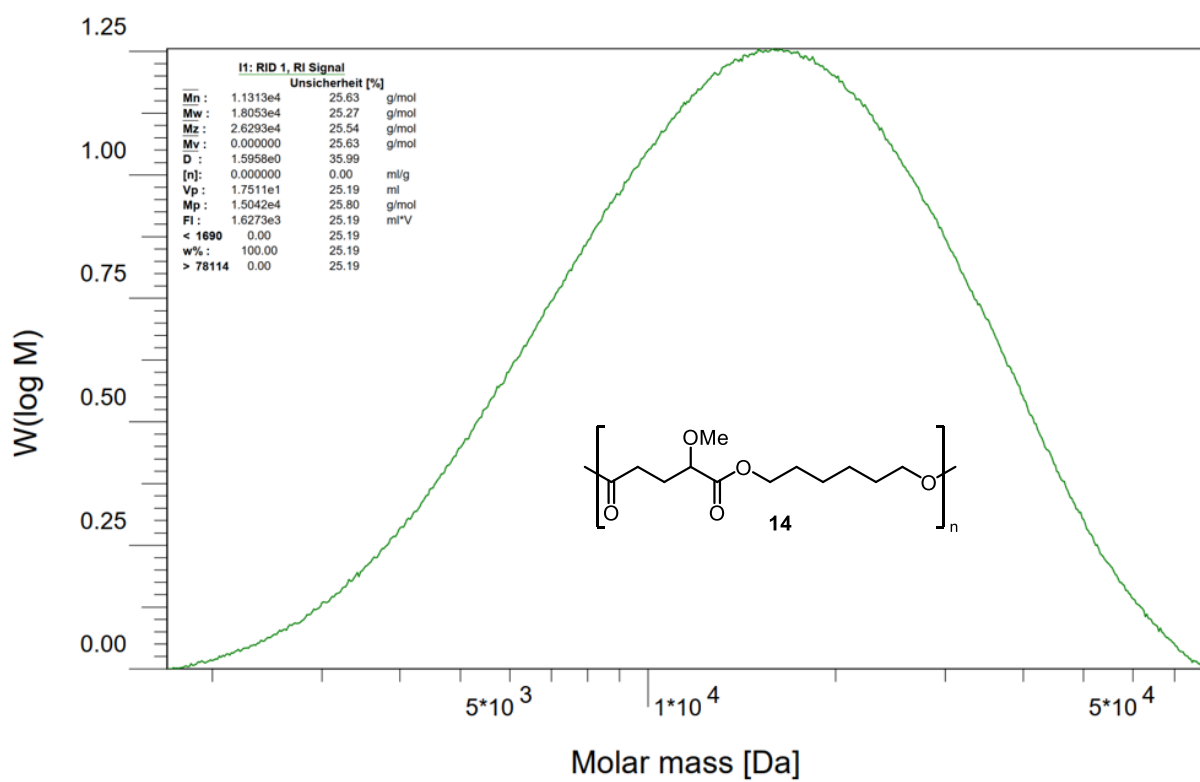




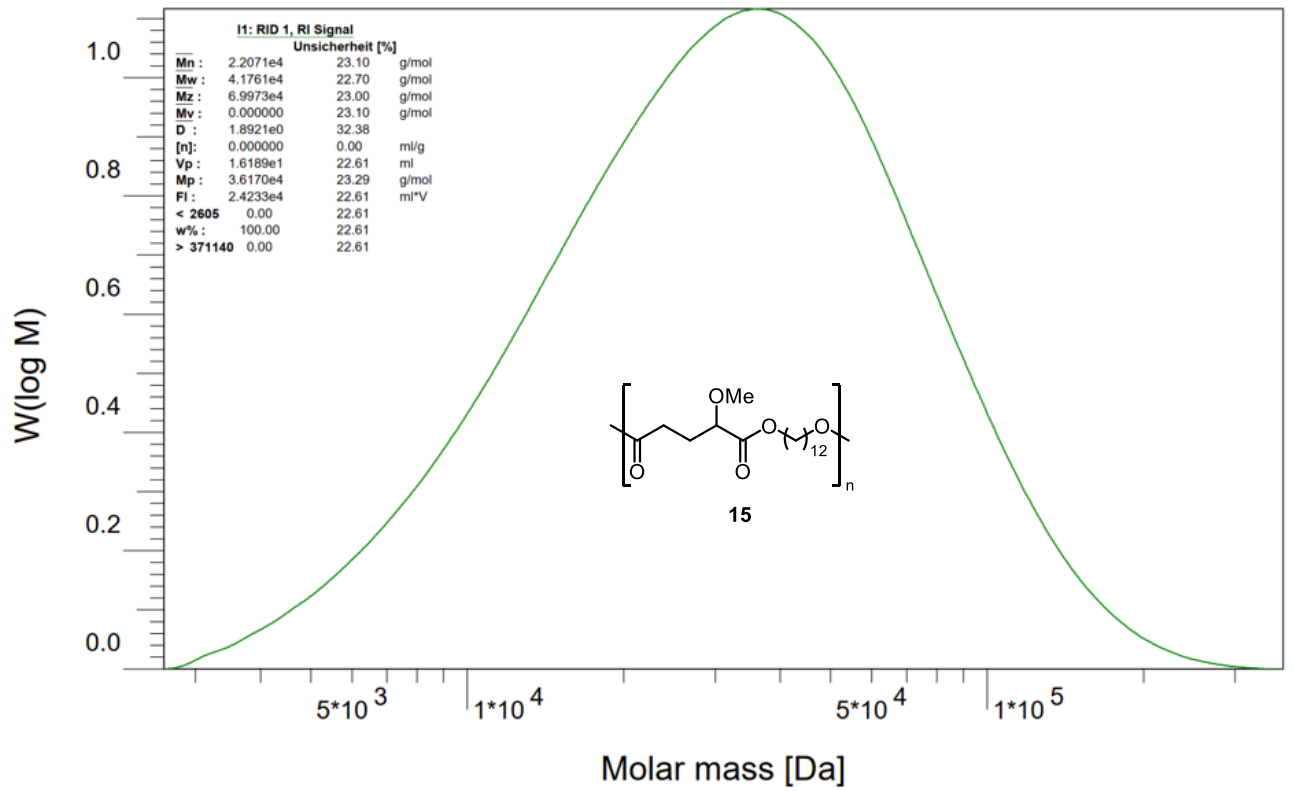
GPC Chromatograms



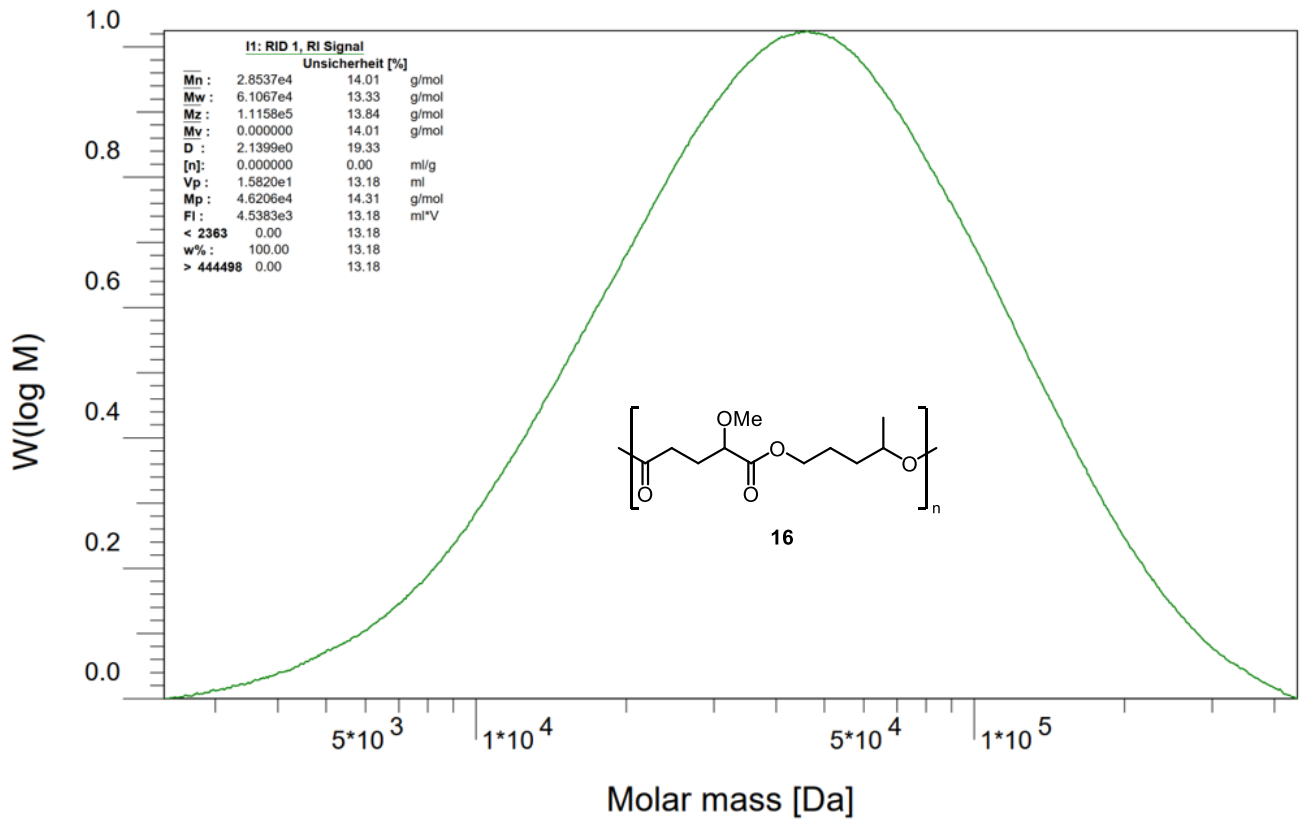
PSS WinGPC UniChrom, Build 5350, AN017, Instanz #1



PSS WinGPC UniChrom, Build 5350, AN017, Instanz #1

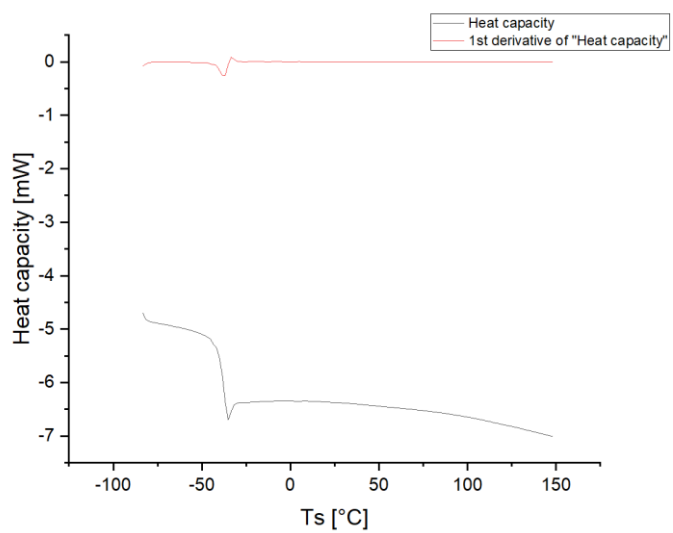
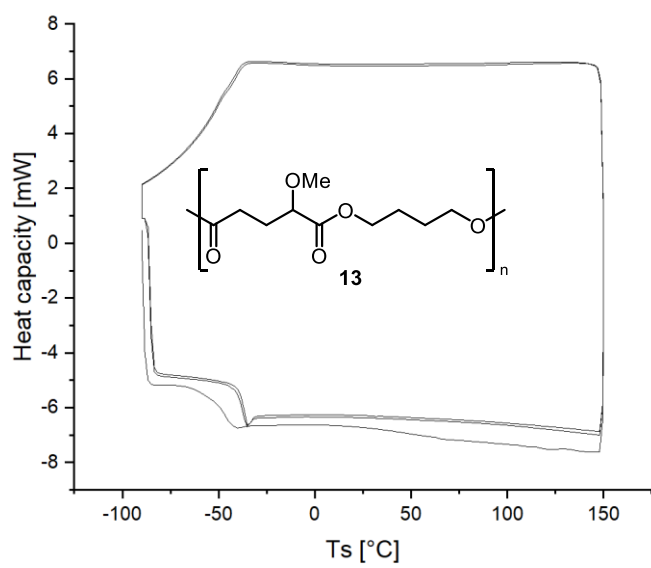


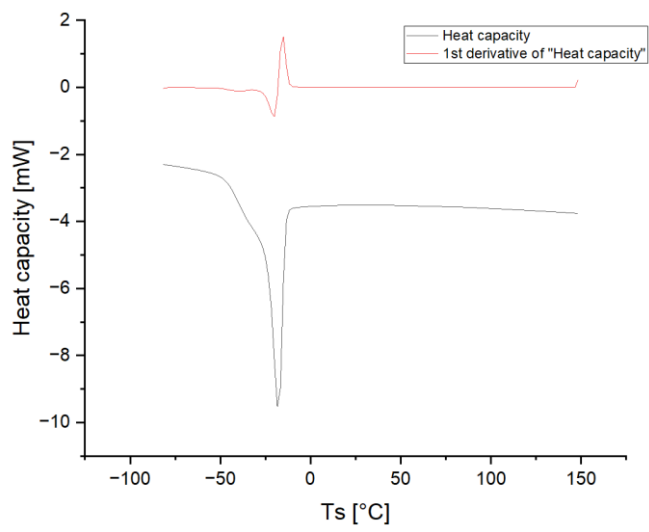
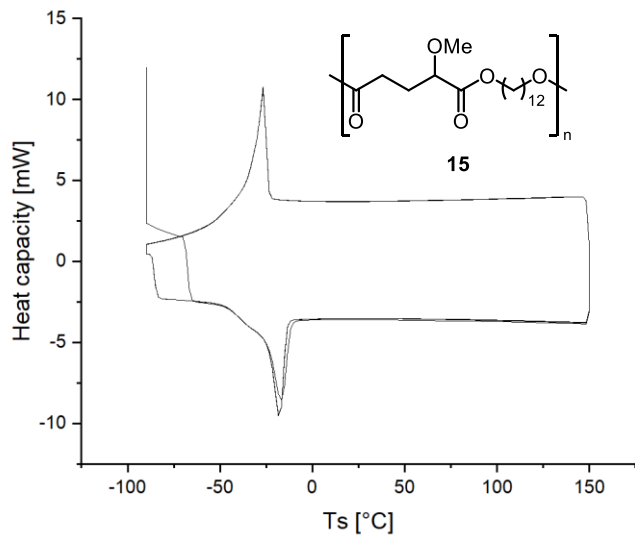
PSS WinGPC UniChrom, Build 5350, AN017, Instanz #1

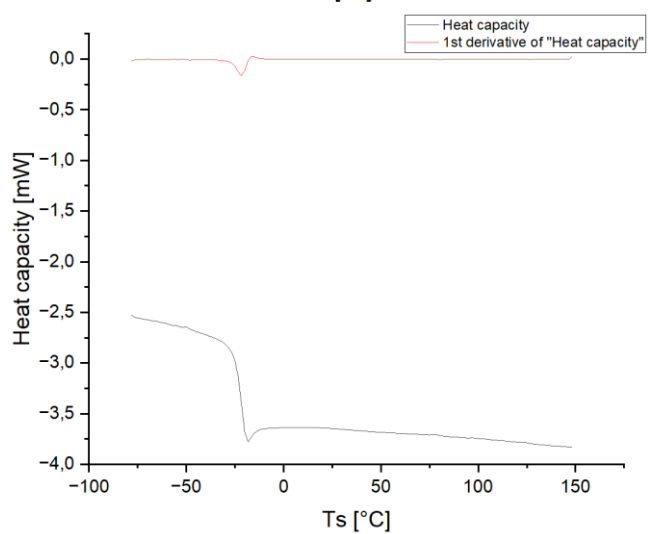
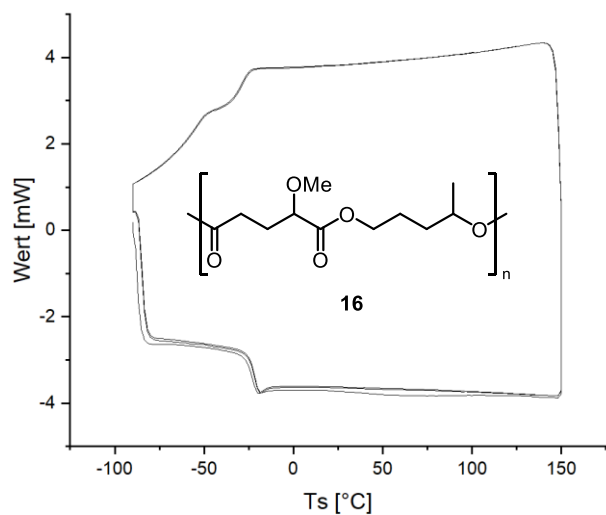


PSS WinGPC UniChrom, Build 5350, AN017, Instanz #1

DSC







6. References

1. J. Savard and P. Brassard, *Tetrahedron*, 1984, **40**, 3455-3464.
2. B. M. Jessen, J. M. Ondozabal, C. M. Pedersen, A. Sølvhøj, E. Taarning and R. Madsen, *ChemistrySelect*, 2020, **5**, 2559-2563.

7.3 Curriculum Vitae

Personal information

<i>First name, Surname</i>	Andrea Dell'Acqua
<i>Address</i>	Voßstraße 14, 18059 Rostock (Germany)
<i>e-mail</i>	and.dellacqua@gmail.com
<i>Telephone</i>	+49 1522 240 8513
<i>Nationality</i>	Italian
<i>Date of birth (mm/gg/aa)</i>	02/18/1994

Education and Training

<i>October 2019 – September 2022</i>	PhD, Dr. Rer. Nat. Leibniz Institute for Catalysis, Rostock, Germany <i>PhD Thesis</i> <i>Value-added products from bio-based platform chemicals</i> <i>Supervisor</i> Prof. Dr. Johannes Gerardus de Vries
<i>October 2016 – October 2018</i>	Master of Science in <i>Chemical Sciences</i> Università Degli Studi Di Milano, Milan, Italy <i>Master Thesis</i> <i>Base-metal catalysts for carbon-carbon and carbon-heteroatom multiple bonds reduction</i> <i>Supervisors</i> Prof. Dr. Cesare Gennari (Tutor: University of Milan) Dr. Luca Pignataro (Co-Tutor: University of Milan) Prof. Dr. Johannes Gerardus de Vries (Leibniz Institute for Catalysis, Rostock, Germany)
<i>Erasmus + Placement, 6 months (March-August 2018)</i>	Leibniz Institute for Catalysis, Rostock, Germany <i>Synthesis, characterization and applications in hydrogenation reactions of cobalt-NNS pincer complexes</i>
<i>October 2013 - July 2016</i>	Bachelor of Science in <i>Chemistry</i> Università Degli Studi Di Milano, Milan, Italy <i>Thesis</i> <i>Preparation of synthetic intermediates of RGD-Paclitaxel conjugates for 'Tumor targeting' applications</i> <i>Supervisors</i> Prof. Dr. Cesare Gennari (Tutor: University of Milan) Dr. Luca Pignataro (Co-Tutor: University of Milan)
<i>Pre-academic studies</i>	High School Diploma: <i>Maturità Scientifica</i> Liceo Scientifico <i>Edith Stein</i> , Gavirate, Italy

Professional Experience

October 2018 – September 2019

Laboratory technician

Catalysis with renewables & platform chemicals; Leibniz Institute for Catalysis, Rostock, Germany

November 2016 – March 2017

Laboratory technician

R&D department for fire-resistant coating; Aithon Ricerche International S.R.L., Ternate, Italy

Volunteering

October 2015 – February 2018

Emergency/urgency rescuer; SOS dei Laghi Onlus, Travedona Monate, Italy

Publications

1. "Phosphine-free cobalt catalyst precursors for the selective hydrogenation of olefins", *Catal. Sci. Technol.* 2019, 9, 61-64
2. "Additive Free Isomerization of Allylic Alcohols to Ketones with a Cobalt PNP Pincer Catalyst", *Chem. Eur. J.* 2019, 25, 7820-7825
3. "Scalable synthesis and polymerisation of a β -angelica lactone derived monomer", *Green Chem.* 2020, 22, 5267-5273
4. "Metal-catalysed selective transfer hydrogenation of α,β -unsaturated carbonyl compounds to allylic alcohols", *Green. Chem.* 2020, 22, 3323-3357
5. "HMF-glycerol acetals as additives for the debonding of polyurethane adhesives", *Green Chem.* 2021, 23, 957-965
6. "Ozonolysis of α -angelica lactone: a renewable route to malonates", *Chem. Commun.*, 2021, 57, 10524-10527
7. "Glycolaldehyde as a Bio-based C1 Building Block for Selective N-Formylation of Secondary Amines", *ChemSusChem.*, 2022, DOI: 10.1002/cssc.202201264

Contributions at conferences

1. *International Symposium on Homogeneous Catalysis*, Amsterdam (Netherlands), 8-13/07/2018: Flash talk and poster (“Additive Free Isomerization of Allylic Alcohols to Ketones with a Cobalt PNP Pincer Catalyst”)
2. *52. Jahrestreffen Deutscher Katalytiker*, Weimar (Germany), 13-15/03/2019: poster (“Phosphine-free cobalt catalyst precursors for the selective hydrogenation of olefins”)
3. *International Symposium on Green Chemistry*, La Rochelle (France), 13-17/05/2019: Oral communication (“Phosphine-free cobalt catalyst precursors for the selective hydrogenation of olefins”)
4. *54. Jahrestreffen Deutscher Katalytiker* (online), 16-19/03/2021: poster (“New and atom economic synthetic route towards a biobased angelica lactone cyclopentadiene polymer”)
5. *ACS Spring 2021* (online), 05-16/04/2021: Oral talk (“New and atom economic synthetic route towards a biobased angelica lactone-cyclopentadiene polymer”)
6. *Freiburg Macromolecular Colloquium 2022* (online), 23-25/02/2022: Poster presentation (“Angelica Lactones: renewable intermediates for the synthesis of monomers and polymers”)
7. *International Symposium on Green Chemistry*, La Rochelle (France), 16-20/05/2022: Oral communication (“Angelica Lactones: renewable intermediates for the synthesis of monomers and polymers”)
8. *55. Jahrestreffen Deutscher Katalytiker*, Weimar (Germany), 27-29/06/2022: Lecture (“Use of Iridium-Catalyzed Transfer Vinylation as an Efficient Synthetic Route towards Bio-Based (bis)-Vinyl Ether”)

Awards - Best Master thesis by *Fondazione Legnanese*, Legnano (Italy), 18/11/2018